"Study on All-Optical Logic and Arithmetic Operations using the Non-Linear Optical Material"

Thesis submitted for the Degree of

Doctor of Philosophy in Science

of

Jadavpur University

2025

By

Apurba Guchhait

Department of Physics

Jadavpur University

Kolkata-700032, West Bengal,

India.

''Study on All-Optical Logic and Arithmetic Operations using the Non-Linear Optical Material''

Thesis submitted for the Degree of

Doctor of Philosophy in Science

of

Jadavpur University

by

Apurba Guchhait

Under The Supervision of

Prof. Nabin Bran Manik

Department of Physics, Jadavpur University

Kolkata-700032, West Bengal, India.

&

Dr. Nirmalya Pahari

Department of Physics, Vivekananda College

Thakurpukur, Kolkata-700063, West Bengal, India

August 2025

Dedicated

to my reverend

Mother, Late ***Dipali Guchhait,***

Mother-in- law, Late ***Asa Maiti***

&

Father, Late ***Adwaita Guchhait***

Declaration by the Author

I hereby declare that this thesis entitled "**Study on All-Optical Logic and Arithmetic Operations using the Non-Linear Optical Material**" is my own work and that, to the best of my knowledge and belief, it contains neither any material previously published or written by another person nor any material which has been accepted for the award of any other degree or diploma of the university or other institute of higher learning, except where due acknowledgement has been made in the text.

Apurba Guchhait.

(Apurba Guchhait)

Date: 20/08/2025

Program: Ph.D.

Department: Physics

Institution: Jadavpur University, Kolkata, WB, India

Certificate from supervisors

This is to certify that the thesis entitled **"Study on All-Optical Logic and Arithmetic Operations using the Non-Linear Optical Material"** submitted by Apurba Guchhait, who had got his name registered on 27th February,2018 for the award of the degree of Doctor Philosophy (Science) of Jadavpur University, is absolutely based upon his own work under the supervision of Prof. Nabin Baran Manik and Dr. Nirmalya Pahari, and that neither this thesis nor any part of it has been submitted for either any degree / diploma or any other academic award anywhere before.

We believe the readers will certainly get some new interesting ideas from this thesis.

20.08.25

Prof. Nabin Baran Manik
Supervisor
Professor
Department of Physics,
Jadavpur University,
Kolkata- 700032,
West Bengal, India
Date: 20.08.25
Place: JADAVPUR, KOLKATA

Dr. NABIN BARAN MANIK
Professor
Department of Physics
Jadavpur University
Kolkata - 700 032

Nirmalya Pahari

Dr. Nirmalya Pahari
Supervisor
Associate Professor
Department of Physics,
Vivekananda College,
Kolkata-700063,
West Bengal, India.
Date: 20/08/2025
Place: KOLKATA

Dr. Nirmalya Pahari
Associate Professor
Dept. of Physics (UG & PG)
VIVEKANANDA COLLEGE
Thakurpukur, Kol-63

Acknowledgement

I would like to take this opportunity to express my heartfelt gratitude to all those who have supported me, directly or indirectly, in the preparation and completion of this thesis.

First and foremost, I extend my deepest respect and sincere thanks to Prof. Nabin Baran Manik, Professor, Department of Physics, Jadavpur University, and Dr. Nirmalya Pahari, Department of Physics, Vivekananda College, for granting me the opportunity to pursue research in the field presented in this thesis. I am profoundly grateful for their constant inspiration, invaluable guidance, and unwavering encouragement throughout my research journey. Their deep understanding of the subject and steadfast commitment to academic excellence have greatly enriched the quality of my work.

I would like to express my heartfelt gratitude to the revered person whose inspiring teaching first sparked my interest in this field of research. His loving guidance and profound wisdom have been the cornerstone of my academic journey. I remain ever grateful to him for granting me the invaluable opportunity to be mentored by Dr. Nirmalya Pahari Sir. This respected individual is none other than my esteemed postgraduate teacher from Vidyasagar University — Prof. Sourangshu Mukhopadhyay, the Honourable Vice Chancellor of Mahatma Gandhi University. His blessed presence continues to be a guiding force in my educational life.

I sincerely acknowledge Jadavpur University for providing the opportunity to carry out my research, and I thank all the staff members of the Department of Physics, Jadavpur University, as well as my colleagues at Panithar Gram Sava Mahendra Sikshasadan, Sabang, Paschim Medinipur, for their unstinting support and cooperation.

I bow in reverence to my beloved parents, Late Dipali Guchhait and Late Adwaita Guchhait (Retired Lecturer, Sabang Sajanikanta Mahavidyalaya). Their blessings, support, and values continue to guide me in every step of my life. I owe them my deepest respect and gratitude. My heartfelt gratitude also goes to my maternal grandparents, Late Lilarani Samanta and Late Ramkrishna Samanta, as well as to my respected father-in-law Nirad Baran Maiti and my maternal uncle Dr. Dilip Samanta (who was also my teacher during my undergraduate studies), for their constant inspiration, affection, and goodwill.

I would like to sincerely thank Dr. Jitendra Nath Acharyya (Postdoctoral Researcher, Laboratoire Photonique, Institut d'Optique Graduate School, France) and my cousin Dr. Debajyoti Samanta (Associate Professor, Department of Physics, Rampurhat College, Birbhum) for their valuable advice and suggestions. Special thanks are due to my beloved student and mentor, Debabrata Ganthya (Research Scholar, Department of Physics, Vidyasagar University and Assistant Teacher at Ramchandrapur Baikuntha Vidyapith), for his thoughtful suggestions, timely support, and collaborative spirit. His friendship and encouragement have meant a lot to me during the course of this work. I am also grateful to my dear student Samaybrata Paria (Research Scholar, Department of Physics, IIT Kharagpur), my friend Sourabh Kumar Das (Assistant Professor, Department of Physics, Raja N.L. Khan Women's College, Paschim Medinipur) and my brother-in-law Sourav Sundar Maity for their assistance with computer simulations and their insightful discussions.

Last but not least, I would like to express my sincere appreciation to Dr. Kanailal Paria (Retired Principal, Sabang Sajanikanta Mahavidyalaya, Paschim Medinipur) for his blessings, guidance, and unwavering support throughout this research.

Finally, I am deeply indebted to my family for their endless support, encouragement, and sacrifices, without which this journey would not have been possible. Thank you for standing by me.

Apurba Guchhait

Abstract

The increasing demand for high-speed computing and efficient data transmission has positioned optical systems as promising alternatives to traditional electronic approaches, owing to their natural ability to handle operations in parallel. This thesis explores a fully photonic framework that employs nonlinear optical materials primarily Kerr-type media for constructing a wide range of digital logic and arithmetic operations.

Beginning with an all-optical scheme for serial information transfer between storage units, the work utilizes nonlinear switching mechanisms to execute fundamental logic using optical NAND and NOT functions. Image edge recognition, a cornerstone in visual data analysis, is then addressed through a method that simulates edge extraction using intensity-dependent refractive changes in nonlinear substances.

The investigation proceeds by incorporating optical switching techniques to reinterpret digital logic elements. A binary encoding structure is proposed that translates decimal inputs into binary without relying on conventional or hybrid gate components. Following this, an all-optical decoding method is introduced, allowing for reverse transformation from binary to decimal optimized for rapid response and integration into purely photonic computational systems.

Further sections develop multi-valued logic encoders and decoders. Decimal-to-ternary and ternary-to-decimal translation mechanisms are designed using discrete light intensity levels, beam combiners, and splitters eliminating the need for logic gates entirely. The ternary system, defined through absence and variations of light, supports broader data expressiveness and high operational efficiency.

Advancing to four-level logic, a quaternary encoder is conceptualized to convert base-10 numbers into 4-ary code, further highlighting the scalability and adaptability of all-optical schemes. The architecture benefits from eliminating both optical and electronic gate components while facilitating broad parallel signal handling capabilities.

An innovative device is subsequently introduced to represent trigonometric ratios of compound angles using intensity-encoded light beams. This system leverages ternary encoders and coherent light manipulation to encode angular values, making it suitable for specialized scientific and engineering applications.

Finally, a binomial expansion device is presented, which optically computes binomial coefficients for any positive integer index using layered intensity inputs and a systematic light-routing design. This optical binomial processor showcases the extensibility of photonic methods in symbolic mathematics.

In conclusion, the study systematically demonstrates the capability of optical circuits built on nonlinear media and devoid of conventional logic gates to carry out encoding, decoding, computation, and mathematical operations. The proposed all-optical mechanisms hold significant potential in the design of future ultra-fast, gate-free photonic computing and communication technologies.

Acronyms

BC	-	Beam Combiner
BS	-	Beam Splitter
CD	-	Compact Disc
CKT	-	Circuit
CL	-	Constant Light
CLS	-	Constant Light Source
FF	-	Flip Flop
GOLES	-	Generalized Optical Logic Elements
I/P	-	Input
LM	-	Linear Material
LSB	-	Low Significant Beat
MCL	-	Multiple Constant Light Source
MSB	-	Most Significant Beat
MSD	-	Modified Signed-Digit
MISD	-	Multiple Instruction Single Data
NLM	-	Non-Linear Material
O/P	-	Output
OBED	-	Optical Binomial Expansion Device
OC	-	Output Controller
OD	-	Optical Device
OP	-	Optical Port
OR	-	Optical Regulator
OS	-	Optical Switch
ODC	-	Optical Divider Circuit
OQE	-	Optical Quaternary Encoder
OTE	-	Optical Ternary Encoder
OTFD	-	Optical Trigonometric Functional Device
OTD	-	Optical Ternary Decoder
R	-	Reflector

RI	-	Refractive Index
NOM	-	Non-linear Optical Material
PL	-	Pulse Setting Laser
SEM	-	Scanning Electron Micrograph
SIMD	-	Single Instruction Multiple Data
SISD	-	Single Instruction Single Data
VLSI	-	Very Large-Scale Integration

List of Figures

Chapter - 4

Chapter - 5

Chapter - 6

List of Tables

Chapter - 5

Chapter - 6

Contents

Preface

The very nature of the limitations of the traditional electronic digital computers has motivated the creation of a new technological philosophy that utilizes optics for computation. The basic aim in this new field is to increase the speed of computation while reducing system size at the same time. Optical computing, which is an evolving field, has attracted significant attention based on the inherent nature of optics to accomplish both analog and digital computations. In recent decades, there has been an increasing interest in all-optical data processing and it has thus been the focal point of study.

My personal journey into the subject started when I was working part-time as a lecturer in Sabang Sajanikanta Mahavidyalaya. I first came across the idea of optical computing there. The notion of parallel processing through light intrigue me and kindled a profound enthusiasm. It finally grew into a firm desire to make significant contributions to this prospective and interdisciplinary field.

Prominent progress has been achieved in parallel computing in optics and optoelectronics over the past several years. Most importantly, optical devices enable the implementation of multiple logic functions with a single nonlinear optical medium, which is impossible for electronic circuits with one logic gate. Researchers have suggested a number of models and methods based on different nonlinear crystals and metamaterials with the aim of efficient modulation of light. Yet, there are still difficulties in designing all-optical logic and arithmetic systems with satisfactory functional requirements.

In our research, we intend to convert traditional digital electronic devices into optical devices through the application of intensity-based optical gates or switches. In this work, we try to build different all-optical logic and arithmetic circuits through the exploitation of Kerr-type nonlinear optical materials' distinctive characteristics. Here, binary data are encoded in light: the presence of polarized light signifies a binary '1' and its absence signifies a binary '0'. I hope this research will be useful for future work in the area.

This thesis is organized into seven chapters. The first chapter offers introductory concepts. Chapters 2 to 6 detail our proposed optical computing schemes, while Chapter 7 presents the overall conclusions and suggests possible directions for future work. Finally, APPENDICES and a list of my publications are provided at the end of this thesis.

Chapter -1

Motivation and outline of the thesis

1.1. Introduction

1.2. Advantages of optical computing and photonic data processing

1.3. Optical or Photonic computing and its need

1.4. Optical encoding and decoding techniques

1.5. Optical isotropic nonlinear materials

1.6. Optical isotropic Kerr nonlinear material as a light-controlled switch

1.7. Objectives of the proposed thesis

1.8. Organization of the work

1.9. Background of optical computation

1.10. Overview of optical computing techniques

1.11. Conclusions

1.12. References

Chapter 1

Motivation and outline of the thesis

1.1. Introduction

The increasing demand for high-speed data transmission has become a driving force behind modern technological development. With the surge in global digital communication needs, conventional electronic systems are increasingly struggling to keep up due to inherent physical limitations. Although advancements in microelectronics have led to faster and more compact computing devices, the movement of electrons which forms the basis of traditional computation is restricted by factors such as limited mobility, thermal issues, and bandwidth constraints. These limitations have become significant barriers to achieving the ultra-fast processing speeds required in current and future applications.

In search of a better alternative, the scientific community turned its attention to optics. This shift began in the 1970s, when light-based (photonic) systems showed promise in data transmission and processing. Unlike electrons, photons can travel at the speed of light and do not suffer from the same propagation delays or thermal inefficiencies. The use of photons as information carriers introduced the possibility of all-optical computing a concept that allows data to be processed entirely using light, bypassing the limitations of electronics. Optical computing offers numerous advantages over electronic systems. With the ability to handle operations at frequencies as high as 10^{15} Hz compared to the 10^{10} Hz limit of electronic devices optical systems support much higher processing speeds. Additionally, photonic signals do not interfere with each other, enabling multiple data streams to travel simultaneously through a single system. This parallelism, along with minimal signal distortion and reduced energy consumption, makes optics particularly attractive for high-speed computing and communication tasks.

Recent research efforts have focused on developing components such as all-optical logic gates, multiplexers, cross-bar switches, and ultra-fast photonic switches. These innovations are crucial for building efficient and scalable optical systems. Moreover, optical technologies like wavelength division multiplexing (WDM) allow multiple signals

of different wavelengths to be processed simultaneously, further enhancing the potential for parallel processing.

Over the years, optical computing has evolved from an analog concept to practical digital implementations. Researchers and engineers across the globe are continuously investigating innovative architectures and advanced materials to unlock the full potential of photonic technologies [1, 2, 3, 4, 5, 6, 7].

As a result, optical computing is now seen as a powerful solution for overcoming the speed, scalability, and energy limitations of electronic systems. In our ongoing research, we have designed innovative schemes to implement algebraic, arithmetic, mathematical, digital(electronic) and image processing operations.

1.2. Advantages of optical computing and photonic data processing

As technological demands increase for faster, more efficient, and scalable computing systems, optical methods have emerged as a promising alternative to traditional electronic systems. Light-based computing technologies, driven by innovations in nonlinear optics and photonic integration, offer several significant benefits over conventional electronic approaches particularly in speed, energy efficiency, scalability, and signal integrity.

Superior Processing Speed

Optical computing systems exhibit the potential for extremely fast operation due to the inherent properties of light [8, 9]. In contrast to electrical signals which experience resistance, capacitance, and inductive delays within metallic conductors light pulses travel at extremely high velocities, enabling near-instantaneous signal propagation. With the operational ceiling for electronic logic typically capped at around 10^{10} operations per second, optical systems theoretically support logic operations in the order of 10^{15} per second, demonstrating a quantum leap in processing capability. Additionally, since photons are not affected by electron drift or capacitance effects, optical systems can support real-time computation without propagation delay.

Parallelism and Non-Interference

One of the defining strengths of optical systems is their ability to process multiple data channels simultaneously. This is achieved through two key principles: first, by increasing the volume of information transmitted and processed concurrently within the central system; and second, by allowing optical paths to intersect without mutual disturbance.

Multiple light beams, especially when multiplexed by wavelength (WDM), can travel together through a single fiber, supporting massive parallelism that is extremely difficult to replicate in traditional digital systems.

Low Energy Consumption and Thermal Efficiency

Electronic systems typically consume significant amounts of power during operation ranging from 80 to 250 watts depending on system state. In contrast, photonic devices operate with minimal energy requirements due to the absence of resistive heating and lower voltage demands [10]. Optical switches, for example, do not require line charging like electronic components, and as such, heat generation is vastly reduced. This allows the elimination of large cooling systems, fans, or heat sinks, leading to more compact and thermally efficient hardware configurations.

Reduced Noise and Acoustic Output

Mechanical components such as fans, present in nearly all electronic computing systems, are known sources of audible noise. Optical systems, by nature of their static operation and lack of moving parts, produce negligible sound, making them ideal for applications where silent operation is preferred.

Design Flexibility and Scalable Architecture

In electronic systems, device layout is largely constrained by the physical limitations of signal transmission speeds and interference among copper traces. Optical communication, however, is nearly immune to distance-related delays and interference, allowing flexible placement of system components. For instance, the different parts of an optical computing system can be distributed across large physical areas within a building, across a vehicle, or even an entire campus without degrading performance. This is made possible by the low attenuation and high data rate capabilities of fiber optics.

Immunity to Electromagnetic Interference

Unlike electrons, photons do not interact with external electric or magnetic fields. This property ensures that data traveling through optical channels is not distorted by environmental noise, eliminating problems such as cross-talk, interference, or short-circuiting commonly found in electronic circuits. This makes optical communication highly stable and reliable, particularly in high-noise environments such as industrial or medical settings.

Support for Multi-Valued Logic

While electronic computing systems typically rely on binary logic (two voltage states), optical systems can easily support multi-level logic through modulation of light intensity, phase, or frequency. This opens up possibilities for more compact and efficient encoding schemes, such as ternary or quaternary logic, which are much harder to implement using conventional electronics.

Efficient Bandwidth and Compact Design

Optical systems require fewer physical channels due to their ability to multiplex multiple signals within a single transmission line. **This reduces the space needed for routing and simplifies the hardware design, leading to smaller, lighter, and more cost-effective devices.** Additionally, since there is no electrical charging involved, signal lines can be thinner and more energy-efficient.

1.3. Optical or Photonic computing and its need

Prior to the invention of the transistor, performing logical or arithmetic operations through machines was a slow and hardware-intensive process. Early computing systems were large, inefficient, and limited in processing capability. The introduction of the transistor significantly transformed this landscape, enabling faster and more compact electronic devices [11]. This breakthrough marked the beginning of digital computation, and with ongoing improvements in semiconductor fabrication especially through Very Large-Scale Integration (VLSI) computing systems achieved clock speeds in the gigahertz range.

However, as integration density increased, further performance improvements began to plateau due to inherent limitations. Challenges such as interconnect delays, restricted pin counts, and limited bandwidth have created obstacles to scaling electronic systems. Although electronic circuits have become faster and smaller, the growing demand for even higher data rates and lower latency has outpaced the capabilities of current silicon-based platforms.To overcome these limitations, the field of photonic or optical computing has emerged. This approach replaces electrical signals and copper interconnects with photons and optical pathways, offering solutions that operate at the speed of light. Systems utilizing photonic components promise substantial improvements in speed, parallelism, energy efficiency, and signal fidelity.

Unlike conventional computation that relies on electrons, optical systems manipulate light using nonlinear media, waveguides, fibers, and optical switches. Such systems are capable of executing not only data transmission tasks but also complex signal processing. Applications of optical computing extend beyond communications and include memory storage, image analysis, Fourier-based processing, correlation techniques, optical neural networks, holographic computing (2D and 3D), pattern recognition, fuzzy logic processing, multiplexing and demultiplexing, and artificial intelligence architectures.

A fundamental concept behind all-optical systems is that one light beam can control another, implementing switching or logic functionality without requiring any electrical signal for operation. The performance of these systems often lies in the picosecond to femtosecond range, far surpassing what is achievable with electronics.

Photonic computation uses devices that transmit or block light to represent logical states. By exploiting multiple wavelengths and polarizations, such systems can process several data streams concurrently. As a result, photonic systems not only reduce size and power consumption but also offer higher reliability and freedom from electromagnetic interference. In essence, replacing electrons with photons opens the possibility of a new generation of computing devices optical computers that are smaller, faster, more robust, and capable of parallel operations that traditional electronics cannot match. This transformation is not only about communication speed, but also about revolutionizing how information is processed, stored, and interpreted in intelligent systems.

1.4. Optical encoding and decoding techniques

In recent decades, optical techniques have gained prominence for performing various functions in data manipulation and processing. Numerous studies [12-41] have recognized the advantages of using light-based signals over electronic ones. This shift is largely due to the superior properties of optical communication, including high speed and natural parallelism.

When light signals are employed for transmitting digital information, the need arises for effective methods to represent and interpret data states. Different encoding approaches have been explored, involving the signal's polarization, intensity level, or phase. In one commonly used strategy—intensity modulation—the complete absence of light is considered a low state ('0'), while the presence of light at a predetermined strength is interpreted as a high state ('1').

Now it is fact that a conventional computing machine cannot comprehend the mathematical digit like zero (0) and one (1) for binary system. So, to encode the mathematical data, difference optical symbols here to be utilize. Several symbolic coding and decoding techniques can be adopted to communicate data from one unit of a system to another and to utilize the parallelism of optical signals to perform various computer operations. Some reports here also noted the use of tri-state or other multivalued logic [42]. Various techniques of data encoding and decoding can be utilized to implement optical data processors. These processes can be like intensity. Polarization [43], phase or frequency-based encoding [44]. In our journey we adopt intensity-based coding system where logic '1' (high state) and logic '0' (low state) are represented by presence of a pre-fixed intensity (I) of light signal and absence of any light signal respectively for binary operation.

However, for realizing such all-optical data systems, nonlinear optical media and photorefractive compounds have played a crucial role in many published methods [45-49]. There are also notable contributions where logic schemes beyond binary, such as ternary and quaternary, have been demonstrated with light-based circuits. In these types of systems, the precise intensity of the signal is critical to the behaviour of optical switches formed from nonlinear materials. Specifically, in isotropic Kerr-type media, the refractive index varies as the signal strength changes, affecting the medium's ability to guide or switch the signal appropriately. This property is foundational for constructing optical switching mechanisms.

1.5. Optical isotropic nonlinear materials

Isotropic nonlinear optical substances play a pivotal role in the development of light-based switching systems. These materials exhibit Kerr-type nonlinear behaviour, meaning their refractive index varies based on the intensity of the incident optical wave. This intensity-dependent index shift enables the redirection of light through different optical paths, making them highly suitable for designing switching circuits.

Consider a scenario (**Fig. -1.1**) where a light pulse labelled "AO_1" is launched into the medium with a predefined standard intensity denoted by 'I'. Under these conditions, the refractive property of the nonlinear medium causes the beam to emerge from a designated output channel, say "P_1", while no light appears at an alternate path "P_2". However, when the incident light intensity is increased to '2I', the nonlinear medium responds by altering

its refractive index (typically increasing in this case), whereas the linear medium remains unaffected. As a result, the beam is rerouted, now exiting through channel "P_2" instead of "P_1". This controllable behaviour forms the basis for implementing all-optical switching mechanisms [50]. Such switching operations are discussed in more detail in next section, where the material's behaviour is exploited to manipulate light paths without the need for electrical control. Traditionally, these systems utilize pulsed Nd: YAG laser sources due to their ability to generate short, high-power pulses suitable for triggering nonlinear effects. However, these lasers often require substantial electrical input, which may be impractical in compact or energy-sensitive setups. To address this, tunable diode lasers can serve as an alternative source, offering adjustable output while consuming less power. For this reason, nonlinear materials with strong Kerr responses are preferred those capable of generating significant optical nonlinearities even under moderate-intensity beams. It's also important that these substances exhibit minimal nonlinear absorption, ensuring that the majority of the signal energy is used for switching rather than being lost as heat or scattered light [51]. Among such materials, chalcogenide glasses are particularly noteworthy. They possess a third-order nonlinear susceptibility ($\chi 3$) that is approximately a thousand times greater than that of conventional silica-based media. This makes them ideal candidates for efficient optical switching in low-power regimes. Additionally, Q-switching methods can be implemented to transform continuous-wave laser outputs into high-peak-power pulse beams, further improving the performance of light-controlled switching.

1.6. Optical isotropic Kerr nonlinear material as a light-controlled switch

Certain isotropic substances with nonlinear optical properties exhibit what is known as the **Kerr effect**, where their refractive index varies in response to the light intensity that interacts with them. These materials are known to support **self-focusing** behaviour [52], which can be effectively utilized in designing photonic switching elements. In such media, the **second-order nonlinear term** in the dielectric polarization equation becomes prominent and must be considered while ignoring higher-order effects.

According to the refractive index relation (equation 3.5), these materials show a **linear increase** in refractive index when the intensity of the passing light beam is increased. This unique characteristic enables their application as optical switches, as illustrated conceptually in **Figure 1.1**.

Explanation

Now the basic famous Kerr nonlinear equation on which the optical switching action depends is- $n_{NLM} = n_0 + n_2 I$ -----(1)

where n_0 is the constant (linear) refractive index, n_2 is the second-order nonlinear coefficient, and I is the light intensity passing through the medium. This indicates that the refractive index of such materials increases with increasing intensity of the incident beam, making them good candidates for optical switching applications. For implementing a switching mechanism, a composite structure involving both linear and nonlinear materials can be used. Let (in **figure 1.1**) the light beam propagates from a linear medium (refractive index n_L) to a nonlinear medium (with intensity-dependent index n_{NLM}). For some intensity (say intensity I), the light can propagate along a certain path, say path P_1 of intensity I. When the intensity is increased, the refractive index of the nonlinear medium varies but not the refractive index of the linear medium. This produces a change in the refraction angle, according to Snell's Law,

$n_{LM} \sin\theta_1 = n_{NLM} \sin\theta_2$ -----(2)

so that the refracted beam travels nearer to the normal (along path P_2 of intensity 2I), for instance). This serves to make the composite act as an intensity-sensitive optical switch. Optical materials such as carbon disulphide (CS_2), silica glass, and gallium arsenide (GaAs) are used mostly for this purpose owing to their highly nonlinear optical properties. For example, CS_2 has a linear refractive index $n_0 = 1.62$ and nonlinear coefficient $n_2 = 0.22 \times 10^{-19} m^2/W$ [53]. A CS_2-based system has the capability to focus a laser beam of radius 1 cm and 10 MW power at a distance of 10 cm because it has self-focusing property. This focusing capability is important in optical switching and is determined by the focusing length L, which depends on the beam power P and the beam cross-section 'a' according to:

$$P = \frac{\pi \varepsilon_0 n_0 C a^4}{8 n_2 L^2} \quad \text{----(3)}$$

Here, ε_0 is free-space permittivity and C is the speed of light in a vacuum. From here, it can be understood that a reduction in beam radius or a rise in power decreases the focusing length, rendering such materials useful in photonic integrated circuits where there is limited space.The change in output beam refraction as a result of variation in input intensity can be analyzed quantitatively as well. Consider, for instance, fused silica with

$n_0 = 1.46$ and $n_2 = 3.2 \times 10^{-20} m^2/W$. A standard laser of 100 mW power and 50 μm beam diameter produces an intensity of $2 \times 10^9 \mathrm{W}/m^2$, leading to a refractive-index change $\Delta n = n_{NLM} - n_0 = 6.4 \times 10^{-12}$, a value that appears to be very small. But employing a pulsed laser rather than a continuous one significantly changes this effect. A Q-switched laser with a 10^{-7}second pulse duration can produce an appreciable angular deviation $\Delta\theta_2$ of 0.013° (or 0.24×10^{-3}rad) when intensity is doubled, with the angle of incidence held constant at 45°.

In addition, if the pulse duration is shortened to 10^{-9} seconds, the angular deviation increases considerably to 1.2°. CS_2, which has a greater n_2 value, on the other hand, exhibits even larger deviation, and its higher performance in this switching application is thus shown.

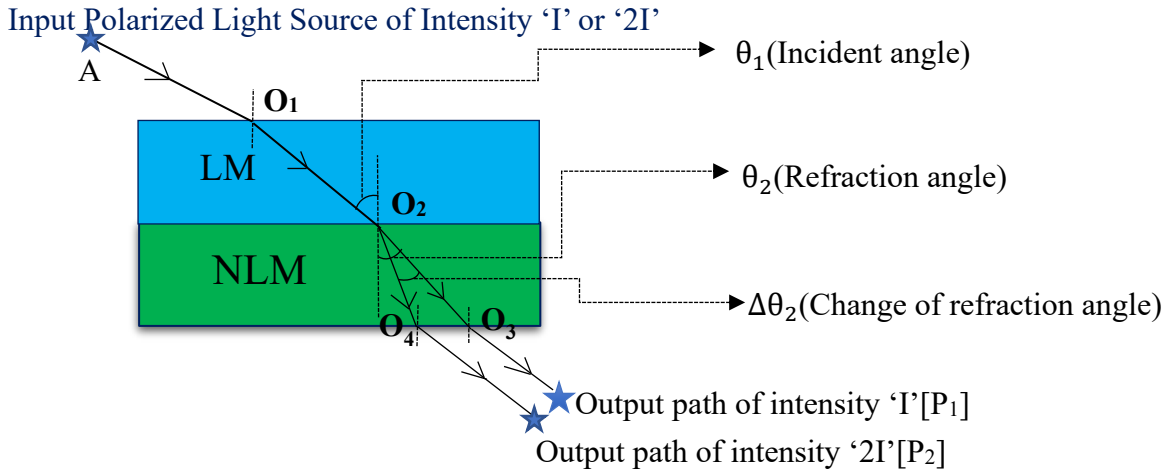

Fig. 1.1 Optical linear and nonlinear materials act as an optical switch or regulator

For a nonlinear medium with 1 cm thickness, this angular variation causes a lateral separation of approximately 0.3 mm between exit points "O_3" and "O_4". In micro-optical systems, this displacement is quite significant, allowing for clearly distinguishable output paths. By adjusting the intensity of nanosecond-duration pulses, light can be directed to specific output channels forming the foundation for digital optical logic devices.

To effectively utilize these nonlinear characteristics, the system must operate in a pulsed or discrete signal mode. Continuous-wave signals without modulation would demand impractically high-power levels to achieve similar nonlinear responses. Some modern

materials are capable of responding within sub-picosecond timescales, making them suitable for ultrafast logic applications. Several designs for optical logic circuits based on this switching principle have already been proposed in research literature.

Additionally, there exist other nonlinear media where the intensity-dependent index change behaves in the opposite manner i.e., increasing beam intensity results in a reduction of the refractive index. This thesis focuses specifically on the first category of nonlinear materials, where the refractive index increases with optical power. By encoding logical states using the strength of the light signal where a predetermined intensity (e.g., 'I') signifies logic "1", and the absence of light signifies logic "0" various all-optical logic gates can be effectively implemented using such Kerr-type nonlinear isotropic materials.

1.7. Objectives of the proposed thesis

The primary aim of this research is to explore and design all-optical systems capable of performing logic and arithmetic operations using nonlinear optical materials, particularly those exhibiting Kerr-type behaviour. The motivation stems from the increasing demand for ultra-fast, parallel, and low-power computational systems, where optics has emerged as a promising alternative to traditional electronic computation.

The specific objectives of the work are outlined as follows:

1. To develop an all-optical mechanism for serial data transfer between registers by implementing fundamental logic operations (e.g., NAND, NOT) using nonlinear optical components.
2. To design an optical image processing scheme that enables real-time edge detection through intensity-sensitive refractive index changes in nonlinear materials.
3. To construct multi-valued optical encoders and decoders (binary, ternary, quaternary) using nonlinear switches, beam splitters, and combiners, eliminating the need for conventional logic gates.
4. To propose an optical framework for computing trigonometric ratios of compound angles by manipulating light intensities to represent angle values and their functional combinations.
5. To realize an all-optical system for the calculation of binomial coefficients based on input light intensity levels, without using any digital arithmetic units.

6. To demonstrate, through design and simulation, that the proposed optical circuits can be utilized as core components in future photonic computing systems and high-speed optical communication technologies.

By achieving the above goals, the research aims to contribute towards scalable, high-throughput, and fully optical computation platforms, reducing the dependency on electronic processing and paving the way for next-generation photonic technologies.

1.8. Organization of the work

The thesis has been organized into seven chapters. The content of each chapter is concisely alluded here.

Chapter- 1: Motivation and outline of the thesis

In Chapter 1, we mentioned the increased need for high-capacity communications systems in order to sustain the fast pace of technological progress at the global level. We highlighted that current electronic computing methods could become inadequate in addressing the requirements of ultra-high-speed data transmission in the near future. Consequently, research is more and more concerned with the development of all-optical computation, which has significant prospects for replacing the conventional electronic devices in high-speed communication applications. The chapter also delineates the importance of all-optical computing and presents the necessary requirements for practical implementation.

Moreover, Chapter 1 discusses the contribution of nonlinear optics to the construction and development of contemporary optical devices, components, and systems. We explained the basic nature of nonlinear optical materials, with specific reference to Kerr nonlinear materials. The working principle of optical switches based on Kerr nonlinearity is investigated, noting their promise as crucial elements in optical networks and other optical computing systems.

Chapter- 2: All-Optical Serial Data Transfer Between Registers

This chapter focuses on designing a system that enables data transfer between memory registers using only optical components. The method relies on nonlinear optical materials to construct logic gate equivalents such as NAND and NOT, eliminating the need for any electronic or electro-optical logic devices. Data is moved serially through controlled light pulses, which trigger logic transitions and maintain consistency across register positions.

The architecture is structured to ensure signal fidelity during transmission, and offers a foundation for expanding into all-optical memory systems and processing architectures. Its serial data handling approach makes it a candidate for compact and high-speed optical hardware implementations.

Chapter- 3: Image Edge Extraction using Nonlinear Optical Media and verification by computer simulation

In this chapter, a novel edge detection mechanism is explored using intensity-dependent refractive behaviour in nonlinear optical substances. Instead of relying on algorithmic digital filtering, this method leverages variations in refractive index to amplify image contrast along object boundaries.

The proposed system involves projecting the image onto a Kerr-type medium, where changes in light intensity correlate with structural differences in the image. The setup is verified through numerical simulation, and its effectiveness demonstrates how light can be used to directly process and analyse visual data at high speed.

Chapter- 4: Optical Logic for Multi-Valued Encoding and Decoding

This chapter presents multiple encoding and decoding schemes that operate using optical principles to represent binary, ternary, and quaternary logic states. Beginning with a binary encoder, the system converts numerical values into binary outputs through nonlinear switching behaviour, entirely within the optical domain. A corresponding decoder interprets these signals without requiring digital logic gates.

The chapter expands into ternary and quaternary formats, where distinct light intensity levels represent multi-valued logic states. Encoding and decoding mechanisms are constructed using beam splitters, combiners, and absorption elements. These systems provide efficient, parallel data processing while maintaining simplicity and eliminating traditional gate dependencies.

Chapter 5: Optical Computation of Trigonometric Ratios

This section introduces an optical configuration for computing compound angle trigonometric values. Using a pair of ternary encoders, each representing a separate angular input, the system produces intermediate outputs in light intensity form. These signals are then optically combined either by addition or subtraction to realize compound trigonometric expressions. Through fixed-intensity light sources and well-positioned

optical components, the system offers a real-time, fully optical method for trigonometric computation. Applications of this approach span fields like geophysics, astronomy, and medical imaging, where rapid and parallel angular analysis is valuable.

Chapter 6: Optical System for Binomial Coefficient Calculation

This chapter proposes a photonic framework to compute binomial coefficients for any positive integral exponent. The system receives light input at an intensity level proportional to the binomial index, which is then routed through an array of nonlinear optical switches. Each output path corresponds to one term in the expansion, activated based on specific threshold criteria.

Strategic use of beam splitters and combiners allows the system to function without digital arithmetic units. The structure illustrates how symbolic mathematical tasks can be executed with light, offering opportunities in real-time optical computation.

Chapter 7: Conclusions and future scope of works

The final chapter consolidates the contributions made throughout the thesis. It emphasizes the advantages of using all-optical systems in digital logic, arithmetic, signal processing, and functional computation. Each proposed design demonstrates how nonlinear optical behaviour, light routing, and intensity modulation can be combined to eliminate dependence on electronic components.

Future work may involve experimental validation of the designs, integration with photonic integrated circuits, and the extension of current systems to handle more complex computations and logic operations. The research lays the groundwork for practical implementation of high-speed, scalable optical computing architectures.

1.9. Background of optical computation

Photonic devices have become increasingly vital across numerous scientific and technological fields due to their substantial advantages over conventional electronic methods. Traditional digital systems face limitations, particularly with regard to speed and thermal constraints. Optical systems provide a compelling alternative, capable of overcoming these barriers by leveraging the properties of light.

All-optical parallel computing represents a fundamental strength of photonic systems and forms a core component in the design of future optical computers. These systems operate at significantly higher speeds than conventional electro-optic technologies. Researchers

globally are dedicating substantial effort to advance this field, aiming to transition from conceptual designs to practical, fully operational optical machines.

In recent years, considerable progress has been made in areas such as light-based logic operations, optical interconnects, memory modules, and switching systems. The performance of these systems, especially their speed and energy efficiency, depends heavily on the nonlinear characteristics of the materials used. As a result, investigations into novel nonlinear optical media have intensified, as these materials are key enablers of all-optical logic operations.

The 21st century is increasingly seen as the era of photonics, where advancements in light-based technologies are reshaping computing and communication systems. Numerous optical computing techniques exist, each with specific benefits and constraints. In such architectures, **synchronization**, **memory**, and **switching efficiency** play crucial roles in ensuring correct and timely computation. Various unconventional techniques have also emerged, pushing the boundaries of optical signal processing beyond the limitations of traditional models.

1.10. Overview of Optical Computing Techniques

Optical methods have firmly positioned themselves as transformative in the domain of information processing. While electronic computers process data sequentially, optical counterparts enable operations to be performed in parallel, capitalizing on the natural parallelism of light propagation. Through this property, optical computing achieves faster data throughput and accelerated decision-making capabilities.

Historically, computing systems were limited to a set of predefined tasks. The introduction of stored program architectures such as the von Neumann model was a breakthrough, combining instruction storage with processing logic. This architecture includes four main components: the processor, memory, control unit, and input/output system. However, having both data and instructions share the same communication path (bus) introduces a speed bottleneck.

Depending on how many instruction and data streams are handled simultaneously, systems are categorized into models such as Single Instruction Single Data (SISD), Single Instruction Multiple Data (SIMD), Multiple Instruction Single Data (MISD), and Multiple Instruction Multiple Data (MIMD) [54]. The SISD model corresponds to the original von Neumann structure. SIMD models are further subdivided into array, pipeline, and associative processors.

To develop an optical computing platform, each of these architectural elements must be reengineered with optical components. Progress has been made in designing both numeric and symbolic optical processors. While numeric processors include devices for logic, arithmetic, and correlation tasks, symbolic units handle tasks like optical pattern interpretation and language-based data processing [55].

Since the laser's invention in the 1960s, the development of optical computing has gained momentum. Ruby and helium-neon lasers led to the discovery of solid-state and gas-based light sources, which paved the way for semiconductor and dye-based laser systems. These breakthroughs catalyzed a transformation in how data is transmitted, processed, and stored.

Researchers recognized that the principles of classical optics could be adapted to perform digital operations. Early proposals emphasized that unless the nonlinearity of the optical medium was sufficiently high, building practical optical logic gates would remain out of reach. Approaches such as symbolic substitution were explored for image handling, and simple optical processors were developed from these ideas. Today, compact laser diodes are widely available, and optical data storage (e.g., CDs) has become commonplace.

Several designs for optical logic circuits and arithmetic processors have emerged using a variety of innovative strategies [56-75]. Notably, Heinz et al. proposed a light-based solution for matrix operations [76], and Mukhopadhyay et al. developed a real-time binary adder using optical logic [77]. In other designs, **tristate logic** and the **modified signed-digit (MSD)** system were employed [78-81]. The MSD format simplifies subtraction and addition by avoiding carry and borrow logic and facilitates easy handling of negative numbers using complement rules.

Although debates about the viability of optical computers still exist [3], the field continues to evolve rapidly [82]. Integrated optical logic circuits are becoming more practical, with some passive logic gates like XOR and COINC already demonstrated using low-energy principles [83-84].

Various encoding strategies have been introduced to implement photonic logic, including **polarization-based encoding**. Alam et al. designed logic circuits using **shadow-casting with polarized light** [85], and others have demonstrated binary logic using linearly polarized waves [86-87]. Zaghloul et al. introduced an architecture called **orthoparallel optical logic**, enabling implementations of gates like AND, OR, and NAND using polarization angles of +45° and -45° to represent logic levels.

All-optical switching mechanisms are foundational in building these systems, relying heavily on the nonlinear optical response of the materials. For example, **Pahari et al. proposed a** light-controlled binary addition method using nonlinear interaction in suitable media [88]. Optical comparison between multi-bit values has also been demonstrated [89], achieving high-speed operation with nonlinear effects. Their approach can theoretically reach speeds between 1–10 terabits per second. Additionally, they introduced a 1's complement comparison method for digital signals [90].

Advanced photonic components like **generalized optical logic elements (GOLEs)** have also been introduced. Caulfield et al. demonstrated devices capable of executing all 16 Boolean logic functions on optical beams with rapid switching capability [91]. Other proposals employed **Mach–Zehnder interferometers** to achieve lossless computation, and **GaAs-AlGaAs microring resonators** were used to realize all-optical switches [92]. Polarization-controlled switching is another route for logic gate implementation [93].

The **optical tree network**, as shown in **Figure 1.2**, is another example of intelligent routing [94-97]. Here, the light path from a constant source (CLS) through branch "a" is redirected based on control beams. When signal "P" is off, the light moves to the lower path "c." When "P" is on, it redirects the signal to upper channel "b." Likewise, control inputs "Q" further govern the branching at subsequent levels. The behaviour for all control input combinations is summarized in **Table 1.1**.

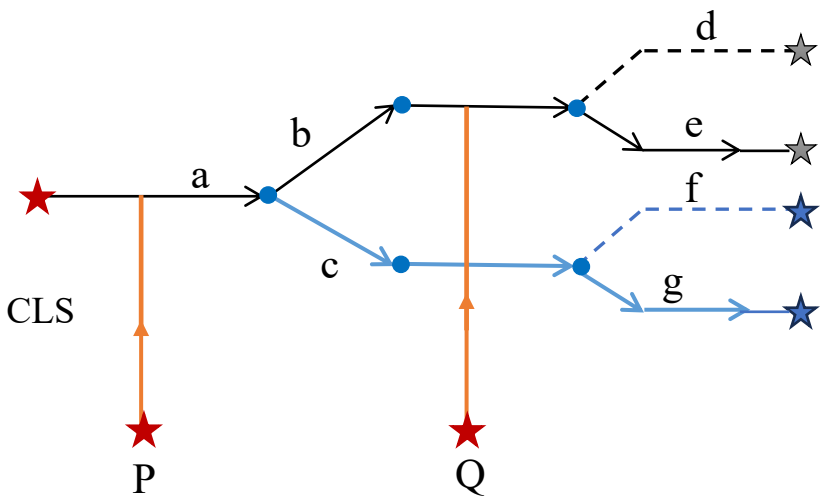

Fig. -1.2: Optical tree structure

Table – 1.1: Output states of tree structure

Control Inputs		Outputs			
P	Q	d	e	f	g
0	0	0	0	0	1
0	1	0	0	1	0
1	0	0	1	0	0
1	1	1	0	0	0

1.11. Conclusion

The advancement of optical computing has reached a significantly developed state since its early conceptualization. Despite this progress, it continues to evolve alongside and in comparison, with traditional electronic computing methods. With ongoing innovations in light-based and hybrid optoelectronic systems, the realization of ultrafast processing through optical means appears increasingly achievable.

Simultaneously, the area of **quantum computation**—which leverages the inherent quantum properties of photons—is also experiencing substantial growth. Devices that operate using **linear optical logic** are showing promise as fundamental building blocks for implementing future **quantum optical processors**.

As we move forward, **fully optical digital processing** is poised to become a defining feature of next-generation computing architectures. Furthermore, this approach is expected to play a vital role in emerging applications such as **quantum-level information security**, particularly in the realm of **quantum cryptography**, where light-based systems can offer enhanced performance and robustness.

In conclusion, the advantages of optical computing ranging from unmatched data throughput and parallelism to low power requirements and interference immunity make it a compelling direction for the future of information processing. As technologies involving nonlinear materials, optical switches, and photonic integration continue to mature, the vision of fully optical computing systems becomes increasingly attainable. These features make optics not only a substitute but a superior alternative to electronics in data processing, logic operation, and high-speed communication environments.

1.12. References

1. T. Main, R. J. Feuerstein, H. F. Jordan, V. P. Heuring, J. Feehrer, C. E. Love, "Implementation of a general-purpose stored-program digital optical computer," *Applied Optics*, **33(8)**, 1619-1628 (1994).
2. A. Sinha, S. Mukhopadhyay, "Effect of higher order nonlinearity in frequency variation of self-phase modulation in optical fiber communication," *Chinese Optics Letters*, **2(9)**, 500-502 (2005).
3. J. Hardy, J. Shamir, "Optics inspired logic architecture," *Optics Express*, **15(1)**, 150-165 (2007).
4. V. A. Sautenkov, Y. V. Rostovtsev, C. Y. Ye, G. R. Welch, O. Kocharovskaya, M. O. Scully, "Electromagnetically induced transparency in rubidium vapor prepared by a comb of short optical pulses," *Physical Review A*, **71(6)**, 063804 (2005).
5. H. J. Caulfield, S. Dolev, "Why future supercomputing requires optics," *Nature Photonics*, **4**, 261-263 (2010).
6. S. Mukhopadhyay, "Optical computation and parallel processing" *Classique Books* (9, Radhanath Mallick Lane, Kolkata 700012, India), (2000).
7. P. Ghosh, S. Mukhopadhyay, "Some digital approaches in optical computation," *Premier Books* (32/3 Old Ballygunge First Lane, Kolkata -19, India), (2004).
8. N. Pahari, S. Mukhopadhyay, "New method of all-optical data comparison with nonlinear material using 1"s compliment method," *Optical Engineering*, **45(1)**, 015201 (2006).
9. N. Pahari, S. Mukhopadhyay, "New scheme for image edge detection using the switching mechanism of nonlinear optical material," *Optical Engineering*, **45(3)**, 037003 (2006).
10. D. Miller, "Device requirements for optical interconnects to silicon chips," *Proceedings of the IEEE*, **97(7)**, 1166-1185 (2009).
11. R. Arrathooon, "Optical computing", *Marcel Dekker Inc.*, (1989).
12. H. C. Neitzert, "A Wannier- Stark waveguide electroabsorption modulator as a low-power switch and its application as NAND, NOR or Ex-OR all-optical logic gates," *Journal of Optics A: Pure and Applied Optics*, **3(3)**, 218-221 (2001).

13. P. O. Hedekvist, A. Bhardwaj, K. Vahala, H. Anderson, "Advanced all-optical logic gates on a spectral bus," *Applied Optics*, **40(11)**, 1761-1766 (2001).

14. J. Barbe, J. Campos, J. Nicolas, C. C. Iemmi, "Multichannel optical correlator for texture classification," *Optical Engineering*, **42(7)**, 2062-2067 (2003).

15. D. Dragoman, M. Dragoman, "Biased micromechanical cantilever arrays as optical image memory," *Applied Optics*, **42(8)**, 1515-1519 (2003).

16. P. Boffi, D. Piccinin, M. C. Ubaldi, M. Martinelli, "All-optical pattern recognition for digital real-time information processing," *Applied Optics*, **42(23)**, 4670-4680 (2003).

17. G. J. Liu, J. Liu, B. M. Liang, Q. Li, G. L. Jin, "Nonlinear optical switching matrix," *Optics Letters*, **28(15)**, 1347-1349 (2003).

18. D. J. Blumenthal, J. E. Bowers, L. Rau, C. Hsu-Feng, S. Rangarajan, W. Wei, K. N. Poulsen, "Optical signal processing for optical packet switching networks," *IEEE Communications Magazine*, **41(2)**, 23-29 (2003).

19. N. K. Nishchal, J. Joseph, K. Singh, "Fully phase encryption using fractional Fourier transform," *Optical Engineering*, **42(6)**, 1583-1588 (2003).

20. N. K. Nishchal, G. Unnikrishnan, J. Joseph, K. Singh, "Optical encryption using a localized fractional Fourier transform," *Optical Engineering*, **42(12)**, 3566- 3571 (2003).

21. N. K. Nishchal, J. Joseph, K. Singh, "Optical phase encryption by phase contrast using electrically addressed spatial light modulator," *Optics Communications*, **217(1-6)**, 117-122 (2003).

22. A. Sinha, K. Singh, "A technique for image encryption using digital signature," *Optics Communications*, **218(4-6)**, 229-234 (2003).

23. D. Ganotra, J. Joseph, K. Singh, "Second and first order phase-locked loops in fringe profilometry and application of neural networks for phase-to-depth conversion," *Optics Communications*, **217(1-6)**, 85-96 (2003).

24. A. A. Awwal, K. M. Iftekharuddin, M. A. Karim, R. D. Juday, "Optical pattern recognition algorithms, architecture and applications: introduction to the future issue," *Applied Optics*, **42(23)**, 4647-4648 (2003).

25. J. B. Fasquel, M. M. Bruynooghe, "New hybrid opto-electronic method for fast and unsupervised object detection," *Optical Engineering*, **42(11)**, 3352- 3364(2003).

26. S. Roychowdhury, V. K. Jaiswal, R. P. Singh, "Implementing controlled NOT gate with optical vortex," *Optics Communications*, **236(4-6)**, 419-424 (2004).

27. F. G. Haibach, M. L. Myrick, "Precision in multivariate optical computing," *Applies Optics*, **43(10)**, 2130-2140 (2004).

28. P. K. Kwan, Y. Y. Lu, "Computing optical bistability in one-dimensional nonlinear structures," *Optics Communications*, **238(1-3)**, 169-175 (2004).

29. C. M. Greiner, D. Iazikov, T. W. Mossberg, "Wavelength division multiplexing based on apodized planar holographic Bragg reflectors," *Applied Optics*, **43(23)**, 4575-4583 (2004).

30. G. Dyankov, H. Y. Chen, S. Chao, S. Chi, "Optimization of second harmonic generation in nonlinear film structure," *Optics Communications*, **236(1-3)**, 203- 208 (2004).

31. J. J. Ju, J. Kim, J. Y. Do, M. S. Kim, S. K. Park, S. Park, M. H. Lee, "Second harmonic generation in periodically poled nonlinear polymer waveguides," *Optics Letters*, **29(1)**, 89-91 (2004).

32. O. Wada, "Femtosecond all-optical devices for ultrafast communication and signal processing," *New Journal of Physics*, **6(1)**, 183 (2004).

33. D. Ganotra, J. Joseph, K. Singh, "Object reconstruction in multilayer neural network based profilometry using grating structure comprising two regions with different spatial periods," *Optics and Lasers in Engineering*, **42(2)**, 179-192 (2004).

34. D. Ganotra, J. Joseph, K. Singh, "Modified geometry of ring-wedge detector for sampling Fourier transform of fingerprints for classification using neural networks," *Optics and Lasers in Engineering*, **42(2)**, 167-177 (2004).

35. M. Chen, S. Zhang, M. A. Karim, "Modification of standard image compression methods for correlation-based pattern recognition," *Optical Engineering*, **43(8)**, 1723-1730 (2004).

36. M. Guignard, V. Nazabal, J. Troles, F. Smektala, H. Zeghlache, Y. Quiquempois, A. Kudlinski, G. Martinelli, "Second-harmonic generation of thermally poled

chalcogenide glass," *Optics Express*, **13(3)**, 789-795 (2005).

37. R. S. Fyath, S. A. Ali, M. S. Alam, "Four operand parallel optical computing using shadow-casting technique," *Optics & Laser Technology*, **37(3)**, 251-257 (2005).

38. R. Clavero, F.Ramos, J.M. Martinez, J. Marti, "All-optical flip-flop based on a single SOA-MZI," *IEEE Photonics Technology Letters*, **17(4)**, 843-845(2005).

39. Y. Wu, "All-optical logic gates by using multibranch waveguide structure with localized optical nonlinearity," *IEEE Journal of Selected Topics in Quantum Electronics*, **11(2)**, 307-312(2005).

40. J. Wang, J. Sun, Q. Sun, "Experimental observation of a 1.5 μm band wavelength conversion and logic NOT gate at 40 Gbit/s based on sum- frequency generation," *Optics Letters*, **31(11)**, 1711-1713 (2006).

41. H. Jung, "2×2, 1×4 Ti:$LiNbO_3$ digital optical switches," *Optical Engineering*, **46**(3), 034602 (2007).

42. Bhowmik P, Roy JN, Chattopadhyay T. Designing of all optical generalized circuit for two-input binary and multi-valued logical operations. *Optics Commun.* 2014;15(331):14–27.

43. H. Y. Tu, C. J. Cheng, M. L. Chen, "Optical image encryption based on polarization encoding by liquid crystal spatial light modulators," *Journal of Optics A: Pure and Applied Optics*, **6(6)**, 524-528 (2004).

44. S. K. Garai, S. Mukhopadhyay, "A method of optical implementation of frequency encoded different logic operations using second harmonic and difference frequency generation techniques in nonlinear material," *Optik – International Journal for Light and Electron Optics*, **121(8)**, 715-721 (2010).

45. K. Roychowdhury, S. Mukhopadhyay, "An all-optical binary comparator using nonlinear material," Journal of Optics, 33(2), 81-85 (2004).

46. A. K. Das, S. Mukhopadhyay, "General approach of spatial input encoding for multiplexing and demultiplexing," *Optical Engineering*, **43(1)**, 126-131 (2004).

47. S. Dhar, S. Mukhopadhyay, "All-optical implementation of ASCII by use of nonlinear material for optical encoding of necessary symbols", *Optical Engineering*, **44(6)**, 065201 (2005).

48. J. Ma, M. L. Povinelli, "Mechanical Kerr nonlinearities due to bipolar optical forces between deformable silicon waveguides," *Optics Express*, **19(11)**, 10102- 10110 (2011).

49. A. Srivastava, S. Medhekar, "Switching of one beam by another in a Kerr type nonlinear Mach-Zehnder interferometer," *Optics & Laser Technology*, **43(1)**, 29-35 (2011).

50. K. Roychowdhury, S. Mukhopadhyay, "An all-optical scheme of signed digit binary addition based on optical nonlinear material," *Optoelectronics Letters*, **4(6)**, 447-451 (2008).

51. J. S. Sanghera, I. D. Aggarwal, L. B. Shaw, C. M. Florea, P. Pureza, V. Q. Nguyen, F. Kung, I. D. Aggarwal, "Nonlinear properties of chalcogenide glass fibers," *Journal of Optoelectronics and Advanced Materials*, **8(6)**, 2148-2155 (2006).

52. A. N. Matveev, "Optics," *Mir Publishers*, Moscow, 427- 428 (1988).

53. M. C. Gupta, J. Ballato, "The handbook of photonics," *CRC Press*, 2nd edition.

54. M. J. Flynn, "Some computer organizations and their effectiveness," *IEEE Transaction on Computers*, **C-21(9)**, 948-960 (1972).

55. D. Goswami, "Optical computing: Research trends," *Resonance*, **July issue**, 8- 21 (2003).

56. C. C. Yang, "All-optical ultrafast logic gates that use asymmetric nonlinear directional coupler," *Optics Letters*, **16(21)**, 1641-1643 (1991).

57. L. A. Wang, S. H. Chang, Y. F. Lin, "Novel implementation method to realize all-optical logic gates," *Optical Engineering*, **37(3)**, 1011-1018 (1998).

58. C. P. Singh, S. Roy, "All-optical switching in bacteriorhodopsin based on M state dynamics and its application to photonic logic gates," *Optics Communications*, **218(1-3)**, 55-66 (2003).

59. H. Soto, J. D. Topomondzo, D. Erasme, M. Castro, "All-optical NOR gates with two and three input logic signals based on cross-polarization modulation in a semiconductor optical amplifier," *Optics Communications*, **218(4-6)**, 243-247 (2003).

60. C. P. Singh, S. Roy, "Dynamics of all-optical switching in C_{60} and its application to optical logic gates," *Optical Engineering*, **43(2)**, 426-431 (2004).

61. M. Naruse, H. Mitsu, M. Furuki, I. Iwasa, Y. Sato, S. Tatsuura, M. Tian, F. Kubota, "Terabit all-optical logic based on ultrafast two-dimensional transmission gating," *Optics Letters*, **29(6)**, 608-610 (2004).

62. H. Soto, E. Alvarez, C. A. Diaz, J. Topomondzo, D. Erasme, L. Schares, L. Occhi, G. Guekos, M. Castro, "Design of an all-optical NOT, XOR gate based on cross-polarization modulation in a semiconductor optical amplifier," *Optics Communications*, **237(1-3)**, 121-131 (2004).

63. N. Iizuka, K. Kaneko, N. Suzuki, "Sub-picosecond all-optical gate utilizing GaN intersubband transition," *Optics Express*, **13(10)**, 3835-3840 (2005).

64. M. S. Alam, M. A. Karim, "Biometric recognition systems: introduction," *Applied Optics*, **44(5)**, 635-636 (2005).

65. C. Yu, L. Christen, T. Luo, Y. Wang, Z. Pan, L. S. Yan, A. E. Willner, "All optical XOR gate using polarization rotation in single highly nonlinear fiber", *IEEE Photonics Technology Letters*, **17(6)**, 1232-1234 (2005).

66. P. Li, D. Huang, X. Zhang, G. Zhu, "Ultrahigh-speed all-optical half adder based on four-wave mixing in semiconductor optical amplifier," *Optics Express*, **14(24)**, 11839-11847(2006).

67. S. Medhekar, P. P. Paltani, "Proposal for optical switch using nonlinear refraction," *IEEE Photonics Technology Letters*, **18(15)**, 1579-1581(2006).

68. Q. Wang, H. Dong, G. Zhu, H. Sun, J. Jaques, A. B. Piccirilli, N. K. Dutta, "All optical logic OR gate using SOA and delayed interferometer," *Optics Communication*, **260(1)**, 81-86 (2006).

69. H. J. Caulfield, C. S. Vikram, A. Zavalin, "Optical logic redux," *Optik-International Journal for Light and Electron Optics*, **117**, 199-209 (2006).

70. P. Mondal, S. Mukhopadhyay, "Method of conducting an all-optical NAND logic operation controlled from a long distance", *Optical Engineering*, **46(3)**, 035009 (2007).

71. J. Zhang, J. Wu, C. Feng, K. Xu, J. Lin, "All-optical logic OR gate exploiting nonlinear polarization rotation in an SOA and red-shifted sideband filtering," *IEEE Photonics Technology Letters*, **19(1)**, 33-35 (2007).

72. J. Wang, J. Sun, Q. Sun, "Single PPLN based simultaneous half-adder, half – subtracter and OR logic gate: proposal and simulation," *Optics Express*, **15(4)**, 1690-1699 (2007).

73. H. L. Yan, W. He, J. Huan, G. Y. Li, Z. H. Yi, "All-optical AND logic gate without additional input beam by utilizing cross polarization modulation effect," *Chinese Physics Letters*, **25(11)**, 3901 (2008).

74. B. M. Isfahani, T. A. Tameh, N. Granpayeh, A. R. M. Javan, "All-optical NOR gate based on nonlinear photonic crystal microring resonators," *JOSA B*, **26(5)**, 1097-1102 (2009).

75. A. Rostami, H. Nejad, R. M. Qartavol, H. R. Saghai, "Tb/s optical logic gates based on quantum-dot semiconductor optical amplifiers," *IEEE Journal of Quantum Electronics*, **46(3)**, 354-360 (2010).

76. R. A. Heinz, J. O. Artman, S. H. Lee, "Matrix multiplication by optical methods," *Applied Optics*, **9(9)**, 2161-2168 (1970).

77. S. Mukhopadhyay, A. Basuray, A. K. Datta, "A real-time optical parallel processor for binary addition with a carry," *Optics Communications*, **66(4)**, 186- 190 (1988).

78. S. Mukhopadhyay, A. Basuray, A. K. Datta, "New coding scheme for addition and subtraction using the modified signed-digit number representation in optical computation," *Applied Optics*, **27(8)**, 1375-1376 (1988).

79. A. K. Ghosh, A. Basuray, "Trinary optical logic processors using shadow casting with polarized light," *Optics Communications*, **79(1-2)**, 11-14 (1990).

80. A. Basuray, S. Mukhopadhyay, H. K. Ghosh, A. K. Datta, "A tristate optical logic system," *Optics Communications*, **85(2-3)**, 167-170 (1991).

81. R. S. Fyath, A. A. W. Alsaffar, M. S. Alam, "Optical two-step modified signed-digit addition based on binary logic gates," *Optics Communications*, **208(4-6)**, 263-273 (2002).

82. H. J. Caulfield, C. S. Vikram, A. Zavalin, "Optical logic redux," *Optik-International Journal for Light and Electron Optics*, **117**, 199-209 (2006).

83. H. J. Caulfield, J. Westphal, "The logic of optics and the optics of logic, "*Information Sciences*, **162(1)**, 21-33 (2004).

84. L. Qian, H. J. Caulfield, "Abstract passive interferometers with applications to conservative logic," *Optik – International Journal for Light and Electron Optics*, **116(8)**, 404-408 (2005).

85. M. S. Alam, M. A. Karim, "Efficient combinational logic circuit design using polarization encoded optical shadow-casting," *Optics Communications*, **93(3-4)**, 245-252 (1992).

86. Y. A. Zaghloul, A. R. M. Zaghloul, "Complete all-optical processing polarization based binary logic gates and optical processors", *Optics Express*, **14(21)**, 9879-9895(2006).

87. Y. A. Zaghloul, A. R. M. Zaghloul, "Unforced polarization-based optical implementation of Binary logic," *Optics Express*, **14(16)**, 7252-7269(2006).

88. N. Pahari, D. N. Das, S. Mukhopadhyay, "All-optical method for the addition of binary data by nonlinear materials," *Applied Optics*, **43(33)**, 6147-6150 (2004).

89. K. RoyChowdhury, A. Sinha, S. Mukhopadhyay, "An all-optical comparison scheme between two multi-bit data with optical nonlinear material," *Chinese Optics Letters*, **6(9)**, 1-4 (2008).

90. N. Pahari, S. Mukhopadhyay, "New method of all-optical data comparison with nonlinear material using 1"s compliment method," *Optical Engineering*, **45(1)**, 015201 (2006).

91. H. J. Caulfield, R. A. Soref, L. Qian, A. Zavalin, J. Hardy, "Generalized optical logic elements –GOLEs," *Optics Communications*, **271(2)**, 365-376 (2007).

92. T. A. Ibrahim, W. Cao, Y. Kim, J. Li, J. Goldhar, P. T. Ho, C. H. Lee, "All- optical switching in a laterally coupled microring resonator by carrier injection," *IEEE Photonics Technology Letters*, **15(1)**, 36-38 (2003).

93. N. Calabretta, Y. Liu, F. M. Huijskens, M. T. Hill, H. de Waardt, G. D. Khoe, H. J. S. Dorren, "Optical signal processing based on self-induced polarization

rotation in a semiconductor optical amplifier," *Journal of Lightwave Technology*, **22(2)**, 372-381 (2004).

94. K. Roychowdhury, S. Mukhopadhyay, "Binary optical arithmetic operation scheme with tree architecture by proper accommodation of optical nonlinear material," *Optical Engineering*, **43(1)**, 132-136 (2004).

95. D. K. Gayen, J. N. Roy, "All-optical arithmetic unit with the help of terahertz-optical asymmetric-demultiplexer-based tree architecture," *Applied Optics*, **47(7)**, 933-943 (2008).

96. J. N. Roy, "Mach-Zehnder interferometer-based tree architecture for all-optical logic and arithmetic operations," *Optik – International Journal for Light and Electron Optics*, **120(7)**, 318-324 (2009).

97. J. N. Roy, A. K. Maity, D. Samanta, S. Mukhopadhyay, "Tree-net architecture for integrated all-optical arithmetic operations and data comparison scheme with optical nonlinear material," *Optical Switching and Networking*, **4**, 231- 237(2007).

Chapter - 2

All-Optical Serial Data Transfer Between Registers

Chapter

2

All-Optical Serial Data Transfer Between Registers

The inherent parallelism of optical signal is an advantageous feature for high-speed computations and other digital logic operations. Different techniques have been proposed for performing arithmetic, algebraic and logic operations using light as the information-carrier. Here we propose a new method for Serial Data Transfer between Registers using optical non-linear material. This system is all-optical in nature. Optical NAND gate and NOT gate are the basic building blocks of this system.

2.1. Overview

In the last few decades, it has been established that there is no other alternative of optics in case of high-speed computation. Even an operation of terahertz speed can be achieved when photon is used as an information-carrier. To use photon as information carrier one should use optical switch, where non-linear materials play important role [1]. Scientists and technologists are trying to construct a hybrid structure where the conventional electronic Arithmetic Logical Unit will be replaced by an optical parallel processor. Here binary data '1' is expressed as the presence of light and '0' is considered as the absence of light. In achieving this goal there are several established techniques for conducting all-optical arithmetic, algebraic and logic operations [2–8]. In the present communication we introduce a new concept of Serial Data Transfer between Registers. We show that such transfer is possible using optical non-linear material based optical NAND and NOT gates which are the basic building blocks of this system.

2.2. Optical nonlinear materials (NLM) as optical switch

It is known that there occurs no change in the Refractive Index (R.I.) of a linear material if light (polarized laser radiation) of any intensity is incident upon it. However, for some non-linear materials Refractive Index (R.I.) changes according to the intensity of incident light [9,10]. The equation of change in R.I. of the non-linear material related with the intensity of incident light is

$$n_{NLM} = n_0 + n_2 I \quad (1)$$

where n_{NLM} is the refractive index (R.I.) of non-linear material (N.L.M.), n_0 is constant R.I. term of N.L.M. n_2 is 2nd order non-linear correction term. '**I**' is intensity of incident light that penetrates through the non-linear material.

[considering up to the second order nonlinear term and ignoring the higher order terms, the dielectric polarization (P) of the nonlinear material can be revealed as-

$$P = \varepsilon_0\chi^{(1)}E + \varepsilon_0\chi^{(2)}EE + \varepsilon_0\chi^{(3)}EEE \quad \text{(i)}$$

Here, ε_0 and $\chi^{(n)}$ denote the free-space permittivity and the n-th order component of the electric-susceptibility of that material.

Now for isotropic optical materials, $P(-E) = -P(E)$ (ii)

So, the above equation becomes $P = \varepsilon_0\chi^{(1)}E + \alpha_3 E_0^2 E$ (iii)

Where $\alpha_3 = \varepsilon_0\chi^{(3)}$. Now the displacement vector $\vec{D}$ is as

$$\vec{D} = \varepsilon\vec{E} = \varepsilon_0\vec{E} + \vec{P} = [\varepsilon_0(1 + \chi^{(1)}) + \alpha_3 E_0^2]\vec{E} \quad \text{(iv)}$$

Hence the expression of the refractive index (RI) of the isotropic nonlinear material becomes $n_{NLM} = \sqrt{\frac{\varepsilon}{\varepsilon_0}} = \sqrt{1 + \chi^{(1)} + \alpha_3 \frac{E_0^2}{\varepsilon_0}}$

$n_{NLM} \approx \sqrt{(1 + \chi^{(1)})}[1 + \frac{\alpha_3}{2\varepsilon_0(1+\chi^{(1)})}E_0^2]$ as $[\frac{\alpha_3}{\varepsilon_0(1+\chi^{(1)})}E_0^2] \ll 1$

Thus, $n_{NLM} = n_0 + n_2 I$ (v)

Where $n_0 = \sqrt{(1 + \chi^{(1)})}$ is the constant linear RI term,

$n_2 = \frac{\alpha_3}{2\varepsilon_0\sqrt{(1+\chi^{(1)})}}$ is the 2nd order NLM correction term and $I = E_0^2$ is the intensity of the optical signal passing through the NLM.]

Carbon disulphide (CS2), pure silica glass, GaAs, etc. are the example of such type of non-linear materials. In case of CS_2, the value of n_0 is 1.62 and n_2 is $0.22 \times 10^{-19}\, m^2/W$. When it is used as non-linear material it can focus a laser beam of cross-section 1 cm radius and 10 MW power at a distance of 10 cm. This character of a material is known as self-focusing character. Not only carbon disulphide, all the materials which have the self-focusing character can be used easily for all-optical switching operations. The focusing length (L) of non-linear material depends on the power (P) and the area of cross-section

(a) of the laser beam with the relation $P=\frac{\pi\varepsilon_0 n_0 ca^4}{8n_2L^2}$ where ε_0 and C are the free space permittivity and free space velocity of light. From the above equation it is clear that the focusing length (L) will be shorter with the increase of the power of the beam and with the optimum decrease of the radius of the beam. In the integrated optical system, all the components (switches) are in sub-micron-level dimension. So, to implement an integrated optical system with this type of non-linear material we require a very high-power laser with a diffraction limited standard beam size.

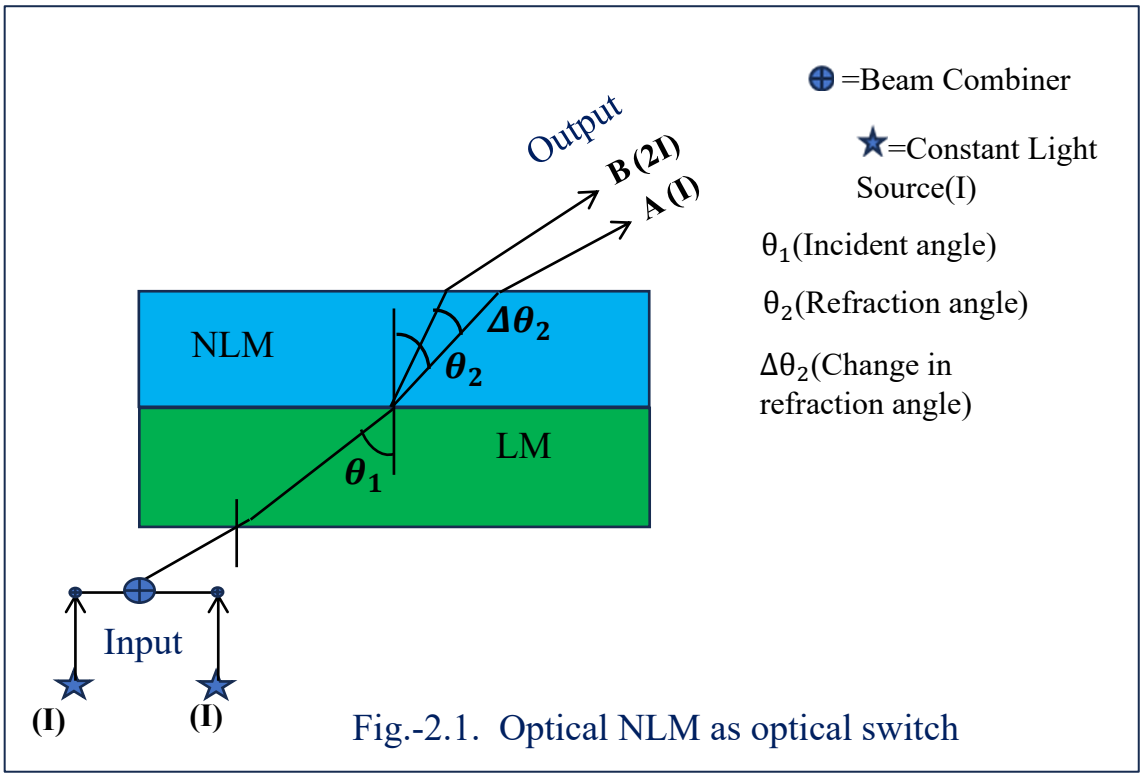

Fig.-2.1. Optical NLM as optical switch

An optical switch can be prepared using this intensity-based R.I. property of non-linear material. For this we make a combination of linear and non-linear media, where n_{LM} and n_{NLM} are the R.I. of linear and non-linear materials respectively. Suppose, a beam of polarized laser light of intensity '**I**' is incident upon the linear medium **(Fig.-2.1)** in a certain angle and passes through the non-linear medium to give an emergent ray in direction 'A'. Now, if the intensity of incident light increases then the light ray goes to direction 'B'. From Eq. (1), it is seen that n_{NLM} is increased when '**I**' is increased. Also, as n_{NLM} is increased, obeying Snell's law [$n_{LM} \sin\theta_1 = n_{NLM} \sin\theta_2$] θ_2 is decreased and incident light of higher intensity passes through the N.L.M. following direction (B). In this switching scheme, CS_2 or pure silica glass may be used as an optical non-linear material.

Nd: YAG laser with 1.064 μm wave length is an ideal source to activate the non-linear material in the switching operation.

Now we discuss about the change of output refraction angle from the non-linear material due to the change of input intensity level. If pure fused silica is used as non-linear material, the n_0 and n_2 for it are 1.46 and $3.2 \times 10^{-20}\ m^2/W$. respectively. When an ordinary laser of power 100 mW and cross-section 50 μm^2 is taken, we can get its intensity of about $2 \times 10^9\ W/m^2$. This produces a change in the refractive index ($\Delta n = n - n_0$) of the non-linear material which is 64×10^{-12}. Apparently, this change is irrelevant. But the situation will be changed if we use pulse laser instead of a continuous laser beam. An ordinary Q-switched pulse laser having 10^{-7} s on time duration for each pulse can be used as input signal. For pure fused silica if the above laser (100 mW continuous power) is used for getting 10^{-7} s on-time duration pulse laser, we can achieve $\Delta\theta$ (the angular change of the direction of the output light from nonlinear material after refraction) as 0.013◦ or 0.24×10^{-3} rad, when the intensity is increased twice keeping the input incident angle fixed at 45°. The value of $\Delta\theta$ will be 1.20°, when 10^{-9} s on-time duration pulses are used from 100 mW continuous laser keeping other requirements constant. For CS_2, $n_2 = 0 \cdot 22 \times 10^{-19}\ m^2/W$, so the value of $\Delta\theta$ is higher than that of silica.

2.3. Optical NAND and NOT logic gate by optical NLM

2.3.1. Optical NAND gate

For an optical NAND gate, we make a composite slab of linear and non-linear material as shown in **Fig.-2.2**. There A, B are input beams of same intensity 'I'. C.L. is a constant light source of intensity 'I'. When intensity of incident light is I then rays of light go along the path 'A1'. When intensity of incident light is 2I (I + I) then it goes along the path B1. When intensity of incident light is 3I (I + I + I) then it goes along the path 'C1'. With the help of the beam splitter (BS), on the path of 'B1' Y is taken as the output of optical NAND gate.

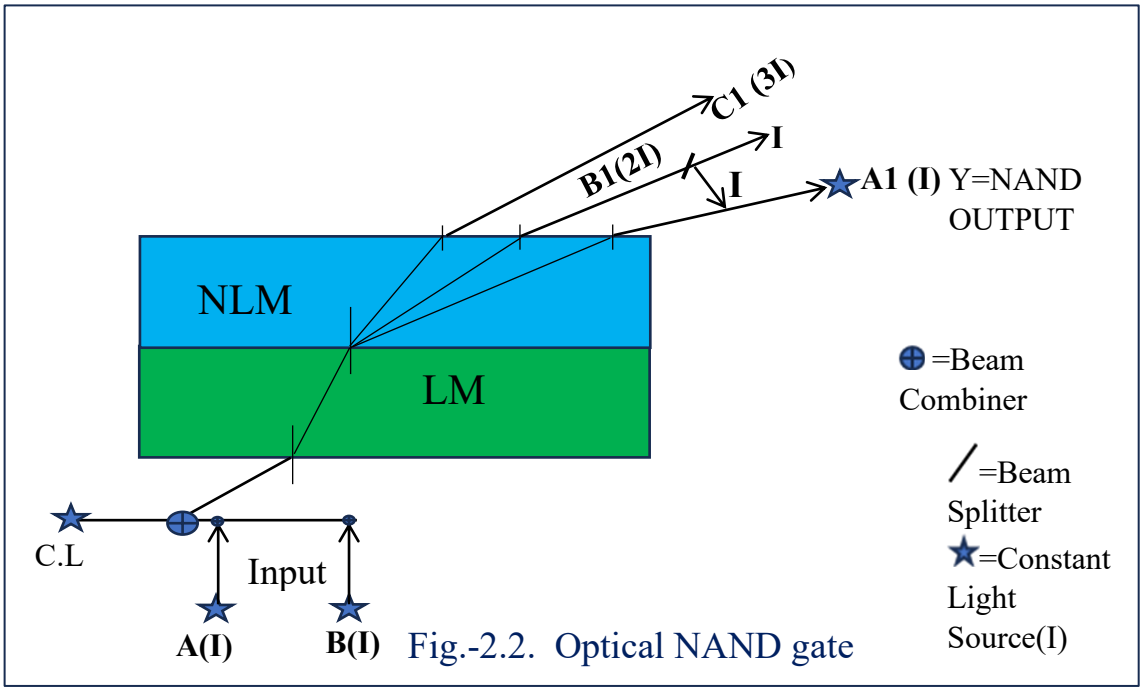

Fig.-2.2. Optical NAND gate

Table- 2.1: Truth table of optical NAND gate

Input		Output
A	**B**	**Y (=A_1)**
0	0	1(I)
0	0	1(I)
1(I)	0	1(I)
1(I)	1(I)	0

Switching operation for NAND gate:

(i) When A = B = 0, then only for C.L. the intensity of incident light ray is I and goes through N.L.M. along with path (A1), at this stage output Y = 1.

(ii) When A = B = 1, then intensity of incident light ray is I for A, I for B and I for C.L. in total 3I. So, ray of light goes through N.L.M. along with path (C1), at this stage output Y = 0.

(iii) When A = 0, B = 1, then the intensity of incident ray is 0 for A, I for B and I for C.L., in total 2I. Then the ray of light passes through N.L.M. along with path (B1). Then facing BS finally intensity at 'Y' is 'I' i.e., output of the optical NAND gate Y = 1.

(iv) When A = 1, B = 0 then intensity of incident ray is in total 2I.

Then the output Y = 1. The truth table of optical NAND gate is given in **Table-2.1**. If necessary, the output intensity level can be maintained at the desired intensity level (I) by proper mechanism **[11]**.

2.3.2. Optical Not gate

To develop an optical NOT gate, we make the composite slab of linear and non-linear material **(Fig.-2.3)**, where 'X' is the only input path and C.L. is the constant light source having intensity 'I'. To select the output of optical NOT gate the path of intensity 'I' (A) is taken.

Switching operation for NOT gate:

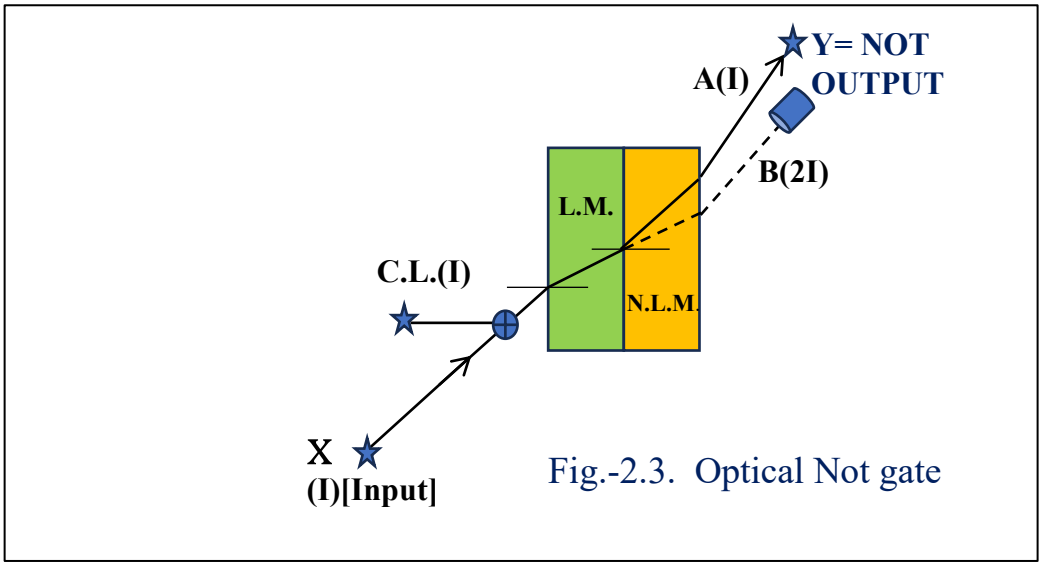

Fig.-2.3. Optical Not gate

Table- 2.2: Truth table of optical NOT gate

Input(X)	Name of the path	Output (Y=A)
1 (I)	B(2I)	0
0	A(I)	1

(i) When X = 0, then only for C.L. source intensity of incident ray of light is I, this light beam passes through N.L.M. along with path (A). As a result, the output Y is 1.

(ii) When X = 1, then intensity of incident light beam is I for A and I for C.L., in total (I + I) = 2I. The light beam passes through N.L.M. along with path (B). Then the output Y is 0. The truth table of optical NOT gate is given in **Table-2.2**.

2.4. Optical D-flip-flop using optical NLM

An optical D-flip–flop can be formed by using one optical NOT gate [E] and four optical NAND gates ([A], [B], [C] and [D]). Here, D input (D for Data) acts as an input of NAND gate [A] and its compliment is the input of NAND gate [B] (**Fig.-2.4**).

Here, [A] NAND gate has two inputs – D input (D for data) and P.L. (pulse setting leaser) input. [B] NAND gate has two inputs, compliment of D and P.L. input. Here, two inputs D input and C.L. are in same intensity (I) of light source. Pulse setting leaser source is also of the same intensity I. We shall see here when pulse setting leaser source is in 'on state' then whatever may be the value of Qt, the value of Q_{t+1} will depend upon the value of D input (**Table-2.3**).

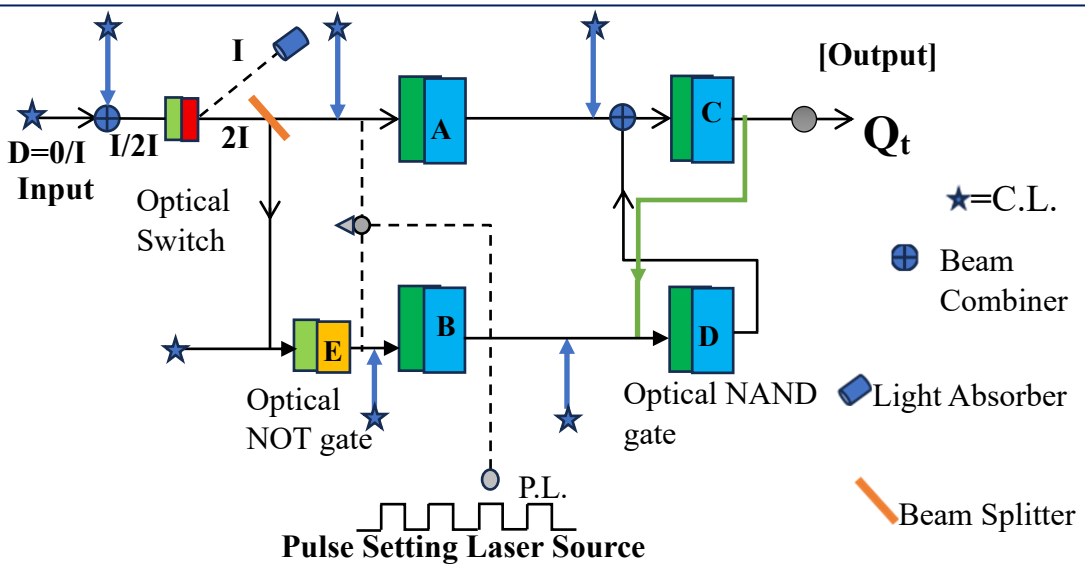

Fig.-2.4. D flip-flop by using optical N.L.M.

Table -2.3: Truth Table of Optical D Flip Flop

Clock **[CK]** (Pulse Setting Laser)	Data**[D]**	First/Primary Output **[Q_t]**	Last/Secondary Output **[Q_{t+1}]**
(Disabled) **0**	×	**0**	**0**
0	×	**1**	**1**
(Enabled)**1**	**0**	**0**	**0**
1	**0**	**1**	**0**
1	**1**	**0**	**1**
1	**1**	**1**	**1**

(1) When P.L. = 1, D = 0 & C.L. = 1 then input of [A] NAND gate is of double intensity (one of C.L. and other of P.L.) and output of [A] NAND gate is 1. Input of [E] NOT gate is '0' and as a result of it output of [E] NOT gate is 1. So, input of [B] NAND gate is of triple intensity (one of C.L., one output of [E] and other P.L.) and hence output of [B] NAND gate is zero.

Let Qt = 0, the input of [D] NAND gate is of single intensity (due to C.L.) hence output of it is 1. Then input of [C] NAND gate is of triple intensity (one of output of [A], one of C.L., and other of output of [D]) and hence output of [C] NAND gate Qt+1 = 0. If Qt = 1, the input of [D] NAND gate is of double intensity (one of C.L. and other of Qt), hence output of the [D] NAND gate is 1. Then input of [C] NAND gate is of triple intensity (one output of [A], one of C.L., one of output of [D]) and hence output of [C] NAND gate Qt+1 = 0. From the above discussion we can conclude that when P.L. = 1 (on state), for any value of Qt (0 or 1), the output Qt+1 depends upon the value of D input.

(2) When P.L. = 1, D = 1 & C.L. = 1 then input of [A] NAND gate is of triple intensity (one of C.L., one of P.L. and other of D input) hence output of [A] NAND gate is 0.

Now input of [E] NOT gate is 1, as a result of it output of [E] NOT gate is 0. So, input of [B] NAND gate is of double intensity (one of C.L. and one of P.L.) and hence output of [B] NAND gate is 1.

Let Qt = 0, the input of [D] NAND gate is of double intensity (one of C.L. and other is of output of [B] NAND gate), hence output of [D] gate is 1. Then input of [C] NAND gate is of double intensity (one of C.L. and other is of output of [D] gate), hence output of [C] NAND gate is Qt+1 = 1.

If Qt = 1, the input of [D] NAND gate is of triple intensity (one of C.L., one of output of [B] and other of Qt) then output of [D] NAND gate is 0. Then input of [C] NAND gate is of single intensity (due to C.L.) and hence output of [C] gate Qt+1 = 1.

Here also we see that whatever be the value of Qt (0 or 1) the output Qt+1 depends upon the value of D input. Between two pulses when P.L. = 0 the outputs of NAND gate [A] and [B] are 1 whatever be the value of D. Hence from figure if Q = 1, it remains 1, whereas if Q = 0, it remains 0. Thus, we can say that this D-flip–flop does not change state between pulses, it is invariant within a pulse period.

2.5. Shift register by optical NLM

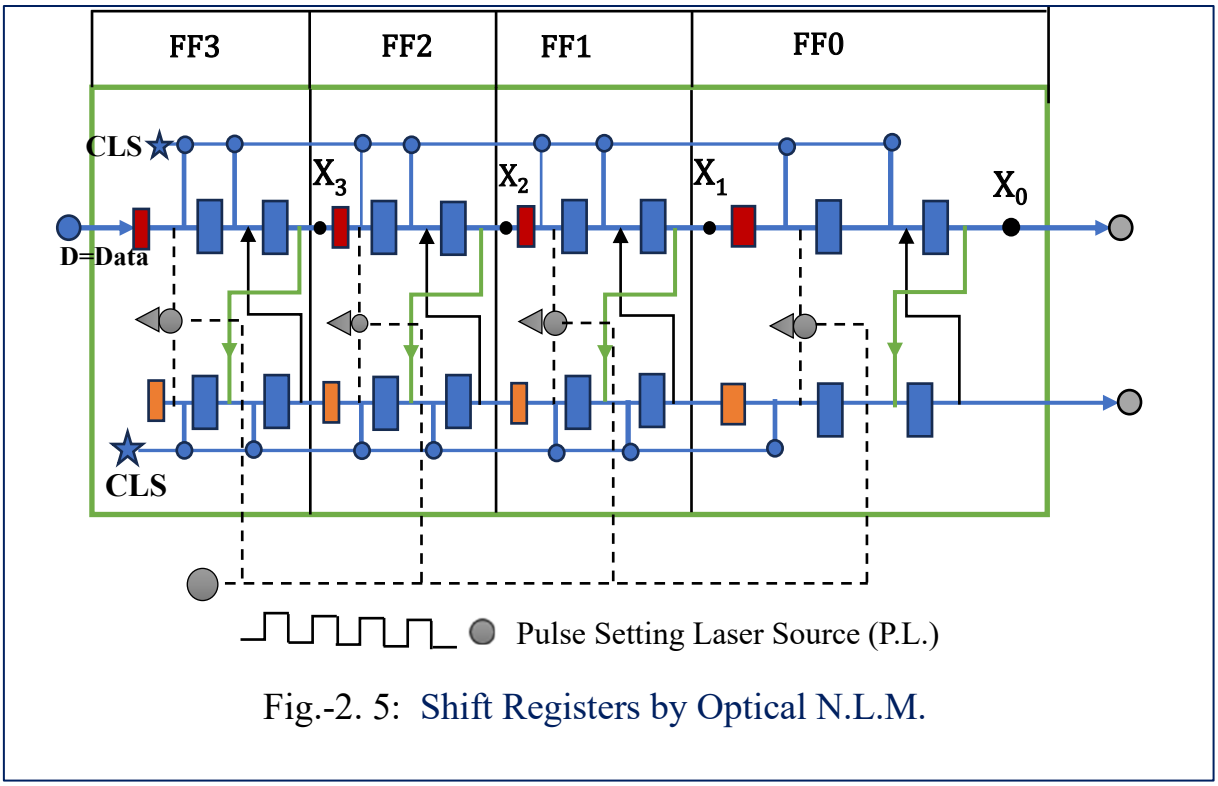

Fig.-2. 5: Shift Registers by Optical N.L.M.

Table- 2.4: Serial data transfer in optical shift register

Input data (D)	**FF-3**	**FF-2**	**FF-1**	**FF-0**	State of shift pulse
1	0	0	0	0	Before shift pulses applied
0	1	0	0	0	After first pulse
0	0	1	0	0	After second pulse
1	0	0	1	0	After third pulse
0	1	0	0	1	After fourth pulse

An optical shift register is a group of flip–flops aligned in such a way that the stored up binary numbers in the flip–flops can shift from one flip–flop to the next for every pulse of pulse setting laser source. **Fig. 2.5** shows a four-bit optical shift register using optical D-flip–flop.

The input data D is fed into FF3, which may be 0 or 1. The output of FF3 is fed into FF2 and so on. C.L. is the constant light source of intensity I. P.L. is the pulse setting laser source of same intensity I. All the C.L., P.L. and input D applied in the scheme are taken from a common source.

The operation of optical shift register can be understood from the following explanation (**Table-2.4**).

Let all the flip–flops in the optical shift register be in 0 state i.e., it contains (0000) initially (before shift pulses is applied). We are intended to register (1001) shifting (0000) in this scheme. Now pulse setting laser source is applied. D is 1 in FF3. After first pulse, FF3 is

set to 1, and the outputs of other flip–flops are in 0. Before the application of second pulse D changes to 0, input of FF3 becomes 0.

After second pulse FF3 is set to 0, the 1 that was previously in FF3 is in FF2, and the outputs of other two flip–flops are in 0. Keeping D in 0 state, third pulse is applied. After third pulse FF3 is set to 0, the 0 that was previously in FF3 is now in FF2, and 1 that was previously in FF2 is now in FF1, and the output of FF0 is 0. Before the application of fourth pulse D changes to 1, input of FF3 becomes 1. After fourth pulse FF3 is set to 1, the 0 that was previously in FF3 is now in FF2, the 0 that was previously in FF2 is now in FF1, and the 1 that was previously in FF1 is now in FF0. Finally, 1001 is registered in the optical shift register.

2.6. Serial data transfer between registers by optical NLM

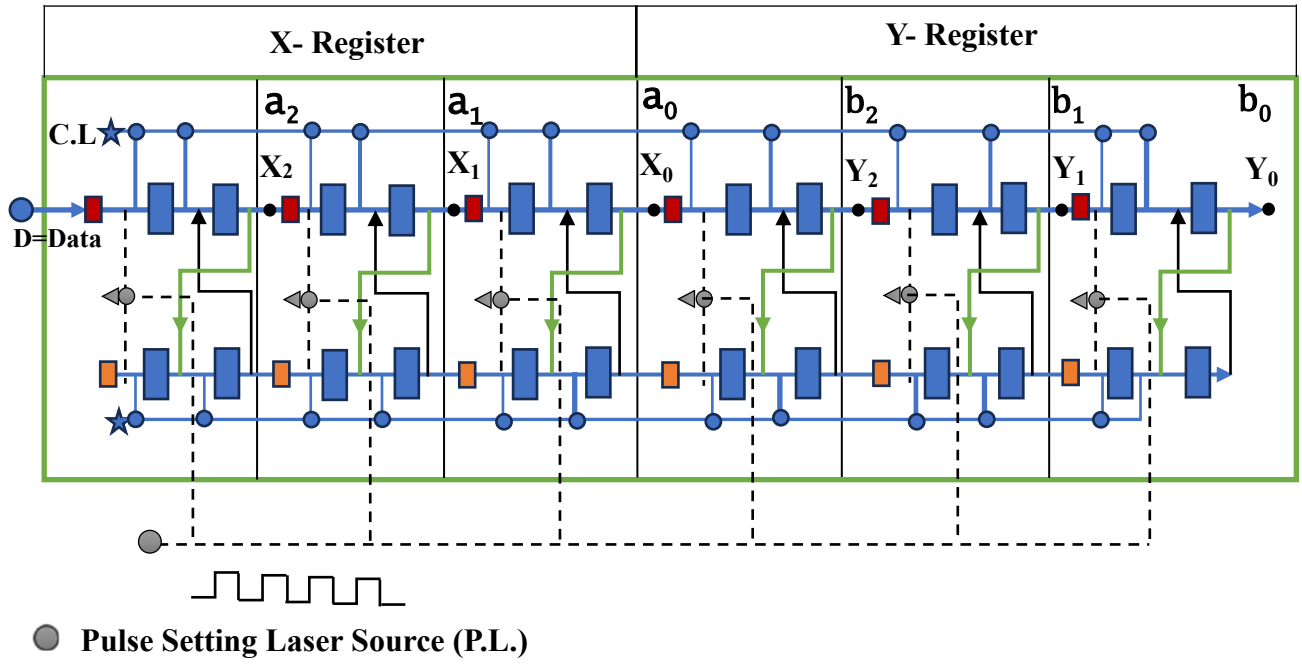

Fig.-2.6: Serial Data Transfer between Registers by Optical N.L.M.

The optical counterpart of Serial Data Transfer between Registers by optical N.L.M. is shown in **Fig.-2.6**. In this scheme we will study how stored binary numbers can be serially shifted from one register to another. Figure shows a three-bit data transfer scheme, where the contents of the X register (011) will be serially transferred into Y register.

In X register, there are three flip–flops a2, a1 and a0. In Y register there are also three flip–flops b2, b1, and b0. The output of a2 flip–flop is X2, which is the input of a1 flip–flop.

The output of a1 flip–flop is X1, which is the input a0 flip–flop. The output of a0 flip–flop is X0, which is the input of b2 flip–flop of Y register; the output of b2 flip–flop is Y2 which is input of b1 flip–flop. The output of b1 flip–flop is Y1 which is input of b0 flip–flop. The output of b0 flip–flop is Y0.

The P.L. of a2, a1, a0, b2, b1 and b0 flip – flops of X and Y registers are connected together at one point where the pulse setting laser source is applied. The C.L. source of each optical NAND gate of all D flip – flops of X and Y registers are connected together at one point, where the laser source is applied. C.L., P.L., and D input all are of same prefix intensity, say 'I'. During operation the value of input D is 1 (**Table-2.5**).

In the 'on state' of pulse setting laser source the applied data transfer occurs as follows:

X2–X1–X0–Y2–Y1–Y0.

Before the application of pulse setting laser source the contents of X-register are **011** i.e.,

X2 = 0, X1 = 1, X0 = 1 and that of Y register is **000** i.e., Y2 = 0, Y1 = 0, Y0 = 0.

Table -2.5: Serial Data Transfer scheme between Registers by Optical N.L.M.

Input	X- Register			Y- Register			Pulse Setting Laser
D	**X_2**	**X_1**	**X_1**	**Y_2**	**Y_1**	**Y_0**	State of Shift Pulse
1	0	1	1	0	0	0	Before Shift Pulses applied
1	1	0	1	1	0	0	After 1_{st} Pulse
1	1	1	0	1	1	0	After 2_{nd} Pulse
1	1	1	1	0	1	1	After 3_{rd} Pulse

Now from the knowledge of D-flip–flop the output Q is same as input when pulse setting laser is in 'on state' and that value remains up to the next pulse.

To understand the mechanism of optical shift register:

(1) When 1st pulse is occurring, the output of

(i) a_2 flip–flop is 1 i.e., X2 = 1 (since D is 1)

(ii) a_1 flip–flop is 0 i.e., X1 = 0 (since X2 was at 0)

(iii) a_0 flip–flop is 1 i.e., X0 = 1 (since X1 was at 1)

(iv) b_2 flip–flop is 1 i.e., Y2 = 1 (since X0 was at 1)

(v) b_1 flip–flop is 0 i.e., Y1 = 0 (since Y2 was at 0)

(vi) b_0 flip–flop is 0 i.e., Y0 = 0 (since Y1 was at 0)

(2) When 2nd pulse is occurring, the output of

(vii) a_2 flip–flop is 1 i.e., X2 = 1 (since D is 1)

(viii) a_1 flip–flop is 1 i.e., X1 = 1 (since X2 was at 1)

(ix) a_0 flip–flop is 0 i.e., X0 = 0 (since X1 was at 0)

(x) b_2 flip–flop is 1 i.e., Y2 = 1 (since X0 was at 1)

(xi) b_1 flip–flop is 1 i.e., Y1 = 1 (since Y2 was at 1)

(xii) b_0 flip–flop is 0 i.e., Y0 = 0 (since Y1 was at 0)

(3) When 3rd pulse is occurring, the output of

(xiii) a_2 flip–flop is 1 i.e., X2 = 1 (since D is 1)

(xiv) a_1 flip–flop is 1 i.e., X1 = 1 (since X2 was at 1)

(xv) a_0 flip–flop is 1 i.e., X0 = 1 (since X1 was at 1)

(xvi) b_2 flip–flop is 0 i.e., Y2 = 0 (since X0 was at 0)

(xvii) b_1 flip–flop is 1 i.e., Y1 = 1 (since Y2 was at 1)

(xviii) b_0 flip–flop is 1 i.e., Y0 = 1 (since Y1 was at 1)

From the above discussion, it is seen that after three pulses the contents of X register (011) shift to Y register. The X register is now at 111, losing its original data. Now X register is ready to accept new data.

2.6.1. Python simulation result

Python simulation result for serial data transfer between two optical registers (‘X’ to ‘Y’) when stored binary number of ‘X’ register is 011which is shown in **Fig.-2.7.**

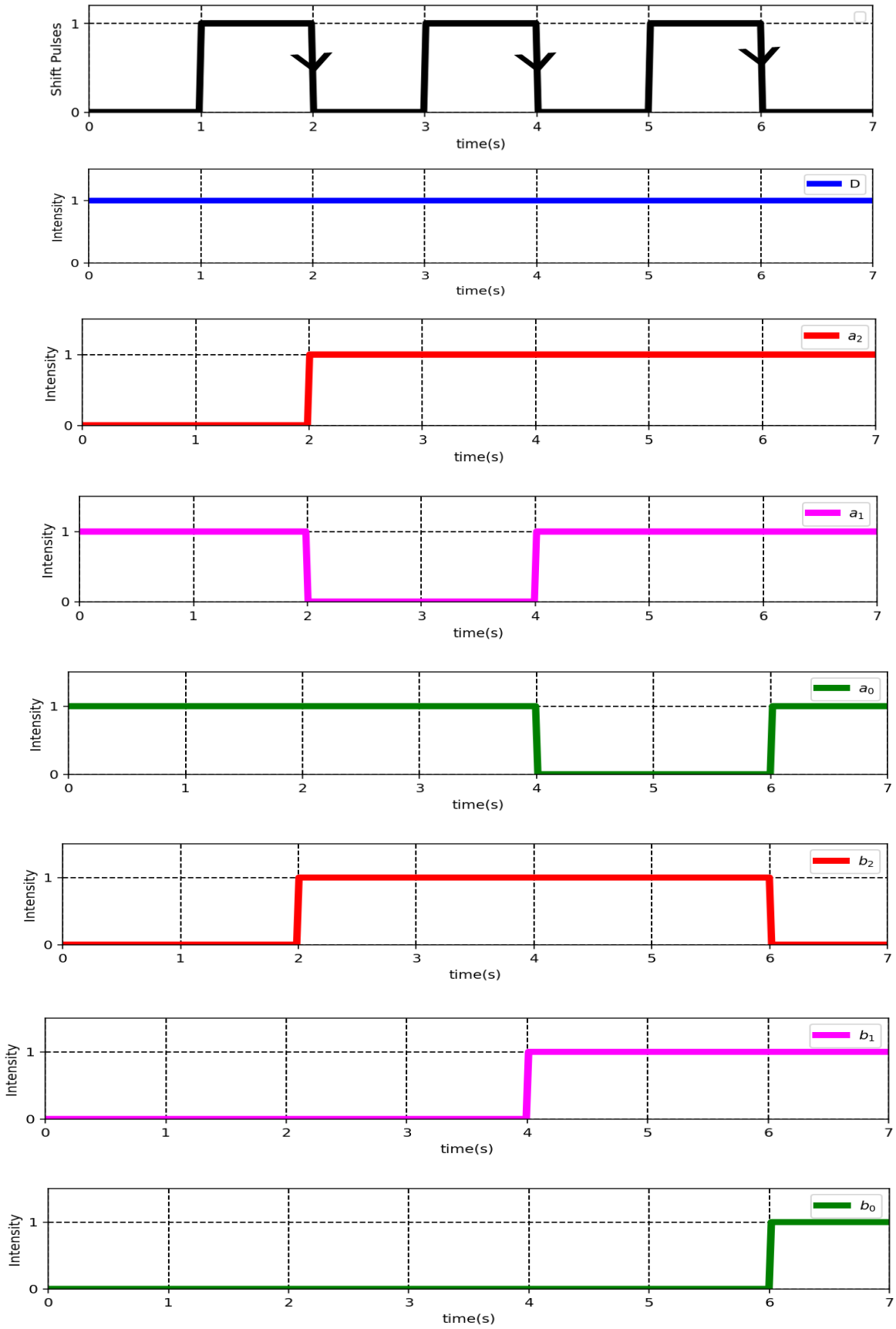

Fig.-2.7: Python simulation result for serial data transfer

2.7. Conclusion

In this scheme the operation of data shifting (serial in–serial out) from one register to another has been explained with optical equivalent D-flip–flop. This shift register is all-optical in nature. Consequently, speed of operation of this optical shift register is very high compared to its electronic counterpart. The D-flip–flop is constructed with the help of non-linear material. Here, input light beam is polarized and should be coherent in nature for activating a suitable non-linear material. The circuit used in Fig. 5 is the counterpart of the basic electronic shift register. In Fig.2.6 we have given a scheme of implementing the transfer process of data from one 3 bit register to another by serial in serial out mechanism. Introduction of each pulse helps the transfer of one bit from one register to other. This scheme may be enlarged by introducing the same number of flip–flops in each register. Similarly, number of registers can also be increased as much as possible. As the basic switches operation is done by the active use of non-linear material, so a very high-speed operation can be experienced from the system. The switch can run with femtosecond response time. In implementing all these schemes each of the input data D, C.L. (constant light), and P.L. (pulse setting laser) is of the equal intensity ‘I’ level.

2.8 References

[1] S.P. Medhekar, P. Paltani, Proposal for optical switch using nonlinear refraction, IEEE Photon. Technol. Lett. 18 (15) (2006) 1579–1581.

[2] N. Pahari, D.N. Das, S. Mukhopadhyay, All-optical method for the addition of binary data by nonlinear materials, Appl. Opt. 43 (33) (2004) 6147–6150.

[3] K.R. Choudhury, A. Sinha, S. Mukhopadhyay, An all-optical comparison scheme between two multi-bit data with optical nonlinear material, Chin. Opt. Lett. 6 (9) (2008) 693–696.

[4] J. Wang, G. Meloni, G. Berrettini, L. Poti, A. Bogoni, All-optical binary counter based on semiconductor optical amplifiers, Opt. Lett. 34 (22) (2009) 3517–3519.

[5] T. Chattopadhyay, C. Taraphdar, J.N. Roy, Quaternary Galois field adder based all-optical multivalued logic circuits, Appl. Opt. 48 (22) (2009) E36–E44.

[6] B. Chakraborty, S. Mukhopadhyay, Alternative approach of conducting phase-modulated all-optical logic gates, Opt. Eng. 48 (3) (2009) 5201–5205.

[7] J.N. Roy, A.K. Maity, D. Samanta, S. Mukhopadhyay, Tree-net architecture for integrated all-optical arithmetic operations and data comparison scheme with optical nonlinear material, Opt. Switch. Network. 4 (2007) 231–237.

[8] T. Haist, W. Osten, Ultrafast digital-optical arithmetic using wave-optical computing, in: OSC 2008, LNCS 5172, 2008, pp. 33–45.

[9] N.V. Kukhtarev, H.J. Caulfield, T. Kukhtarev, P. Buchave, S.F. Lyuksyuto, Nonlinear optical and electrical materials in high-contrast dynamic holography, in: SPIE CR64, 1996, pp. 280 307.

[10] H.J. Caulfield, N. Kukhtarev, T. Kukhtareva, M.P. Schamschula, P. Banerjee, One-, two-, and three-beam optical chaos and self-organization effects in photorefractive materials, Mater. Res. Innov. 3 (1999) 194–199.

[11] D. Samanta, S. Mukhopadhyay, A method of maintaining the intensity level of a polarization encoded light signal, J. Phys. Sci. 11 (2007) 87–91.

Chapter - 3

Image Edge Extraction using Nonlinear Optical Media and Verification by Computer Simulation

Chapter

3

Image Edge Extraction Using Nonlinear Optical Media and Verification by Computer Simulation

Image edge detection is an important part of image processing. There are many established techniques for extracting image edge. In this present scheme we show how the edges of an image can be extracted using Kerr type of nonlinear material and the implementation of the same scheme through computer simulation.

3.1. Brief overview

The edges of an image is not a physical entity; it is an impression. It is the portion where the picture ends and the surrounding starts. Edges of an image are the points where there is a large variation of luminance in going from interior of the image to that of the surroundings. The importance of detecting the edges of images span over various fields of applied science and technology. To give a few examples of it, detection of edge is important in properly locating the edge of digitized images in the field of medical sciences for estimating the size of cancerous tissues, counting and estimating the number density of astrophysical objects in the photometric images of an area of the sky and also detecting the number of particles per unit area in the scanning electron micrograph (SEM) images of nano-particles. There are many ways to perform edge detection. Up to 1960 the edge detection was done by Discrete Gradients and Laplacian methods. Canny edge detector [1] was invented in 1983.

From 1985 a new idea is introduced in the field of edge detection, which are linear and nonlinear scale-spaces. Optics with its inherent property is a very successful candidate to achieve very high-speed image operations [2, 3]. There are several established techniques of image edge detection in both analog and digital optical processing [4–10]. This paper presents a proposal of a method for image edges detection by proper use of intensity based NOT switching operations with Kerr type of nonlinear optical material. In the last section, musing a six-step algorithm it has been shown how edges of digitized images can efficiently be detected.

3.2. Edge detection by optical NLM

Nonlinear optical material as an optical switch and it's NOT functioning. There are some other types of nonlinear material for which β1 (1st order non-linear coefficient) = 0 and the lowest order non-linearity is due to β2 i.e. the 2nd order nonlinear term is active here. This nonlinear behaviour of the medium introduces the intensity-dependent lensing (focusing or defocusing) of propagating beams.

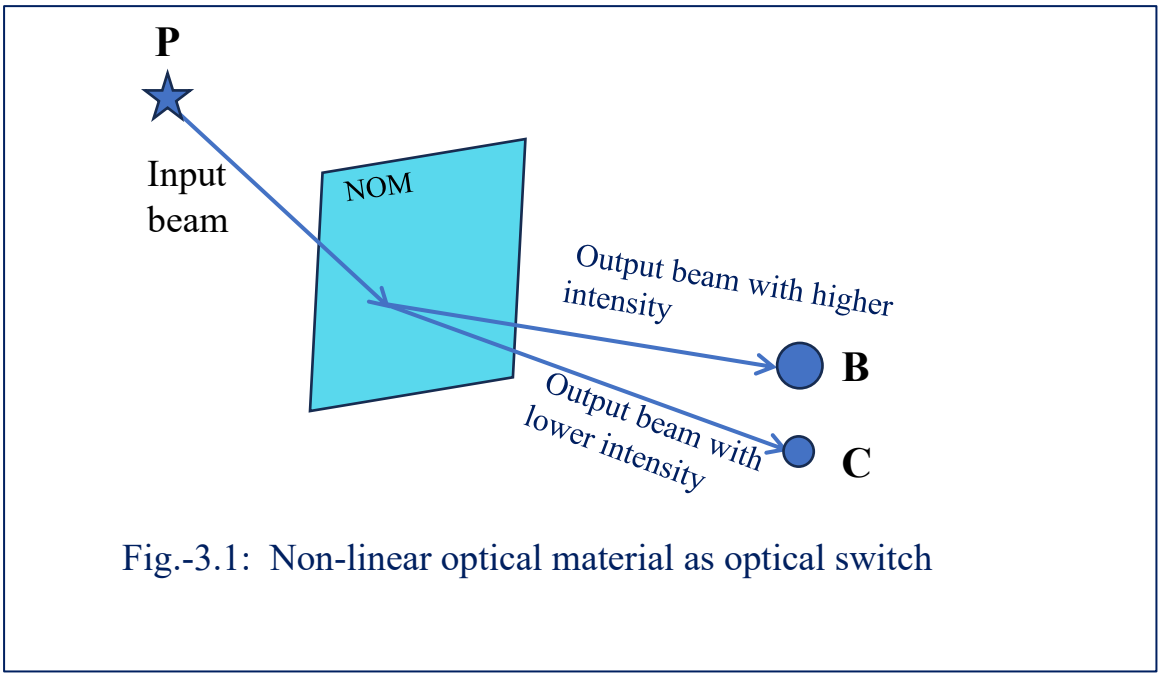

Fig.-3.1: Non-linear optical material as optical switch

For this non-linear material the refractive index can be expressed as $n = n_0 + n_2 I$, where n_0 is a constant refractive index term, n_2 is a second order non-linear correction term and 'I' is the intensity of light beam that passes through the material. According to this equation, the refractive index of the nonlinear material increases with the increase of intensity of the passing light.

To develop the switching scheme a non-linear medium is considered which is shown in Fig. 1. In **Fig.3.1** for a particular intensity, the beam approaches in the C direction. But for a light beam with higher intensity the refractive index of the non-linear medium increases which leads to a decrease in the angle of refraction in the medium. For this reason, the light beam with the higher intensity passing through the nonlinear medium comes closer (say along B) to the normal of the air-non-linear medium boundary plane. Thus, the non-linear material can act as intensity based optical switch.

Figure 3.2 shows NOT switching by this type of nonlinear material. Here P is the input light beam and C.L is the constant light source. Output is taken from the single intensity path (solid line). C.L. is always 1, so the input P will be inverted at the output.

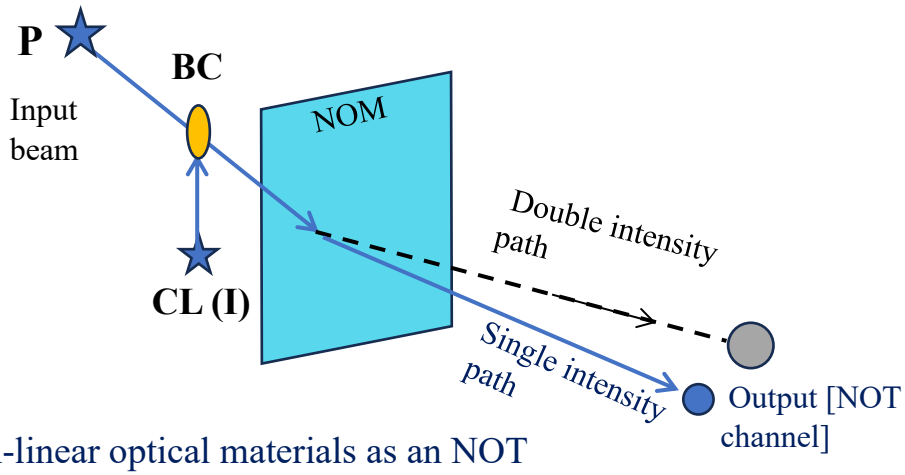

Fig.-3.2: Non-linear optical materials as an NOT switch

3.2.1. Inversion of the input image

In **Fig. 3.3**, A is a supplied image (developed positive photographic plate), whose edges are to be detected. In the image A the central portion is transparent and marginal portion is opaque. This image 'A' is placed on one side (say left side) of the nonlinear optical material (NOM), which acts as the NOT switch. Here the intensity label of the input light 'P' is I. C.L. is the constant light source of same intensity I. Due to NOT switching operation of NOM, we get the inverted image $\overline{A}$ at the output, which is taken in a positive photographic plate, as shown in the Fig. 3. In the inverted image $\overline{A}$, marginal portion is transparent and central portion is opaque. This is obtained in accordance with the NOT interaction between the beam P and C.L. Thus, we get the inverted image $\overline{A}$ of the supplied input image A. In the edge detection process this inverted image $\bar{A}$ can be used to get the sharp edges of the original image A.

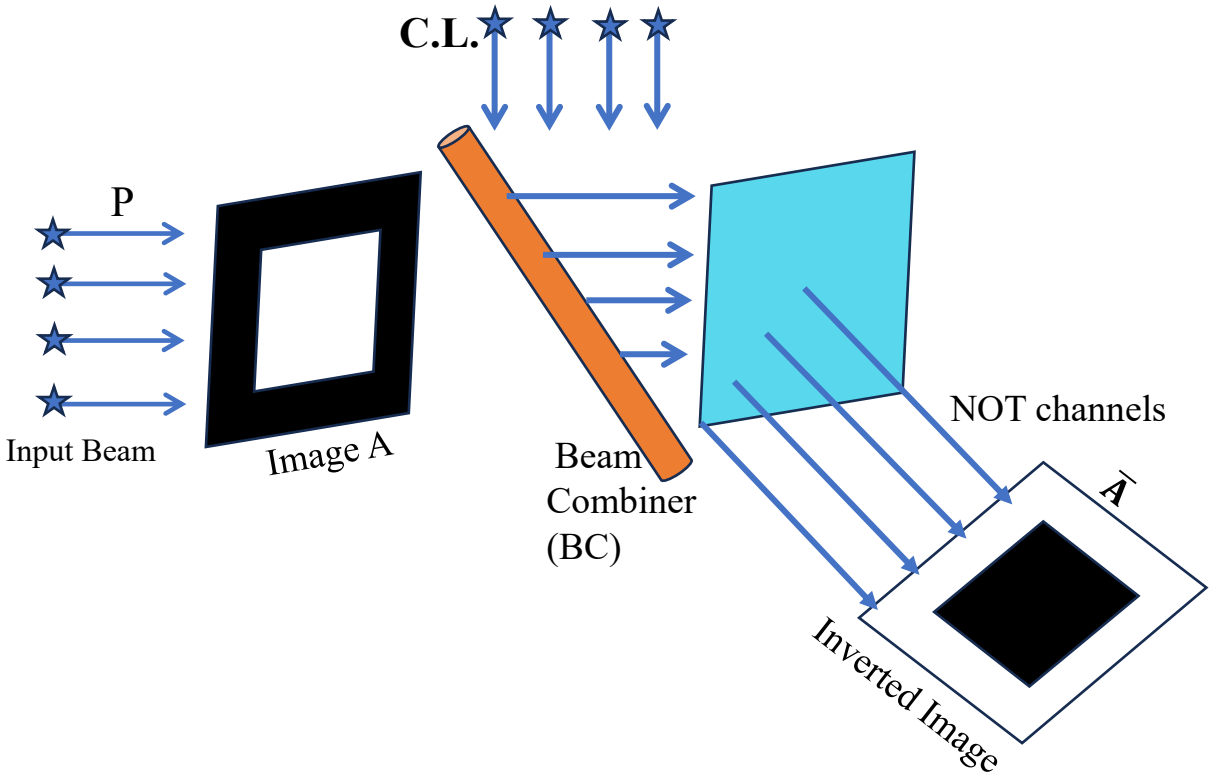

Fig.-3.3: Optical setup for obtaining inverted image

3.2.2. Edge detection

Figure 3.4 represents an optical setup for image edge detection. Here input image A and inverted image $\bar{A}$ are kept on opposite sides of a two-lens magnification system. NOM is intensity based NOT gate with nonlinear optical material. Light from an extended source is incident on image A. After passing through the image A the light beam comes to fall on the two-lens magnification system to provide some magnification of the input image. Passing through the lens system the beam is allowed to fall on the inverted image $\bar{A}$ by which we can get edges of the images at the output. To get the sharp image edge the magnification is adjusted so that the optical image of A is amplified a little bit by the lens system. The light beam emerging from inverted image is incident on the NOM and gives the sharp image edge at the output by NOT switching operation. The output from NOM is taken on a positive photographic plate.

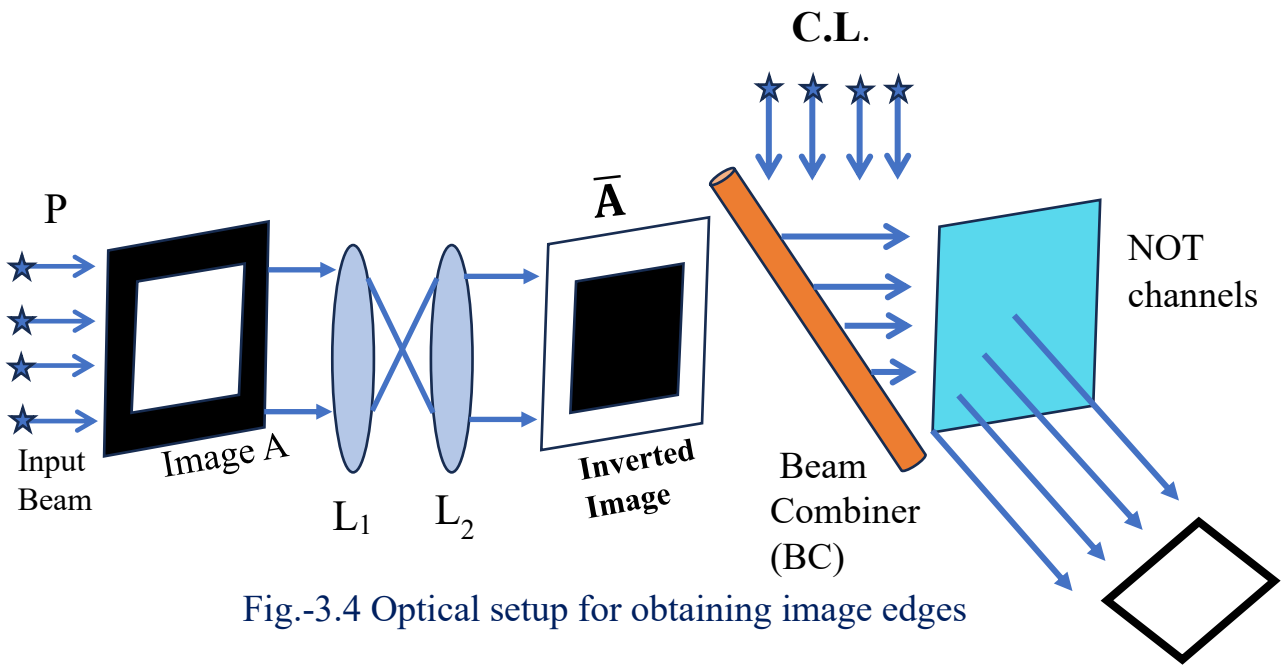

Fig.-3.4 Optical setup for obtaining image edges

3.3. Implementation of the concept at the software level: computer assisted image edge detection

In this section, we would discuss how the concept of image edge-detection, which has been described in the previous sections can also be applied for the purpose of edge extraction of binary two level (0 and 1) black and white images through computer simulation. For showing the validity of the concept and to keep the procedure simple we consider images having no spatial variation of intensity. So, the image can be simply represented by presence of light (0) and absence of light (1) (a negative logic has been assumed). The whole sequence of operations is a six-step process consisting of ----------

(i) In the first step the black and white image is converted into a binary matrix of 1's and 0's

(ii) One has to note that actually the contour of 0's represents the edge of the image which we want to detect. To do this we first carry out an operation by which any 1 adjacent to a 0 is converted to 0. This is equivalent to binary expanded image.

(iii) To produce binary inverted image of the input image we make an operation on matrix form of input image by which each '0' of matrix is converted into '1' and each '1' is converted into '0' simultaneously.

(iv) After then AND operation is made between the binary expanded image and binary inverted image, which gives the binary inverted image edge.

(v) Next the binary inverted image edges are converted to binary image edges by performing the same operation as describe in step (iii).

(vi) In the final step the output binary image of step (v) is converted into real edge of the input image.

The popular image manipulation program GIMP [11] is used to convert black and white image into the binary matrix and the output binary matrix into real edge. The rest of the operations, expansion the contours of 0's i.e., the creation of binary expanded image, creation of binary inverted image, the AND operation of these two binary images and the creation of binary image edges from output of AND operation are carried by the C program. Below we show the implementation of this sequence of operations on sample images. **Figure 3.5** is the input image. **Figure 3.6** (Matrix-1) represents the input image in binary matrix form. The edge expanded matrix of the input matrix, where the adjacent 1 of each 0 is converted to 0, is represented in **Fig.3.7** (Matrix-2). **Figure 3.8** (Matrix-3) is the binary inverted image of the input image, where each '0' of Fig. 6 (Matrix-1) is converted into '1' and each '1' is converted into '0'. **Figure 3.9** (Matrix-4) is the output of AND operation of Fig. 7 (Matrix-2) and Fig. 8 (Matrix-3). Figure 3.9 (Matrix-4) represents the inverted binary image edge of the input image. **Figure 3.10** (Matrix-5) represents the binary image edge of the of the input image. **Figure 3.11** represents the edge of the input image (Fig. 5). Figure 12 represents a series of image and their edges extracted in this proposed scheme.

Fig.-3.5: Input image

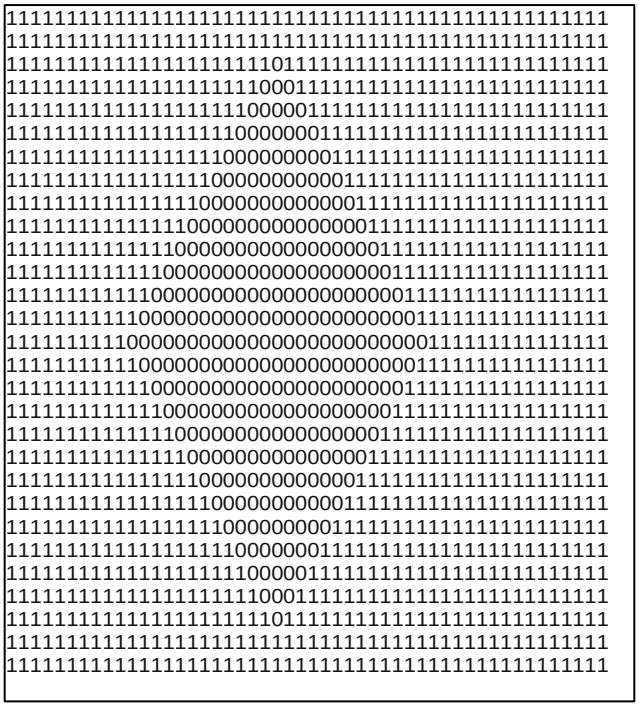

Fig.-3.6: (Matrix-1): input image in binary matrix form

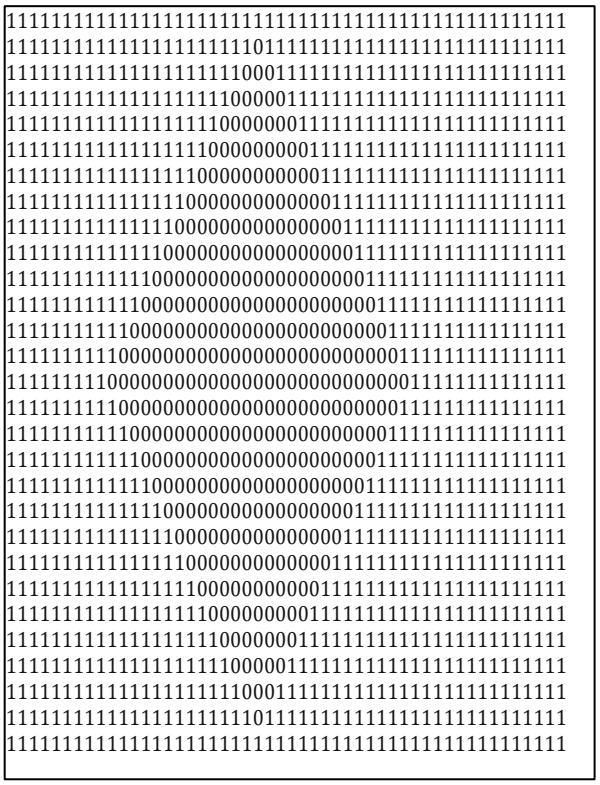

Fig.-3.7: (Matrix-2): edge expanded matrix

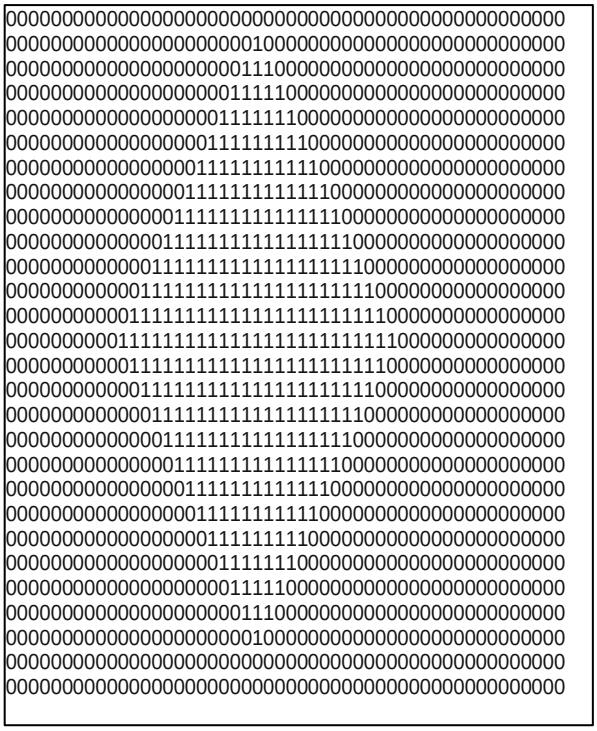

Fig.-3.8: (Matrix-3): inverted image in binary matrix form

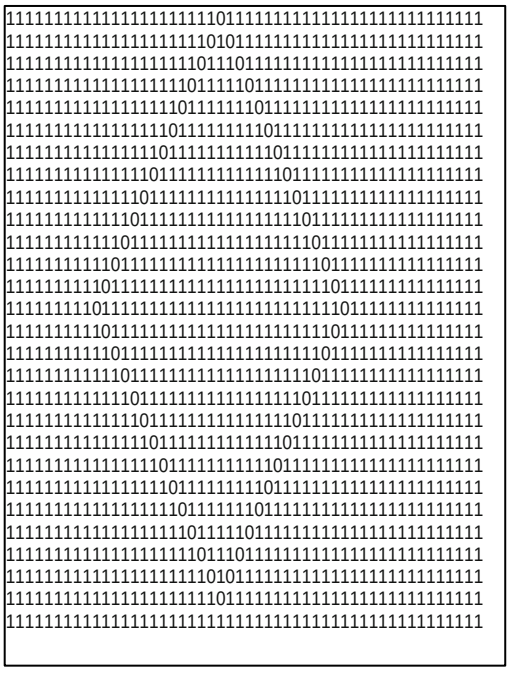

Fig.-3.9: (Matrix-4): inverted image edge in binary matrix form

```
00000000000000000000000000000000000000000000000000
00000000000000000000001000000000000000000000000000
00000000000000000000101000000000000000000000000000
00000000000000000001000100000000000000000000000000
00000000000000000100000100000000000000000000000000
00000000000000001000000100000000000000000000000000
00000000000000010000000100000000000000000000000000
00000000000000100000000100000000000000000000000000
00000000000001000000000100000000000000000000000000
00000000000010000000000100000000000000000000000000
00000000000100000000000100000000000000000000000000
00000000001000000000000100000000000000000000000000
00000000010000000000000100000000000000000000000000
00000000100000000000000100000000000000000000000000
00000001000000000000000100000000000000000000000000
00000010000000000000000100000000000000000000000000
00000100000000000000000100000000000000000000000000
00001000000000000000000100000000000000000000000000
00010000000000000000000100000000000000000000000000
00100000000000000000000100000000000000000000000000
01000000000000000000000100000000000000000000000000
00100000000000000000000100000000000000000000000000
00010000000000000000000100000000000000000000000000
00001000000000000000000100000000000000000000000000
00000100000000000000000100000000000000000000000000
00000010000000000000000100000000000000000000000000
00000001000000000000000100000000000000000000000000
00000000100000000000000100000000000000000000000000
00000000010000000000000100000000000000000000000000
00000000001000000000000100000000000000000000000000
00000000000100000000000100000000000000000000000000
00000000000010000000000100000000000000000000000000
00000000000001000000000100000000000000000000000000
00000000000000100000000100000000000000000000000000
00000000000000010000000100000000000000000000000000
00000000000000001000000100000000000000000000000000
00000000000000000100001000000000000000000000000000
00000000000000000010001000000000000000000000000000
00000000000000000001010000000000000000000000000000
00000000000000000000100000000000000000000000000000
00000000000000000000000000000000000000000000000000
```

Fig.-3.10: (Matrix -5)- image edge in binary matrix notation

Fig.-3.11: Edge of the input image

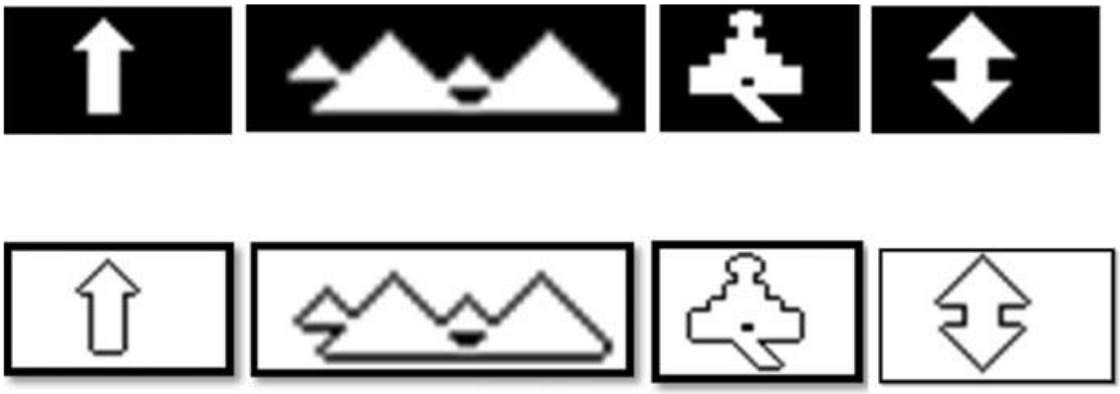

Fig.-3.12: A series of image and their edges

3.4. Conclusion

This system of image edge detection with nonlinear material is an all-optical one, so its speed of operation is very high and the whole operation is parallel. To activate the nonlinear material, one should use a suitable polarized laser light. To maintain the coherency, condition all inputs should be derived from a single source. Carbon bi Sulphide (CS_2) or Silica glass can be used as Kerr type nonlinear materials for getting NOT switching operation. Nd: YAG laser with 1.064 μm wave length is an ideal source to activate the non-linear material in the switching process. At the time of transmission through A and $\overline{A}$ diffraction problem may come, but after NOT

operation the output will be free from such problem, because in the diffraction affected edges there is a variation of intensity from 'I' to 0 in the image edge region. The non-linear material functioning as directional filter separates the 'I' intensity-based image edges in a different direction. So, after NOT operation at the output, we get edges of the input image which are free from diffraction problem. The same algorithm can directly be applied to extract the edges of any digitized image of objects. A software implementation and verification of the concept is done here for simple black and white images. In future, this will be extended for the gray level variation as well as coloured images.

3.5 References

1. J.F. Canny, A computational approach to edge detection. IEEE Trans. Pattern. Anal. Mach. Intell. 8(6), 679–698 (1986)
2. N. Pahari, S. Mukhopadhyay, New scheme for image edge detection using the switching mechanism of nonlinear optical material. Opt. Eng. 45, 037003–037005 (2006)
3. D.N. Das, S. Mukhopadhyay, Image edge detection and enhancement by an inversion operation. Appl. Opt. 37 (35), 8254–8257 (1998)
4. X. Jiang, H. Bunke, Edge detection in range images based on scan line approximation. Comput. Vis. Image Underst.73(2), 183–199 (1999)
5. G.W. Wei, Y.Q. Jia, Synchronization-based image edge detection. Europhys. Lett. 59(6), 814–819 (2002)
6. G. Welch, W.T. Rhodes, Imaging through a random phase screen by enhanced backscatter: a physical interpretation. Appl. Opt. 32(15), 2692–2696 (1993)
7. Y.-K. Lee, W.T. Rhodes, Nonlinear image processing by a rotating kernel transformation. Opt. Lett. 15(23), 1383– 1385 (1990)
8. A. Sinha, K. Singh, A technique for image encryption using digital signature. Opt. Commun. 218(4–6), 229–234 (2003)
9. G.S. Pati, G. Unnikrishnan, K. Singh, Multichannel image addition and subtraction using joint-transform correlator architecture. Opt. Commun. 150(1-6), 33–37 (1998)
10. Z. Chen, M.A. Karim, M.M. Hayat, Displacement cooccurance statistics for binary digital images. J. Electron. Imaging 11(02), 127–135 (2002)
11. http://www.gimp.org/

Chapter - 4

Optical Logic for Multi-Valued Encoding and Decoding

Chapter

4

Optical Logic for Multi-Valued Encoding and Decoding

Optics and photonics have come forward as promising substitutes for traditional electronics in computation and communication due to their natural parallelism and high-speed processing. Taking advantage of the nonlinear switching behaviour of Kerr-type optical media, this chapter introduces new all-optical schemes for number system conversion. In particular, encoder and decoder structures are constructed to effectively convert decimal numbers into binary, ternary, and quaternary representations, and vice versa to decode binary and ternary codes into decimal. Such all-optical structures not only reduce operations but also improve processing efficiency, which proves the capability of Kerr-based photonic switches in future data processing and computing systems.

4.1. Brief Overview

During the past few decades, optics and photonics have been developing as strong technologies for computing and communication, prompted by the shortcomings of traditional electronics in providing ultra-high processing rates. Compared to electrons, photons can provide intrinsic parallelism and be used as good information carriers, allowing quicker arithmetic, algebraic, and logic operations. Nonlinear Kerr-type optical material properties have been central to the design of intensity-based optical switches, which are basic building blocks for encoding and decoding strategies. Number system conversions—binary, ternary, quaternary—have been proposed by researchers as several methods of performing such conversions based on all-optical architectures, showcasing the potential of all-optical structures for facilitating multi-valued logic and increasing data processing capacity. This work adds to that effort by introducing new all-optical encoder and decoder designs based on Kerr nonlinear materials, providing efficient and high-speed alternatives for future computing systems.

4.2. Optical Binary Encoder to Code Decimal Number

Optics has steadily revealed as a potential candidate in the realms of data processing as well as in computing system on the ground of its inherent parallelism. In the present work,

a renovated approach is penetrated in digital electronic circuit to enhance and ease the operation process by leveraging the optical switch in place of electronic one. Here, an all-optical binary encoder scheme has been specifically devised to interpret the coding of decimal number to its binary form with hasty and easy operation whose rudimentary foundation is the Kerr-optical nonlinear material. Since the presented scheme is all-optical in nature, in addition to providing high speed computation, the key advantage of this optical binary encoder is that unlike electronic encoder which relies on the electronic gate as an essential part, the proposed scheme does not demand any gate either electronic or optical or electro-optical. Thus, the proposed scheme can be appointed to the all-optical computing system as well as the photonic device application.

Over the past few decades, photonic device has become impressive tool owing to its numerous advantages in various application in computation as well as communication. Manifold schemes have enriched the field of opto-electronics parallel communication process and optical computing system where photon as high-speed information carrier [**1-4**]. Within this context, an intensity based an all-optical decimal to binary code encoder is designed by utilizing the switching capacity of Kerr-type optical non-linear material N.L.M[**4-5**]. In this proposed scheme, the intensity levels I, 2I, 3I, 4I, -----, nI are corresponded to the decimal numbers 1, 2, 3, 4, -----, n respectively which serve as the input signal. The output states of the binary encoder are 0 and 1, where these states are represented by the absence of light and the presence of polarized light of standard intensity level I respectively. To maintain the schematic intensity levels, beam-combiners (BC) and 50% beam-splitters (BS) are designedly utilized [**5-8**].

4.2.1. Optical switch (or regulator) by N.L.M: -

To develop the optical switch a composite slab of L.M & N.L.M is taken together as shown in **Fig: - 4.2.1**, where n_{NLM} and n_{LM} are the refractive index (R.I.) of nonlinear and linear material respectively. Here θ_1 and θ_2 are incident and refraction angle respectively.

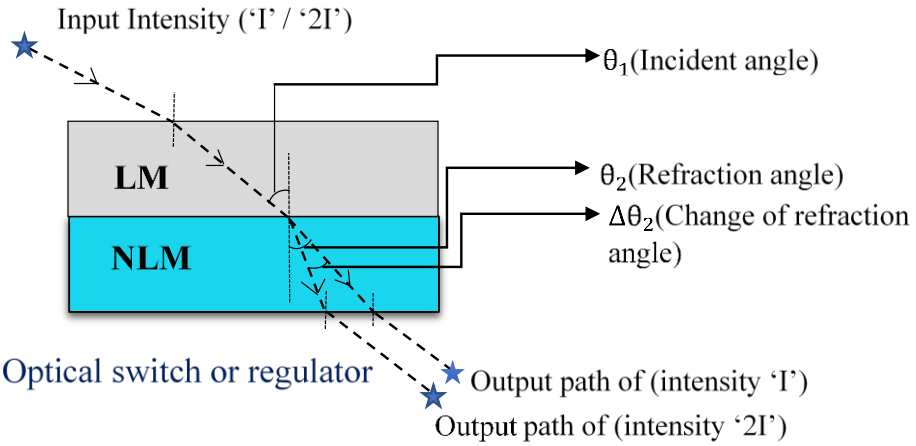

Fig.-4.2.1: Optical switch or regulator

To create optical switch if we take only N.L.M. then incident polarized laser beam upon the N.L.M. (of high relative refractive index with respect to air) is deflected from N.L.M. as large variation. To reduce this large variation of deflected output beam, we should take linear and non-linear material together as optical switch.

4.2.2. Design of Optical Binary Encoder

The proposed optical binary encoder consists of following four parts as –

4.2.2.1. Input section

In our presented scheme there are 9 numbers of constant light (CL)sources (as like S_1, S_2, S_3, S_4, ……S_9) each of the same and standard intensity level I i.e. proposed binary encoder can convert any decimal number into its binary form from decimal number 1 up to 9. A definite number of constant light sources must be stimulated to express the definite decimal number into its equivalent binary from. Here particular decimal number is represented by certain number times standard intensity level (I), i.e.,1,2,3,4, ----- etc. decimal numbers are illustrated by I,2I,3I,4I, respectively. To express the particular decimal number into its binary form, the particular number of light sources are to be in HIGH state (Light is present). Here, it is strictly noted that these 9 numbers of constant light (CL) sources are coherent in nature.

4.2.2.2. Optical switch (A)

Optical switch(A) acts as an optical regulator. Output intensity of 'A' is treated as decimal number which is converted into binary form. For expressing definite decimal number,

particular number of C.L. are in high state. As a consequence, depending upon input light intensity level into 'A' there are several output paths of definite light intensity level from 'A'. Then all output paths (of respective definite intensity) are linked into processing section.

4.2.2.3. Processing section

For coding gradually 'n' number of decimal number into its binary form there are $(n-1)$ number of (m: n) optical devices [(m: n) OD] are placed in front of output path from OS(A). The table. -4.1.1 shows which type of [(m: n) OD] will be connected in which output path from OS(A). All [(m: n) OD] are implemented with help of 50% B.S, constant light source (C.L.), B.M and reflector.

Behavior of (m: n) optical device [(m: n) OD]: -

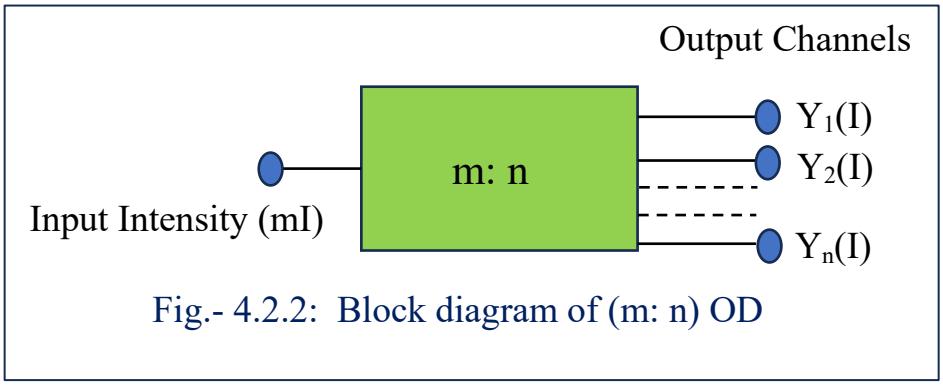

Fig.- 4.2.2: Block diagram of (m: n) OD

It is developed in such a way that for fixed input intensity 'mI', it provides 'n' numbers of different output lines of the same and standard intensity 'I'. Here, 'm' and 'n' are natural numbers except m = 1. The m: n OD (shown in **Fig.- 4.2.2:**) is constructed with help of beam combiner (BC) and 50% beam splitter (BS). In our proposed scheme, decimal numbers1 to 9 are coded to its binary form. So, in this case m= 2,3,4, -------,9 and value of 'n' is either 1or 2 or 3. In presented scheme, required (m: n) of OD are (2:1), (3:2), (4:1), (5:2), (6:2), (7:3), (8:1), (9:2). To design (2: 1) OD, only one 50% BS is required. Block diagram of this OD is shown in **Fig.- 4.2.3:** Here, a polarized light of input intensity 'I' enters into the device. Then with help of BS, finally, there is single output channel of intensity 'I' from the OD. Similarly, for designing [(3: 2) OD], (which is shown in **Fig.- 4.2.4:**) the polarized light of intensity '3I'is combined with another light from CL at the point 'a'. As result, united light of intensity '4I' advances towards the point 'b' and encounters the 50% BS. Then, there are two emergent light beams from the point 'b'. One

is absorbed by the wall of the device and another of intensity '2I' moves towards the point 'c' and by dint of BS it is split into two parts. Both of them act as output channels, where each of them has same intensity level 'I'. Here, two output channels from [(3: 2) OD] are denoted by $3Y_1$ and $3Y_2$. In this way, other [(m: n) Optical Device] can be developed. Now the input intensity versus number of output lines of [(m: n) OD] are shown in **Table. - 4.2.1**. This table also shows how the output lines from each [(m: n) OD] are associated to the different optical ports.

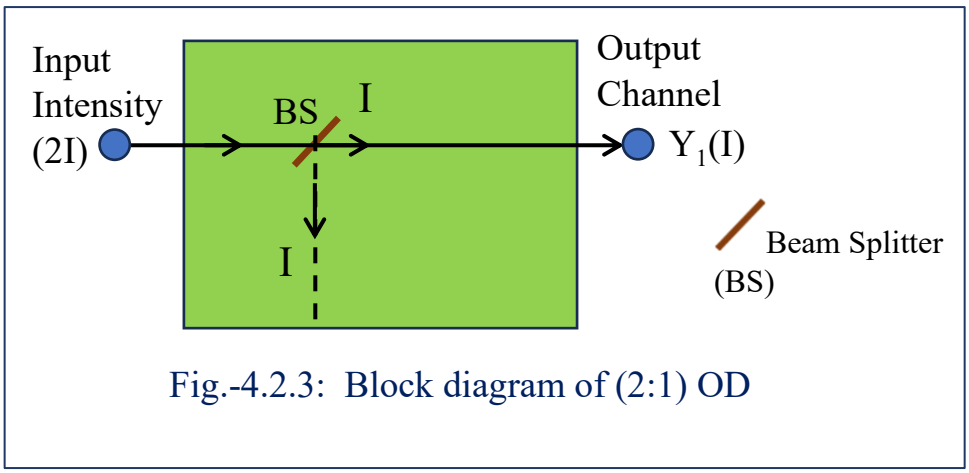

Fig.-4.2.3: Block diagram of (2:1) OD

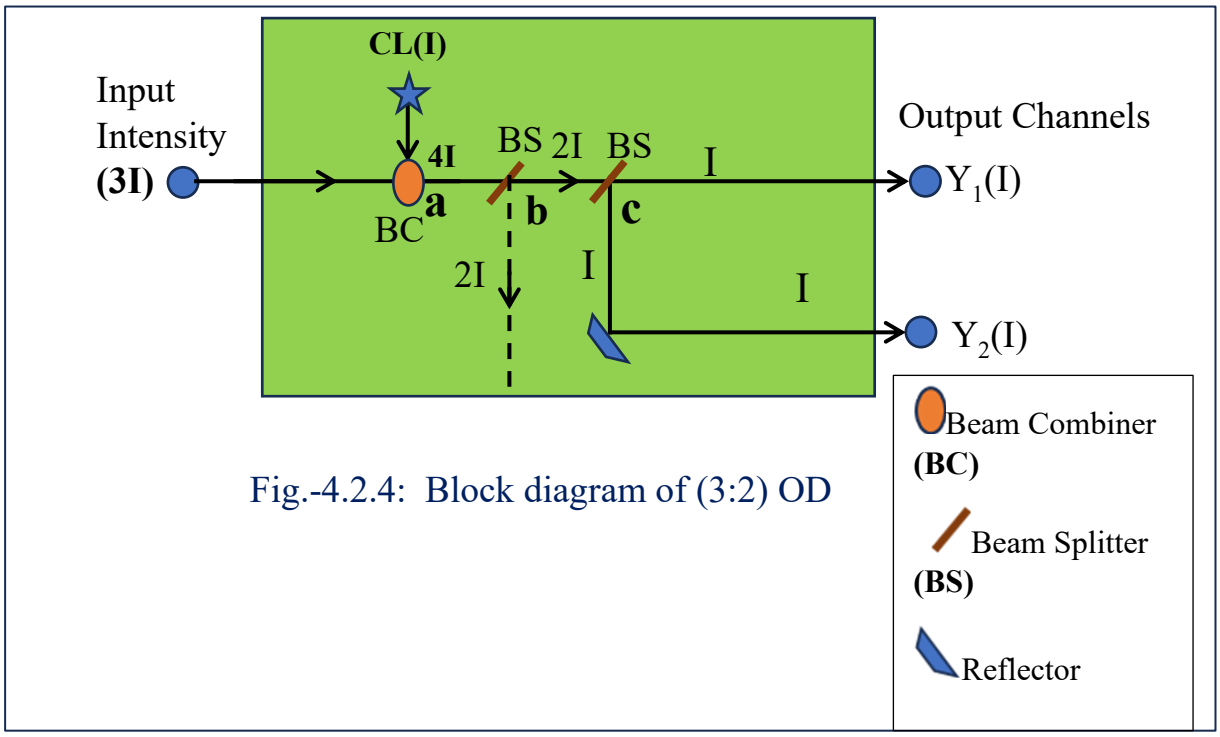

Fig.-4.2.4: Block diagram of (3:2) OD

4.2.2.4. Output division

Output division of proposed optical binary encoder (OBE) consists of four optical ports such as – B_1, B_2, B_3 & B_4 where B_1 & B_4 are treated as M.S.B & L.S.B respectively. Now relation between output lines (intensity) of [(m: n) OD] in processing section and connected optical ports in output division is as-

$$B_1 = 8Y_1(I) + 9Y_1(I) \quad (1)$$

$$B_2 = 4Y_1(I) + 5Y_1(I) + 6Y_1(I) + 7Y_1(I) \quad (2)$$

$$B_3 = 2Y_1(I) + 3Y_1(I) + 6Y_2(I) + 7Y_2(I) \quad (3)$$

$$B_4 = D(I) + 3Y_2(I) + 5Y_2(I) + 7Y_3(I) + 9Y_2(I) \quad (4)$$

Here D(I) denote that output path of intensity I from optical switch (A) is continued directly into the port 'B_4' (LSB) without collaboration of any (m: n) optical device. Now from the relation (1), (2), (3) & (4), the binary form of any decimal number is displayed at output section of OBE.

4.2.3. Operation of OBE (decimal to binary)

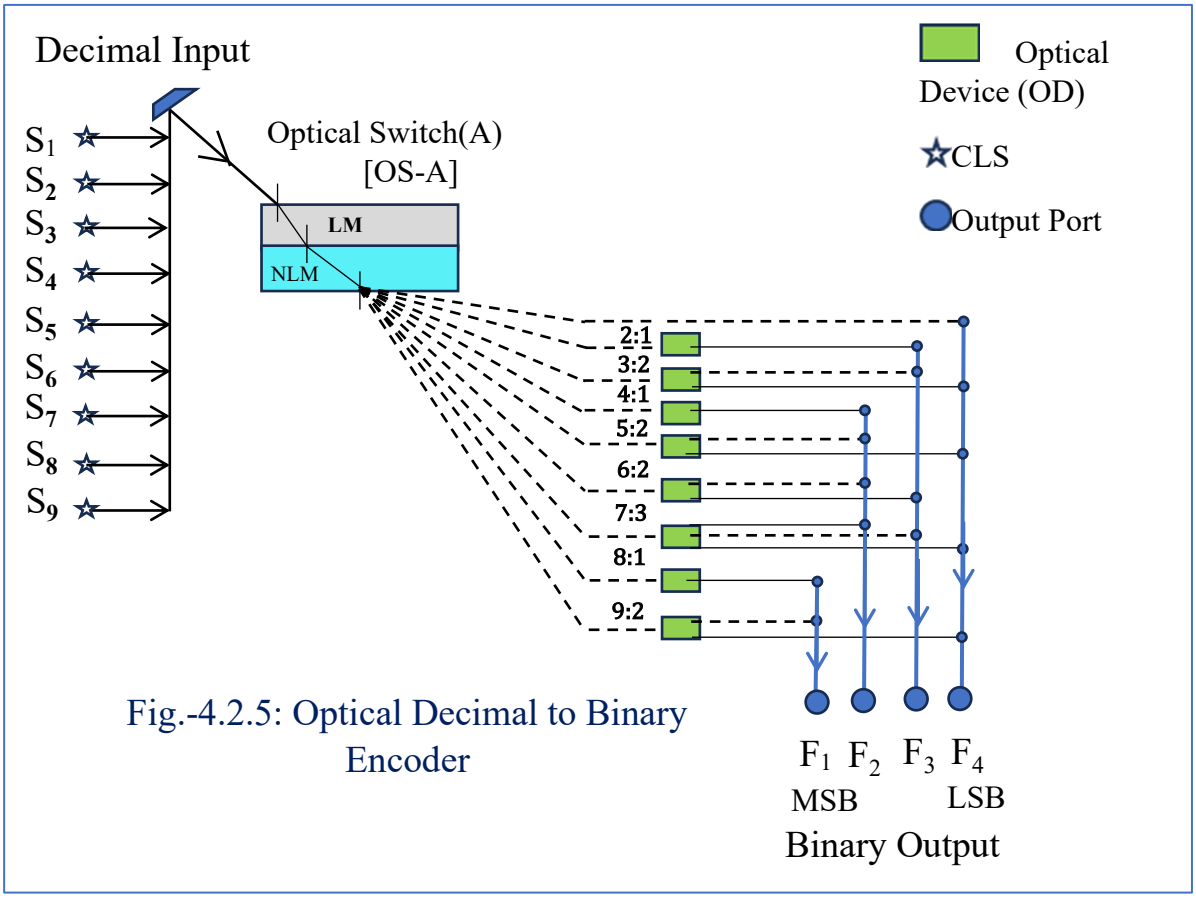

Fig.-4.2.5: Optical Decimal to Binary Encoder

The operation of the optical Encoder (shown **in Fig. -4.2.5**) will be perceived from the following example-

Now to code decimal number 7 to its equivalent binary form, any seven numbers of CLS (of input section of presented scheme) are in high state. As a result, output path of intensity level 7I is refracted from OS-A and then it is associated to 7:3 OD of processing section. Now from the relation (2), (3) and (4), optical port B_2, B_3 and B_4 are shined i.e., $B_1 = 0$; $B_2 = B_3 = B_4 = 1$. As an outcome, binary answer of decimal number 7 is = 001. [A python computational simulation for conversion of decimal number 7 to its equivalent binary form is shown in **Fig. -4.2.6**]. Thus, in this way, any decimal number is converted to its equivalent decimal. The presented design is schemed for conversion of decimal number 1 to 9, which is shown in **Table-4.2.1**.

Table. -4.2.1 Decimal number versus binary output form

Decimal Number	No. of Lighted Source	Intensity of Output path from Optical Switch (OS)	(m: n) Optical Device (OD)	Name of the Output Channel (Y_n) from OD	Nane of the connected Optical Port	Binary Output Form			
						F_1 (MSB)	F_2	F_3	F_4 (LSB)
1	1	I	Direct	Direct	F_4	0	0	0	1
2	2	2I	2 :1	$2Y_1$	F_3	0	0	1	0
3	3	3I	3 :2	$3Y_1$	F_3	0	0	1	1
				$3Y_2$	F_4				
4	4	4I	4 :1	$4Y_1$	F_2	0	1	0	0
5	5	5I	5 :2	$5Y_1$	F_2	0	1	0	1
				$5Y_2$	F_4				
6	6	6I	6 :2	$6Y_1$	F_2	0	1	1	0
				$6Y_2$	F_3				
7	7	7I	7 :3	$7Y_1$	F_2	0	1	1	1
				$7Y_2$	F_3				
				$7Y_3$	F_4				
8	8	8I	8 :1	$8Y_1$	F_1	1	0	0	0
9	9	9I	9 :2	$9Y_1$	F_1	1	0	0	1
				$9Y_2$	F_4				

This proposed all-optical encoding scheme offers ultrafast operation (terahertz range) surpassing electronic and electro-optic devices. Unlike traditional encoders that rely on specific key inputs and OR gates, this design requires only setting selected light sources (of equal intensity) to high state eliminating the need for any logic gates. Its simplicity and speed make it suitable for all-optical computing and photonic applications.

4.2.4. Python simulation result

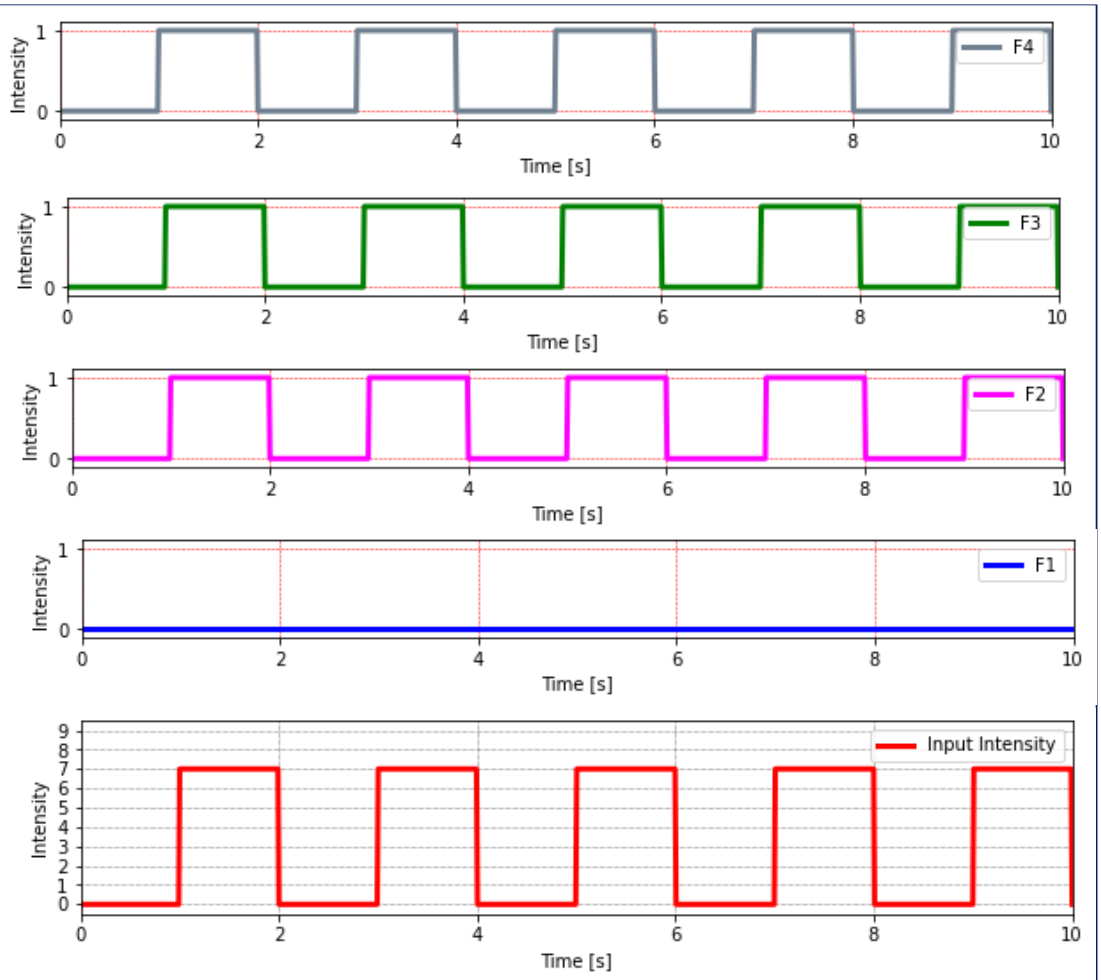

Fig.-4.2.6: Python computational simulation for conversion of decimal number 7 to its equivalent binary form 0111[where F_1=MSB & F_4=LSB].

4.3. Optical Binary-Decoder for decoding binary data to decimal number

To achieve the high degree of processing speed in the field of computation and communication process, it has been undoubtedly proven that there is no alternative way of optics due to inherent parallelism of optical signal. On the basis of this thought the nonlinear materials act as an optical switch and for proper functioning of such optical

switch a constant intensity level of the input data is the necessary condition. Here, in this communication, we propose a new scheme for decoding of binary number to decimal number by optical decoder which is all optical in nature. The rudimentary foundation of this optical decoder is optical positive non-linear material. The process of the proposed scheme is very easy and the fastest in operation. It can be included in all optical computing system as well as in the optical communication process.

The limitation of electronics in parallel arithmetic, algebraic and logic processing are well known. Very high-speed computation cannot be expected in conventional electronic systems. Present scientist and technologist all over the world are constant working to achieve terabit speeds of operation Some technologist believe this speed of operation may be achieved by replacing electron particle by photon as information carrier. Different crystals and met materials are used to control the light signal. In the last few decades, there have been many proposals in the field of optical computing system and in optoelectronic parallel communications process. By many significant and successful developments in this field has been prospered and prolonged [4, 9-15]. In our present journey we introduce a new concept for decoding of binary number to decimal number. For implement this process we use optical positive nonlinear material (NLM). based optical gate or optical switch. This optical gate or optical switch is the basic building blocks of our proposed optical decoder. Here binary data '1' is expressed as the presence of light and '0' is considered as the absence of light.

4.3.1. Optical Switch by positive NLM [Shown in Fig. -4.3.1]

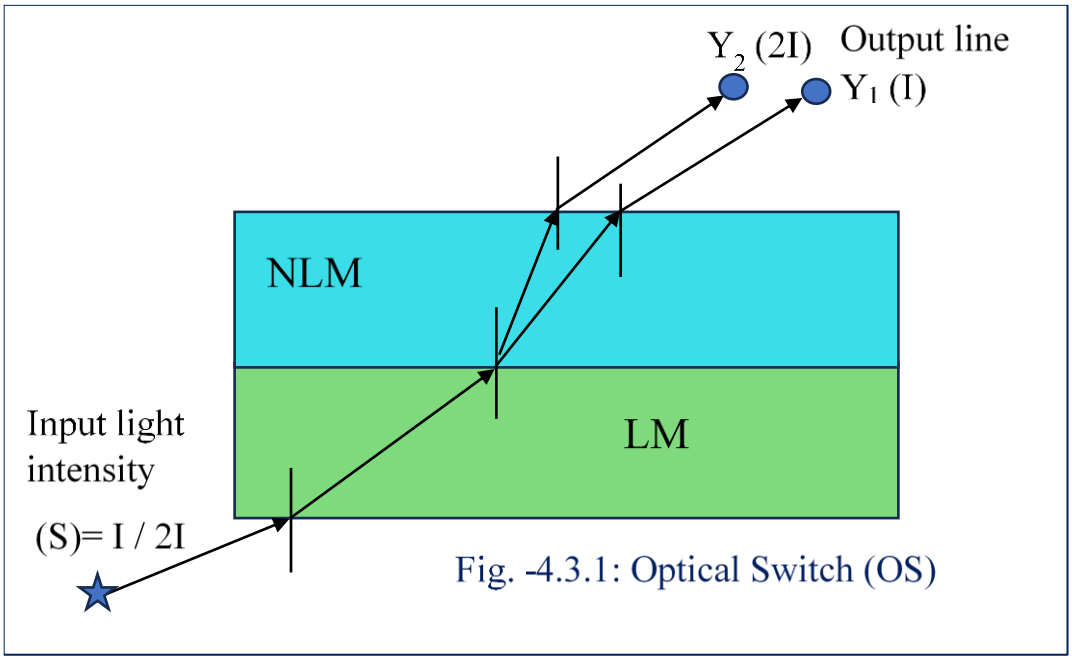

Fig. -4.3.1: Optical Switch (OS)

4.3.2. Design of optical decoder [circuit-1] by Kree-type N.L.M.

An optical circuit which transforms binary coded information to decimal coded information be revealed as optical decoder (shown in **Fig. -4.3.2**). In my proposed optical decoder, there are four numbers of coherent sources by naming 'A', 'B', 'C' and 'D' acting as input line, where 'A' and 'D' are in MSB (most significant bit) and LSB (low significant bit) respectively. All input sources are remaining in high state (1) and low state (0) by the presence and absence of triggering optical signal (of standard intensity level 'I') respectively. In this presented optical decoder, there are nine number of output channels. They are denoted by the order Y_1 to Y_9 representing the finite decimal number 1 to 9 respectively. When input intensity of incident polarized on optical switch (OS-4) is 'I' / '2I' / '3I'/ --------/ '9I', there is several output beams passing through the channel Y_1 / Y_2 / Y_3 / ------- / Y_9 respectively and definite O/P line of definite intensity level from OS-4 denote the conversion of definite binary number to its equivalent decimal number. In operation while any one output channel out of nine is in high state, then the rest of the channels are in low state and at the same time high state output channel represents the definite decimal number.

To design optical decoder, there are four numbers of optical switches such as OS-1, OS-2, OS-3 and OS-4 in proposed scheme, where OS-1 to OS-3 are linked with input data line 'A' to 'C' via 'a' (C.L.S of intensity level '7I'), 'b' (C.L.S of intensity level '3I') and 'c' (C.L.S of intensity level 'I') respectively. Here, OS-4 acts as an output controller (OC) of the scheme, where outputs (O/P) of OS-1, OS-2, OS-3 and directly input line 'D' are associated with it (OC) by the help of beam combiner (B.C.). As a result, for a particular input intensity OS-1 to OS-3 are ready to join with the OS-4 (OC) otherwise they [OS-1 to OS-3] are disconnected from OC. Such for OS-1, when 'A' =1, then input intensity on it (I + 7I =) 8I, then it is connected with OC. Again, 'A' =0, then input intensity on it (0 + 7I =) 7I, then it is inactive to join with OC. Similarly, active input intensity of OS-2 and OS-3 to link with OC are '4I' and '2I'.

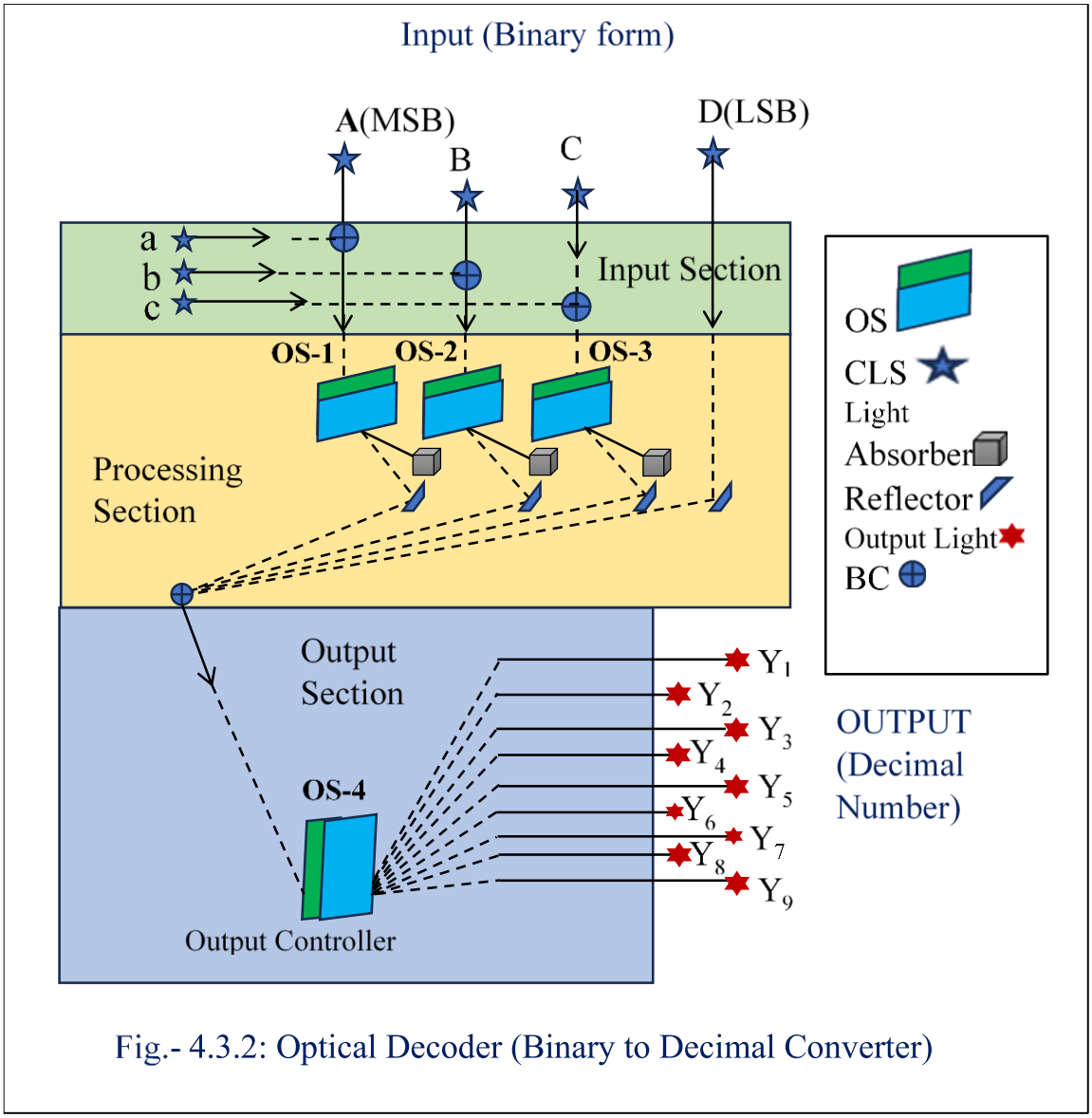

Fig.- 4.3.2: Optical Decoder (Binary to Decimal Converter)

4.3.3. Operation of the optical decoder

The whole operation of the optical decoder will be clear from the following example - when 'A' =1, 'B' = 0, 'C' = 0, & 'D' = 1, then total input intensity into OC is = 8I (O/P of OS-1) + 0 + 0 + 1 (for input data 'D') = 9I. So, we get positional O/P beam only at channel Y_9 i.e., $\mathbf{Y_9}$ will glow at an intensity level **9I**. Thus, positional $\mathbf{Y_9}$ is the decimal equivalent of binary form **1001.** In the similar way, any binary data can be converted into its equivalent decimal number. By the presented design, here 0001 to 1001 binary number conversion is showed in **table-4.3.1.** A python computational simulation for conversion of binary number 1001 to its equivalent decimal number 9 is shown in **Figure- 4.3.3**.

Table.4.3.1– Binary data to Decimal number conversion

Input (Binary form)				Output Intensity From				Total Input Intensity on O/P Controller	Output (Decimal Number)
A	B	C	D	$(OR)_A$	$(OR)_B$	$(OR)_C$	D	$(OR)_A+(OR)_B+(OR)_C+D$	$\mathbf{Y_n}$
0	**0**	**0**	**1**	0	0	0	I	0+0+0+I = **I**	$\mathbf{Y_1}$
0	**0**	**1**	**0**	0	0	2I	0	0+0+2I+0 = 2**I**	$\mathbf{Y_2}$
0	**0**	**1**	**1**	0	0	2I	I	0+0+2I+I = 3**I**	$\mathbf{Y_3}$
0	**1**	**0**	**0**	0	4I	0	0	0+4I+0+0 = 4**I**	$\mathbf{Y_4}$
0	**1**	**0**	**1**	0	4I	0	I	0+4I+0+I = 5**I**	$\mathbf{Y_5}$
0	**1**	**1**	**0**	0	4I	2I	0	0+4I+2I+0 = 6**I**	$\mathbf{Y_6}$
0	**1**	**1**	**1**	0	4I	2I	I	0+4I+2I+I = 7**I**	$\mathbf{Y_7}$
1	**0**	**0**	**0**	8I	0	0	0	8I+0+0+0 = 8**I**	$\mathbf{Y_8}$
1	**0**	**0**	**1**	8I	0	0	I	8I+0+0+I = 9**I**	$\mathbf{Y_9}$

This binary to decimal conversion scheme is entirely optical, based on nonlinear materials, enabling ultrafast computation. Unlike electronic decoders that rely on AND and NOT gates, this design requires no logic gates of any kind electronic, optoelectronic, or optical. Its simplicity and speed make it well-suited for all-optical computing and advanced photonic applications.

4.3.4. Python simulation result

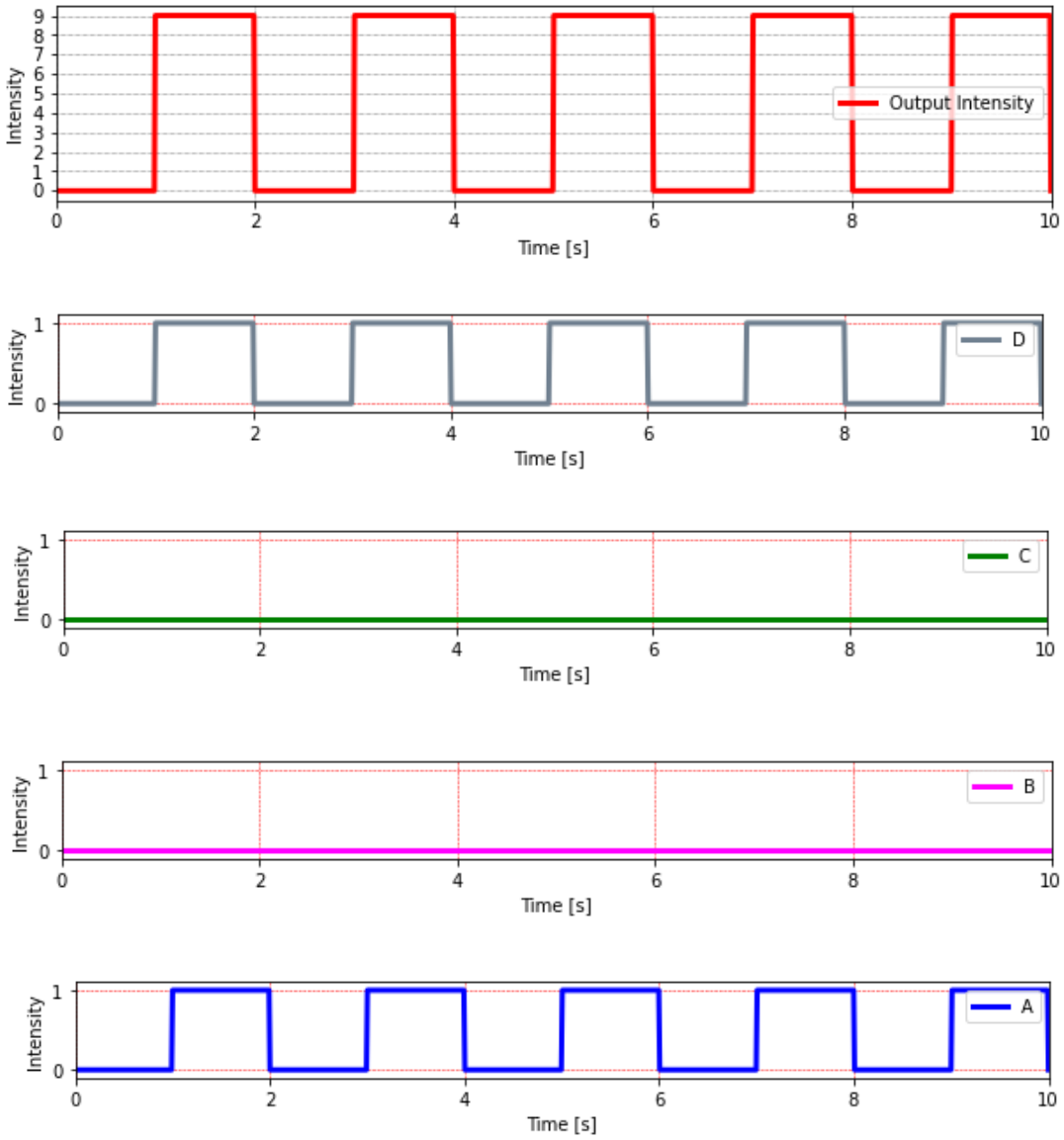

Fig.-4.3.3: Python computational simulation for conversion of binary number 1001 to its equivalent decimal number 9 [where A=MSB & D=LSB].

4.4. Optical Ternary-Encoder for coding decimal input

In the last few decades, it has been established that optics has adequate potential to perform super-fast computation in the field of communication [11,12,15,16]. Many proposals have already been proposed in many fields in support of this, where non-linear optical material plays an important role in constructing intensity based superfast optical switching system [4,9,10]. Here an all-optical scheme of decimal to ternary encoder is proposed with the proper use of optical non-linear material as switching device. Beam splitter and beam combiner are used here to maintain the desire intensity level. Here we represent a paper on optical ternary encoder which is wholly all-optical in nature on the basis of intensity based refractive index (R.I.) property of positive non-linear material (N.L.M.) and inherent advantage of parallelism of optical signal. For this type of NLM R.I of N.L.M. will increase with the increase of intensity of applied optical signal on it. In this context positive N.L.M. acts as optically controlled switching system. An all-optical system to convert the decimal number to ternary number is proposed here with the proper use of switching mechanism of Kerr type optical non-linear material. In this scheme the intensity level I, 2I, 3I, 4I respectively represents the decimal number 1, 2, 3, 4 which is used as the input bit. The output of the optical ternary state is represented by absence of light (0), presence of light with intensity level I (1) and the light of 2I intensity ($\bar{1}$). Beam splitter and beam combiner are used here to maintain the desire intensity level.

4.4.1. N.L.M. acts as Optical Switch [Fig. -4.4.1.]

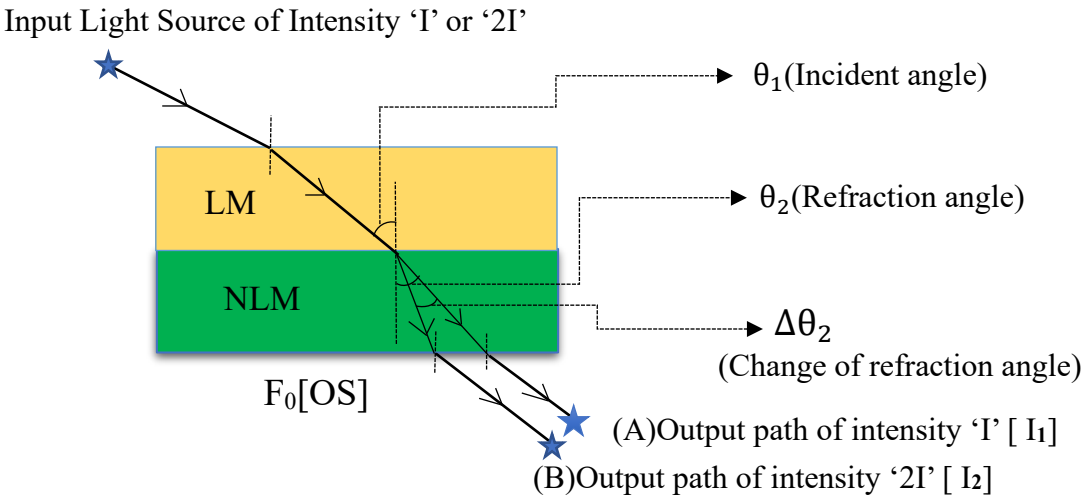

Fig. -4.4.1: Optical NLM act as an optical switch (F_0)

We know the relation between R.I. of the N.L.M. and intensity of incident polarized light is written as $n_{NL} = n_0 + n_2 I$ ……. (1),

where n_{NL}= the intensity-based R.I. of N.L.M., n_0= arbitrary constant term whose value depends upon what type of N.L.M. is used. n_2 = 2nd order nonlinear correction term. I =intensity of polarized light that passes through the linear material (L.M.) firstly and then secondly through the N.L.M. There are many such type of NLM having self-focusing character that are CS_2, GaAs, pure silica glass etc. We can use such materials (which have the self-focusing character) as optical switch for all-optical switching process in lieu of electronic gates. Now the focusing length (L) of NLM, power of laser beam (P) and area of cross-section (a) of the applied laser beam are related by the equation

$$P = \frac{\pi \epsilon_0 n_0 c a^4}{8 n_2 L^2} \qquad \ldots\ldots\ldots\ldots (2)$$

where ϵ_0 and c denote the free space permittivity and velocity of light in free space respectively. Now from the above relation it is known that the focusing length will be reduced with enhancing the power of the applied optical beam and also with when the radius of the beam is decreased optimally. As all the components i.e., optical switches are in sub-micron level dimension in the integrated optical system. Here to develop optical switch CS_2 or pure glass silica can be taken as optical NLM. Nd: YAG laser can be utilized as an incident polarized optical beam to activate the N.L.M.

4.4.2. Optical Ternary Encoder [OTE] by optical switch

In this proposed optical TERNARY encoder, intensity I ,2I ,3I, 4I ,5I ,6I ,7I ,8I & 9I represents the decimal number 1, 2, 3, 4, 5, 6, 7, 8 & 9 respectively. When we want to code particular decimal number into ternary words in that circumstance particular decimal number times standard intensity have to pass through the optical switch F_0 (**Fig.-4.4.1 & Fig.-4.4.9**). Depending upon the values of intensity of input incident polarized light on optical switch (which is constructed by optical L.M. & N.L.M), we get refracted ray passes through it in different refraction angle as well as different direction path by name "I_1", "I_2", "I_3", "I_4", "I_5", "I_6", "I_7", "I_8", & "I_9" of intensity level I, 2I, 3I, 4I, 5I, 6I, 7I, 8I & 9I respectively.

In our proposed optical ternary encoder, there are nine number of coherent constant light (C.L) sources (of same and standard intensity I) containing R, S, T, U, W, X, Y & Z. As and when the definite decimal number, be coded at that time concerned no. of any coherent

C.L sources are to be kept in HIGH state (i.e. light is present) circumstance name of the output intensity path from optical switch (F_0) is expressed by I suffix that no. of lighted sources, which is known as input key of ternary encoder. Thus, in optical ternary encoder decimal number 1, 2, 3, 4, 5, 6, 7, 8 & 9 are represented by input key as I_1, I_2, I_3, I_4, I_5, I_6, I_7, I_8 & I_9 of intensity level I, 2I, 3I, 4I, 5I, 6I, 7I, 8I & 9I respectively.

Now to design optical ternary encoder we take specific seven optical devices named "A", "B", "C", "D", "E", "F", & "G" and there are three optical switches "F_1", "F_2" & "F_3" which act as output of ternary encoder where "F_3" is low significant bit (L.S.B.) and "F_1" is most significant bit (M.S.B.) . Here it is important note that each of F_1, F_2, & F_3 has two output channels where one output channel is of intensity level I and another output channel is of intensity level 2I.The property of these optical switches"F_1", "F_2", & "F_3" is such that when input intensity of incident light on such type optical switch is zero then there is no output light from it but when input intensity of incident polarized light on such type optical switch is not zero then output light from it can be found in either intensity level of I or intensity level of 2I in accordance with input status.

Now we discuss how the input key I_1, I_2, I_3, I_4, I_5, I_6 I_7, I_8, & I_9 are connected with optical switches "F_1", "F_2", & "F_3" via optical devices named "A", "B", "C", "D", "E", "F", & "G" where F_3 is low significant bit (L.S.B.) and F_1 is most significant bit (M.S.B).Here it is to be noted that when we construct optical devices "A", "B", "C", "D", "E", "F", & "G", we use C.L for particular intensity level I and placed a 50% beam splitter (B.S) whose function is to divide the intensity of incident light on it into two parts of equal intensity [**3**].

The input key I_1 & I_2 are directly connected to the input of the optical switch "F_3". The input key I_3 is connected to the input of optical switch "F_2" via optical device "A". The input key I_4 is connected with optical switch "F_2" & "F3" via optical device "B". The input key I_5 is connected with optical switch "F_2" & "F3" via optical device "C". The input key I_6 is connected to the input of optical switch "F_2" via optical device "D". The input key I_7 is connected with optical switch "F_2" & "F3" via optical device "E". The input key I_8 is linked with optical switch "F_2" & "F3" via optical device "F". The input key I_9 is joined with optical switch "F_1" via optical device "G".

4.4.2.1. Characteristics of optical devices

Optical device "A"

The characteristics of it is such that when input intensity on it is 3I, then output intensity from it is I, which is linked into the input of optical switch "F_2".

Optical device "B"

When input intensity on it is 4I, and then there are two output beams from it, each of which is same intensity I. One of the two output beams from optical device "B" is linked to the optical switch "F_2" and the other into the optical switch "F_3".

Optical device "C"

Here when input intensity of incident polarized light on it is 5I then there are two output optical channels from it. One of them is of intensity level I which is connected to the optical switch "F_2"and another is of intensity 2I which is associated into the optical switch "F_3".

Optical device "D"

The property of optical device "D" is such that when input intensity on it is 6I then output channel from it is of intensity 2I which is joined into the optical switch "F_2"

Optical device "E"

When input intensity on it is 7I 'and then there are two output beams from it. One output of them is of intensity level I which is connected to the optical switch "F_3" and another output is of intensity level 2I, which is linked into the input of optical switch "F_2".

Optical device "F"

The property of it is such that when input intensity of incident light on it is 8I then there are two output beams of same intensity level 2I. One of this two output channels is connected into the input of optical switch "F_2" and another is joined into the optical switch "F_3".

Optical device "G"

The characteristics of optical device "G" is such that when input intensity level of incident light on it is 9I then there is only one output channel of intensity level I which is linked into the optical switch "F_1".

Table-8 shows how the output line/lines of each optical device are connected to the optical switches 'F_1', 'F_2' and 'F_3', where 'F_1' and 'F_2' are MSB and LSB respectively.

4.4.2.2. Working principle of optical devices

Optical device "A" (fig-4.3.2.)

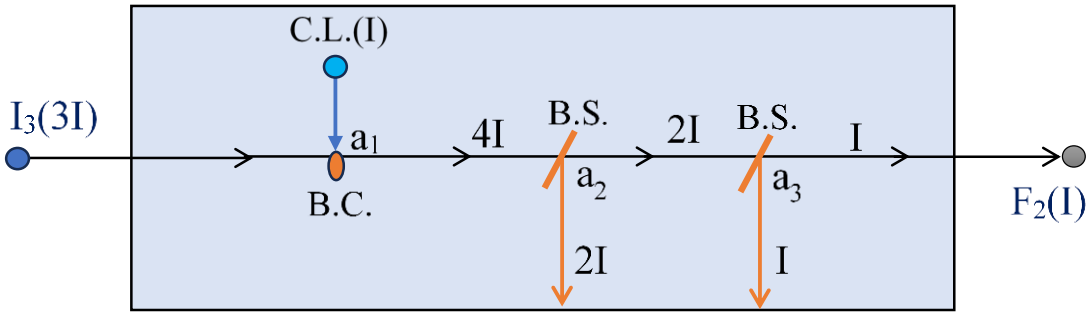

Fig. -4.4.2: Block diagram of Optical Device 'A'

Here the given input intensity of incident light on it is 3I due to I_3.the other source of light from C.L (of standard intensity I) is added at the point a_1, with the help of beam combiner (B.C). The combined beam of intensity 4I (3I for I_3, I for C. L in total 3I+I=4I) is split into two beams at the point a_2 with the help of 50% beam splitter (B.S). Now, light of intensity 2I from the point a_2 is again split at the point a_3. Finally, the light from the point a_3 of intensity I is added to the optical switch "F_2" (**Table-4.4.1**).

Table-4.4.1: Intensity level at different points and final output intensity of optical device "A"

Input intensity	At the Specific point	With the help of B.C. (Beam Combiner) Or B.S. (Beam splitter)	Output Intensity of Light at specific point	Connected optical switch
3I	a_1	B.C.	4I	
4I	a_2	B.S.	2I	
			2I	
2I	a_3	B.S.	I	F_2
			I	

Optical device "B" (fig-4.4.3.)

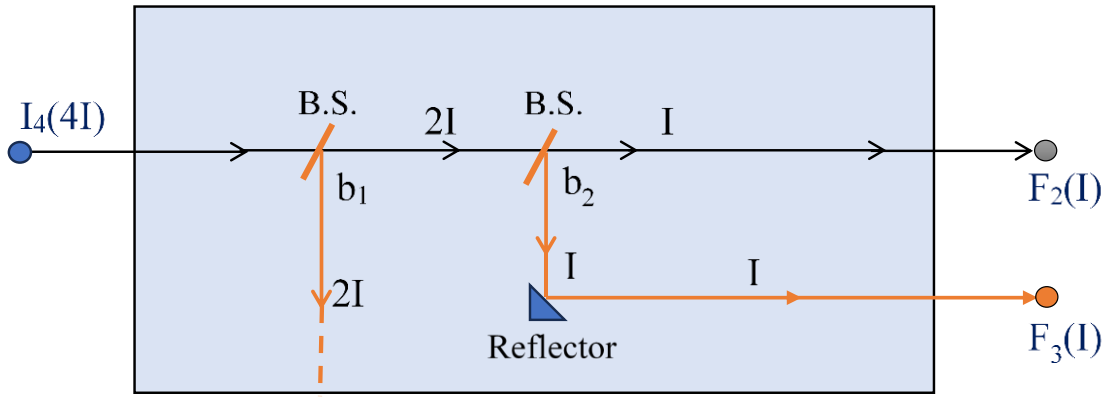

Fig. -4.4.3: Block diagram of Optical Device 'B'

Here the given input intensity of incident light on it is 4I due to I_4. This light is split into two parts of equal intensity 2I at the point b_1 by B.S. (50% beam splitter). Now, of intensity 2I moves forward to the point b_2. Now at the point b_2 light is again split into parts of same intensity I. They are separately joined to the optical switches "F_2" & "F_3" (**Table-4.4.2**).

Table-4.4.2: Intensity level at different points and final output intensity of optical device "B"

Input intensity	At the Specific point	With the help of B.C. (Beam Combiner) Or B.S. (Beam splitter)	Output Intensity of Light at specific point	Connected optical switch
4I	b_1	B.S.	2I	
			2I	
2I	b_2	B.S.	I	F_2
			I	F_3

Optical device "C" (fig-4.4.4.)

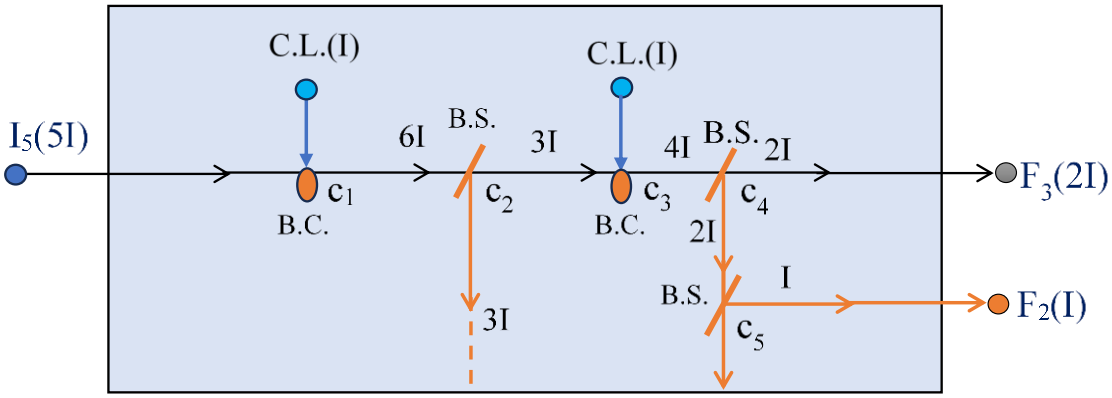

Fig. -4.4.4: Block diagram of Optical Device 'C'

The given input light intensity on it is 5I due to I_5. This light and another polarized light from C.L are combined at the point c_1 with the help of B.C. Now intensity of combined beam is 6I (5I for I_5, I for C.L in total 5I+I=6I). Now using B.S this combined beam of intensity 6I is split at the point C_2. As a result, the light of intensity 3I propagates to the point C_3 and at this point presence of C.L and with the help of B.C this light changes its intensity level 3I to 4I. This present light of intensity 4I from the point C_3 is split into two equal parts with the help of B.S at the point C_4. Then one (which intensity level is of 2I) of them is directly joined to optical switch "F_3" and another part is again split at the point C_5 by B.S. Now light of intensity I from the point C_5 is connected with optical switch "F_2" (**Table-4.4.3**).

Table-4.4.3: Intensity level at different points and final output intensity of optical device "C"

Input intensity	At the Specific point	With the help of B.C. (Beam Combiner) Or B.S. (Beam splitter)	Output Intensity of Light at specific point	Connected optical switch
5I	c_1	B.C.	6I	
6I	c_2	B.S.	3I	
			3I	
3I	c_3	B.C.	4I	
4I	c_4	B.S.	2I	F_3
			2I	
2I	c_5	B.S.	I	F_2
			I	

Optical device "D" (fig-4.4.5.)

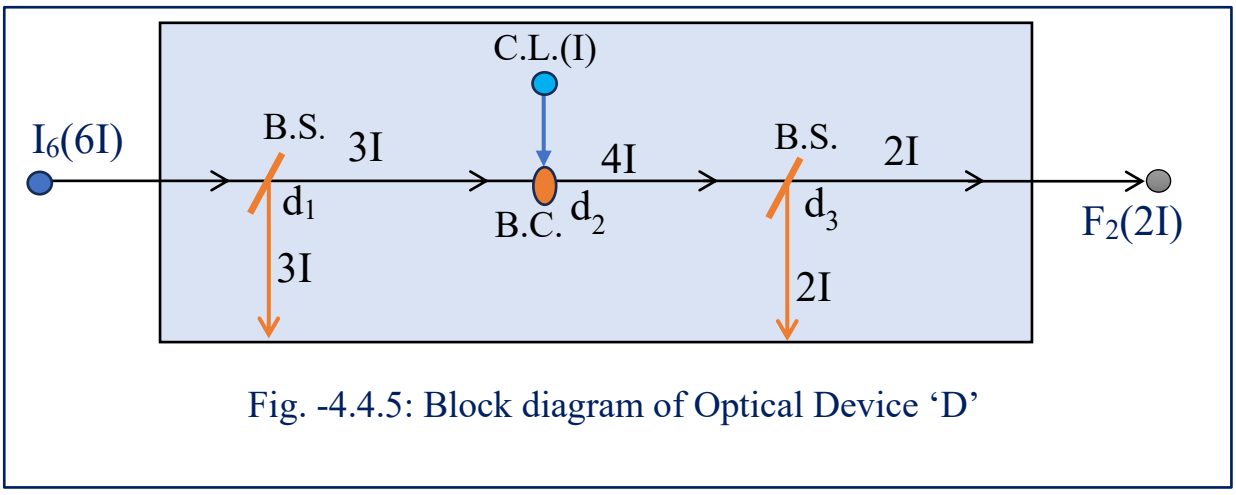

Fig. -4.4.5: Block diagram of Optical Device 'D'

Due to I_6 the supplied input light intensity on it is 6I. This light is split into two parts of equal intensity 3I at the point d_1 with the help of B.S. Now light of intensity 3I from the point d_1 is combined with another polarized light coming C.L (I) at the point d_2 using B.C. Now intensity of this combined light is 4I (3I+I). This combined beam is split at the point d_3 using B.S. Now light of intensity 2I from the point d_3 is connected with optical switch "F_2" (**Table-4.4.4**)

Table-4.4.4: Intensity level at different points and final output intensity of optical device "D"

Input intensity	At the Specific point	With the help of B.C. (Beam Combiner) Or B.S. (Beam splitter)	Output Intensity of Light at specific point	Connected optical switch
6I	d_1	B.S.	3I	
			3I	
3I	d_2	B.C.	4I	
4I	d_3	B.S.	2I	F_2
			2I	

Optical device "E" (fig-4.4.6.)

Here supplied input intensity level on it is 7I due to I_7. Now this light is combined with another light from C.L (I) at the point e_1 with the help of B.C. Now intensity level of combined light beam is 8I (7I+I). Using B.S. this combined beam is split into two equal parts at the point e_2. Now new light of intensity 4I coming from the point e_2 is again split into two parts by B.S at the point e_3. One light beam (of intensity 2I) of them is joined into optical switch "F_2" and another light beam from the point e_3 is again split at the point e_4 by B.S. Now there are two emergent lights from this point e_4. One of them (of intensity I) is joined to optical switch "F_3" (**Table-4.4.5**).

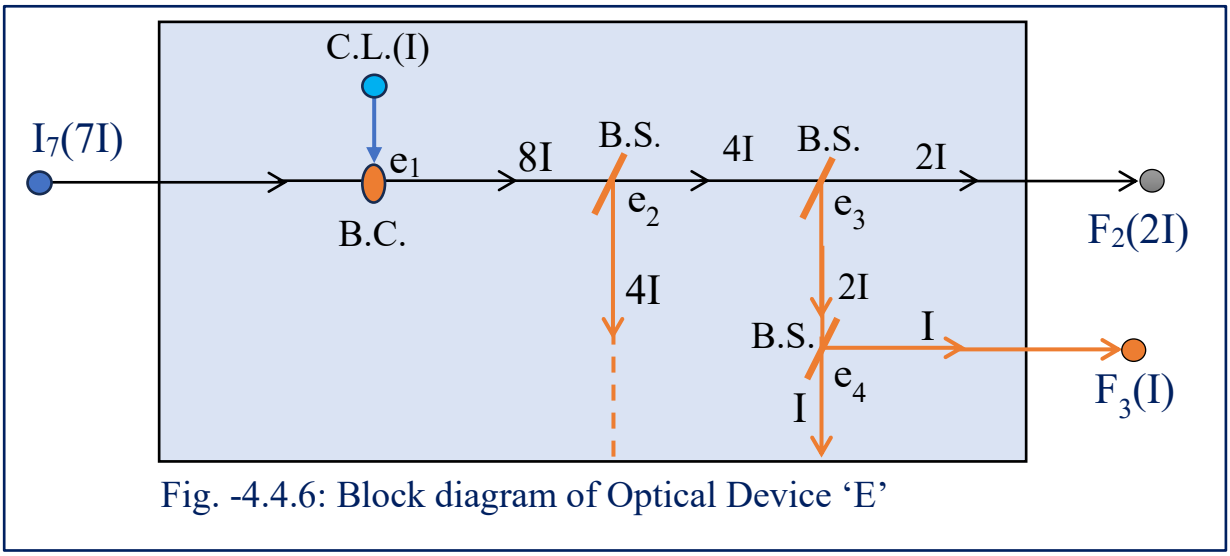

Fig. -4.4.6: Block diagram of Optical Device 'E'

Table-4.4.5: Intensity level at different points and final output intensity of optical device "E"

Input intensity	At the Specific point	With the help of B.C. (Beam Combiner) Or B.S. (Beam splitter)	Output Intensity of Light at specific point	Connected optical switch
7I	e_1	B.C.	8I	
8I	e_2	B.S.	4I	
			4I	
4I	e_3	B.S.	2I	F_2
			2I	
2I	e_4	B.S.	I	F_3
			I	

Optical device "F" (fig-4.4.7.)

Here the given input light intensity on it is 8I due to I_8. Using B.S. this light is split into two parts of equal intensity 4I at the point f_1. Now one light beam of them is again split into two parts with the help of B.S at the point f_2. These two emergent lights of equal intensity 2I from the point f_2 are separately connected with the optical switches "F_2" & "F_3" (**Table-4.4.6**).

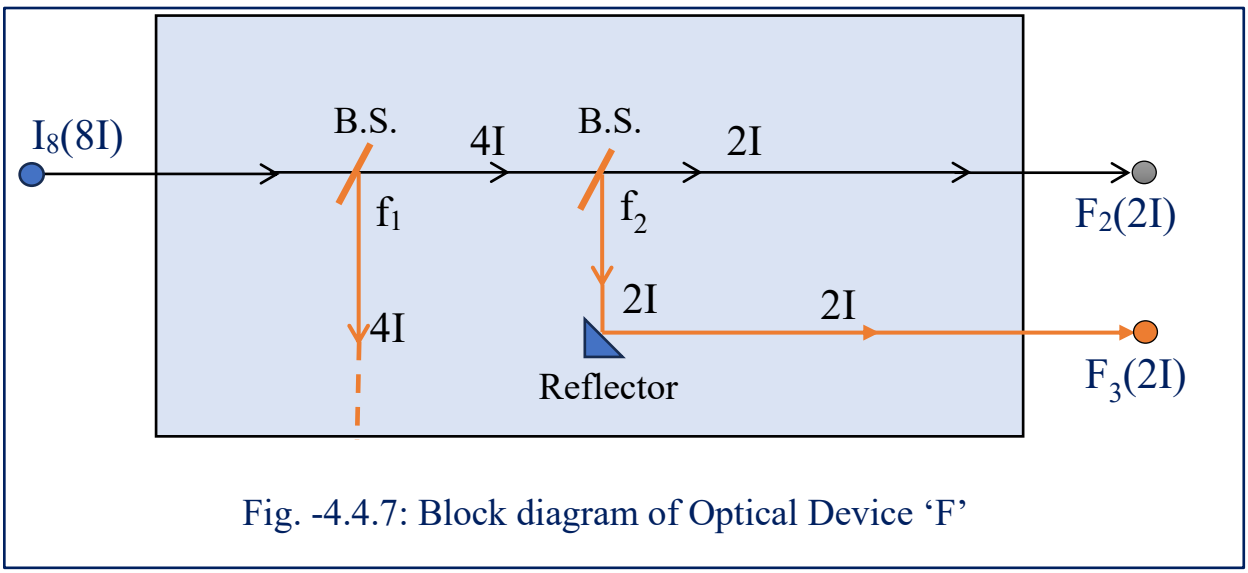

Fig. -4.4.7: Block diagram of Optical Device 'F'

Table-4.4.6: Intensity level at different points and final output intensity of optical device "F"

Input intensity	At the Specific point	With the help of B.C. (Beam Combiner) Or B.S. (Beam splitter)	Output Intensity of Light at specific point	Connected optical switch
8I	f_1	B.S.	4I	
			4I	
4I	f_2	B.S.	2I	F_2
			2I	F_3

Optical device "G" (fig-4.4.8.)

In optical device "G" the given input intensity level on it is 9I due to I_9. Now this light is combined with another component of light from C.L (I) at the point g_1. The intensity of combined beam is 10I (9I+I). This light of intensity 10I is split into two beams at the point g_2 with the help of B.S, where each beam will have intensity level 5I. Now one light beam of them propagates to the point g_3 and combined with light of intensity I coming from C.L using B.C at the point g_3. As a result, we get a combined beam of intensity 6I (5I+I). This combined beam is split into two parts at the point g_4 using B.S. Now we get a new beam of intensity 3I. This beam is combined with another light from C.L with the help of B.C at the point g_5. So, we get a beam of intensity 4I from the point g_5. . At the point g_6 this light is again split into two beams each having intensity 2I. Now one light beam from the point g_6 is again split into two beams at the point g_7 using B.S. We get finally two emergent beams from the point g_7 each of which same intensity I. Now one light (of intensity I) of them is added into optical switch "F_1" (**Table-4.4.7**).

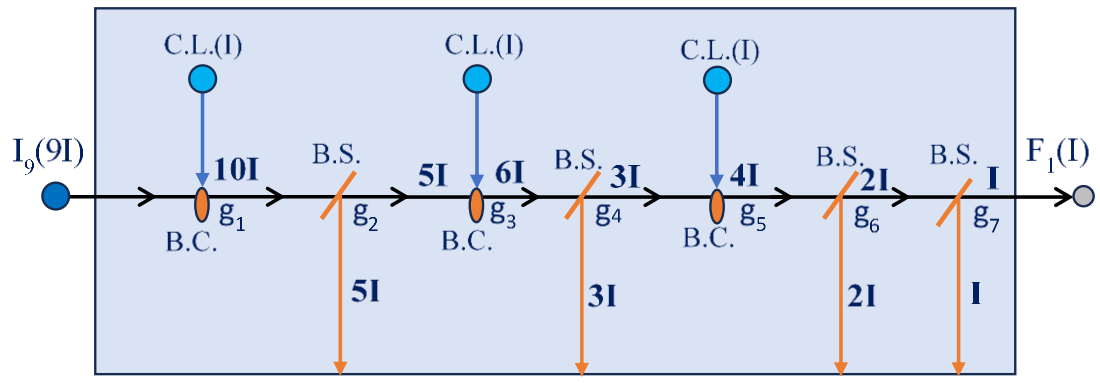

Fig. -4.4.8: Block diagram of Optical Device 'G'

Table-4.4.7: Intensity level at different points and final output intensity of optical device "G"

Input intensity	At the Specific point	With the help of B.C. (Beam Combiner) Or B.S. (Beam splitter	Output Intensity of Light at specific point	Connected optical switch
9I	g_1	B.C.	10I	
10I	g_2	B.S.	5I	
			5I	
5I	g_3	B.C.	6I	
6I	g_4	B.S.	3I	
			3I	
3I	g_5	B.C.	4I	
4I	g_6	B.S.	2I	
			2I	
2I	g_7	B.S.	I	F_1
			I	

4.3.3. Operation of Optical Ternary Encode [Fig.- 4.4.9]

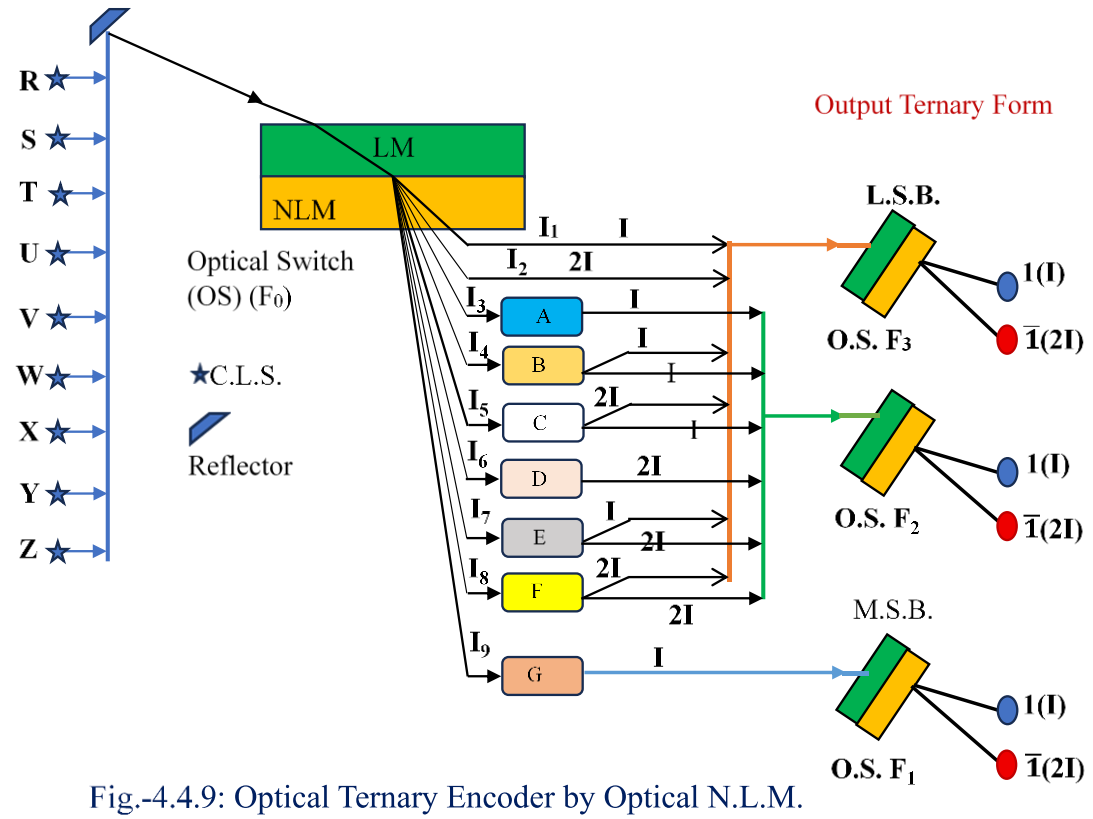

Fig.-4.4.9: Optical Ternary Encoder by Optical N.L.M.

From the relation between input key by name "I_1", "I_2", "I_3", "I_4", "I_5", "I_6", "I_7", "I_8", & "I_9" and output channels"F_1", "F_2", & "F_3" (where "F_3" is low significant bit and "F_1" is most significant bit) via using optical devices named "A", "B", "C", "D", "E", "F", & "G", we can achieve the following situations-

1. When input source "R" is in high state then input intensity of incident light on optical switch (F_0) is I, so input key is I_1 then refracted ray from F_0 follows the path of intensity I, which is directly concerted to the input of optical device "F_3". As a result, output of optical switches "F_1", "F_2", & "F_3" are 0, 0, 1 respectively which represent the ternary form decimal number 1.

2. When input sources "R" & "S" are in high state then input intensity of incident light on optical switch (F_0) is 2I, so input key is I_2 then refracted ray from F_0 follows the path of intensity 2I, which is directly joined to "F_3". As a result, output of optical switches "F_1", "F_2", & "F_3" are 0, 0, 1 respectively which represent the ternary form decimal number 2.

3. When "R", "S" & "T" are in high state then input intensity of incident light on optical switch (F_0) is 3I, so input key is I_3 then refracted ray from F_0 follows the path of intensity 3I, which is directly joined to the optical switch "F_2" via optical device "A". So that input intensity of "F_2" is I. As a result, output of optical switches "F_1", "F_2", & "F_3" are 0, 1, 0 respectively which represent the ternary form decimal number 3.

4. When input sources "R", "S", "T" & "U" are in high states, then refracted ray from optical switch (F_0) along the path of intensity level 4I, as input key is I_4, in front of which is an optical device "B". The two outputs of "B" are path of same intensity level I which are connected with "F_2" & "F_3". As a result, output of optical switches "F_1", "F_2", & "F_3" are 0, 1, 1 respectively which represent the ternary form decimal number 4.

5. When input sources "R", "S", "T", "U", & "V" are in high states, then refracted ray from optical switch (F_0) along the path of intensity level 5I, as input key is I_5 and it is connected with optical switches "F_2", & "F_3" via optical device "C". The two outputs of "C" are path of intensity I & 2I which are connected with "F_2" & "F_3" respectively. Then output of optical switches "F_1", "F_2", & "F_3" are 0, 1, 1 respectively which represent the ternary form decimal number 5.

6. When input sources “R”, “S”, “T”, “U”, “V” & “W” are in high states, then refracted ray from optical switch (F_0) along the path of intensity level 6I, as input key is I_6. Now an optical device “D” is placed in front of path of intensity 6I. The property optical device “D” is such that when input intensity of it is 6I then output from it 2I, which acts as only input of “F_2”. So, output of “F_1”, “F_2”, & “F_3” are 0, 1, and 0 respectively which represent the ternary form decimal number 6.

7. When input sources “R”, “S”, “T”, “U”, “V”, “W” & “X” are in high states, then refracted ray from optical switch (F_0) along the path of intensity level 7I, as input key is I_7. Now I_7 is connected with optical device “E” then two outputs of intensity level 2I & I of “E” are again connected with “F_2” & “F_3” respectively. Now output form of “F_1”, “F_2”, & “F_3” are 0, 1, 0 respectively which represent the ternary form decimal number 7.

8. When input sources “R”, “S”, “T”, “U”, “V”, “W”, “X” & “Y” are in high states, then refracted ray from optical switch (F_0) along the path of intensity level 8I, as input key is I_8. Now input key is I_8 is joined with optical device “F”, where two outputs of same intensity 2I are also connected with “F_2”, & “F_3”. Now output form of “F_1”, “F_2”, & “F_3” are 0, 1, 1 respectively which represent the ternary form decimal number 8.

9. When all input sources (“R”, “S”, “T”, “U”, “V”, “W”, “X, “Y” & “Z” are in high state then input intensity of incident light on optical switch (F_0) is 9I. Hence input key is I_9 and refracted ray from F_0 follows the path of intensity 9I, which is again associated with an optical device “G”. Here it is noted that when input intensity of “G” is 9I then output intensity of “G” is only I. This output of “G” is again connected with only optical device “F_1”. So, for input intensity 9I the output of form of “F_1”, “F_2”, & “F_3” are 1, 0, 0 respectively which represent the ternary form decimal number 9.

Ternary conversion of decimal number 1 to 9 is shown in **Table-4.4.8**. Also, python computational simulation is shown in **Figure -4.4.10** & **Figure-4.4.11**.

Table –4.4.8: Input versus Output Ternary Form of Optical Ternary Encoder

Input Decimal Number	Number of any lighted coherent sources	Total input intensity on optical switch	Name of the output (O/P) intensity path from optical switch	Intensity of the O/P intensity path from optical switch	Name of the connecting optical device on the fixed intensity path	O/P intensity from optical device at specific point	Con-nect-ed optic-al swit-ch	Output Ternary form		
								F_1 MSB	F_2	F_3 LSB
0	0	0	-	-	-	-	-	0	0	0
1	1	I	I_1	I	-	I	F_3	0	0	1
	2	2I	I_2	2I	-	2I	F_3	0	0	$\bar{1}$
3	3	3I	I_3	3I	A	I	F_2	0	1	0
4	4	4I	I_4	4I	B	I	F_2	0	1	1
						I	F_3			
5	5	5I	I_5	5I	C	I	F_2	0	1	$\bar{1}$
						2I	F_3			
6	6	6I	I_6	6I	D	2I	F_2	0	$\bar{1}$	0
7	7	7I	I_7	7I	E	I	F_3	0	$\bar{1}$	1
						2I	F_2			
8	8	8I	I_8	8I	F	2I	F_2	0	$\bar{1}$	$\bar{1}$
						2I	F_3			
9	9	9I	I_9	9I	G	I	F_1	1	0	0

Here in this scheme for coding of decimal number to ternary number by optical ternary encoder of which rudimentary foundation is optical switch. So, this ternary encoder is wholly all- optical in nature. As a result, speed of operation of this optical ternary encoder is very high compare with electronic encoder. On the other hand, when we can express (2^n-1) different signals with the help of n bit binary state at the same time we can express (3^n-1) different signals by same n bit ternary state. In electronic encoder for coding of decimal number definite key has to be pressed but here in optical ternary encoder to code particular decimal number concerned number of any optical input sources (each of same and standard intensity I) are to be kept on HIGH state. Thus, this proposed optical ternary encoder has as in one side speedy operation, highest number of different signal encoder with respect to binary encoder for same fixed bit and other side lays easy mechanism compare to electronic encoder. This scheme will be highly applicable in any N.L.M. based optical communication and optical processing system. The optical circuit used in **fig-4.4.9** is basic building block of 3-bit ternary encoder. It is able to code decimal number 1 to 26 whereas 3-bit binary encoder is able to code decimal number 1 to 7 only. Here in this scheme, we show ternary conversion decimal number 1 to 9.

In this optical ternary encoder, there are three states namely **0, 1 and $\bar{1}$**. We represent 0 by absence of light, we represent **1 and $\bar{1}$** by presence of light of intensity level I and 2I respectively. Here all input sources are in same standard intensity of I. The input light beam is polarized (preferably a laser beam from Nd: YAG source with wavelength of 1.064 μm) and should be coherent to activate N.L.M. (CS_2 or pure silica glass) and optical functioning.

To create optical switch if we take only N.L.M. then incident polarized light (laser) upon the N.L.M. (of high relative refractive index with respect to air) is deflected from N.L.M. as large variation. To reduce this large variation of deflected output beam, we should take linear and nonlinear material together as optical switch.

4.3.4. Python simulation result of OTE

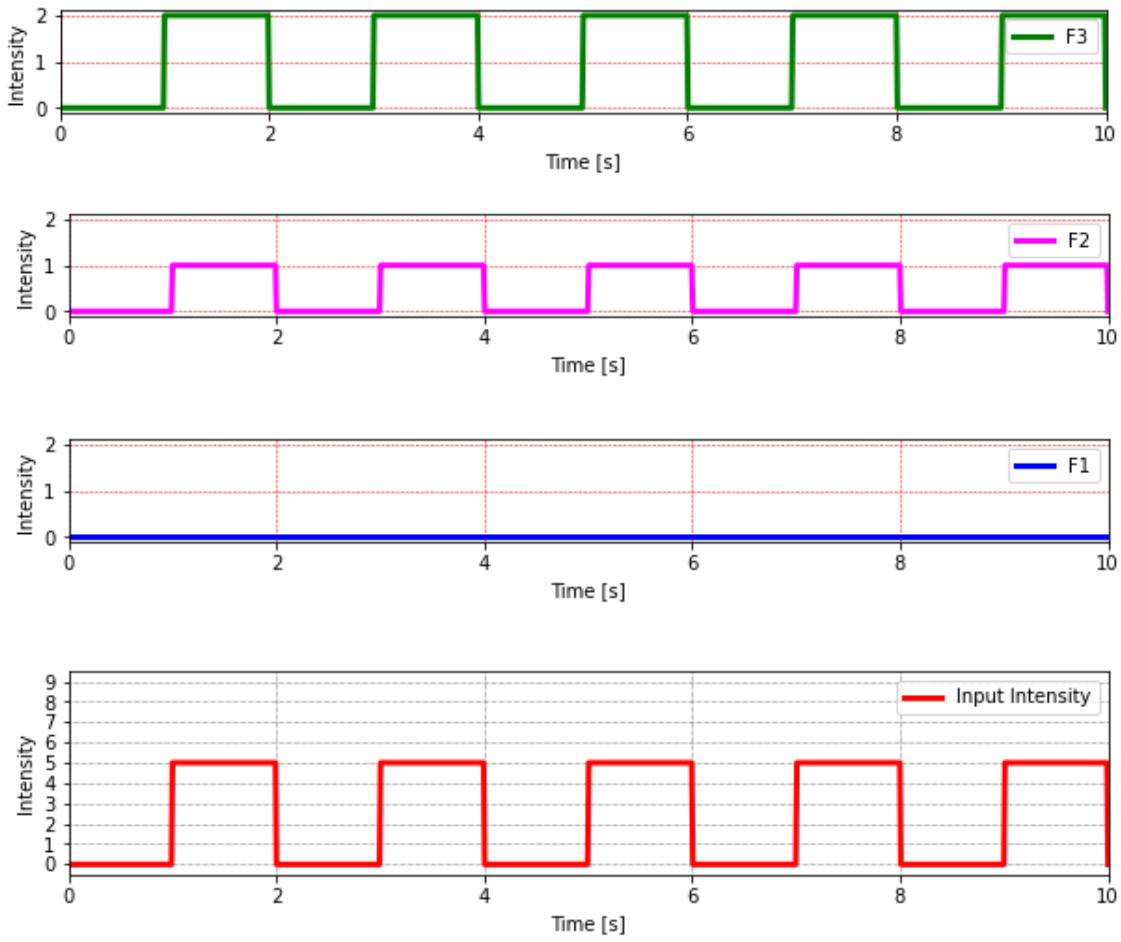

Fig.-4.4.10: Python computational simulation for conversion of decimal number **5** to its equivalent ternary form **01$\bar{1}$** [where F_1=MSB & F_3=LSB].

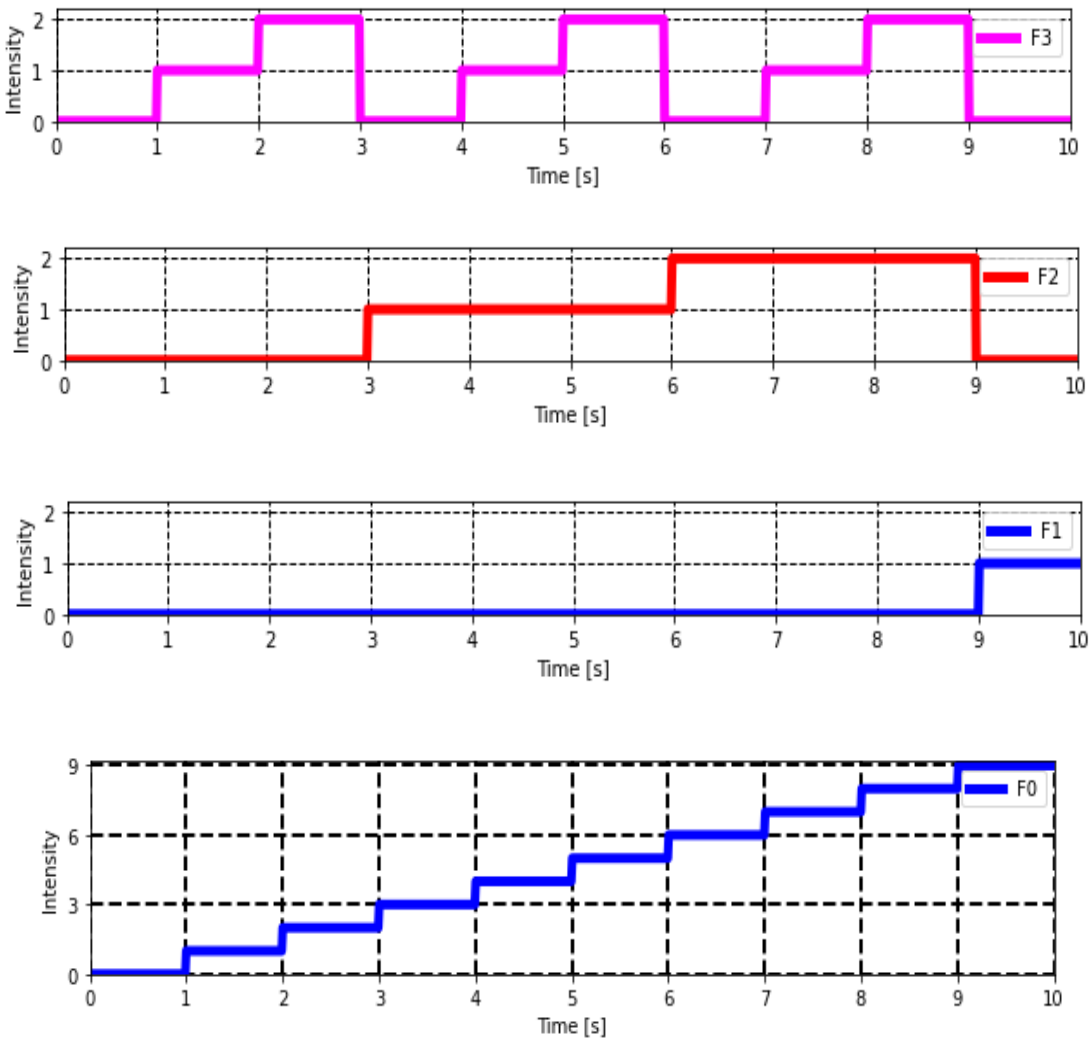

Fig.-4.4.11: Python computational simulation for conversion of decimal number **1-9** to its equivalent ternary form [where F_0=input intensity- level F_1= MSB & F_3=LSB].

4.5. Kerr-Based Optical Circuit for Ternary to Decimal Conversion

In data processing and computing systems, encoding and decoding are crucial processes. In recent decades, photonic processing has emerged as a promising technology for data processing and computation. In the present study, we propose an all-optical decoder for converting ternary code into its equivalent decimal number. In the present scheme, a Kerr type optical nonlinear material is used as an optical switch or regulator. Multiple coherent laser sources of single intensity 'I', beam combiner and some light absorbing materials are properly utilized to implement the proposed scheme. The presented scheme is purely optical in nature. As a result, three benefits can be enjoyed from this proposed optical ternary decoder. Firstly, it occupies a high degree of operational speed. Secondly, $(3^n - 1)$ different input signals can be decoded by 'n' bits ternary states [here number of output channel of optical ternary decoder $(m) < 3^n - 1$ where n = number of bit or number of input channels of proposed optical ternary decoder]. Thirdly, the conventional electronic decoder (binary to decimal) is built on an electronic AND gate and electronic NOT gate, but no gate, either electronic or optoelectronic or only optical, is required in the presented scheme. Thus, the proposed optical circuit can be assigned in the field of optical computing system and communication process.

The data transfer rate is increasing every day. So, it demands a computing device that can provide high processing speed. This is possible by shifting to the optical domain from the electro-optic and most definitely electronic one. Over the past few decades optics has been resolutely presiding as a significant and successful applicant as the efficient information carrier for data technology cum communication of information. This upgradation will also take the concept of multi-valued logic (radix > 2) [17-18]. Here in this paper, we theoretically convert especially decoded ternary form or code to its decimal equivalent by utilizing the switching potency of the optical Kerr nonlinear material [4,5,6,7,8,13,18,19]. In this proposed architecture, input code is of three optical states i.e. ternary form like as 0(zero), 1(one) and $\bar{1}$ (one bar) where they are represented as an absence of light, and presence of polarized light (Nd: YAG acts as laser source) of standard intensity level 'I' & '2I', respectively. The output of optical Ternary Decoder (OTD) is denoted by 'nI' (here 'n' a is natural number). For each value of 'n', there is a separate output line from the device. For particular ternary form, output line 'nI' signifies the decimal number 'n' (block diagram of OTD is shown in **Fig.-4.5.1**).

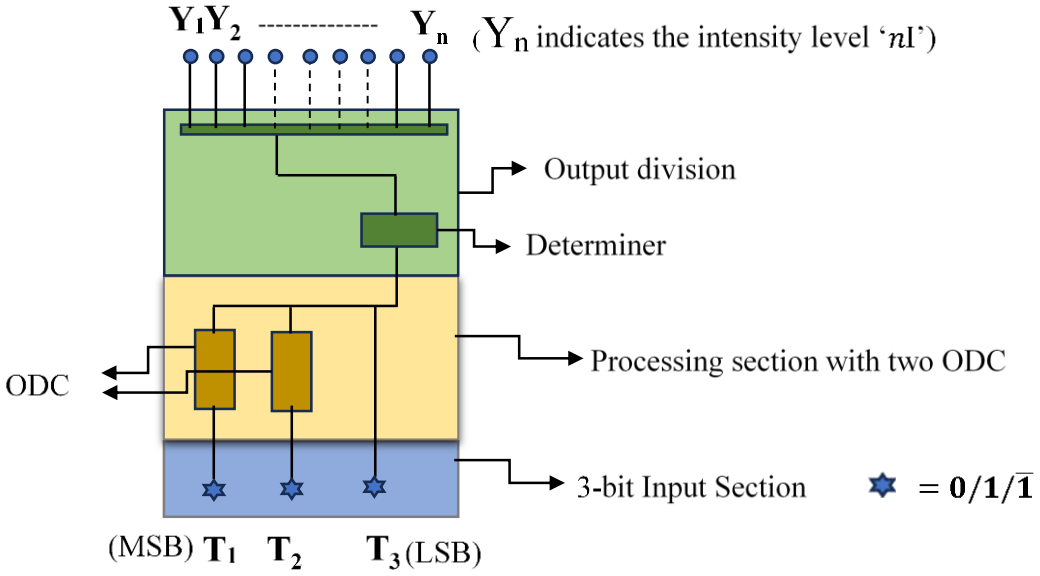

Fig.-4.5.1: Block diagram of optical ternary decoder (OTD)

4.5.1. Kerr Optical Regulator [Fig.-4.5.2]

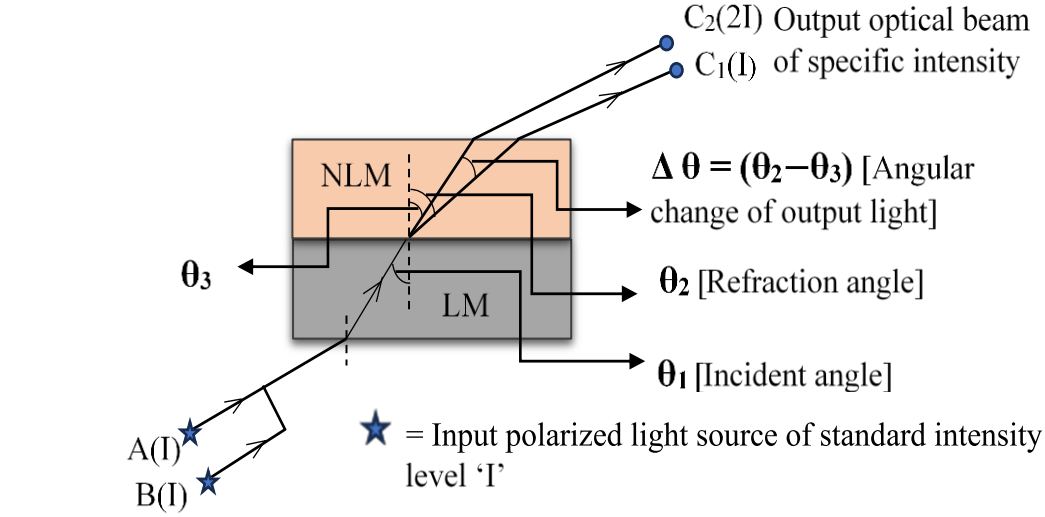

Fig.-4.5.2: Kerr switch or regulator with help of optical nonlinear material (NLM)

4.5.2. Optical divider circuit (ODC) [Fig. -4.5.3]

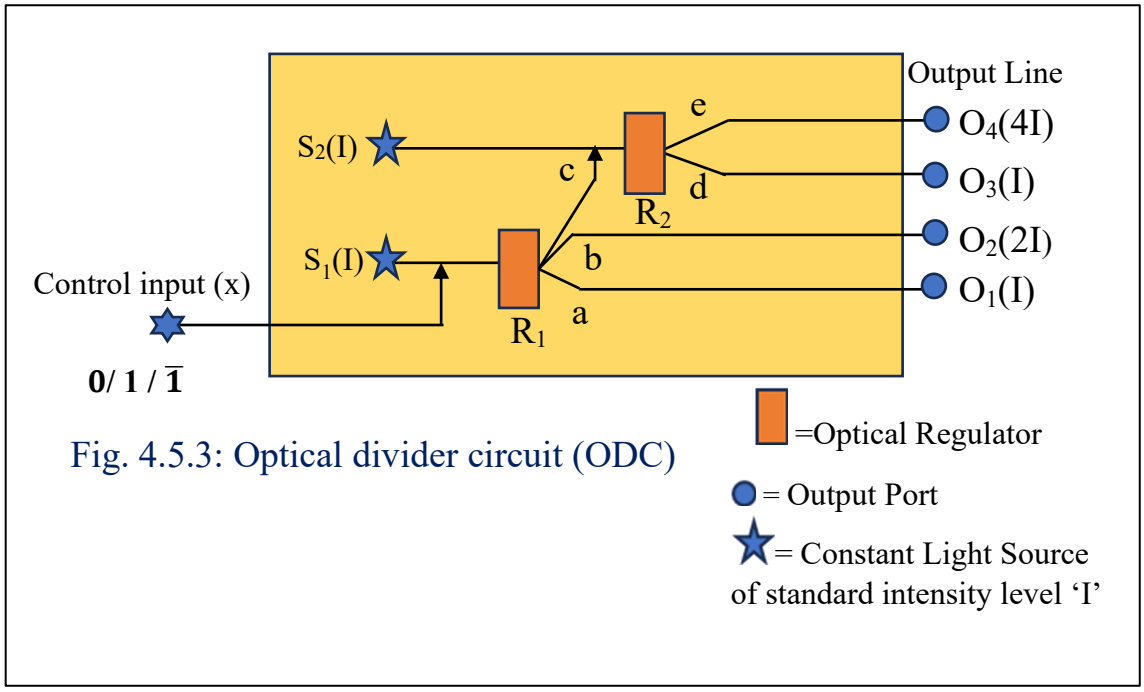

Fig. 4.5.3: Optical divider circuit (ODC)

Optical divider circuit consist of two optical regulators (R_1 and R_2), two coherent light sources of standard intensity level 'I' (S_1 and S_2) and one control input 'x' where optical state of 'x' is either 0(zero) or 1(one) or $\bar{1}$(one bar). The structure of ODC is depicted in **Fig.-4.5.3**. Here the optical regulator (OR) 'R_1' activates any one port out of three different lines 'a', 'b' and 'c' according to the input optical state of control input (x). Similarly, OR 'R_2' provides output lines either 'd' or 'e' according to absence or presence of active optical path 'c', which acts as controller of OR 'R_2'. Now working principle of ODC is explained as-

When the optical state of control input 'x' is 0(zero), there are always only two output lines as O_1 and O_3 due to the presence of $S_1(I)$ and $S_2(I)$. But when optical state of 'x' is 1(one) and $\bar{1}$ (one bar) then the light beam from R_1 is directed to the line 'b' or 'c' of intensity level '2I' or '3I' accordingly. As a consequence, for 'x' =1, there are two active output lines 'O_2' and 'O_3'. Again, if the optical value of 'x' is $\bar{1}$ (one bar), then the refracted output line from 'R_1' is along the direction 'c' of intensity level '3I'. In this case, the active output port of ODC is only 'O_4'. The entire result of ODC depending upon input optical state of control input is shown in **Table-4.5.1**. Now, utilizing this ODC, an all-optical ternary decoder is implemented for ternary to decimal conversion.

Table – 4.5.1: [Input state versus active output line of ODC (where active output port of any intensity level is denoted by solid circle)]

Input	Output of optical divider circuit (ODC)			
	O_1 (I)	O_2 (2I)	O_3 (I)	O_4 (4I)
0 (zero)	●		●	
1(one)		●	●	
$\bar{1}$(one bar)				●

4.5.3. Design of an all-optical Ternary Decoder

In this paper an all-optical ternary decoder (OTD) device for the conversion of ternary form to an equivalent decimal number has been proposed. This proposed scheme is developed based on the optical divider circuit (ODC), which is depicted in fig.- 3. Here, a 3-bit ternary decoder is designed with the help of two ODCs in number. As a result, 0 to maximum (3^3-1) = 26 numbers coded signal (form) can be decoded into its original equivalent decimal number by the presented circuit but here only eighteen number output lines are designed i.e. 0—18 decimal numbers are decoded from equivalent ternary code (schematic diagram of all-optical 3-bit ternary decoder is shown in **Fig.- 4.5.4**). Here, T_A, T_B and T_C are three control input ports where T_A and T_C function as the most significant bit (MSB) and low significant bit (LSB) respectively in the presented scheme. Now to implement optical ternary decoder, input port T_C (LSB) is directly connected to the determiner ('D') via the point O_C. Input port T_B is connected with a determiner through optical divider $[(ODC)_B]$. Here, $S_1 = S_2 = 2I$. When optical state of input port T_B = 0, 1 and $\bar{1}$ (one bar) then there are output lines namely 'B_1' & 'B_3', 'B_2' and 'B_4' respectively. The intensity level of 'B_1', 'B_2', 'B_3' and 'B_4' are '2I', '3I', '2I' and '4I' orderly. Here, 'B_1' and 'B_3' are blocked by light absorbing material and 'B_2' & 'B_4' are adjoined to the point 'O_B'. Similarly, the input port 'T_A' (MSB) is connected with a determiner via another optical divider circuit $[(ODC)_A]$, where $S_1 = S_2 = 8I$. When T_A= 0, there are output line A_1 [from R_1 of $(ODC)_A$] and A_3 [from R_2 of $(ODC)_A$] of the same intensity level '8I'. For T_A= 1, the output line A_2 is activated at intensity level '9I' but other rest output lines of $(ODC)_A$ are inactive. Again, for T_A= $\bar{1}$, then only one output line A_4 of intensity level '18I' will be

effective. In this design, A_1 & A_3 are obstructed by light absorbing material. Only A_2 and A_4 are continued to the point 'O_A'.

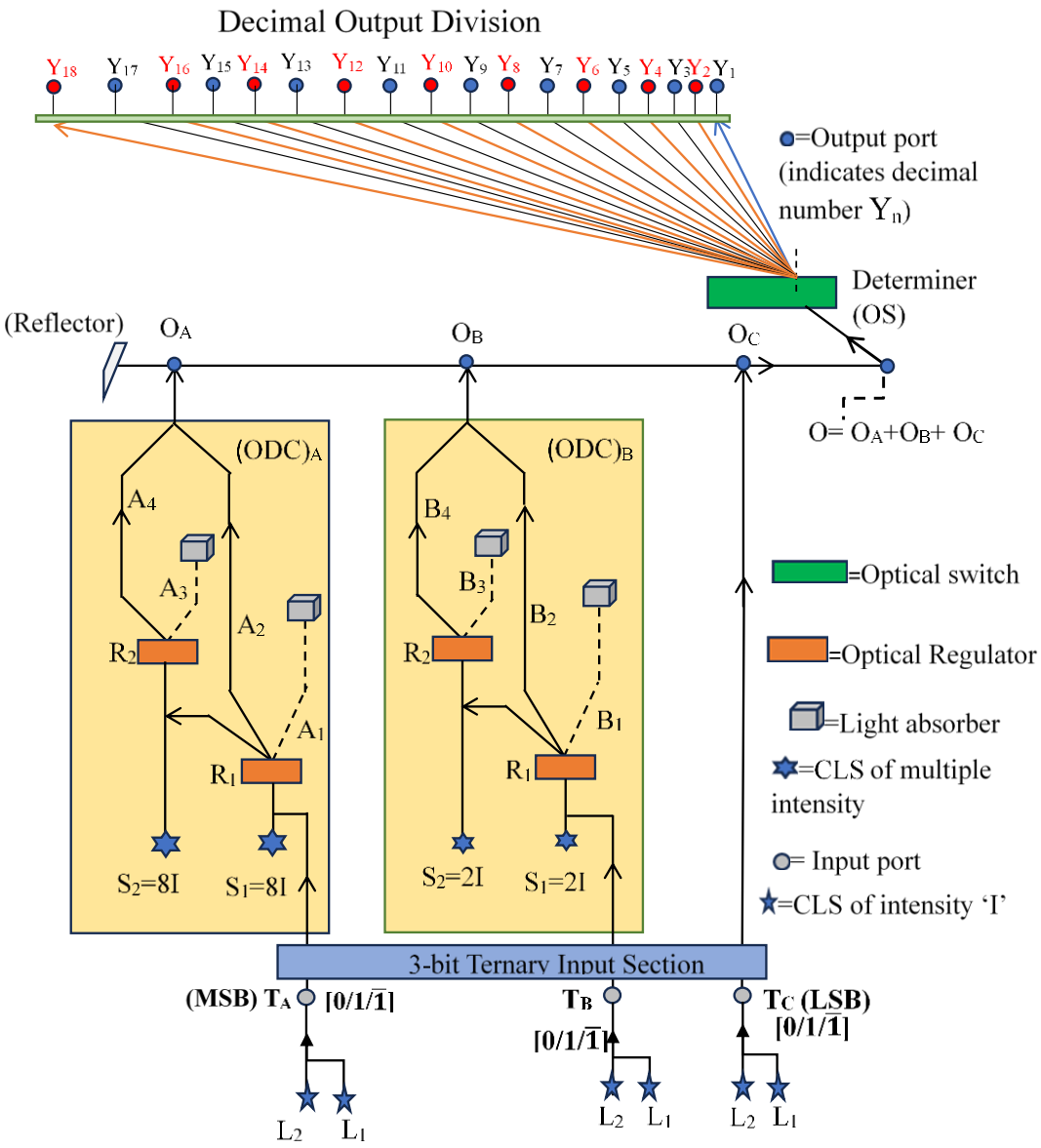

Fig. 4.5.4: (schematic diagram of all-optical 3-bit ternary decoder)

So, total input intensity into the determiner (it is basically an optical switch or regulator) at the point 'O' (I_O)is calculated by-

$I(O)=I(O_A)+I(O_B)+I(O_C)$. Now for different optical states of each input port of the ternary input section versus intensity level at the specific points O_A, O_B and O_C are shown in **Table- 4.5.2(a)**. Now according to total intensity at the point 'O', determiner select several marking output port Y_1 to Y_{18}, where specific output port indicates specific intensity level i.e. Y_n represents intensity level 'nI', which means it represents the decimal number 'n'. Now for a particular ternary form, total intensity at 'O' has to be calculated. Then depending upon intensity level at 'O', light will glow at output port Y_n, where 'n' indicates the equivalent or original decimal number of concerned ternary form (code). Ternary form versus equivalent decimal number is shown in **Table -4.5.2(b)**.

Table. -4.5.2(a): [Input optical state versus intensity level at specific points of the all-optical ternary decoder]

Control Input	Input optical state	Name of the output line from ODC	Intensity at the specific points		
			O_A	O_B	O_C
(MSB)T_A	0 (zero)	A_1 & A_3	0	-	-
	1 (one)	A_2	9I	-	-
	$\bar{1}$ (one bar)	A_4	18I	-	-
T_B	0 (zero)	B_1 & B_3	-	0	-
	1 (one)	B_2	-	3I	-
	$\bar{1}$ (one bar)	B_4	-	6I	-
(LSB)T_C	0 (zero)	-	-	-	0
	1 (one)	-	-	-	I
	$\bar{1}$ (one bar)	-	-	-	2I

Table. -4.5.2(b): [Ternary form versus corresponding output intensity level cum decoding decimal number]

3-bit Ternary form			Intensity level at the specific points			Total input intensity into determiner at the point 'O'= $O_A+O_B+O_C$	Decoding decimal number
(MSB)T_A	T_B	(LSB)T_B	O_A	O_B	O_C		
0	0	0	0	0	0	0+0+0=0	0
0	0	1	0	0	I	0+0+I=I	1
0	0	$\bar{1}$(one bar)	0	0	2I	0+0+2I=2I	2
0	1	0	0	3I	0	0+3I+0=3I	3
0	1	1	0	3I	I	0+3I+I=4I	4
0	1	$\bar{1}$(one bar)	0	3I	2I	0+3I+2I=5I	5
0	$\bar{1}$ (one bar)	0	0	6I	0	0+6I+0=6I	6
0	$\bar{1}$(one bar)	1	0	6I	I	0+6I+I=7I	7
0	$\bar{1}$(one bar)	$\bar{1}$(one bar)	0	6I	2I	0+6I+2I=8I	8
1	0	0	9I	0	0	9I+0+0=9I	9
1	0	1	9I	0	I	9I+0+I=10I	10
1	0	$\bar{1}$(one bar)	9I	0	2I	9I+0+2I=11I	11
1	1	0	9I	3I	0	9I+3I+0=12I	12
1	1	1	9I	3I	I	9I+3I+I=13I	13
1	1	$\bar{1}$(one bar)	9I	3I	2I	9I+3I+2I=14I	14
1	$\bar{1}$(one bar)	0	9I	6I	0	9I+6I+0=15I	15
1	$\bar{1}$(one bar)	1	9I	6I	I	9I+6I+I=16I	16
1	$\bar{1}$(one bar)	$\bar{1}$(one bar)	9I	6I	2I	9I+6I+2I=17I	17
$\bar{1}$(one bar)	0	0	18I	0	0	18I+0+0=18I	18

4.5.4. Operation of optical 3-bit Ternary Decoder (ternary to decimal)

To decode ternary form to its original equivalent decimal number, input ternary form as optical state ($0/1/\bar{1}$) at different input port has to be kept in the input section of the 3-bit ternary decoder. According to the value of T_A, T_B & T_C, the determiner acquires total input intensity at 'O'. Depending upon it, there is a specific shining output port of intensity level 'nI', where 'n' indicates the decimal number 'n'. Now entire operation of OTD will be understandable from the following example-For changing ternary form $11\bar{1}$ to its decimal number, input ports T_A (MSB) & T_B are illuminated with same intensity level 'I' and input port T_C (LSB) with intensity level '2I'. As 'R_1' of $(ODC)_A$ and 'R_1' of $(ODC)_B$ are actuated with intensity level 'I', two light beams are refracted along the path 'B_2' and 'A_2' of intensity level '3I' and '9I' respectively. Now total intensity at 'O' is = $O_A + O_B + O_C$ =9I+3I+2I=14I. So, determiner will incite the 14^{th} output port i.e. 'Y_n' = 'Y_{14}' or 'n' =14. As an outcome, conversion of ternary form $11\bar{1}$ to its decimal equivalent number is 14. Thus, any ternary form is decoded to its equivalent decimal number by the help of proposed device OTD. Python computational simulation is shown in **Figure-4.5.5(a) and 4.5.5(b)**.

This proposed all-optical ternary decoder (OTD) introduces multi-valued logic into optical computing, enabling high-speed conversion of ternary codes to their decimal equivalents. It offers three key advantages: (1) ultrafast processing due to its all-optical nature, (2) extended decoding range up to $3^n - 1$ for n bits, surpassing binary decoders, and (3) complete elimination of logic gates (AND, NOT, etc.), unlike traditional electronic decoders. This marks a significant step toward advanced, gate-free optical computing systems.

4.5.5. Python simulation result

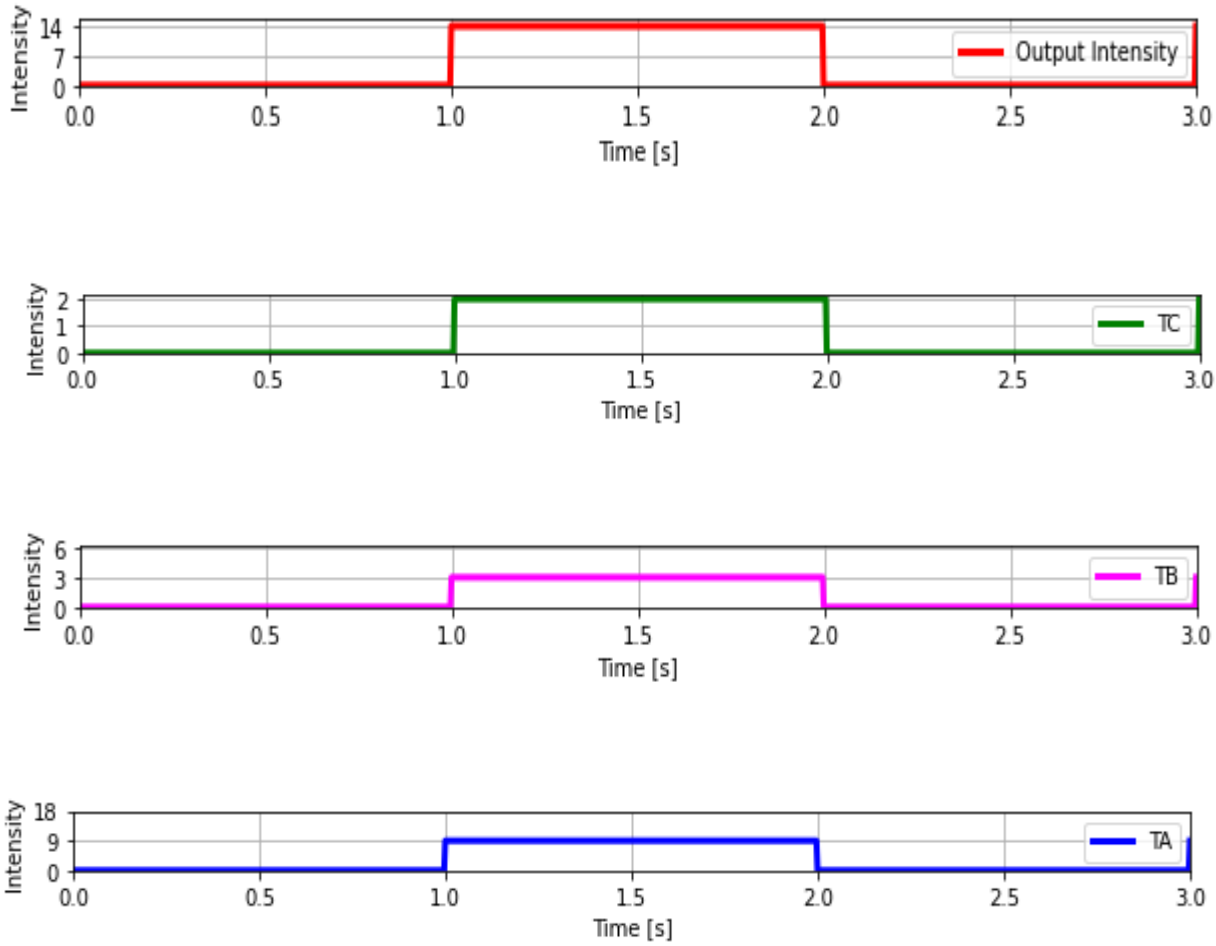

Fig.-4.5.5 (a): Python computational simulation for conversion of ternary number **11$\bar{1}$** to its equivalent decimal number **14** [where T_A=MSB & T_C =LSB].

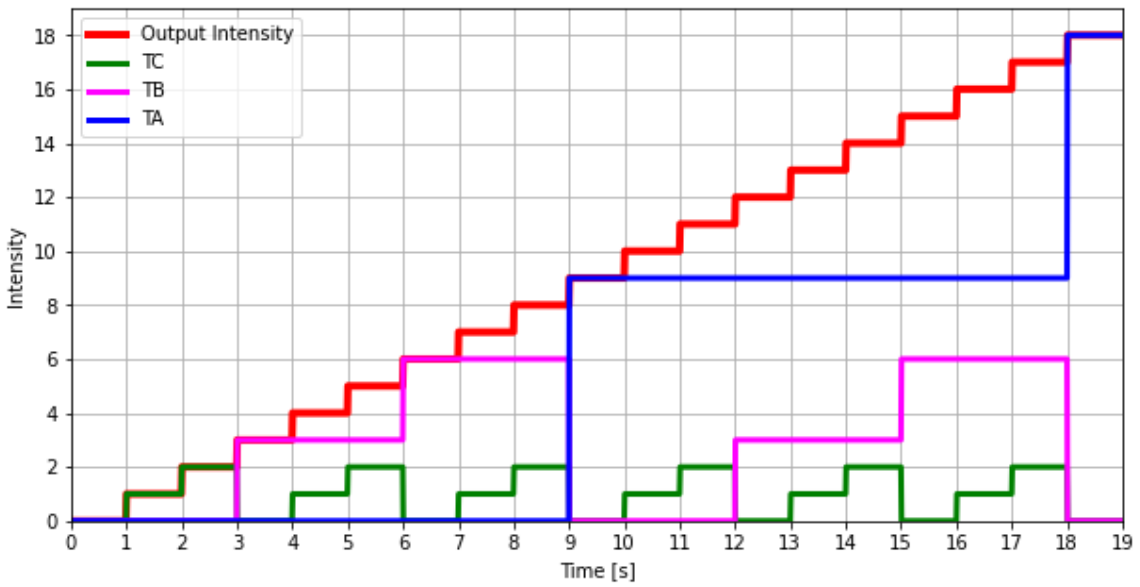

Fig.-4.5.5 (b): Python computational simulation for conversion of ternary number **000-$\bar{1}$00** to its equivalent decimal number **0-18** [where T_A = MSB & T_C = LSB].

4.6. Design of Optical Quaternary Encoder with Kerr-Effect

Optics and photonics offer significant advancements in the rapidly evolving fields of data processing and communication owing to their inherent parallel-processing capabilities. This paper presents a novel all-optical quaternary encoder that efficiently encodes decimal numbers by leveraging the nonlinear switching properties of Kerr-type optical materials. The proposed encoder operates entirely within the optical domain and offers multiple benefits. First, it achieves exceptionally high processing speeds owing to its optical nature. Secondly, it supports the simultaneous encoding of $(4^n - 1)$ different input signals expressed in 'n' bit quaternary states, enhancing parallel data handling. Third, unlike conventional electronic encoders that depend on electronic OR gates, this scheme eliminates the need for both electronic and optical gates, making it a versatile solution for optical communication, all-optical computation, and various photonic-device applications.

The proposed approach underscores the potential for advancing optical technologies and expanding their applicability across diverse fields.

Over the past few decades, optics have emerged as a powerful and essential technology for efficient information and data processing. The inherent parallelism of optical signals provides a significant advantage for high-speed computations and various digital logic operations. Numerous approaches have been proposed to harness photons as high-speed information carriers, enabling arithmetic, algebraic, and logic operations [1, 19-30, 36-50]. In parallel, the field of computing has seen growing interest in multivalued logic (radix > 2), which offers the potential for enhanced data-carrying capacity and faster arithmetic operations [6,17, 51-68]. However, despite the progress in this area, the development of a robust all-optical quaternary encoder remains a challenge and warrants further exploration. Over the decades, various techniques have been developed to manipulate photon propagation. Photonic crystals have emerged as one of the most effective platforms for controlling photon propagation, leading to significant advancements in high-speed information processing. A photonic crystal is an artificial medium composed of materials with varying refractive indices, allowing precise control of photon movement within the structure. Over the years, different photonic crystals—incorporating both linear and nonlinear materials—have been utilized in the design of sequential and combinational logic circuits [30-35]

This paper presents the design of an intensity-based all-optical decimal-to-quaternary code encoder utilizing the switching capabilities of a Kerr-type optical nonlinear material (NLM). In the proposed scheme, decimal values 1, 2, 3, 4, and 5 are encoded using the corresponding intensity levels I, 2I, 3I, 4I, and 5I, which act as the input signals. The output states of quaternary encoders 0, $\bar{0}$ (zero bar) 1, and $\bar{1}$ (one bar) are represented by the absence of light and the presence of light at intensity levels I, 2I, and 3I, respectively. To maintain the required intensity levels, 50% beam splitters and beam combiners are strategically employed [3,7,8]. Section 2 discusses an optical switch or regulator utilizing a Kerr-type positive nonlinear material. Section 3 describes the design of the proposed optical circuit in detail. The operation of the proposed optical scheme is described in Section 4.

4.6.1. Kerr-optical regulator

The crucial element of the proposed device, which relies on an optical switch [2,4,5,10,56] is shown in **Figure-4.6.1**. Here, positive Kerr-type optical nonlinear materials (NLMs) act as an optical switch based on the following equations-

$$n_{NLM} = n_0 + n_2 I \qquad \text{---(1);}$$

$$n_{LM} \sin\theta_1 = n_{NLM} \sin\theta_2 \qquad \text{---(2);}$$

$$P = \frac{\pi \varepsilon_0 n_0 c a^4}{8 n_2 L^2} \qquad \text{---(3);}$$

Here, symbols used in the conventional sense.

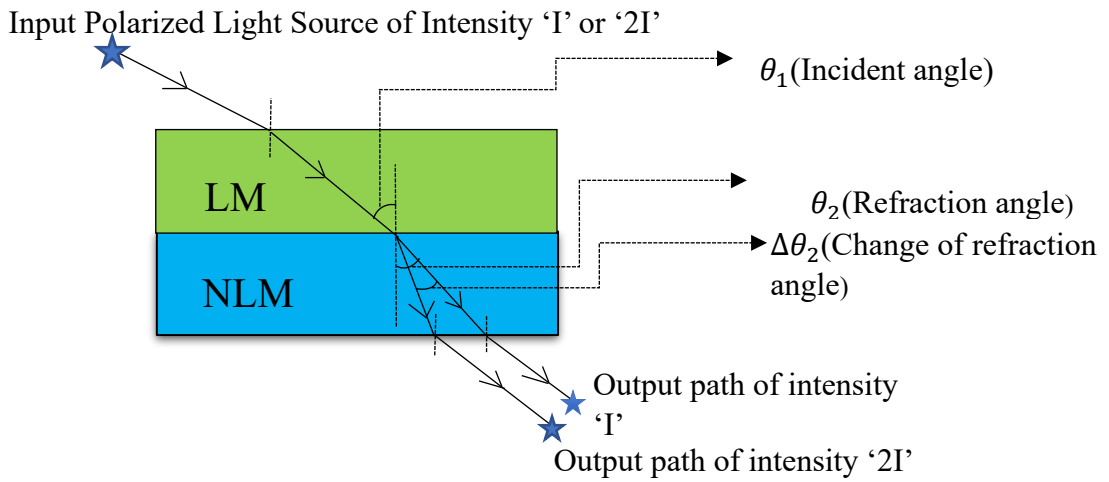

Fig. 4.6.1 Optical linear and nonlinear materials act as an optical switch or regulator

4.6.2. Design of Optical Quaternary Encoder (OQE):

4.6.2.1. Input section:

In the proposed scheme there are 16 numbers of coherent constant light sources (such as i_1, i_2, i_3, i_4, ……i_{16}) each of the same and standard intensity levels 'I.' The proposed quaternary encoder can convert any decimal number into a quaternary form by utilizing decimal numbers 1 to 16. A definite number of light sources must be activated to express a definite decimal number in its quaternary form. Here, a definite decimal number is denoted by a definite number times the standard intensity level, i.e.,1,2,3,4,5, etc. and the decimal number is represented by I,2I,3I,4I,5I. To express a definite decimal number in a quaternary form, a definite number of light sources must be activated in the HIGH state

(i.e., light is present). It should be noted that these 16 constant light sources are coherent. Here, it is noted that the input power level depends on the Kerr coefficient of the selected material. For example, in the case of CS_2, the nonlinear refractive index parameter n_2 is $0.22\times10^{-19}m^2/W$. Using a 10 MW laser with a 1 cm beam radius, the material exhibits significant self-focusing effects at a distance of 10 cm. For pure fused silica, with $n_2=3.2\times10^{-20}m^2/W$, an ordinary laser with 100 mW power and a 50 μm^2 cross-section results in an intensity of approximately 2×10^9 W/m^2.

4.6.2.2. Optical regulator:

An optical switch (M) acts as an optical regulator. The output intensity of 'M' is treated as a decimal number, which is converted into the quaternary form by the process for expressing a definite decimal number and a definite number of C.L., which are in the High state. As a result, depending upon the input intensity level into 'M' there are several output lines of definite intensity level from 'M.' All output lines (of respective definite intensity) are individually connected to a specific optical device of the processing section (which are shown in the Appendix-A, Table. - s2).

4.6.2.3. Processing section

To continue coding gradually 'n' number of decimal numbers into quaternary form, (n− 3) numbers optical devices (all of which are of single input but have single or double output lines) have to be present in the scheme. In our scheme for coding decimal numbers from 1 to 16, (16–3) = 13 optical devices (namely, N, O, P, Q, R, S, T, U, V, X, Y, and Z) are required to complete the process. Here, the characteristics of all-optical devices (O.D) are such that if their input intensity is n4I (n= natural number), then those optical devices are single-input and single-output systems; otherwise, they will be single-input and double-output systems. The working principle of all-optical devices is explained using a block diagram and a relevant table. The optical device named 'N' is the first OD in our scheme. Based on this OD(N), the end user OD 'Z' is developed. Similarly, depending upon OD 'P,' other ODs', 'T, 'and 'U' are founded. Again, depending upon OD 'Q,' other ODs 'W and 'X' are constructed. The optical device 'Y is formed depending on OD' R.' The input and output intensity distribution of optical devices 'N, 'Z, 'P,' 'S,' 'Q,' 'W,' 'R' and 'Y' are depicted in Fig. – 4.6.2.1 to 4.6.2.8 and in Table 4.6.1.1 to 4.6.1.8. Other ODs 'O', 'T', 'U', 'V', and 'X' are shown in the Appendix-A, Fig. – S1.1 to S1.5 and Table s1.1 to s1.5. All optical devices were implemented with the help of a 50% beam splitter (BS), beam combiner (BM), constant light source (CL), and reflector. Here, it is noted that the power losses may occur due to absorption, scattering, and coupling inefficiencies in

the nonlinear material. However, the system compensates for this by using beam splitters, beam combiners, and optical regulators to maintain consistent intensity levels required for encoding.

Optical device 'N' [Fig.-4.6.2.1]

It consists of one input device and one output device. When O.D. 'N' is activated at definite intensity level 4I, then a propagated polarized light beam of that intensity is parted into two beams (each of intensity 2I) at the point 'n_1' with the help of 50% B.S. Then one of them is absorbed and another beam of intensity 2I is confronted with B.S. at the point 'n_2'. As a result, there are two light beams of the same intensity 'I' from that point 'n_2'. One of them is absorbed and the other is treated as the output line ('N_1') of the optical device 'N.' The operation of optical device 'N' is shown in **Table-4.6.1.1**.

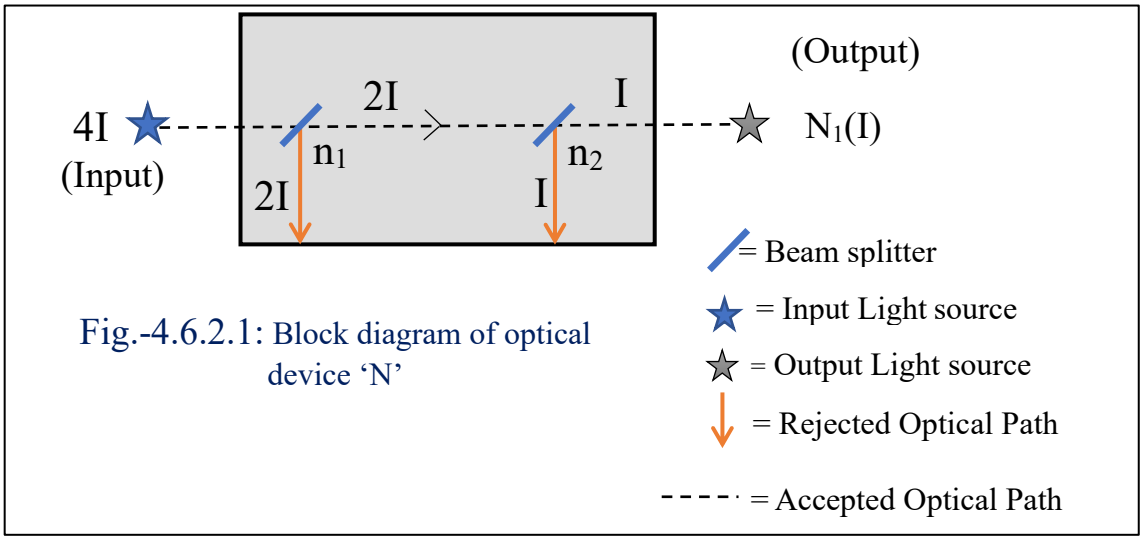

Fig.-4.6.2.1: Block diagram of optical device 'N'

Table – 4.6.1.1: Input intensity versus Output intensity of the optical device 'N'

Name of the specific point of O.D. 'N'	Input intensity into the specific point	Helping element [Beam splitter (B.S.)/ Beam combiner (B.C.)/another O.D.]	Output intensity of progressive light beam from the specific point by the helping element	Name of the output line from the O.D. 'N' (with the intensity level)
n_1	4I	B.S.	2I	
n_2	2I	B.S.	I	N_1(I)

Optical device 'Z' [Fig.-4.6.2.2]

It is also a single-input (16I) and single-output (I) device. It is formed with the help of OD 'N'. The OD 'Z' functionates at input intensity level 16I. After the activation of 'Z' there is output intensity level 'I' from it [which is revealed by **Table - 4.6.1.2**].

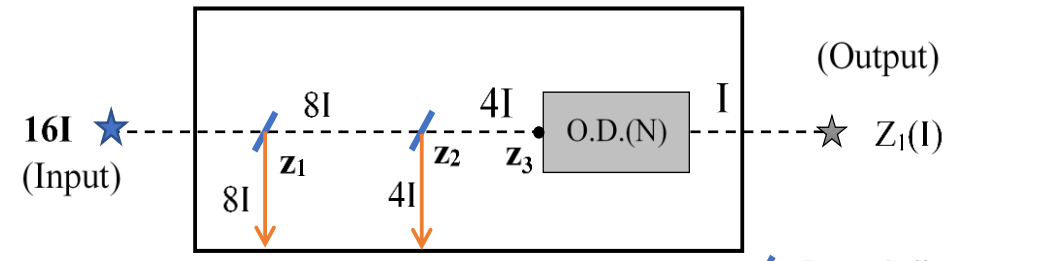

Fig. -4.6.2.2 Block diagram of optical device 'Z'

= Beam Splitter
= Connector
= Input Light Source
= Output Light Source

Table 4.6.1.2: Input intensity versus Output intensity of the optical device 'Z'

Input intensity [into the specific point]	Helping element [Beam splitter (B.S.)/ Beam combiner (B.C.) /another O.D.]	Output intensity of progressive light beam from the specific point by the helping element	Name of the output line from the O.D. 'Z' (with the intensity level)
16I [z_1]	B.S.	8I	
		8I	
8I [z_2]	B.S.	4I	
		4I	
4I [z_3]	O.D.(N)	I(N_1)	Z_1(I)

Optical device 'P' [Fig. -4.6.2.3]

Single input and double output are the features of this device. It was enacted for an intensity level of 6I. The output paths (with intensity) are $P_1(I)$ and $P_2(2I)$ [which are shown in **Table - 4.6.1.3**]

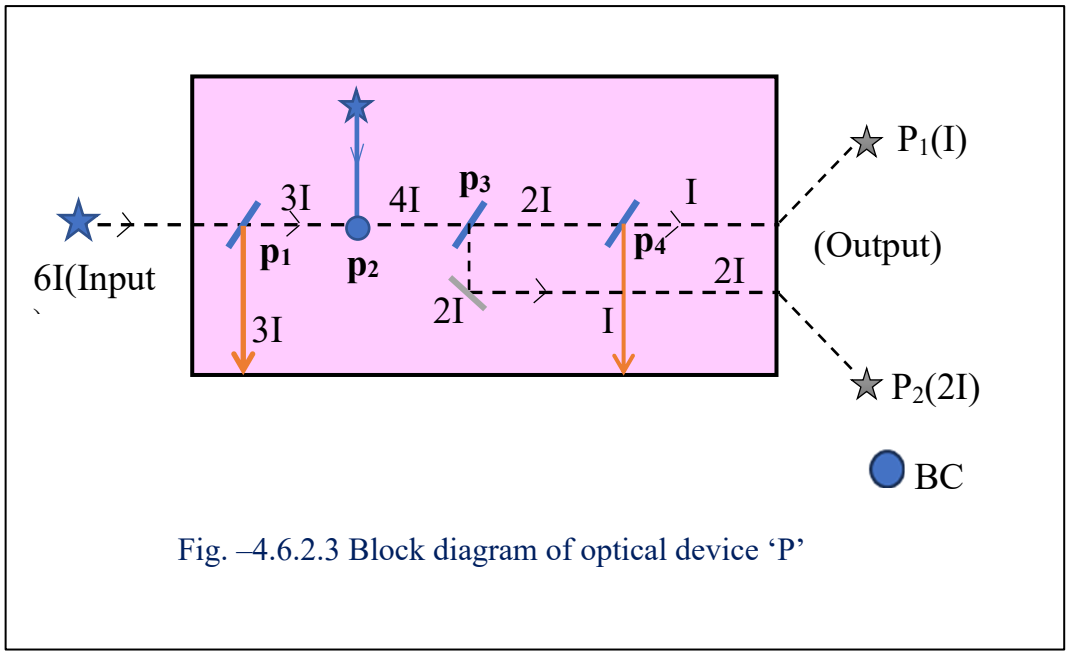

Fig. –4.6.2.3 Block diagram of optical device 'P'

Table 4.6.1.3: Input intensity versus Output intensity of the optical device 'P'

Name of the specific point of O.D. 'P'	Input intensity into the specific point	Helping element [Beam splitter (B.S.)/ Beam combiner (B.C.) /another O.D.]	Output intensity of progressive light beam from the specific point by the helping element)	Name of the output line from the O.D. 'P' (with the intensity level)
p_1	6I	B.S.	3I	
			3I	
p_2	3I	B.C.	4I	
p_3	4I	B.S.	2I	
			2I	$P_2(2I)$
p_4	2I	B.S.	I	$P_1(I)$
			I	

Optical device 'S' [Fig. -4.6.2.4]

The characteristic of OD 'S' is that it is a single input and two outputs device. There are two output lines 'S_1' and 'S_2' of intensity 'I' and '2I' respectively for input intensity 9I [which is revealed by **Table: -4.6.1.4].**

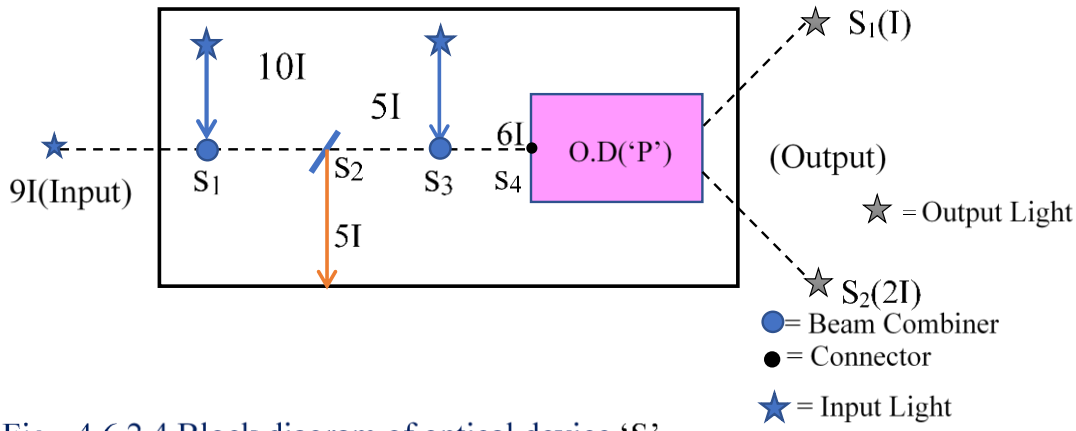

Fig. -4.6.2.4 Block diagram of optical device 'S'

Table 4.6.1.4: Input intensity versus Output intensity of the optical device 'S'

Input intensity (into the specific point)	Helping element [Beam splitter (B.S.)/ Beam combiner (B.C.) /another O.D.]	Output intensity of progressive light beam from the specific point by the helping element	Name of the output line from the O.D. 'S' (with the intensity level)
9I(s_1)	B.C.	10I	
10I(s_2)	B.S.	5I	
		5I	
5I(s_3)	B.C.	6I	
6I(s_4)	O.D.(P)	I(P_1)	S_1(I)
		2I(P_2)	S_2(2I)

Optical device 'Q' [Fig. -4.6.2.5]

It also has a single-input and double-output device. This was performed at an intensity level of 7I. Then there are two output lines 'Q_1' and 'Q_2' with intensity levels 'I' and '2I' respectively [which is revealed by **Table: -4.6.1.5**].

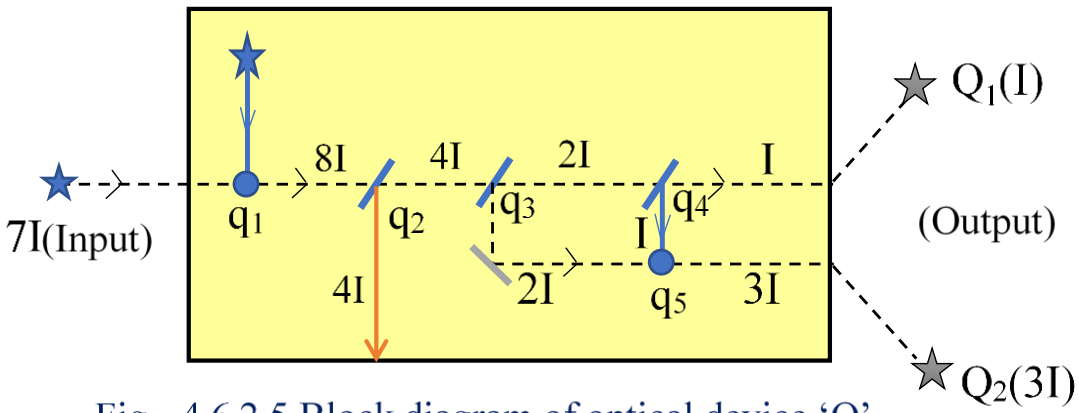

Fig. -4.6.2.5 Block diagram of optical device 'Q'

Table 4.6.1.5: Input intensity versus Output intensity of the optical device 'Q'

Input intensity (into the specific point)	Helping element [Beam splitter (B.S.)/ Beam combiner (B.C.) /another O.D.]	Output intensity of progressive light beam from the specific point by the helping element	Name of the output line from the O.D. 'Q' (with the intensity level)
7I(q_1)	B.C.	8I	
8I (q_2)	B.S.	4I	
		4I	
4I (q_3)	B.S.	2I	
		2I	
2I (q_4)	B.S.	I	Q_1(I)
		I	
2I (q_5)	B.C.	3I	Q_2(3I)

Optical device 'W' [Fig. -4.6.2.6]

In this case, there are two output lines $W_1(I)$ and $W_2(3I)$ for the input intensity level 13I [shown in Table: -4.6.1.6].

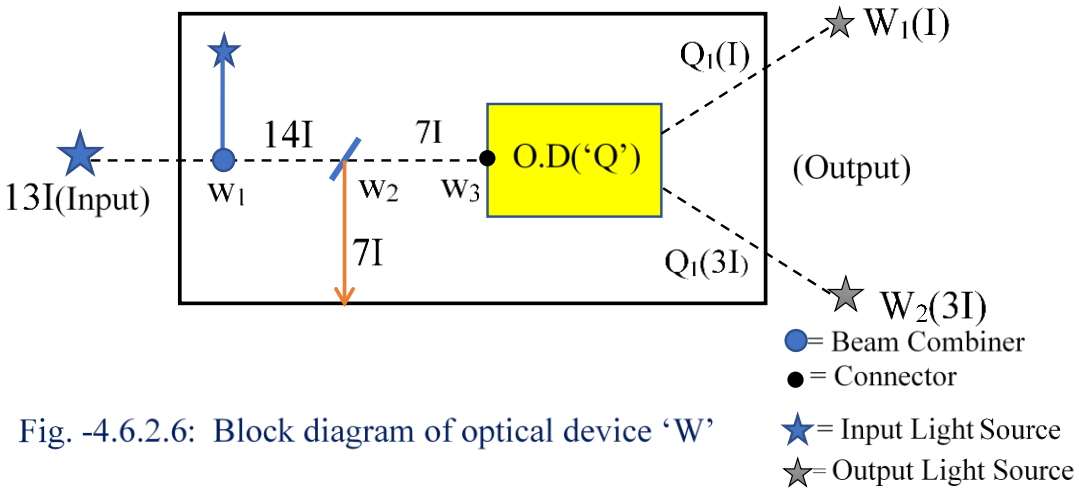

Fig. -4.6.2.6: Block diagram of optical device 'W'

Table 4.6.1.6: Input intensity versus Output intensity of the optical device 'W'

Input intensity [into the specific point]	Helping element [Beam splitter (B.S.)/ Beam combiner (B.C.) /another O.D.]	Output intensity of progressive light beam from the specific point by the helping element	Name of the output line from the O.D. 'W' (with the intensity level)
13I [w_1]	B.C.	14I	
14I [w_2]	B.S.	7I	
		7I	
7I [w_3]	O.D.(Q)	I(Q_1)	$W_1(I)$
		3I(Q_2)	$W_2(3I)$

Optical device 'R' [Fig. -4.6.2.7]

It is formed using a single input line and a single output line. When it is incited at intensity level 8I then there is output line 'R_1' of intensity level '2I' from 'R' [which is shown by **Table- 4.6.1.7**].

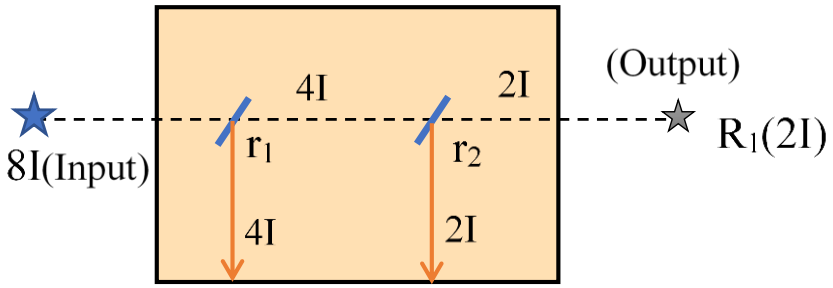

Fig. -4.6.2.7: Block diagram of optical device 'R'

Table 4.6.1.7: Input intensity versus Output intensity of the optical device 'R'

Input intensity (into the specific point)	Helping element [Beam splitter (B.S.)/ Beam combiner (B.C.) /another O.D.]	Output intensity of progressive light beam from the specific point by the helping element	Name of the output line from the O.D. 'R' (with the intensity level)
$8I(r_1)$	B.S.	4I	
		4I	
$4I(r_2)$	B.S.	2I	$R_1(2I)$
		2I	

Optical device 'Y' [Fig. -4.6.2.8]

It was stimulated at an input intensity of 15I. Subsequently, there are two output lines of the same intensity level 3I [which is displayed in **Table: -4.6.1.8**].

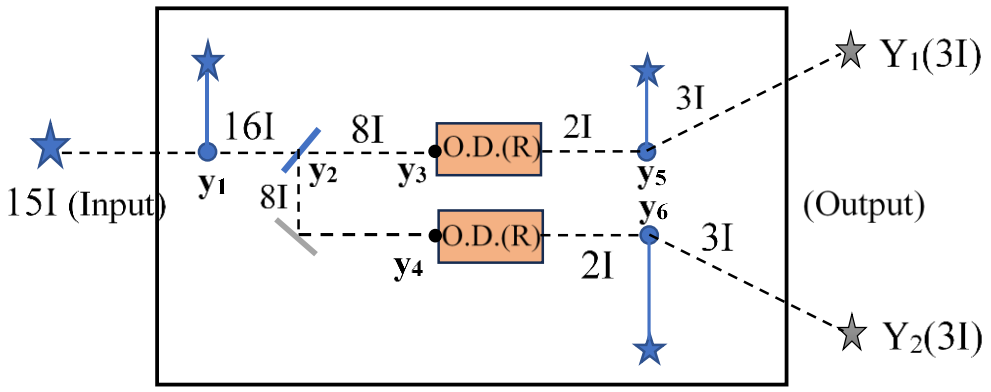

Fig. -4.6.2.8 Block diagram of optical device 'Y'

Table 4.6.1.8: Input intensity versus Output intensity of the optical device 'Y'

Input intensity [into the specific point]	Helping element [Beam splitter (B.S.)/ Beam combiner (B.C.) /another O.D.]	Output intensity of progressive light beam from the specific point by the helping element	Name of the output line from the O.D. 'Y' (with the intensity level)
15I [y_1]	B.C.	16I	
16I [y_2]	B.S.	8I	
		8I	
8I [y_3]	O.D.(R)	2I(R_1)	
8I [y_4]	O.D.(R)	2I(R_1)	
2I(R_1) [y_5]	B.C.	3I	Y_1(3I)
2I(R_1) [y_6]	B.C.	3I	Y_2(3I)

4.6.3. Output division: [Fig.-4.6.3]

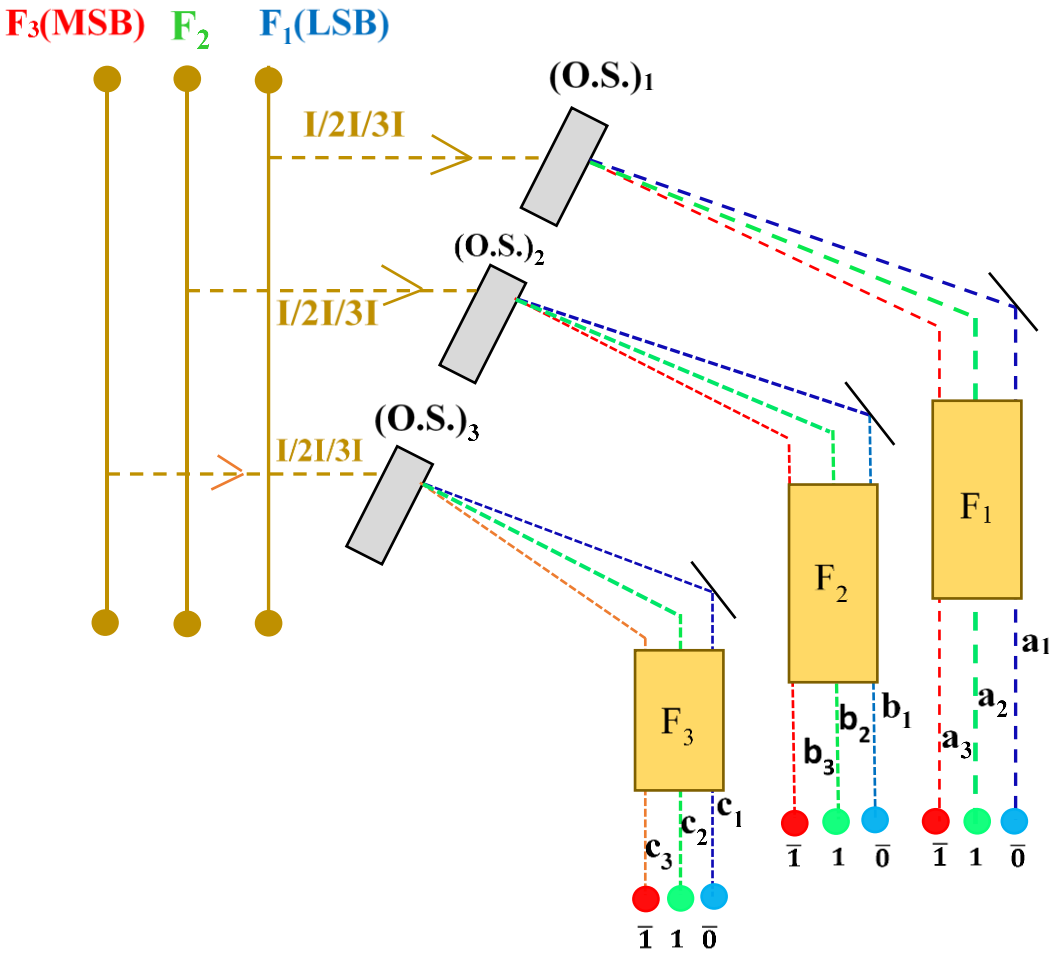

Fig. -4.6.3 Schematic illustration of output division of Optical Quaternary Encoder

The output division of the proposed optical quaternary encoder (shown in **Fig. 4.6.3**) consists of three optical ports, F_1, F_2, and F_3 where F_1 and F_3 are treated as the L.S.B and M.S.B, respectively, and three optical switches, namely $(O.S.)_1$, $(O.S.)_2$, and $(O.S.)_3$. Here, F_1, F_2, and F_3 are connected to optical switches $(O.S.)_1$, $(O.S.)_2$, and $(O.S.)_3$ respectively. It should also be noted that at the end of every port, there are three output lines (as shown in **Fig. 4.6.3**). Here output line is denoted by the symbol j_i where the value of 'j'= 'a' or 'b' or 'c' and numerical value of 'i' = 1 or 2 or 3. The significance of 'j' is as when 'j'= 'a' or 'b' or 'c' then it denotes the optical port – F_1 or F_2 or F_3 respectively. On the other hand, when 'i' = 1, 2, or 3, it represents intensity level I or 2I or 3I, respectively. Now, the relationship between the output lines (intensity) of the optical devices in the processing section and the connected optical ports in the output division is

$F_1 = D(I) + D(2I) + D(3I) + O_1(I) + P_2(2I) + Q_2(3I) + S_1(I) + T_1(2I) + U_2(3I) + W_1(I) + X_1(2I) + Y_1(3I)$ ---(1)

$F_2 = N_1(I) + O_2(I) + P_1(I) + Q_1(I) + R_1(2I) + S_2(2I) + T_2(2I) + U_1(2I) + V_1(3I) + W_1(3I) + X_2(3I) + Y_2(3I)$ ----(2)

$F_3 = Z(I)$ ----(3)

Here D(I), D(2I) & D(3I) denote that output lines of intensity I, 2I & 3I orderly from the optical regulator are continued directly into the port 'F_1' without the collaboration of any optical device. From relations (1), (2), and (3), it is noted that each port can have three types of intensity levels: I, 2I, and 3I. As a result, the output intensity level of every port either 'I' or '2I' or '3I' will be marked as $\bar{0}$, 1, and $\bar{1}$ respectively. Here it is also noted that in this scheme 'F_1' port acts as L.S.B and 'F_3' port officiates as M.S.B. The output line or several output lines of each

optical device is connected to a definite optical port as well as a definite optical switch in the output division, as shown in **Table 4.6.2**. Here, it is illustrated that for several input intensities to the optical regulator (O.R), there are active optical devices as well as active output lines/lines in the output form.

Table- 4.6.2: (Input intensity level versus output intensity level at several output lines of all-optical devices and name of the connected optical switch)

Value of input intensity level	Name of the optical device	Name of the output line from the definite optical device (with intensity level)	Name of the connected optical port of the output division	Active output line(j_i)
I	None (Direct)	(Direct)	F_1	a_1
2I	None (Direct)	(Direct)	F_1	a_2
3I	None (Direct)	(Direct)	F_1	a_3
4I	'N'	N_1(I)	F_2	b_1
5I	'O'	O_1(I)	F_1	a_1
		O_2(I)	F_2	b_1
6I	'P'	P_1(I)	F_2	b_1
		P_2(2I)	F_1	a_2
7I	'Q'	Q_1(I)	F_2	b_1
		Q_2(3I)	F_1	a_3
8I	'R'	R_1(2I)	F_2	b_2
9I	'S'	S_1(I)	F_1	a_1
		S_2(2I)	F_2	b_2
10I	'T'	T_1(2I)	F_1	a_2
		T_2(2I)	F_2	b_2
11I	'U'	U_1(2I)	F_2	b_2
		U_2(3I)	F_1	a_3
12I	'V'	V_1(3I)	F_2	b_3
13I	'W'	W_1(I)	F_1	a_1
		W_2(3I)	F_2	b_3
14I	'X'	X_1(2I)	F_1	a_2
		X_2(3I)	F_2	b_3
15I	'Y'	Y_1(3I)	F_1	a_3
		Y_2(3I)	F_2	b_3
16I	'Z'	Z_1(I)	F_3	c_1

It is worth noting here that the size of the proposed optical system (OQE) depends on the physical dimensions of the nonlinear materials and beam-splitting optics. The system is designed to be miniaturized by integrating Kerr materials on photonic chips. However, it will likely be larger than an electronic quaternary encoder implemented in CMOS but much faster due to its optical nature.

4.6.4. Operation of Optical Quaternary Encoder (OQE) (decimal to quaternary)

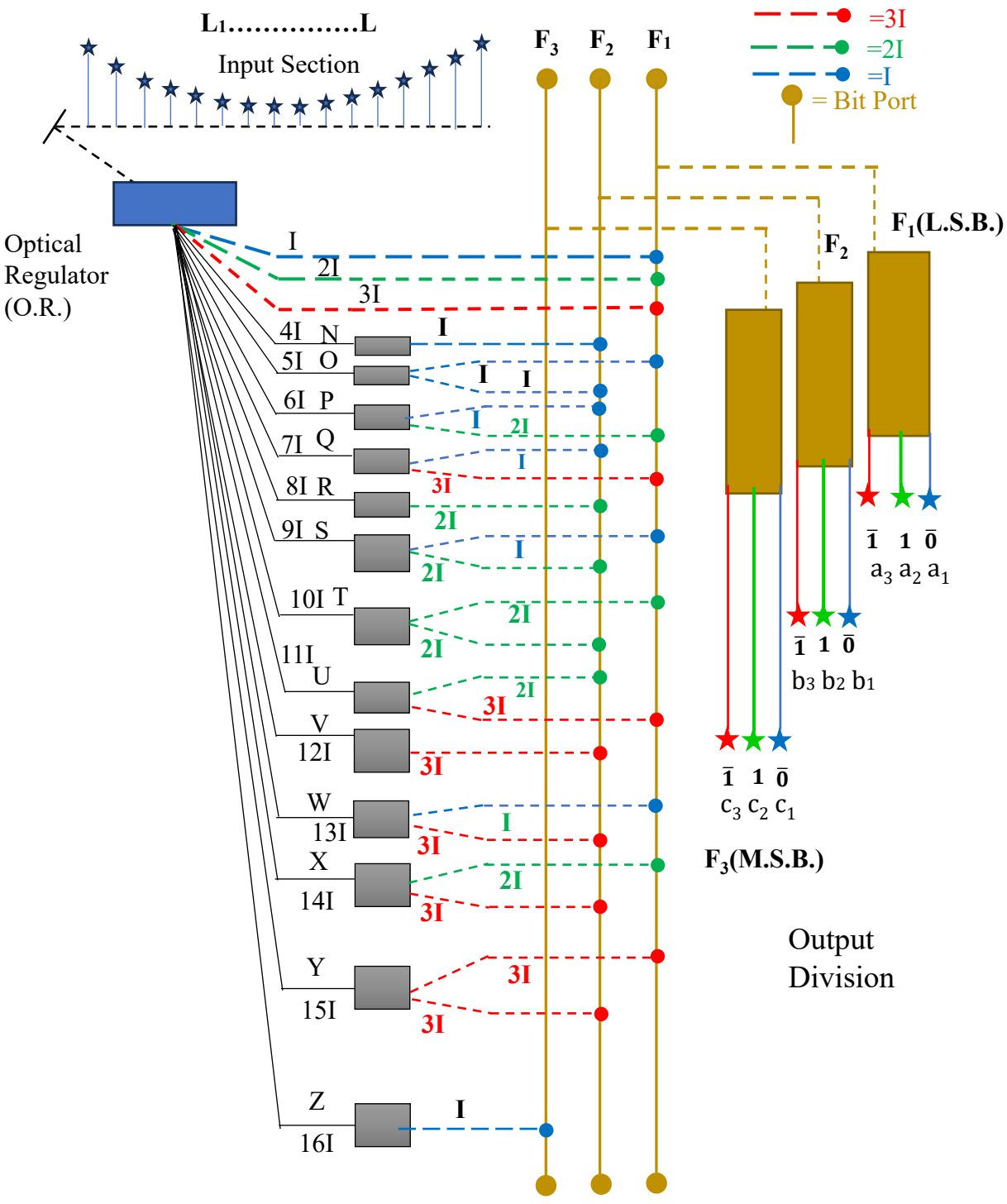

Fig. -4.6.4: Schematic diagram of all-optical decimal to Quaternary Converter [Optical Quaternary Encoder (OQE)]

The present section discusses the implementation and design of the optical quaternary encoder (OQE). To code a particular decimal number, a particular number of input sources must be activated (operation of the proposed scheme OQE is shown in **Fig. 4.6.4**). Depending on the input intensity level, there are active states of different output lines/lines of optical ports F_1, F_2, and F_3 (which is shown in Table 3. In Table 3, the active state is indicated by a solid circle). Now, the operation is simplified using the following examples:

For coding decimal number 5, any five out of 16 input sources must be incited. Thereafter, a polarized ray from the O.R. follows the path of intensity 5I. Then this light beam of intensity 5I enters into the optical device 'O.' Now from the feature of 'O' for input intensity 5I, there are two output lines 'O_1' & 'O_2' from optical device 'O' with the same intensity level 'I,' where 'O_1' & 'O_2' are again joined to the port 'F_1' & 'F_2' respectively. Subsequently, the output quaternary form F_3 F_2 F_1 is 0 $\bar{0}$ $\bar{0}$, Which is a decimal equivalent of 5. A python computational simulation is shown in **Figure-4.6.5**.

4.6.5. Python simulation result

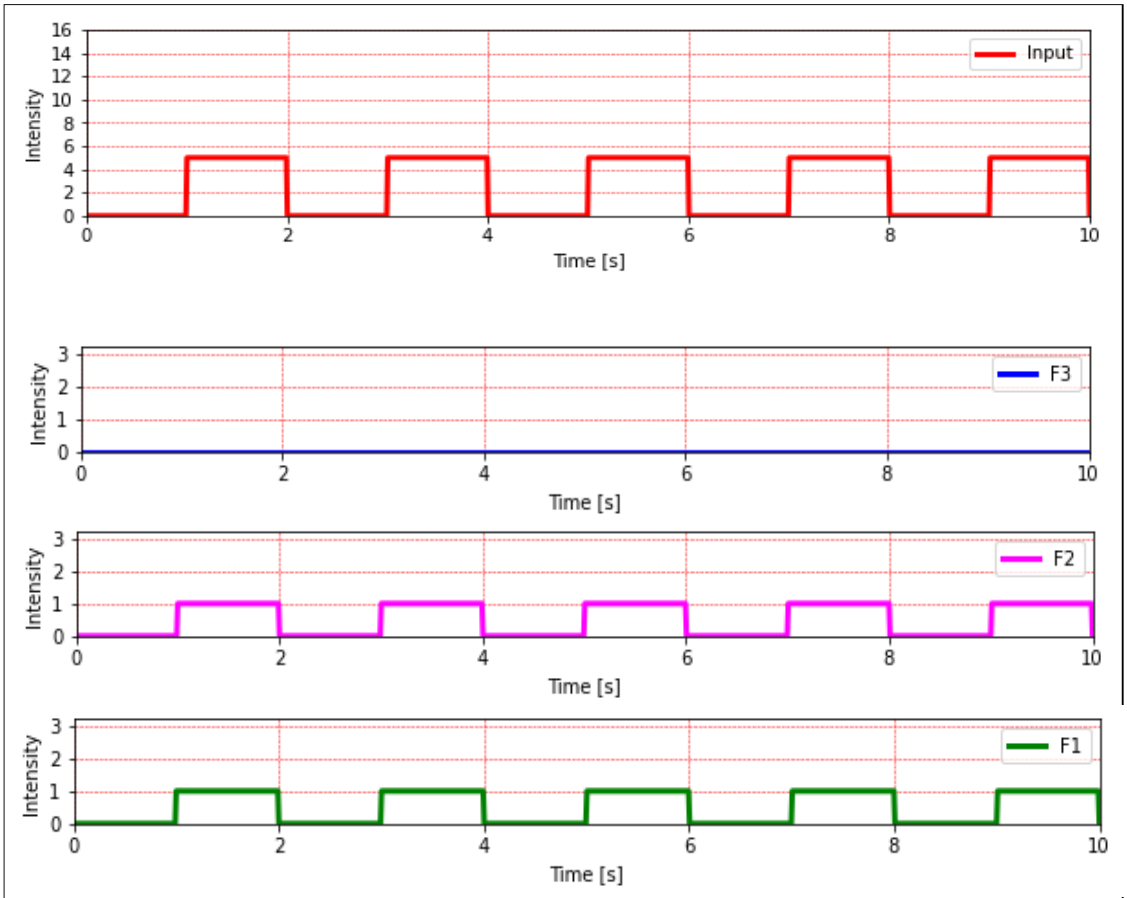

Fig. – 4.6.5: PYTHON simulation result illustrating the conversion of input decimal number '5' to its quaternary form where F3 is MSB and F1 is LSB.

To transform a decimal number14 into its quaternary form, there are 14 input sources out of the 16 sources to be activated. Then the output light beam of intensity 14I from O.R moves towards the O.D 'X.' As a result 'X' is stimulated and offers two output lines X_1(2I) & X_2(3I) where they are adjoined to the optical port (O.P) F_1 and F_2 respectively. Now the output quaternary form of decimal number 14 is as $-F_3 = 0$; $F_2 = \bar{1}$; $F_1 = 1$. A python computational simulation for conversion of decimal number '14' to its quaternary form is shown in **Figure 4.6.6**.

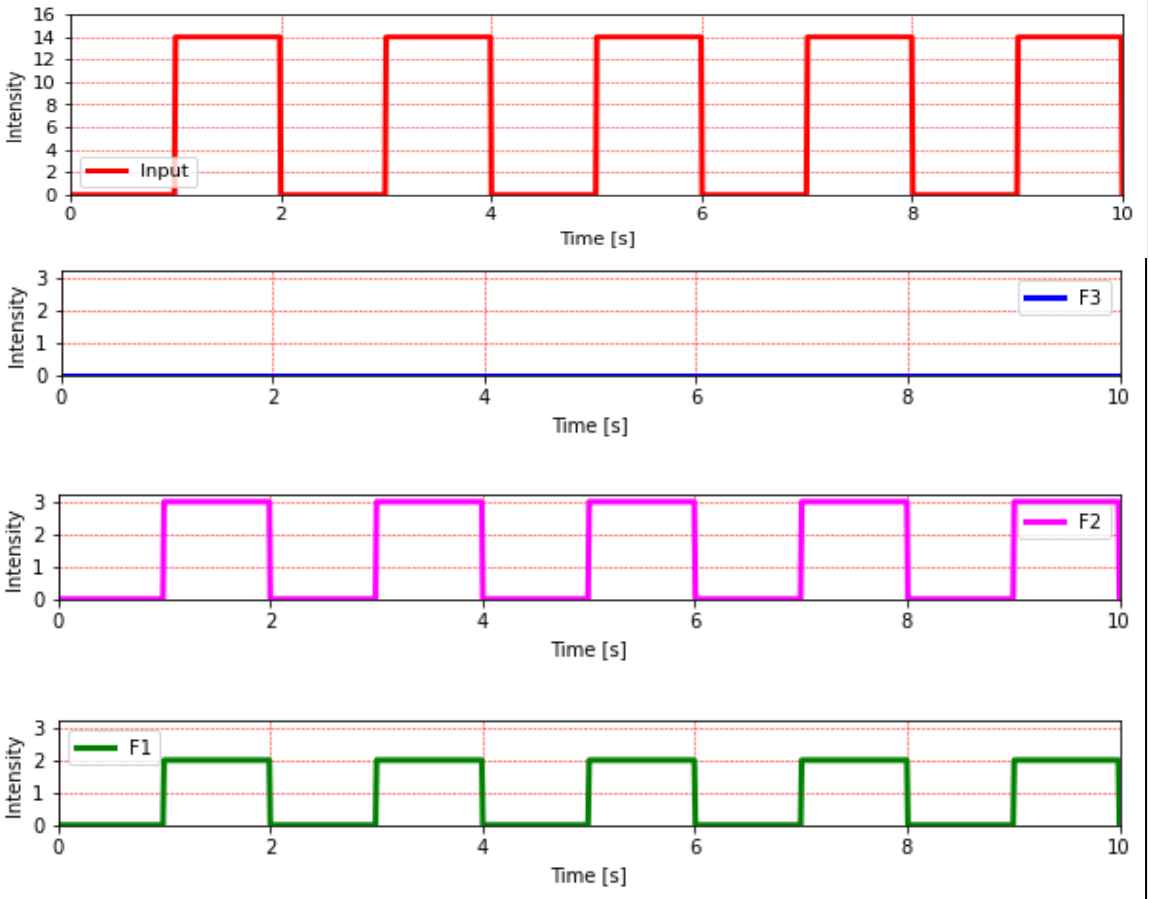

Fig. – 4.6.6: PYTHON simulation result illustrating the conversion of input decimal number '14' to its quaternary form where F3 is MSB and F1 is LSB.

similarly, here any decimal number from 1 to 16 can be converted into its quaternary form which has been broadly discussed in the Appendix-A in the section 'conversion process'. In this way, one can obtain the conversion table, as shown in **Table-4.6.3, Table-4.6.4** and concern python computational simulation is shown in **Figure-4.6.7**. However, the configuration of the OQE can be extended to code higher decimal numbers to its quaternary form.

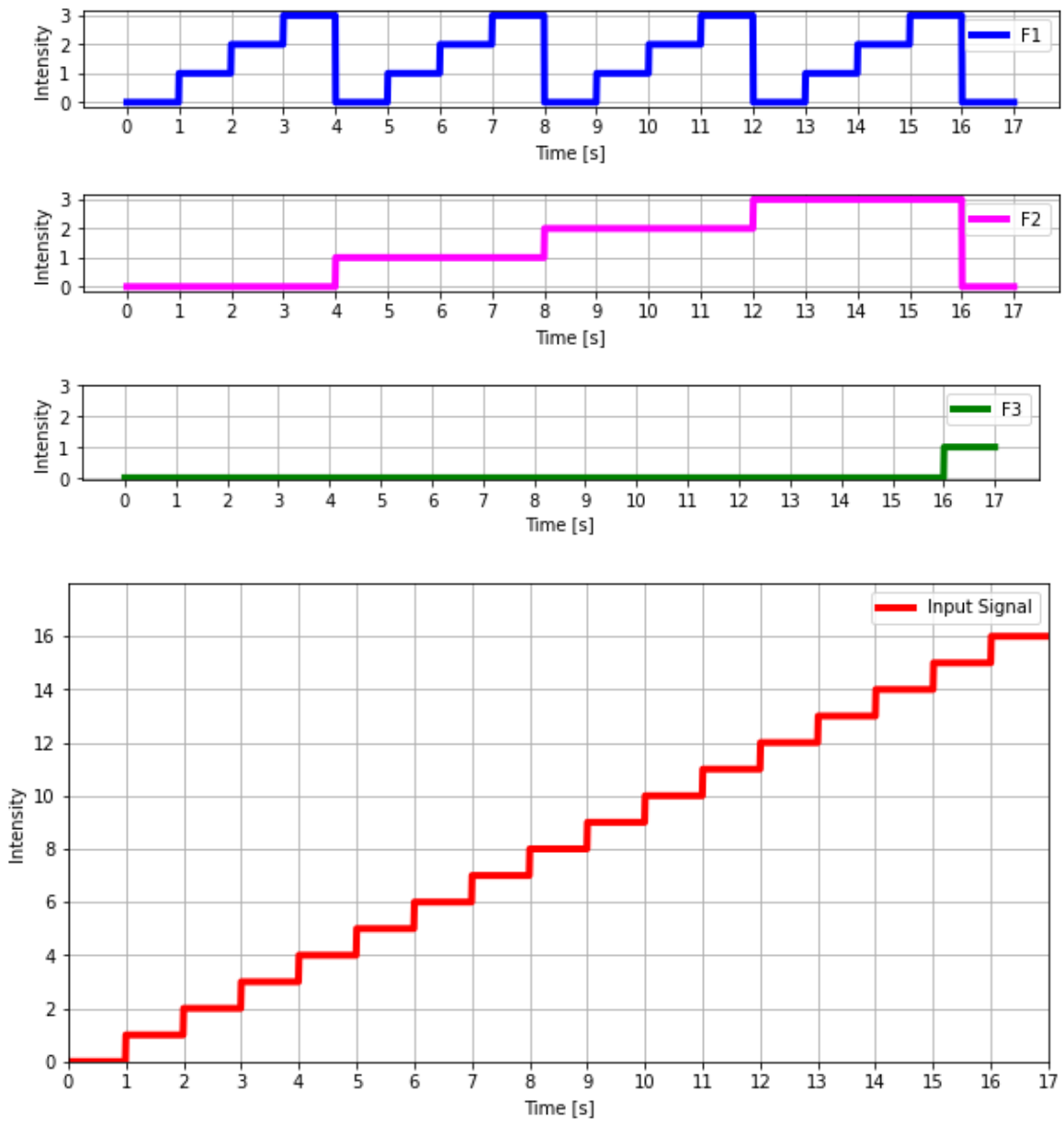

Fig. – 4.5.7: PYTHON simulation result illustrating the conversion of input decimal number '1' to '16' to its quaternary form where F3 is MSB and F1 is LSB.

Table – 4.6.3: Input intensity versus the active state of different output lines of each output port (where the active state = solid circle; Blue= I; Green= 2I; Red= 3I) of OQE

Input intensity	The active output line of the optical port at the output division of OQE								
	F_3 (M.S.B.)			F_2			F_1 (L.S.B.)		
	c_3	c_2	c_1	b_3	b_2	b_1	a_3	a_2	a_1
I									●
2I								●	
3I							●		
4I						●			
5I						●			●
6I						●		●	
7I						●	●		
8I					●				
9I					●				●
10I					●			●	
11I					●		●		
12I				●					
13I				●					●
14I				●				●	
15I				●			●		
16I			●						

Table – 4.6.4: Input versus output of Optical Quaternary Encoder (OQE)

Input (Decimal number)	Input intensity into optical Regulator (O.R.)	Output Quaternary form		
		F_3 (M.S.B.)	F_2	F_1 (L.S.B.)
0	0	0	0	0
1	I	0	0	$\bar{0}$(zero bar)
2	2I	0	0	1
3	3I	0	0	$\bar{1}$(one bar)
4	4I	0	$\bar{0}$(zero bar)	0
5	5I	0	$\bar{0}$ (zero bar)	$\bar{0}$(zero bar)
6	6I	0	$\bar{0}$(zero bar)	1
7	7I	0	$\bar{0}$(zero bar)	$\bar{1}$(one bar)
8	8I	0	1	0
9	9I	0	1	$\bar{0}$(zero bar)
10	10I	0	1	1
11	11I	0	1	$\bar{1}$(one bar)
12	12I	0	$\bar{1}$(one bar)	0
13	13I	0	$\bar{1}$(one bar)	$\bar{0}$(zero bar)
14	14I	0	$\bar{1}$(one bar)	1
15	15I	0	$\bar{1}$(one bar)	$\bar{1}$(one bar)
16	16I	$\bar{0}$ (zero bar)	0	0

The important thing here is that since the system operates entirely in the optical domain, the response time is governed by the Kerr effect, which is typically in the femtosecond range (10^{-15} s). This means that the system can potentially perform encoding at terahertz (THz) speeds, significantly outpacing electronic encoders. Now the following **Table- 4.6.5** can be used to compare the proposed Optical Quaternary Encoder (OQE) with other encoding methods:

Table-4.6.5: Comparison table between proposed Optical Quarter Encoder and other encoding methods

Feature	Electronic Quaternary Encoder	Optical Binary Encoder /BCD to excess 3 code Encoder	Proposed Optical Quaternary Encoder (OQE)
Speed	GHz range	THz range	THz range
Logic Gates	Electronic logic gates	Optical logic gates	No logic gates required
Power Consumption	High	Moderate	Low
Complexity	Moderate	High	Low
Losses	Electrical resistance	Optical losses	Minimal optical losses
Expandability	Limited	Binary / excess 3 code encoding	Can be extended to higher bases

The present work successfully demonstrated the possibility of realizing a Quaternary Encoder using all-optical means. The decimal number is coded to its quaternary form by a quaternary encoder, which can play an undeniable role in the data communication system. Because the proposed scheme is all-optical, its speed of operation is much higher (terahertz) than that of conventional electronic devices and even electro-optic devices. The input light beams are coherent and share the same polarization state, which is necessary for activating the nonlinear material. Again, the dimension of the proposed scheme relies on the size of the selected NLMs; therefore, under proper precautions, the entire scheme can be minimized. On the other hand, whereas the capability of coding range of 'n, bit conventional binary encoder is 1 to $(2^n - 1)$, But that range of 'n' bit quaternary encoder is 1 to $(4^n - 1)$[There is a comparison among Binary, Ternary, and Quaternary Encoder of 3-bit in the **Appendix-A**, **Table- s3**]. An important advantage of this scheme is that coding a decimal number into a quaternary form only requires setting the necessary number of input sources (any number of input sources where each source is of equal intensity) to a high state, unlike electronic encoders that require a specific key to press. In addition, it should be noted that the electronic OR gate is an essential element of the

electronic encoder, but no gate (either electronic or optical) is required in our proposed scheme. Thus, this scheme may be employed in the field of all-optical computation, as well as photonic applications. The Optical Quaternary Encoder (OQE) presents a significant advancement in the field of optical computing and data encoding by eliminating the need for electronic components and leveraging the nonlinear switching properties of Kerr materials. The system enables ultrafast encoding speeds in the THz range, making it a promising candidate for next-generation photonic circuits.

Potential Applications of OQE:

1. Optical Computing:

   Can be integrated into all-optical logic circuits for high-speed arithmetic and data processing.

2. Optical Communication Networks:

   Suitable for high-speed data encoding in Fiber-optic networks. Enables quaternary modulation schemes, increasing data transmission rates compared to traditional binary encoding.

3. Extension to Higher Numerical Bases:

   The concept can be generalized to radix-8 (octal) or radix-16 (hexadecimal) encoders. Future work can explore hybrid nonlinear materials with enhanced Kerr effects for more compact and efficient designs.

4.7. Conclusion

The all-optical encoding and decoding schemes put forward herein, based on the nonlinear switching characteristics of Kerr materials, offer ultrafast operation within the terahertz domain and avoid the necessity for traditional logic gates. In contrast to electronic systems, dependent as they are upon intricate circuitry, these schemes realize simplicity, scalability, and efficiency through the exploitation of equal-intensity optical inputs. Expanding number representations from binary to ternary and quaternary vastly expands the set of signals that can be represented using a fixed bit length, and with this, flexibility and performance over conventional encoders and decoders. These capabilities make Kerr-based photonic architectures strong candidates for future optical computing and communications systems that require compactness, high speed, and multi-valued logic.

4.8. References

1. S. Mukhopadhyay, "An optical conversion system: From binary to decimal and decimal to binary." ***Optics communication***, volume 76, number5,6 (1990).
2. N. Pahari, S. Mukhopadhyay, "An all-optical R-S flip-flop by optical non-linear material." ***J. Opt.*** 34(3), 108–114 (2005).
3. D. Samanta, S. Mukhopadhyay, "All-optical method for maintaining a fixed intensity level of a light signal in optical computation." ***Opt. Commune.*** 281, 4851–4853 (2008).
4. N. Pahari, A. Guchhait, "All-optical serial data transfer between registers using optical non-linear materials." ***Optik***123(5),462–466 (2012).
5. N. Pahari, A. Guchhait, A.D. Jana, "Image edge detection scheme by the use of Kerr type nonlinear material and the verification of the scheme by computer simulation." ***J. Opt.*** 41, 178–183 (2012).
6. A. Guchhait, N. Pahari, N.B. Manik, "All-optical decimal to ternary converter with the proper use of optical non-linear material." ***J. Opt.*** 49, 59–68 (2019) Opt. Soc. India.
7. A. Guchhait, N. Pahari, N.B. Manik, "Optical Kerr nonlinear material for calculating the coefficient of binomial expansion under any positive integral index." ***J. Opt.*** 51, 851–865 (2022).
8. A. Guchhait, N. Pahari, N.B. Manik, "Optical Kerr nonlinear material for expressing the trigonometric ratios of compound angles." ***J. Opt.*** 53(25) (2023).
9. S. P. Medhekar, P. Paltani, "Proposal for optical switch using nonlinear refracton," *IEEE Photon. Technol. Let.* 18 (15) (2006) 1579-151.
10. N. Pahari, D. N. Dash, S. Mukhopadhyay, "All-optical method for the addition of binary data by nonlinear material," *Appl. Opt* 43 (33) (2004) 6147-6150.
11. K. R. Choudhury, A. Sinha, S. Mukhopadhyay, "An all-optical comparison scheme between two multi-bit data with optical nonlinear material," *Chin. Opt. Lett.* 6(9) (2008) 693-696.
12. T. Chattopadhyay, C. Taraphdar, J. N. Roy, "Quaternary Galois field adder based all-optical multivalued logic circuits," *Appl. Opt* 48(22) (2009) E36-E34.

13. J. N. Roy, A. K. Maity, D. Samanta, S. Mukhopadhyay, "Tree-net architecture for integrated all-optical arithmetic operations and data comparison scheme with optical nonlinear material," *Opt. Switch. Network.*4 (2007) 231-237.

14. T. Haist, W. Osten, "Ultrafast digital-optical arithmetic using wave-optical computing," in: *OSC 2008, LNCS 5172*, 2008 33-45.

15. J. Wang, G. Meloni, G. Berrettini, L. Poti, A. Bogoni, "All-optical binary counter based on semiconductor optical amplifiers," *Opt. Lett.* 34 (22) (2009)3517-3519.

16. B. Chakraborty, S. Mukhopadhyay, "Alternative approach of conducting phase-modulated all-optical logic gates," *Opt. Eng.* 48 (3) (2009)5201-5205.

17. P. Bhowmik, J. N. Roy, T. Chattopadhyay, "Designing of all optical generalised circuit for two-input binary and multivalued logical operations," *Optics communication* 331, 14-27 (2014).

18. "Designing of all-optical tri-state logic system with the help of optical nonlinear material," *Journal of Nonlinear Optical Physics & Materials* 17(3), 315 (2008).

19. S. Mukhopadhyay, "Role of optics in super-fast information processing," *Indian J. Phys*, 84.1069-1074 (2010).

20. McMahon P L, "The physics of optical computing," *Nature Reviews Physics* 5, 717–34 (2023).

21. S Mukhopadhyay, A Basuray, AK Datta, "New coding scheme for addition and subtraction using the modified signed-digit number representation in optical computation," *Applied optics* 27 (8), 1375-1376 (1988).

22. S Mukhopadhyay, "Binary optical data subtraction by using a ternary dibit representation technique in optical arithmetic problems," *Applied optics* 31 (23), 4622-4623 (1992).

23. M.A. Karim, A.A.S. Awwal, "Optical computing: an Introduction," *(Wiley, New York)* Chap. 3 pp. 35–56 (2003).

24. D Samanta, S Mukhopadhyay, "A new scheme of implementing all-optical logic systems exploiting material nonlinearity and polarization-based encoding technique," *Optoelectronics Letters* 4, 172-176 (2008).

25. Samanta D, "Implementation of optical Manchester coded data using Kerr type of nonlinear material," *J. Opt.* 51, 899–902 (2022).

26. D Samanta, S Mukhopadhyay, "All-optical method of developing parity generator and checker with polarization encoded light signal," *Journal of Optics* 41, 167-172 (2012).

27. A. Chatterjee, S. Biswas, S. Mukhopadhyay, "Method of frequency conversion of Manchester encoded data from a Kerr type of nonlinear medium," *J. Opt.* (2017).

28. Pahari N and Mukhopadhyay S, "New scheme for image edge detection using the switching mechanism of nonlinear optical material," *Opt. Eng.* 45, 037003–037003 (2006).

29. S. Jiao, J. Feng, L. Zhang, D. Wu and Y. Shen, "Optical logic gate operations with single-pixel imaging," *IEEE Journal of Selected Topics in Quantum Electronics*, 29(2), 7700208 (2022).

30. Parandin, F., & Karami, P., "Numerical analysis of All-Optical universal NAND and NOR photonic crystal logic gates by creating holes in silicon material," *Optics & Laser Technology*, 182, 112197 (2025).

31. Acharyya, Jitendra Nath, Narayana Rao Desai, R. B. Gangineni, and G. Vijaya Prakash, "Effect of photonic cavity interactions on femtosecond multiphoton optical nonlinear absorptions from Bi2O3-based one-dimensional photonic crystal," *ACS Photonics* 9, no. 6 (2022): 2092-2100.

32. Kuriakose, Albin, Jitendra Nath Acharyya, Pankaj Srivastava, and G. Vijaya Prakash, "Photonic Band Gap and Fractal Resonances in Aperiodic Cantor-like Self-Similar a: SiN x Photonic Structures," *ACS Applied Optical Materials* 2, no. 4 (2024): 670-678.

33. JN Acharyya, DN Rao, M Adnan, C Raghavendar, RB Gangineni, "Giant optical nonlinearities of photonic minibands in metal–dielectric multilayers," *Advanced Materials Interfaces* 7, no- 11(2020):2000035.

34. JN Acharyya, NR Desai, RB Gangineni, GV Prakash, "Photonic Cavity-Mediated Tunable Ultrafast Absorption Dynamics in BaTiO3-Based One-Dimensional Photonic Crystal," *ACS Applied Electronic Materials* 3 (4), 1904-1911, (2021).

35. JN Acharyya, AK Mishra, DN Rao, A Kumar, GV Prakash, "Ultrafast Nonlinear Pulse Propagation Dynamics in Metal–Dielectric Periodic Photonic Architectures," *Advanced Materials Interfaces* 8 (19), 2100757, (2021).

36. JN Acharyya, GV Prakash, "Nonlinear optical dispersion and higher-order effects in bulk and wavelength-ordered photonic materials," *Optik* 247, 167944, (2021).

37. S. Biswas, S. Mukhopadhyay, "an all-optical scheme of secured cryptographic communication encoded with decimal data," *Optik* 124, 2376–2378 (2013).

38. JN Acharyya, S Singh, M Shanu, GV Prakash, AK Mishra, "Ultrafast pulse propagation and spectral broadening in metal-dielectric 1D photonic crystal," *Optical Materials* 131, 112688.

39. JN Acharyya, A Kuriakose, G Vijaya Prakash, "Spectrally resolved nonlinearities within a laser pulse in a single-scan and spectrometer-based nonlinear optical probing," *Optics Letters* 49 (7), 1721-172.

40. S.K. Das, N. Pahari, "Binary to the hexadecimal decoder using Pockels' effect guided Mach-Zehnder interferometer (MZI) and optical tree architecture," *Braz. J. Phys.* 54, 26 (2024).

41. Biswas K and Sarkar A, "MEMS-based optical switches," *Optical switching: Device Technology and Applications in Networks. Chapters* 93–106 (2022).

42. E. Garmire, "Nonlinear optics in daily life," *Opt. Express* 21(25), 30532–30544 (2013).

43. R. Bano, M. Asghar, K. Ayub, T. Mahmood, J. Iqbal, S. Tabassum, R. Zakaria, M.A. Gilani, "A theoretical perspective on strategies for modelling high performance nonlinear optical materials," *Front. Mater.* 8, 532 (2021).

44. R.W. Boyd, "Nonlinear optics," *(Academic Press, Massachusetts, 2020)*.

45. S.D. Smith, "Optical bi-stability, photonic logic, and optical computation," *Appl. Opt.* 25, 1550–1564 (1986).

46. H.J. Caulfield, "Perspectives in optical computing," *Computer* 31(2), 22–25 (1998).

47. S.D. Smith, H.A. Mackenzie, J.G.H. Mathew, J.J.E. Reid, M.R. Taghizadeh, F.A.P. Tooley, A.C. Walker, "Nonlinear optical circuit elements, logic gates for optical computers: the first digital circuits," *Opt. Eng.*24(4), 569–574 (1985).

48. S. Sahu, S. Dhar, "All-optical implementation of arithmetic operation scheme using optical nonlinear material-based switching technique," *Photonics Opto-electron* 3, 37–50 (2014).

49. X. Yang, X. Hu, H. Yang, Q. Gong, "Ultracompact all-optical logic gates based on nonlinear plasmonic nanocavities," *Nano Photonics* 6(1), 365–376 (2017).

50. M. Moradi, M. Danaie, A.A. Orujo, "Design of all-optical XOR and XNOR logic gates based on Fano resonance in plasmonic ring resonators," *Opt. Quantum Electron.* 51, 1–18 (2019).

51. D. Psaltis, D. Brady, K. Wagner, "Adaptive optical networks using photorefractive crystals," *Appl. Opt.*27(9), 1752–1759 (1998).

52. S. Saha, de Paromita, S. Mukhopadhyay, "all-optical frequency encoded quaternary memory unit using symmetric configuration of MZI-SOA," *Opt. Laser Technol.* 131, 106386 (2020).

53. S.K. Chandra, S. Biswas, S. Mukhopadhyay, "Phase-encoded all-optical reconfigurable integrated multi-logic unit using phase information processing of four-wave mixing in semiconductor optical amplifier," *IET Optoelectronic* 10(1), 1–6 (2016).

54. S. Biswas, S. Mukhopadhyay, "All-optical approach for conversion of a binary number having a fractional part to its decimal equivalent to three places of decimal using single system optical tree architecture," *J opt* 43(2), 122–129 (2014).

55. S. Biswas, S. Mukhopadhyay, "an all-optical approach for developing a system involving Kerr-material based switches for cryptographic encoding of binary data depending on the input parity," *Optic* 125, 1954–1956 (2014).

56. Pahari N, "All-optical BCD to excess 3 code encoders with proper use of optical non-linear material," *J. Opt.* 47, 110–4 (2018).

57. S. Biswas, S. Mukhopadhyay, "an all-optical approach for developing a system involving Kerr-material based switches for cryptographic encoding of binary data depending on the input parity," *Optic* 125, 1954–1956 (2014).

58. N. Mitra, S. Mukhopadhyay, "Method of developing an all-optical synchronous counter by exploiting the Kerr non-linearity of the medium," *Opt. Photonics Lett.* 3(1), 23–30 (2010).

59. Y. Fairman, C.C. Guest, S.H. Lee, "Optical digital logic operations by two beams coupling in photorefractive material," *Appl. Opt.* 25(10), 1598–1603 (1986).

60. N.L. Kazatsky, M.A. Butt, S.N. Konini, "Optical computing: status and perspectives," *Nanomaterials*12(13), 2171 (2022).

61. Z. Chai, X. Hu, F. Wang, X. Niu, J. Xie, Q. Gong, "Ultrafast all-optical switching," *Adv. Opt. Mater.* 5(7), 1600665 (2017).

62. Pahari N, "All-optical even and odd parity bit generator and checker with optical nonlinear material," *J. Opt.* 46, 336–41 (2017).

63. Pahari N and Mukhopadhyay S, "New method of all-optical data comparison with nonlinear material using 1's complement method," *Opt. Eng.* 45, 015201–015201 (2006).

64. Pahari N, "All-optical binary to gray code converter and gray code to binary converter with proper use of nonlinear material," *International Conference on Optics and Photonics* vol 9654 (SPIE) pp 260–4 (2015).

65. B. Sarkar, S. Mukhopadhyay, "An-optical system for the sharp increase of light frequency by the use of multiple numbers of LiNbO3 crystals biased by sawtooth electronic pulse," *Indian J. Phys.* 95, 1865 (2021).

66. S. Dey, A. Chatterjee, S. Mukhopadhyay, "Photonic scheme for developing Manchester-coded data using laser-based Kerr switch," *J. Opt.* 50, 341–345 (2021).

67. S. Dey, S. Mukhopadhyay, "All-optical integrated square root of Pauli-Z (SRZ) gates using polarization and phase encoding," *J. Opt.* 48, 520–526 (2019).

68. S. Dey, P. De, S. Mukhopadhyay, "an all-optical implementation of Fredkin gate using Kerr effect," *Optoelectronic. Lett.* 15, 317–320 (2019).

Chapter - 5

Optical Computation of Trigonometric Ratios

Chapter

5

Optical Computation of Trigonometric Ratios

An innovative all-optical device is proposed to effectively express the trigonometric ratios of compound angles based on the fascinating intensity dependent changes of refractive index (RI) of a nonlinear material (NLM). The device has profound applications in numerous domains of research, such as astronomy, oceanography, seismology, civil engineering, electronics, phonetics, medical imaging, and the development of computer music. Optical switch and optical Ternary encoder play major role in this proposed device. To effectively execute this process, a single constant light source (SCL) with a standardized intensity level 'I' has been strategically utilized, alongside multiple constant light sources (MCL), a beam combiner, and a beam splitter. In this scheme, different value of angles is represented by the different value of standard intensity level (I) to express the trigonometric ratios of compound angles. Furthermore, in the proposed design, the output expression of the trigonometric ratios of compound angles are illustrated as the sum or subtraction of two outputs (2-bit ternary form) of two number of optical Ternary Encoders. As the proposed scheme is fully optical in nature, so this device can be employed in optical computation as well as photonic application.

5.1. Overview

In contemporary science and technology, nonlinear optics has sparked an immense upsurge in the advancement of modern society. [1-2]. Nonlinear optical (NLO) materials have become a significant area of focus owing to their immense potential for myriad applications in photonics and optoelectronics [3-6].

The elementary manifestations of nonlinear optics (second-order optical nonlinearity) encompass the intensity-dependent refraction and absorption of medium, when the incident light intensity surpasses certain threshold. [7]. This fascinating intensity dependent change of optical constants facilities tremendous possibility of controlling the performance of the optoelectronic devices and leading to an exciting advancement in combing the materials science and optoelectronic technologies.

Optics and photonics possess remarkable potential to achieve exceptional processing speeds, leading to an extraordinary surge in the realms of computation and communication systems [8-13]. In optical computing system, over the last few decades many schemes have already been proposed for executing arithmetic, algebraic and logic operation [14-18] as well as conversion of electronic circuit by optical counterpart where optical Kerr nonlinear material (NLM) [19-20.] has a key role in processing superfast switching mechanism [21-30]. In such logic operations, trigonometric sine and cosine functions are widely utilized as primary operators, finding tremendous applications in radio waves, electrical current fields, and musical tones, etc. Typically, a compound angle is a trigonometric identity which can be expresses as a trigonometric function of (A+B) or (A-B) in terms of trigonometric functions A and B, where A, B, (A+B), (A-B) are acute angles. Moreover, trigonometry ratio is highly utilized in naval and aviation industries, in cartography even in the satellite system for communications [31-34].

Thus, on one hand, there are promising applications of optical NLM. On the other hand, on the other hand there are useful infliction imposed by trigonometric functions. To address this, we propose an all-optical scheme namely optical trigonometric functional device (OTFD) which enables the expression of trigonometric ratios of compound angles through the collaboration of optical switches and optical Ternary Encoders, both of which are based on all-optical NLM. To visualize this proposed scheme, SCL, MCL, BC, 50% BS, are utilized studiedly [35-36]. With the help of our proposed device, the following problems has been addressed:

the expression of

I. sin (A+B) as well as sin 2A or sin 2B
II. cos (A+B) as well as cos 2A or cos 2B

where A, B and (A+B) are positive angles. Also, it is noted that in this scheme A or B is represented by the intensity of the light beam. Thus, in the present paper, a cogitation for expressing trigonometric function of compound angle is introduced which is fully optical in nature which may pave numerous applications in modern optical computing systems.

5.2 Scheme of optical trigonometric functional device (OTFD)

The present paper demonstrates an optical scheme designed for expressing the trigonometric function of compound angle, where the angle is represented by light intensity levels. The final result of this scheme is illustrated by output of two optical

Ternary Encoders [36], wherein the output forms of the Ternary Encoders such as **1 and $\bar{1}$(in this scheme) reveal as $\sin\theta$ and $\cos\theta$,** respectively (here θ is an angle). The proposed OTFD design comprises five sections which are as follows

a) Input section
b) Regulation unit
c) Switching section
d) Processing section
e) Output division

Here it is to be noted that to perform the proposed scheme, there are some important components such as: Single constant light source (SC) of standard intensity level 'I', Multiple constant light sources (MCL), Beam combiner (BC) which helps to unite two polarized light waves, 50%-Beam splitter (BS) which helps in divide polarised light into two equal intensities. The construction of MCL [18] is such that it always provides polarized light with intensity level 'nI', where 'n' is natural number and 'I' refers to standard intensity level which is supplied by SCL. In our design MCL is abbreviated as M(nI).

5.2.1 Input section

The proposed scheme (OTFD) is designed for expressing the trigonometric function of compound angle (A+B) in terms of trigonometric function of 'A' and 'B', where angles A and B are served as input data. Formation of input data are illustrated in **Fig.-5.1**.

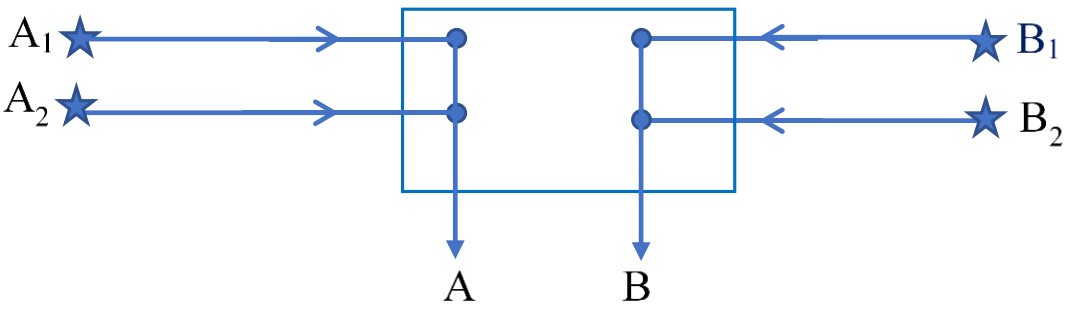

Fig.-5.1: Input section of OTFD

Here input 'A' consists of A_1 and A_2 (where each of them is SCL). Similarly input 'B' is composed by B_1 and B_2 (where both are SCL). As a result, the input data 'A' or 'B' is

represented by light intensity level either '0' (absence of light) or 'I' or '2I', which is shown in **Table-5.1**.

Table-5.1: Different values of light intensity level of input data 'A' & 'B'

A_1 or B_1	A_2 or B_2	$A=A_1+A_2$ or $B=B_1+B_2$
0	0	0
0	I	I
I	0	
I	I	2I

So, on the whole there are five different values of intensity levels of (A+B), such as 0, I, 2I, 3I & 4I (as shown in **Table-5.2**)

Table-5.2: Different values of total intensity level (A+B) of input data 'A' & 'B'

Intensity level of input data		Total intensity level of 'A' & 'B' i.e., value of (A+B)	Different values of (A+B)
A	**B**		
0	0	0	0
	I	I	I
	2I	2I	2I
I	0	I	3I
	I	2I	
	2I	3I	
2I	0	2I	4I
	I	3I	
	2I	4I	

5.2.2 Regulation unit

In the proposed design, the optical switch $(OS)_1$ acts as a regulator which define the output direction of optical ray from it.

Optical switch by NLM (non-linear material)

The fundamental equations of the nonlinear optics which governs the change of refractive index of medium are utilized to construct the optical switch as follows,

1. 2nd-order Kerr non-linearity equation:

$$n_{NL} = n_0 + n_2 I \qquad (1)$$

Where n_{NL} is the refractive index (RI) of NLM having self-focusing character, n_0 is the constant linear refractive index of the NLM. n_2 represents the 2nd order nonlinear correction term, known as nonlinear refractive index of the medium. 'I' represents the intensity of incident polarized light on NLM.

2. From the famous Snell's law of refraction-

$$n_L \sin\theta_1 = n_{NL} \sin\theta_2 \qquad (2)$$

Where n_L is the refractive index (RI) of the linear medium (LM), which is independent of the intensity of the incident light.θ_1 , and θ_2 are the incident refraction angles, respectively.

This is fact that (to minimize the deviation of output optical path from optical switch) linear and nonlinear medium are combined together to form the optical switch operation. The action of an optical switch is schematically shown in **Fig-5.2**

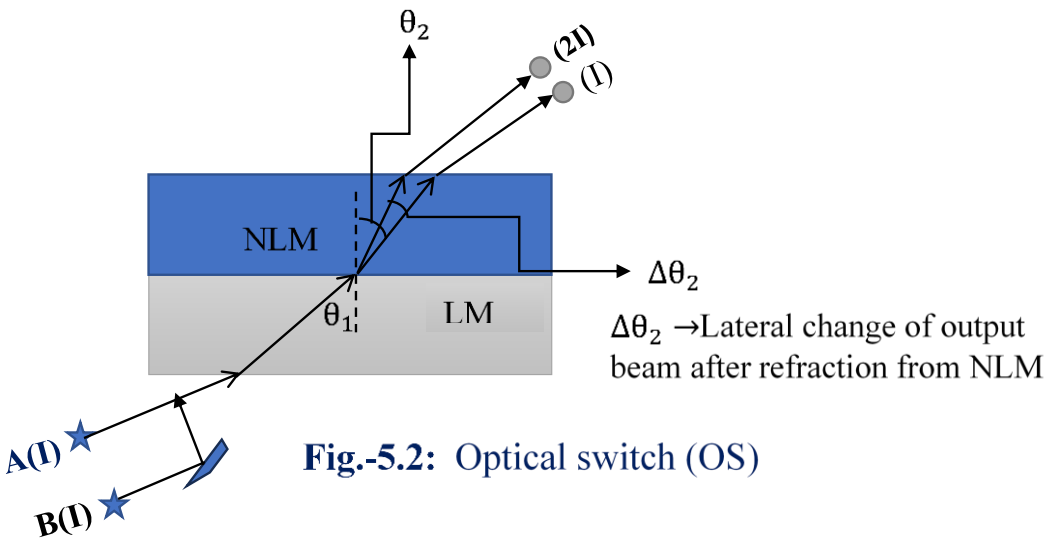

Fig.-5.2: Optical switch (OS)

In this scheme those NLM having self-focussing character (such as Cs_2, GaAs, pure silica etc.) are utilized as optical switch. Here to implement optical switch (OS) another important equation is utilized to calculate the power of the laser beam as follows

$$P = \frac{\pi\varepsilon_0 n_0 c a^4}{8 n_2 L^2} \qquad (3)$$

Here, L is the focal length induced by the NLM. P is the power of Laser beam. a denotes the area of cross-section of the applied Laser beam. ε_0 is the free space permittivity. c is the velocity of light in free space. From equation (3) we can obtain the focal length as

$L \propto \frac{1}{P}$ and $L \propto a$.

So L will be reduced with enhancing the 'P' and also with decreasing the $'a'$ optimally. So integrated optical system has to be implemented by setting a high-power laser source (such as femtosecond laser) with limiting diffraction property.

If we see the phenomena in case of a pure silica which has the following parameters: n_0=1.46; n_2=3.2×$10^{-20} m^2$/w. Now for NLM made of pure SiO_2, $\Delta\theta_2$ (the angular change of direction of the output beam) will be changed by 0.013° when pulse laser (of duration 10^{-7} sec on time and power of 100 mw) instead of continuous laser beam is appointed as input signal for double input intensity and fixed incident angle (45°)[16,18,22.] . The above value of $\Delta\theta_2$ will have 1.20° for 10^{-9} second on time duration pulse are utilized from 100 mw continuous laser keeping other parameters constant. For CS_2 n_0=1.62; n_2=0.22×$10^{-19} m^2$/w; so, the value of $\Delta\theta_2$ for CS_2 is greater than that of SiO_2. For an integrated optical system [37-38], in some cases to activate the nonlinear material, a high power of the laser source with limited diffraction ray may be required. It is also noted that to activate the NLM, coherent laser beams as inputs are also required. In this scheme Q-switched pulse laser (with 10^{-9} s pulse duration) is utilized as coherent light source. For an ordinary CW (continuous wave) laser of average power 100 mw having beam cross-section of 50 μm^2generates the intensity 2×10^9 w/m^2 whereas pulsed beam of pulse duration 10^{-9} s the laser peak intensity arrives a value of 2×10^{18} w/m^2. This pulsed laser beam can be achieved adopting a suitable Q-switching or mode locking mechanism. For example, a frequency doubled Nd: YAG (neodymium yttrium aluminum garnet) laser is capable of gaining an intensity of $megawatts/cm^2$ which is employed as an ideal source to excite the nonlinear material (NLM.) **Thus, in our proposed scheme optical switch $(OS)_1$ acts as Regulator or path finder (which is shown in Fig.-5.3).** Optical switch $(OS)_1$ emerges light ray in different directions according to intensity level of (A+B). So, we obtain different optical path for different intensity level as I, 2I, 3I and 4I. Here it is noted that path of intensities I, 2I, 3I and 4I are added with M(4I), M(3I), M(2I) and SCL(I) respectively. Finally, all output paths are assembled at the definite point 'C'.

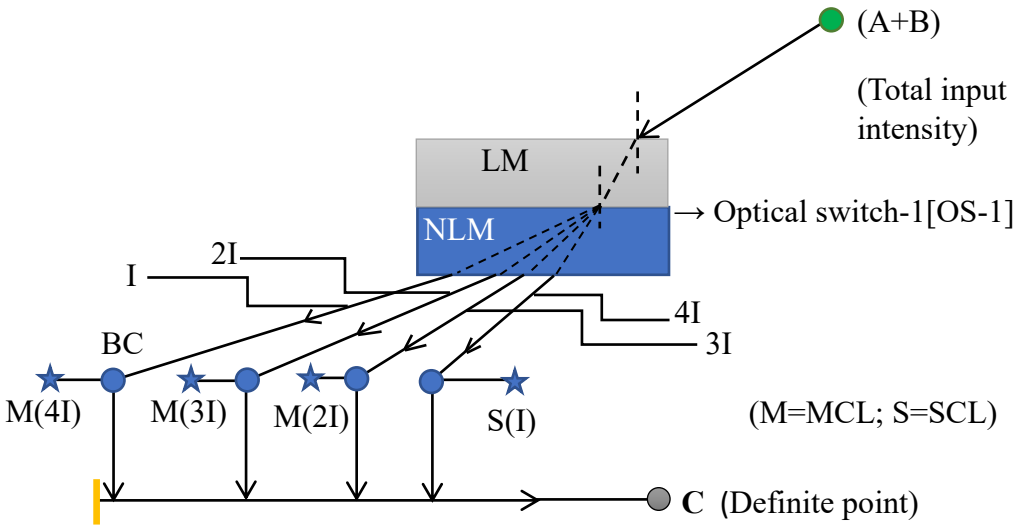

Fig.-5.3: Optical switch-1 $(OS)_1$ acts as regulator

As consequences, at any value of (A+B), the intensity at the point 'C' is found to be 5I (as shown in **Table -5.3**)

Table-5.3: Intensity at definite point 'C' for different value of total input intensity (A+B)

Different value of (A+B)	With the help of SCL(S) or MCL(M)	Intensity at definite point 'C'
I	M(2I)	5I
2I	M(3I)	5I
3I	M(2I)	5I
4I	S(I)	5I

5.2.3 Switching section

This section (which is shown in **Fig.-5.4**) consists of following parts:

I. Sin button and Cos button

II. Optical switch-2 [$(OS)_2$].

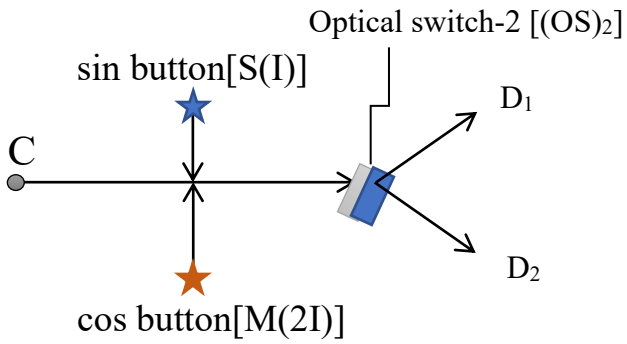

Fig.-5.4: [Switching section of OTFD where $(OS)_2$ acts as controller]

In proposed scheme when the expression of Sin(A+B) and Cos(A+B) have to be displayed then Sin button and Cos button are to be activated respectively but not simultaneously. Here Sin button and Cos button are the sources of polarized light with intensity level I and 2I, respectively. It is also to be noted that $(OS)_2$ acts as controller [25].

The action of $(OS)_2$ is described as follows:

When input light intensity into $(OS)_2$ is = 5I + I (due to Sin button) =6I, then output optical ray from $(OS)_2$ is to be connected into optical device named 'P' with additional intensity 6I [provided by M(6I)]. Whereas input light intensity into $(OS)_2$ is= 5I+ 2I (due to Cos button) =7I, then output optical path from $(OS)_2$ is to be joined into optical device named 'Q' with additional intensity level 5I [provided by M(5I)]. As a result, when Sin button is in the ON mode then optical device 'P' must be active with input intensity level of '12I' and when Cos button is in the ON mode then optical device 'Q' must be active with same intensity level of '12I'.

5.2.4 Processing section

In our proposed scheme, the processing section (shown in **Fig.-5.5**) consists of the following components such as

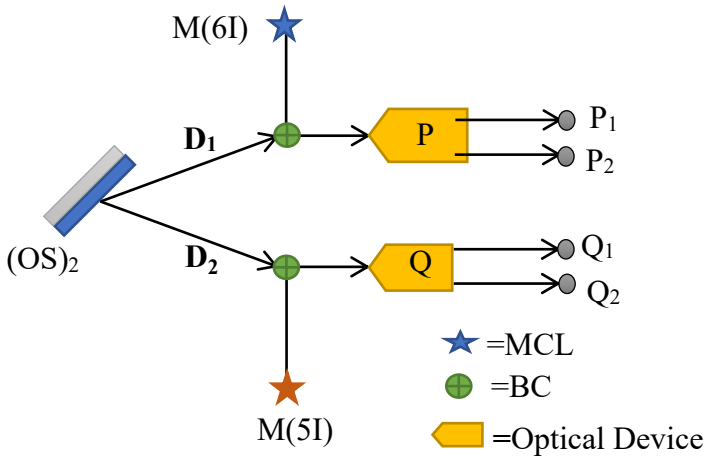

Fig.-5.5: Processing section of OTFD

I. Two MCL like M(7I) and M(6I)

II. Two optical devices (OD) named 'P' and 'Q' where they are single input system having two output channels.

In processing section two OD 'P' and 'Q' functionate as processor with help of two MCL [M(6I) and M(7I)] where input (I_P) of 'P' is combination of two channels as– D_1[one output path of $(OS)_2$] and MCL [M(6I)]. On the other hand, input (I_Q) of optical device of 'Q' is combination of two channels as-D_2 [another output path of $(OS)_2$ and MCL [M(7I)]. Once again in our proposed design (OTFD) the characteristics of optical device 'P' is such that it is actuated with fixed input light intensity of 12I and after activation it provides two output optical paths 'P_1' & 'P_2' of fixed light intensity level 5I & 7I respectively. Similarly feature of OD 'Q' is such that it is incited at fixed input light intensity of 12I and after activation, it provides two output optical lines 'Q_1' & 'Q_2' of fixed light intensity level 8I & 4I respectively. In the following sections the mechanism of optical devices is discussed.

5.2.4.1. Optical device- 'P'

The mechanism of OD 'P' is shown in Fig.-5.6 and Table-5.4.

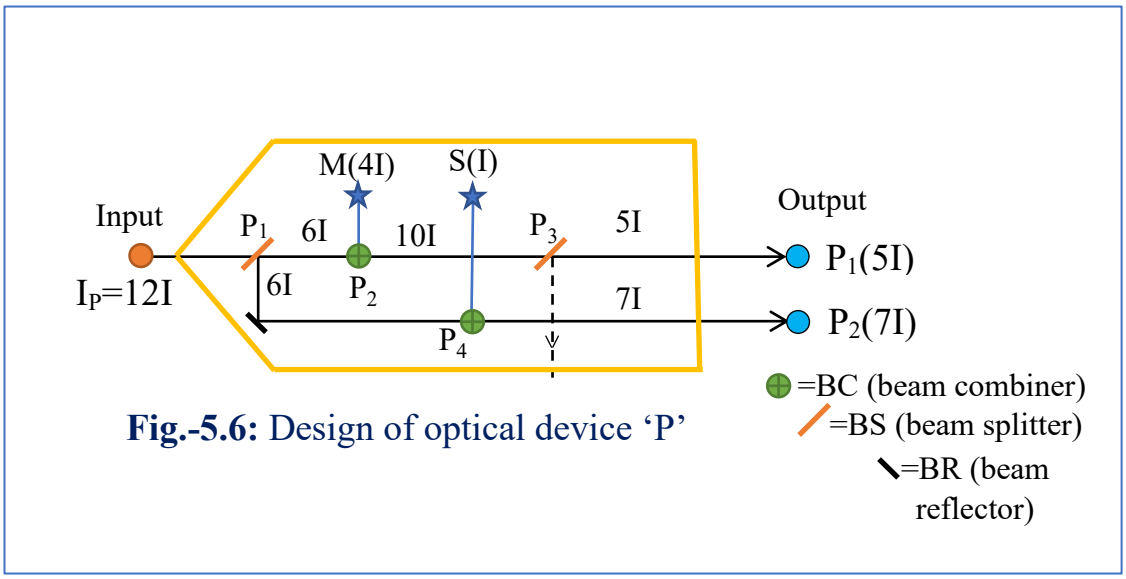

Fig.-5.6: Design of optical device 'P'

It has only one input channel and two output lines named P_1 & P_2. When Sin button is active then OD 'P' is incited with input light intensity level 12I. this polarized light beam of 12I is split at the point p_1 by 50% beam splitter.as a result there are two optical paths of same intensity 6I from the point p_1. Now at the point p_2 with the help of M(4I) and BC, total light intensity level is =(4I+6I) =10I. Then presence of 50% BS at the point p_3 we get two paths of same intensity level(5I) where one of them is acted as one output line (P_1) with intensity level 5I. Now with assistance of SCL & BC, total intensity level at the point p_4 is =(I+6I) =7I, which is another output line 'P_2' from OD 'P'. Finally, two output lines P_1 & P_2 from OD 'P' are connected into optical Ternary Encoder 'E_1' & 'E_2' respectively.

Table-5.4: Conclusive intensity level at different output lines of OD 'P'

Intensity level	At the certain point	With assistance of BC/BS	Output intensity level from that certain point	Output lines with intensity level from the OD
12I	p_1	BS	6I	
			6I	
6I	p_2	BC	10I	
10I	p_3	BS	5I	P_1(5I)
			5I	
6I	p_4	BC	7I	P_2(7I)

5.2.4.2. Optical device- 'Q'

The mechanism of OD 'Q' is shown in **Fig.-5.7** and **Table-5.5**.

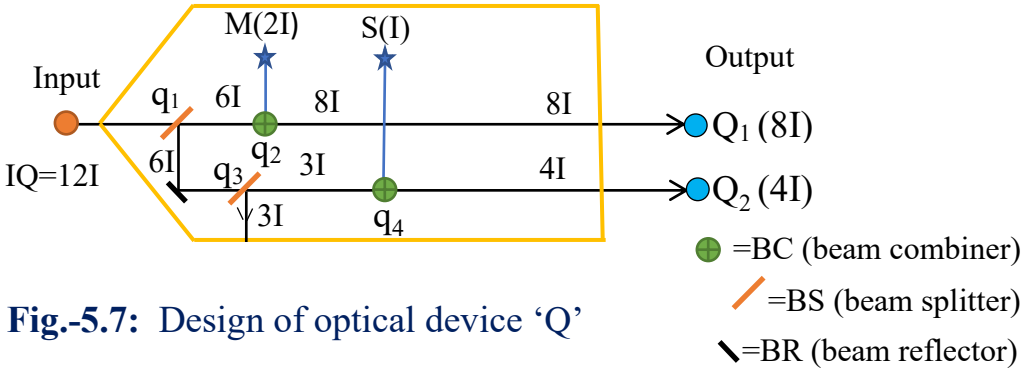

Fig.-5.7: Design of optical device 'Q'

It is also single input device having two output lines namely 'Q_1' and 'Q_2'. When Cos button is active then 'Q' is incited with input intensity level 12I. Then polarized light (of intensity level 12I) is split by 50% BS at the point q_1. Then at the point q_2 with the help of M(2I) and BC, total intensity of light is =(6I+2I) =8I. This polarized light beam is treated as one output line Q_1(8I) of OD 'Q'. Now at the point q_3, with the help of 50% BS, there are two optical lines (each of same intensity level 3I) where one of them approaches to the point q_4 and with help of S(I) and BC, we get new optical ray of intensity 4I(3I+I) from the point q_4. This optical line of intensity 4I serves as another output line Q_2(4I) from OD 'Q'. At last, these two output lines 'Q_1' & 'Q_2' from OD 'Q' are joined into optical Ternary Encoder 'E_1' & 'E_2' respectively.

Table-5.5: Conclusive intensity level at different output lines of OD 'Q'

Intensity level	At the certain point	With assistance of BC/BS	Output intensity level from that certain point	Output lines with intensity level from the OD
12I	q_1	BS	6I	
			6I	
6I	q_2	BC	8I	Q_1(8I)
6I	q_3	BS	3I	
			3I	
3I	q_4	BC	4I	Q_2(4I)

So, on the whole for same input intensity level 12I, it is accomplished that-

For OD 'P'→12I =P_1+P_2 =5I+7I;

For OD 'Q'→12I =Q_1+Q_2 =8I+4I.

5.2.5 Output Division

To implement the proposed device, we take two optical Ternary Encoder [36] where they have key role in displaying output form of trigonometric ratios of compound angle. In our proposed scheme the expansion of Sin (A+B) or Cos (A+B) is represented as sum or subtraction of two outputs (2-bit ternary form) of two optical Ternary Encoders i.e., $Sin(A+B) = Y_1+Y_2$ and $Cos(A+B) = Y_1-Y_2$; where Y_1 & Y_2 are output form of two optical Ternary Encoders E_1 & E_2 respectively. Here sign between Y_1 & Y_2 depends upon nature of the trigonometric function. For odd and even function sign between input data and sign between two output form (Y_1 & Y_2) are same and opposite in nature respectively (which is shown in **Table- 5.6**).

Table-5.6: Nature of sign between two output form of two optical Ternary Encoder

Sign between 'A' & 'B'	Sign between 'Y_1' & 'Y_2' for odd function	Sign between 'Y_1' & 'Y_2' for even function
+	+	−
−	−	+

Moreover, here input data 'A' and 'B' are treated as MSB (most significant bit) and LSB (least significant bit) of output form (2bit- ternary form) respectively of this scheme.

5.2.5.1. Operation of Ternary Encoder

In ternary number system, there are three basic numbers as 0,1 and 2. By Ternary Encoder, all decimal numbers can be expressed by those three basic numbers (0, 1 and 2). In optical Ternary Encoder, three basic numbers 0, 1 & 2 are represented by intensity level 0, I & 2I respectively. Moreover, in optical Ternary Encoder input intensity level I, 2I, 3I, 4I, 5I----------represent the decimal number 1, 2, 3, 4, 5----------respectively but output of optical Ternary Encoder is illustrated by tri-states as 0 (zero),1 (one) &$\bar{1}$ (one bar) where 0, 1 & $\bar{1}$ are represented by absence of light, presence of light with intensity level I and presence of light with intensity level 2I respectively.

5.2.5.2. Block diagram of optical Ternary Encoder

In this scheme optical Ternary Encoder are appointed in output division where any decimal number up to 8 is coded in ternary form. In this optical Ternary Encoder, there are eight number of SCL sources, where they are served as input decimal number. When a decimal

number has to be coded then that number of inputs SCL sources are to be kept in HIGH state (i.e., light is present). Depending upon value of input intensity level, output form is displayed by optical Ternary Encoder. Block diagram of 8-input optical Ternary Encoder and input versus output form in optical Ternary Encoder is shown in **Fig.-5.8** and **Table-5.7** respectively.

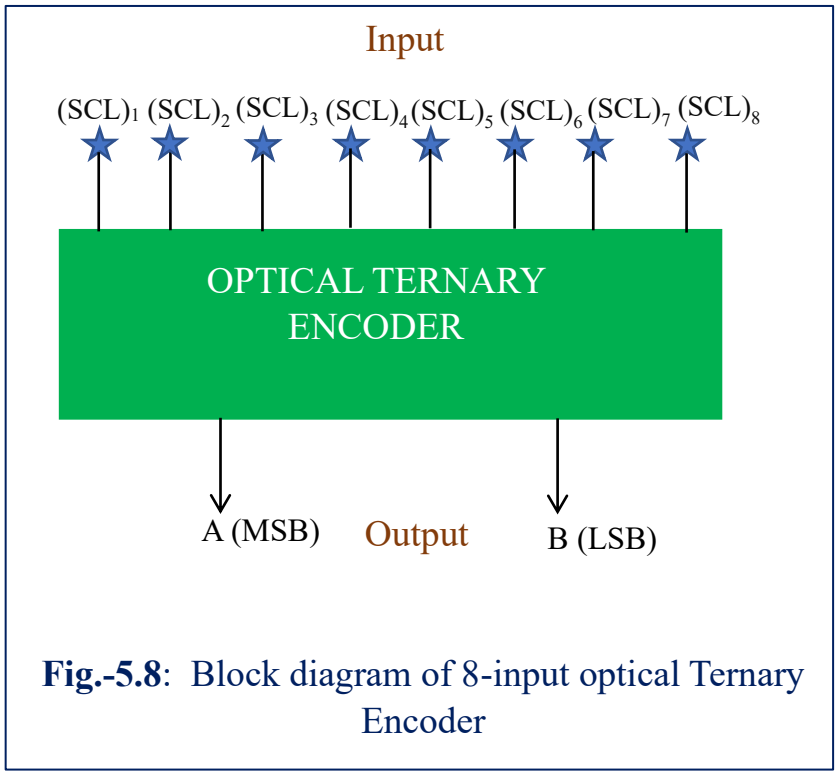

Fig.-5.8: Block diagram of 8-input optical Ternary Encoder

Table-5.7: Input versus output in 8-input optical Ternary Encoder

Decimal number	In terms of intensity level	Output form of optical Ternary Encoder	
		MSB (A)	LSB (B)
1	1	0	1
2	2I	0	$\bar{\mathbf{1}}$
3	3I	1	0
4	4I	1	1
5	5I	1	$\bar{\mathbf{1}}$
6	6I	$\bar{\mathbf{1}}$	0
7	7I	$\bar{\mathbf{1}}$	1
8	8I	$\bar{\mathbf{1}}$	$\bar{\mathbf{1}}$

5.2.5.3. Output of Ternary Encoder as output of proposed design

In general, 2-bit ternary form output (Y) of optical Ternary Encoder is imparted as Y(A)Y(B) where A & B are MSB & LSB of ternary form. In this scheme at MSB 'A', 1 (presence of light with intensity level I) and $\bar{1}$ (presence of light with intensity level 2I) connote sin A and cos A respectively. Similarly, at LSB 'B', 1 and $\bar{1}$ signifies sin B and cos B respectively. Here it is also noted that for position of 0 either at MSB or at LSB means that it is insignificant. Significance of output form of appointed optical Ternary Encoder in this proposed scheme is shown in **Table-5.8**.

Table-5.8: Connotation of ternary form in proposed scheme OTFD

Decimal number in terms of light intensity level	Output form of optical ternary Encoder		Connotation of output ternary form in proposed scheme
	MSB(A)	LSB(B)	
I	0	1	–
2I	0	$\bar{1}$	–
3I	1	0	–
4I	**1**	**1**	**sinAsinB**
5I	**1**	**$\bar{1}$**	sinAcosB
6I	$\bar{1}$	0	–
7I	**$\bar{1}$**	**1**	cosAsinB
8I	**$\bar{1}$**	**$\bar{1}$**	**cosAcosB**

To actualize the proposed scheme, optical Ternary Encoder (OTE) E_1 and E_2 are appointed as output division where outputs of them are-

$Y_1 = Y_1(A)Y_1(B)$ and $Y_2 = Y_2(A)Y_2(B)$ respectively. Finally in our design, output is illustrated as $Y = (Y_1 \pm Y_2) = Y_1(A)Y_1(B) \pm Y_2(A)Y_2(B)$ (which is shown in **Fig.-5.9** and **Table-5.9**). Here, sign between Y_1 & Y_2 depends upon nature of trigonometric function. For odd and even function plus (+) & minus (−) sign is accepted as plus (+) sign between inputs 'A' and 'B' respectively. Here it is also remarkable note that in output form of OTE i.e., in Y [= Y(A)Y(B)], Y(A)Y(B) is the ternary representation of the decimal number (where A= MSB & B= LSB). Y(A)Y(B) is not meaning Y(A) is multiplied by Y(B) but at

output in our proposed design, there is multiplication between connotation of Y(A) and Y(B).

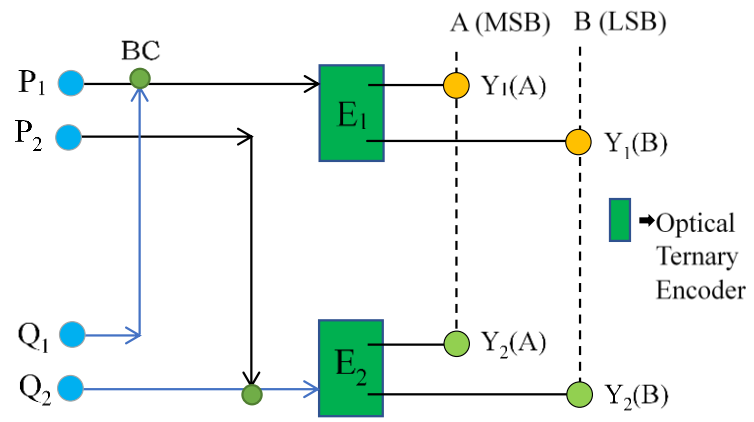

Fig.-5.9: Output division of OTFD

Table-5.9: Output form of proposed device (OTFD) with help of optical Ternary Encoder

Name of the optical Ternary Encoder	Output of optical Ternary Encoder	2-bit output form of optical Ternary Encoder at		Output form (Y) of proposed OTFD with help of two Ternary Encoder 'E_1' & 'E_2'
		MSB 'A' =Y(A)	LSB 'B' =Y(B)	
E_1	Y_1	$Y_1(A)$	$Y_1(B)$	**$Y= Y_1(A)Y_1(B) + Y_2(A)Y_2(B)$**
E_2	Y_2	$Y_2(A)$	$Y_2(B)$	

5.2.5.4. Function of the optical Ternary Encoder in proposed OTFD

To perform the proposed device, we employ two optical Ternary Encoders (OTE) E_1 and E_2 where input of optical Ternary Encoders and output of optical devices (P & Q) are connected by the relation-

$E_1 = P_1 + Q_1 = P_1(5I) + Q_1(8I)$ and $E_2 = P_2 + Q_2 = P_2(7I) + Q_2(4I)$.

Again, it is already discussed that the output of OTFD is represented by –

$Y = Y_1 \pm Y_2 = Y_1(A)Y_1(B) \pm Y_2(A)Y_2(B)$, where Y_1 and Y_2 are 2-bit output form of OTE E_1 and E_2 respectively. Moreover, A and B are MSB and LSB in output form for each OTE.

When optical device 'P' is active with collaboration of Sin button and $(OS)_2$, then input intensity into OTE 'E_1'= P_1= 5I and into OTE 'E_2'= P_2= 7I. So, output form of 'E_1' is = $Y_1(A)Y_1(B)= 1\bar{1}$= sinAcosB (from **Table-5.8**) and output form of 'E_2' is = $Y_2(A)Y_2(B)= \bar{1}\ 1$= cosAsinB (from Table-8). Therefore, final output form of the proposed scheme for sin(A+B) = $Y_1 + Y_2$ = sinAcosB + cosAsinB.

Again, when optical device 'Q' is operative by dint of Cos button and optical switch $(OS)_2$ then input intensity into OTE E_1 =Q_1 =8I and into OTE E_2 =Q_2 =4I. So, output form of 'E_1' is = $Y_1(A)Y_1(B)= \bar{1}\bar{1}$ =CosACosB (from Table-8) and output form of 'E_2' is = $Y_2(A)Y_2(B)= 11$= sinAsinB (from Table-8). So, ultimate output form of the OTFD for Cos(A+B) is = $Y_1 - Y_2$ =cosAcosB – sinAsinB.

The function of OTE at different optical button either Sin button or Cos button [for total input intensity(A+B)] is shown in **Table-5.10**.

Table-5.10: Function of optical Ternary Encoder at different optical button in OTFD

Name of the active button for total input intensity (A+B)	Connecting optical devices (OD)	Name of the output path from OD (with intensity level)	Connecting optical Ternary Encoder (OTE)	Output of OTE	Output of OTE in form Y(A)Y(B); [where 'A' & 'B' acts as MSB & LSB respectively] and its connotation in OTFD		Final output form of OTFD (for particular button) $Y=Y_1 \pm Y_2$
					Y(A)	Y(B)	
Sin	P	P_1(5I)	E_1	Y_1=	$Y_1(A)$=1 =sin A	$Y_1(B)=\bar{1}$ =cos B	Y= sinAcosB+ cosAsinB
		P_2(7I)	E_2	Y_2 =	$Y_2(A)=\bar{1}$ =cosA	$Y_2(B)$=1 =sin B	
Cos	Q	Q_1(8I)	E_1	Y_1=	$Y_1(A)=\bar{1}$ =cosA	$Y_1(B)=\bar{1}$ =cos B	Y= cosAcosB −sin AsinB
		Q_2(4I)	E_2	Y_2=	$Y_2(A)$=1 =sin A	$Y_2(B)$=1 =sin B	

5.3 Operation of Optical Trigonometric Functional Device (OTFD)

Operation of proposed scheme OTFD is shown in **Fig.-5.10**.

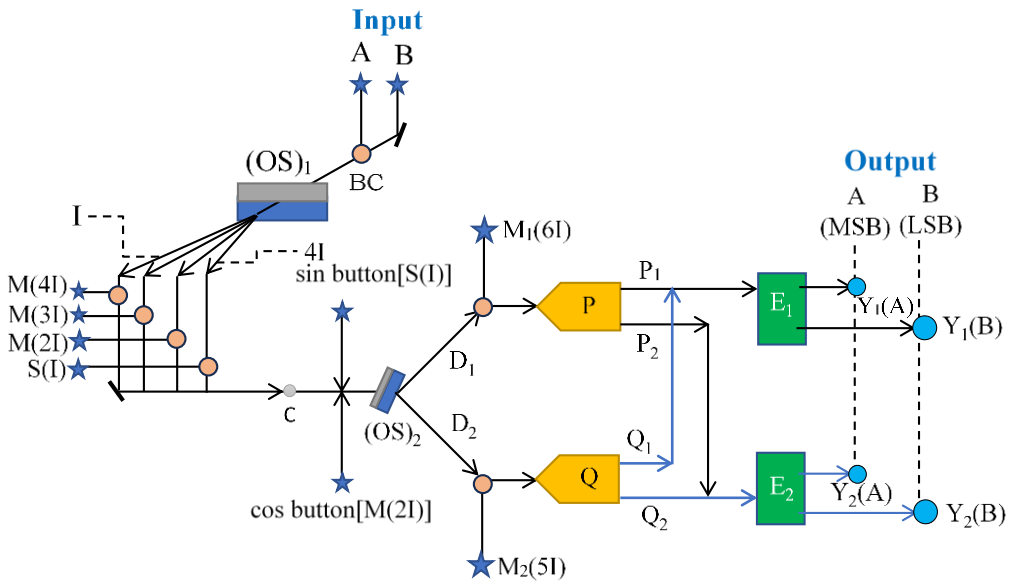

Fig.-5.10: Optical trigonometric functional device (OTFD)

Now to find the value of Sin(A+B) or Cos(A+B), we first take the value A and B. Then with help of the BC, we get total value of (A+B) in terms of light intensity, which serve as total input (light) intensity into $(OS)_1$. In our proposed scheme, there are four different types of values of (A+B) as I, 2I, 3I & 4I (from **Table-5.2**) and in accordance with these input intensity level, the optical output lines from $(OS)_1$ are in various directions with intensity level I, 2I, 3I & 4I respectively. Finally, with help of constant light sources (SCL or MCL) sources all output lines reach the definite point 'C' (input port of controlling section) with definite light intensity level 5I (shown in **Table-5.3**).

Now for expression of either Sin(A+B) or Cos(A+B), we have to actuate the Sin button or Cos button respectively. Now when Sin or Cos button is incited then input light intensity into $(OS)_2$ is 6I(5I+I) or 7I(5I+2I) respectively. So, depending upon ON state of Sin and Cos button, output lines from $(OS)_2$ (impersonate as controller) are directed to the optical path named D_1(6I) & D_2(7I) respectively. Here in this design D_1 & D_2 enter as the input line of OD 'P' & OD 'Q' by connecting with additional sources M_1(6I) & M_2(5I) respectively. As a result, total input intensity into OD 'P' is $=D_1+M_1=6I+6I=12I$ and into OD 'Q' is $= D_2+M_2=7I+5I=12I$.

5.3.1. Expression of sin(A+B)

Here strictly noted that two buttons (Sin & Cos) cannot be activated simultaneously. As consequences when Sin button is ON state then OD 'P' is stimulated, otherwise when Cos button is ON state then OD 'Q' is enlivened by same input intensity level 12I. Thus, to get expression of Sin(A+B), OD 'P' is stimulated by Sin button. Then output lines P_1 & P_2 (with intensity level 5I & 7I respectively) from OD 'P' are connected into OTE E_1 & E_2 respectively.

Now let Y_1 & Y_2 are the output of E_1 & E_2 respectively. So, output form of Y_1 & Y_2 are to be displayed as –

$Y_1 = Y_1(A)Y_1(B)$

$= 1\ \bar{1}$ [due to coefficient of intensity level of P_1]

= sinAcosB [owing to connotation in OTFD from Table-8] and

$Y_2 = Y_2(A)Y_2(B)$

$= \bar{1}\ 1$ [due to coefficient of intensity level of P_2]

=cosAsinB [owing to connotation in OTFD from Table-8] respectively.

As an outcome, final output of the OTFD for sin(A+B) is = $Y = (Y_1 + Y_2)$ = sinAcosB + cosAsinB.

- ***Calculation of sin(A−B)***

  Now from Table-6, sin(A−B) is =$Y = Y_1 - Y_2$ = sinAcosB − cosAsinB

5.3.2. Expression of cos(A+B)

Now to get expression of Cos(A+B) OD 'Q' is stimulated by Cos button. Then from property of OD 'Q' there are two output lines Q_1(8I) & Q_2(4I) from OD 'Q' when input light intensity level OD 'Q' is 12I. Again, Q_1 & Q_2 are joined with OTE E_1 & E_2 respectively. Since coefficient of input intensity into OTE E_1 & E_2 are 8 & 4 respectively. So, output form of OTE E_1 & E_2 are –

$Y_1 = Y_1(A)Y_1(B)$

$= \bar{1}\ \bar{1}$ [due to coefficient of intensity level of Q_1]

= cosAcosB [owing to connotation in OTFD from Table-8] and

$Y_2 = Y_2(A)Y_2(B)$

$= 1\ 1$ [due to coefficient of intensity level of Q_2]

=sinAsinB [owing to connotation in OTFD from Table-8] respectively.

So as ending, output of the OTFD for cos(A+B) is = Y = ($Y_1 - Y_2$) = cosAcosB – sinAsinB.

➢ *Calculation of cos(A−B)*

Now from Table-6, cos(A−B) is =Y = ($Y_1 + Y_2$) = cosAcosB + sinAsinB.

Operation of OTFD is shown in **Table-5.11** and **Table-5.12**.

Table-5.11: Input versus output of OTFD

Input intensity		Intensity at definite point 'C'	Name of the optical button	Name Of the output line from $(OS)_2$	Name of the connected MCL	Connected OD (with total input intensity)	Output line from OD	Connected OTE	Output form of OTE		Output form of OTFD= output of E_1+ output of E_2
A	B								MSB (A)	LSB (B)	
0	I	5I	Sin	D_1	M_1	P (D_1+ M_1)	P_1	E_1	1	$\bar{1}$	Y=1 $\bar{1}$ + $\bar{1}$ 1 =sinAcosB+ cosAsinB
0	2I	5I									
I	0	5I					P_2	E_2	$\bar{1}$	1	
I	I	5I									
I	2I	5I	Cos	D_2	M_2	Q (D_2+M_2)	Q_1	E_1	$\bar{1}$	$\bar{1}$	Y=$\bar{1}$ $\bar{1}$ − 1 1 =cosAcosB −sinAsinB
2I	0	5I									
2I	I	5I					Q_2	E_2	1	1	
2I	2I	5I									

Table-5.12: Calculation of expression of sin(A+B) & cos(A+B) for different value of 'A' & 'B' from OTFD]

Input intensity		Output of OTFD for active Sin button i.e., sin(A+B) = sinAcosB+ cosAsinB	Output of OTFD for active Cos button i.e., cos(A+B) = cosAcosB− sinAsinB
A	B		
0	I	sin0cosI + cos0SinI	cos0cosI - sin0sinI
0	2I	sin0cos2I + cos0sin2I	cos0cos2I - sin0sin2I
I	0	sinIcos0 + cosIsin0	cosIcos0 - sinIsin0
I	I	sinIcosI + cosIsinI	cosIcosI - sinIsinI
I	2I	sinIcos2I + cosISin2I	cosIcos2I - sinIsin2I
2I	0	sin2Icos0 + cos2Isin0	cos2Icos0 - sin2Isin0
2I	I	sin2IcosI + cos2IsinI	cos2IcosI - sin2IsinI
2I	2I	sin2Icos2I + cos2Isin2I	cos2Icos2I - sin2Isin2I

5.3.3. Examples of trigonometric operations by means of light intensity level

Here we discuss some examples of trigonometric operations with some realistic values of light intensities followed by respective angles. By dint of our scheme (OTFD), the expression of sin(A+B) or cos(A+B) is displayed by optically. In this scheme input data (angle) 'A' or 'B' is represented by intensity level as either 0 or I or 2I. So, expression of sin(A+B) or cos(A+B) is displayed by light intensity levels.

Here some specific angles can be determined with help of some commonly known value of $\sin\theta$ and $\cos\theta$ (which is shown in **Table-5.13**) fully optically like as-

Example-1. $\mathbf{\sin 75^\circ}$ & $\mathbf{\cos 75^\circ}$[and then **sin 15° & cos 15°**

Here let A= 30°=I & B= 45°=2I.

Now output form (Y) of OTFD for sin(A+B) i.e., sin(I+2I) is [from **Table-5.11** & **Table-5.12**] as-

Y= $1\bar{1}+\bar{1}1$=sinAcosB + cosAsinB=sinIcos2I + cosIsin2I=$\sin30^\circ\cos45^\circ + \cos30^\circ\sin45^\circ$

$=\frac{1}{2}\frac{1}{\sqrt{2}} + \frac{\sqrt{3}}{2}\frac{1}{\sqrt{2}} = \frac{1+\sqrt{3}}{2\sqrt{2}}$. $\therefore \sin75^\circ = \frac{1+\sqrt{3}}{2\sqrt{2}}$.

Similarly, cos(A+B) = $\bar{1}\bar{1} - 11$=cosAcosB− sinAsinB=cosIcos2I− sinIsin2 = $\cos30^\circ\cos45^\circ - \sin30^\circ\sin45^\circ$

$=\frac{\sqrt{3}}{2}\frac{1}{\sqrt{2}} - \frac{1}{2}\frac{1}{\sqrt{2}} = \frac{\sqrt{3}-1}{2\sqrt{2}}$. $\therefore \cos75^\circ = \frac{\sqrt{3}-1}{2\sqrt{2}}$.

[Now sin(2I-I) =sin (45°-30°)=sin15° or, sin2IcosI-cos2IsinI=sin15°or, sin45°cos30°-cos45°sin30°= sin15° or, $\frac{1}{\sqrt{2}}\frac{\sqrt{3}}{2} - \frac{1}{\sqrt{2}}\frac{1}{2}$=sin15° or, $\sin15^\circ = \frac{\sqrt{3}-1}{2\sqrt{2}}$. Similarly, we can calculate cos(2I-I) = cos (45°-30°)=cos15°]

Example-2. $\mathbf{\sin 90^\circ}$ & $\mathbf{\cos 90^\circ}$

Here let A= 30°=I & B= 60°=2I.

Now output form (Y) of OTFD for sin(A+B) i.e., sin(I+2I) is [from **Table-5.11** & **Table-5.12**] as-

Y= $1\bar{1}+\bar{1}1$=sinIcos2I + cosIsin2I=$\sin30^\circ\cos60^\circ + \cos30^\circ\sin60^\circ = \frac{1}{2}\frac{1}{2} + \frac{\sqrt{3}}{2}\frac{\sqrt{3}}{2} = \frac{1}{4} + \frac{3}{4} = 1$.
$\therefore \sin90^\circ = 1$

Similarly, 'Y' for cos(I+2I) = cosIcos2I − sinIsin2I= $\cos30^\circ\cos60^\circ - \sin30^\circ\sin60^\circ$

$= \frac{\sqrt{3}}{2}\frac{1}{2} - \frac{1}{2}\frac{\sqrt{3}}{2} = 0$. $\therefore \cos90^\circ = 0$.

Example-3. $\mathbf{\sin 105^\circ}$ & $\mathbf{\cos 105^\circ}$

Here let A= 45°=I & B= 60°=2I. Now output form (Y) of OTFD for sin(A+B) i.e., sin(I+2I) is [from Table-11 & Table-12] as- Y= $1\bar{1}+\bar{1}1$=sinAcosB + cosAsinB=sinIcos2I + cosIsin2I=sin45°cos60° +cos45°sin60°=$\frac{1}{\sqrt{2}}\frac{1}{2}$ + $\frac{1}{\sqrt{2}}\frac{\sqrt{3}}{2}$ =$\frac{1+\sqrt{3}}{2\sqrt{2}}$. ∴sin105°=$\frac{1+\sqrt{3}}{2\sqrt{2}}$.

Similarly, cos(A+B) = $\bar{1}\bar{1}$ − 11=cosAcosB− sinAsinB= cosIcos2I− sinIsin2I = cos45°cos60° − sin45°sin60°

=$\frac{1}{\sqrt{2}}\frac{1}{2}$ − $\frac{1}{\sqrt{2}}\frac{\sqrt{3}}{2}$ =$\frac{1-\sqrt{3}}{2\sqrt{2}}$. ∴cos105° =$\frac{1-\sqrt{3}}{2\sqrt{2}}$.

Example-4. **sin 120° & cos 120°**

Here let A= 60°=I & B= 60°=I.Now output form (Y) of OTFD for sin(A+B) i.e., sin(I+I) is [from Table-11 & Table-12] as- Y= $1\bar{1}+\bar{1}1$=sinIcosI + cosIsinI=sin60°cos60° + cos60°sin60°=$\frac{\sqrt{3}}{2}\frac{1}{2}$ + $\frac{1}{2}\frac{\sqrt{3}}{2}$ =$\frac{\sqrt{3}}{2}$. ∴sin120°= $\frac{\sqrt{3}}{2}$.

Similarly, 'Y' for cos(I+I) = cosIcosI − sinIsinI= cos90°cos90° + sin90°sin90°

=$\frac{1}{2}\frac{1}{2}$ − $\frac{\sqrt{3}}{2}\frac{\sqrt{3}}{2}$ = −$\frac{1}{2}$. ∴cos120°=−$\frac{1}{2}$.

Example-5. **sin 180° & cos 180°**

Here let A= 90°=I & B= 90°=I.

Now output form (Y) of OTFD for sin(A+B) i.e., sin(I+I) is [from Table-11 & Table-12] as-

Y= $1\bar{1}+\bar{1}1$=sinIcosI + cosIsinI=sin90°cos90° + cos90°sin90°=1×0 + 0×1=0. ∴sin180°= 0.

Similarly, 'Y' for cos(I+I) = cosIcosI − sinIsinI= cos90°cos90° − sin90°sin90°

= (0× 1) − (1 ×1) =− 1. ∴cos180°=− 1.

Table-5.13: Some commonly known value of sin θ and cos θ.

θ(Angle)	30°	45°	60°
$\sin\theta$	$\frac{1}{2}$	$\frac{1}{\sqrt{2}}$	$\frac{\sqrt{3}}{2}$
$\cos\theta$	$\frac{\sqrt{3}}{2}$	$\frac{1}{\sqrt{2}}$	$\frac{1}{2}$

Similarly, we can calculate the trigonometric ratios of some specific angle with help of commonly known value and determined output value of sinθ and cosθ by OTFD. This is shown by **Table-5.14**.

Table-5.14: Determination of the trigonometric ratios (sin or cos) of some angles with help of known value and determined output value by OTFD (where angle is represented by light intensity level).

Angle represented by intensity level=I	Angle represented by intensity level=2I	Determined output value of sinθ or cosθ where θ=I+2I	Determined output value of sinθ or cosθ where θ=2I−I
30°	45°	75°	15°
30°	60°	90°	Not necessary
45°	60°	105°	-
30°	90°	120°	-
45°	90°	135°	-
60°	90°	150°	-
75°	90°	165°	-
90°	90°	180°	-
75°	120°	195°	-
75°	135°	210°	
75°	150°	225°	-
75°	180°	255°	-
60°	180°	240°	-
90°	180°	270°	-
15°	270°	285°	-
15°	285°	300°	-
15°	300°	315°	-
15°	315°	330°	-
15°	330°	345°	-
180°	180°	360°	0°

In our proposed scheme, output of the device (OTFD) is displayed with collaboration of two optical 2-bit ternary Encoders (where input A & B are treated as MSB & LSB respective of 2- bit output ternary form). Although there are three states $(0,1,\bar{1})$ in optical Ternary Encoder, but in our optical design, two states 1 and $\bar{1}$ are dealt.

I. 1 reveal as Sinθ; θ is acute angle. But in this scheme θ= name of the beat either MSB(A) or LSB(B), wherein 1 is presented in output ternary form.

II. $\bar{1}$ (Presence of light with intensity level 2I) connote Cosθ ; θ= name of the beat either MSB(A) or LSB(B), wherein $\bar{1}$ is located in output ternary form.

In summary, to implement the proposed design, we follow the following criterions.

i. All light must be coherent and same state of polarization in nature.

ii. To minimize the deviation of light beam from optical switch, LM and NLM are coupled for making optical switch.

iii. SCL, MCL, 50% BS, BC are utilized purposefully.

iv. In this design, sin button and cos button are not activated simultaneously.

v. In our proposed scheme, the property of optical devices ('P' & 'Q') such that they are activated by the certain amount of input intensity level (otherwise they will be inactive) and after activation they provide the two output lines of fixed intensity level.

vi. Optical output form of OTFD is $Y= (Y_1 \pm Y_2)$ (where Y_1 & Y_2 are the output form of optical Ternary Encoder E_1 & E_2). Here Sign between Y_1 & Y_2 depends upon nature of odd or even function. For odd function and even function sign between Y_1 & Y_2 same and opposite as sign between inputs 'A' & 'B' respectively.

So, $\sin(A \pm B) = (Y_1 \pm Y_2)$ and $\cos(A \pm B) = (Y_1 \mp Y_2)$.

By virtue of the proposed scheme, the expression of Sin(A+B) and Cos(A+B) are displayed optically, then it can be calculated of Sin(A−B) and Cos(A−B). Thus, output expression of sin(A±B) and cos(A±B), all are optical in nature. So, we are hopeful that our proposed scheme which is wholly optical in nature as well as high degree of processing speed and it can be applied to the field of optical computation.

5.4 Conclusion

In conclusion, an all-optical device is proposed and theoretically presented to effectively express the trigonometric ratios of compound angles (acute). The device is formulated by dint of intensity based refractive index property of isotropic optical nonlinear material and inherent parallelism of optical signal, which can effectively express the values of sin(A+B) and cos(A+B) where acute angles 'A' & 'B' (serve as input) are represented by the light intensity level. The proposed scheme is realised for A or B=0/I/2I. In our proposed scheme, output of the device (OTFD) is displayed with collaboration of two optical 2-bit ternary Encoders (where input A & B are treated as MSB & LSB respective of 2- bit output ternary form). Although there are three states $(0,1,\bar{1})$ in optical Ternary Encoder, but in our optical

design, two states 1 and $\bar{1}$ are dealt. By virtue of the proposed scheme, the expression of Sin(A+B) and Cos(A+B) are effectively displayed by the all-optical means which can further help in calculating the Sin(A−B) and Cos(A−B). Thus, the proposed design facilitates a novel way to express the sin(A±B) and cos(A±B) by an all-optical root. Henceforth, we hold great optimism regarding our envisioned system, which boasts a purely optical foundation accompanied by an exceptional level of processing speed. This innovative scheme has the potential to revolutionize the realm of optical computation, presenting a multitude of promising applications.

5.5 References:

1. E. Garmire, Elsa, "Nonlinear optics in daily life," *Optics express* 21, no. 25, 30532-30544 (2013).
2. Bano, Rehana, Maria Asghar, Khurshid Ayub, Tariq Mahmood, Javed Iqbal, Sobia Tabassum, Rozalina Zakaria, and Mazhar Amjad Gilani, "A theoretical perspective on strategies for modelling high performance nonlinear optical materials," *Frontiers in Materials* 532, (2021).
3. Chatterjee, Agnijita, Subhendu Biswas, Sourangshu Mukhopadhyay, "Method of frequency conversion of Manchester encoded data from a Kerr type of nonlinear medium," *J Opt. The Optical Society of India,* 46, 415-419, (2017).
4. Chandra, Sutanu Kumar, Subhendu Biswas, Sourangshu Mukhopadhyay, "Phase-encoded all-optical reconfigurable integrated multilogic unit using phase information processing of four-wave mixing in semiconductor optical amplifier," *IET Optoelectron.*, Vol. 10, Iss. 1, pp. 1–6 (2016).
5. Saha, Subhendu, Paromita de, Sourangshu Mukhopadhyay, "All optical frequency encoded quaternary memory unit using symmetric configuration of MZI-SOA," *Optics and Laser Technology* ,131, 106386 (2020).
6. Biswas, Subhendu & Mukhopadhyay, Sourangshu, "All-optical approach for conversion of a binary number having a fractional part to its decimal equivalent to three places of decimal using single system optical tree architecture," *J Opt*, 43(2):122–129, (April–June 2014)
7. Boyd, Robert W., "Nonlinear optics," *Academic press*, 2020.
8. S.D. Smith, "Optical bistability, photonic logic and optical computation," *Appl. Opt.* 25, 1550–1564 (1986).
9. G. Li, L. Lin, L. Shao, Y. Yin, J. Hua, "Parallel optical negabinary arithmetic based on logic operations," *Appl. Opt.* 36, 1011–1016 (1997).
10. H.J. Caulfield, "Perspectives in optical computing," *Computer* 31(2), 22-25 (1998).
11. M.A. Karim and A. A. S. Awwal, "Optical Computing: An Introduction," *(Wiley, New York, 2003)*, Chap. 3, pp. 35–56.

12. L.K. Cotter, T.J. Drabik, R.J. Dillon, M.A. Handaschy, "Ferroelectric-liquid-crystal/silicon-integrated circuit spatial light modulator," *Opt. Lett.* 15(5), 291–293 (1990).

13. S.D. Smith, H.A. Mackenzie, J.G.H. Mathew, J.J.E. Reid, M.R. Taghizadeh, F.A.P. Tooley, A.C. Walker, "Nonlinear optical circuit elements, logic gates for optical computers: the first digital circuits," *Opt. Eng.*24(4), 569–574 (1985).

14. N. Pahari, D.N. Das, S. Mukhopadhyay, "All-optical method for the addition of binary data nonlinear materials," *Appl. Opt.* 43(33), 6147–6150 (2004).

15. D. Psaltis, D. Brady, K. Wagner, "Adaptive optical networks using photorefractive crystals," *Appl. Opt.*27(9), 1752–1759 (1998).

16. N. Pahari, A. Guchhait, "All-optical serial data transfer between registers using optical mom-linear materials," *Optik* 123(5), 462–466 (2012).

17. N. Pahari, A. Guchhait, A.D. Jana, "Image edge detection scheme by the use of Kerr-type non-linear material and the verification of the scheme by computer simulation," *Optical Society of India* (2012).

18. A. Guchhait, N. Pahari, N.B. Manik, "Optical Kerr nonlinear material for calculating the coefficient of binomial expansion under any positive integral index," *Journal of optics* 51, 851-865 (2022).

19. Subhendu Biswas, Sourangshu Mukhopadhyay, "An all-optical scheme of secured cryptographic communication encoded with decimal data," *Optik* 124 (2013) 2376–2378.

20. Subhendu Biswas, Sourangshu Mukhopadhyay, "An all-optical approach for developing a system involving Kerr-material based switches for cryptographic encoding of binary data depending on the input parity," *Optik* 125 (2014) 1954–1956.

21. S.P. Medhekar, P. Paltani, "Proposal for optical switch using non-linear refraction," *IEEE photonics Technol. Lett.* 18(15), 1579–1581 (2006).

22. N. Mitra, S. Mukhopadhyay, "Method of developing an all-optical synchronous counter by exploiting the Kerr non-linearity of the medium," *Opt. Photon. Lett.* 3(1), 23–30 (2010).

23. Y. Fainman, C.C. Guest, S.H. Lee, "Optical digital logic operations by two beams coupling in photorefractive material," *Appl. Opt.* 25(10), 1598–1603 (1986).

24. N. Pahari, S. Mukhopadhyay, "An all-optical R-S flip-flop by optical non-linear material," *Journal of optics*,2005, Vol.34, no. 3 page 108-114.

25. J. N. Roy, A. K. Maiti, D. Samanta and S. Mukhopadhyay, "Tree-net architecture for integrated all-optical arithmetic operations and data comparison scheme with optical nonlinear material," *Optical Switching and Networking* 4 (2007) 231-237.

26. Smith, S. D., "Lasers, nonlinear optics and optical computers," *Nature* 316, no. 6026 (1985): 319-324.

27. Nie, Wenjiang, "Optical nonlinearity: phenomena, applications, and materials," *Advanced Materials* 5, no. 7-8 (1993): 520-545.

28. Kazanskiy, Nikolay L., Muhammad A. Butt, and Svetlana N. Khonina, "Optical computing: Status and perspectives," *Nanomaterials* 12, no. 13 (2022): 2171.

29. Chai, Z., Hu, X., Wang, F., Niu, X., Xie, J. and Gong, Q., "Ultrafast all-optical switching," *Advanced Optical Materials*, 5(7), p.1600665 (2017).

30. Sahu, Samir, and Shantanu Dhar, "Implementation of J–K and J K master–slave flip-flops with nonlinear material in all-optical domain," *Optical Engineering* 48, no. 7 (2009): 075401-075401.

31. Sahu, Samir, and Shantanu Dhar, "All-optical implementation of arithmetic operation scheme using optical nonlinear material-based switching technique," *Photonics Optoelectron* 3 (2014): 37-50.

32. Yang, X., Hu, X., Yang, H. and Gong, Q., "Ultracompact all optical logic gates based on nonlinear plasmonic nanocavities," *Nano photonics*, 6(1), pp.365-376 (2017).

33. Wu, Yaw-Dong, Tien-Tsorng Shih, and Mao-Hsiung Chen, "New all-optical logic gates based on the local nonlinear Mach-Zehnder interferometer," *Optics Express* 16, no. 1 (2008): 248-257.

34. Moradi, Marziyeh, Mohammad Danaie, and Ali Asghar Orouji, "Design of all-optical XOR and XNOR logic gates based on Fano resonance in plasmonic ring resonators," *Optical and Quantum Electronics*51 (2019): 1-18.

35. D. Samanta, S. Mukhopadhyay, "All-optical method for maintaining a fixed intensity level of a light signal in optical computation," *Opt. Commun.* 281, 4851–4853 (2008).

36. A. Guchhait, N. Pahari, N.B. Manik, "All-optical decimal to ternary converter with the proper use of optical non-linear material," *Journal of optics* 49 59-68 (2019).

37. B. Sarkar, S. Mukhopadhyay, "An optical system for sharp increase of light frequency by the use of multiple numbers of LiNbO3 crystals biased by sawtooth electronic pulse," *Indian J. Phys.* 95, 1865 (2021).

38. S. Mukhopadhyay, "Role of optics in super-fast information processing," *Indian J. Phys.* 84, 1069 (2010).

Chapter 6

Optical System for Binomial Coefficient Calculation

Chapter

6

Optical System for Binomial Coefficient Calculation

An all-optical scheme, namely optical binomial expansion device (OBED) is proposed based on the inherent convenience of parallelism of optical ray and intensity-dependent refractive index (RI) of isotropic positive optical nonlinear material for calculating the binomial co-efficient of a binomial expansion under any positive integral index. For computing binomial coefficients, the intensity level *'nI'* of the input section functions as the binomial index '*n*', where '*n*' denotes the positive integer number. Moreover, each output channel of OBED is activated by the fixed intensity level of the individual light. The rudimentary foundation of this scheme is an optical switch. Also, the beam combiner and beam splitter have been utilized strategically to implement the optical process. The present study can be envisaged in optoelectronic and photonic applications.

6.1. Overview

Owing to enough potential, optics, and photonics are unique to execute high-speed operation cum computation in the field of computation and communication systems [1-3]. In this regard, the optical switches which invoke the intensity dependent refractive index change based on the optical Kerr nonlinearity are well-known to all [4-6]. Over the last few decades, there have been many proposals in optical computing systems and opto-electronics, where optical nonlinear material (NLM) plays a pivotal role of creating an optical system [7-10].

In this respect, there are many promising applications based on binomial expansion like-higher mathematics, economy, architecture, forecast services, finance, population estimation, probability etc. Here, a scheme is introduced by incorporating the nonlinear optical material for calculating the binomial co-efficient in a binomial term under any positive integral index which acts as an optically controlled switching device.

In this scheme, the value of the binomial coefficient depends on the intensity level. Several intensity levels are represented by specific output channels, i.e., 'Y_t', which always represents the intensity level 'tI'. With the help of this optical device, it has been demonstrated that-

i. For definite value (n) of the index of binomial expansion, the total no. of binomial co-efficient of $(a+x)^n$ is (n+1).
ii. The numerical value of each binomial co-efficient, which is calculated from specific intensity level of specific output channel.

In the present journey, we introduce a concept for calculating binomial coefficients under any positive integral index which is fully optical.

For implementing this process, Kerr-type nonlinear material (NLM) is employed as an optical switch. In this proposed optical architecture some constant light sources (CL) (two types of CL-SCL (single constant light source) & MCL (multiple constant light sources)], beam combiner (BC), and 50% beam splitter (BS) are employed to maintain the intended intensity level [11-12].

6.2 Design of optical binomial expansion device (OBED)

The proposed optical binomial expansion device (OBED) consists of four main parts as follows

- Input section
- Control unit
- Processing section
- Output division

In our proposed OBED, the 'ON' state of each input sources is represented by a polarized light, which can be considered as linearly polarized light signal with the same intensity level (I). On the other hand, each output channel in 'ON' status is associated with its specific intensity level, whereas 'OFF' state of the Input section and output division of OBED is envisaged by the absence of the light signal. Such as in our proposed scheme, 'ON' state of each coherent input source in the input section of OBED is represented by the same and standard intensity level 'I,' and 'ON' state of all output channels, i.e., Y_1, Y_2, Y_3, ……., Y_t of OBED is also considered by intensity level I, 2I, 3I…., tI respectively, where 't' denotes a natural number.

6.2.1. Input Section

On behalf of the proposed scheme, binomial co-efficient of binomial expansion can be computed under the power of any whole number. However, the design of OBED (shown in Fig.-13) is drawn to calculate the binomial coefficient of binomial expansion for indices 0 to 9. The input section of our proposed OBED is composed of several different coherent light sources designated as 'a', 'b', 'c', 'd', 'e', 'f', 'g', 'h' & 'i', where each light source has same and standard intensity level I. In the input section, there is additional CL which is mentioned as 'M'. To compute the binomial coefficients for a particular index of binomial expansion, we have to stimulate the particular number of input sources (i.e., polarized light is present with intensity level 'I' at each input source) in the input section. As a result, to determine binomial co-efficient for n (index of binomial expansion), i.e., for n number of input coherent lighted sources, total intensity of incident polarized light on optical switch (OS) ('N') 'tI'= nI + I (due to additional CL 'M') = (n+1) I …...(A). Consequently, (n+1) is the co-efficient (t) of input intensity of incident polarized light beam on optical switch 'N', which determines the serially 't' number of output channels (in output division of OBED) i.e., Y_1, Y_2, Y_3, ……., Y_t are in ON state.

It is remarked that the volume of the whole scheme (shown in Fig.-6.13) depends on the number of index (n) of binomial expansion. For n>9, extra input sources of same intensity as well as additional no. optical device (OD) are to be included in the scheme. For n=n, then total no. of OD are n and no. of O/P lines from the OD depends upon the serially placement of OD in the system i.e., no. of O/P line from 1st OD =2, no. of O/P line from 2nd OD=3, no. of O/P line from the nth OD = (n+1). Consequently, for n=n, total no. of O/P of OBED are Y_1, Y_2, ……., Y_{n+1}.

6.2.2. Control unit

Here optical switch [which is constructed by linear material (LM) and nonlinear material (NLM)] acts as a control unit of OBED by dint of intensity-based refractive index (RI) property of NLM. The following section is focused on the optical NLM as an optical switch –

From the famed Kerr nonlinearity equation, the nonlinear refractive index can be expresses as

$$n_{NL} = n_0 + n_2 I \quad -------(1)$$

Here $n_{NL}$is the R.I. of the concerned NLM, $n_2$is the second-order nonlinear correction term, n_0 is the constant R.I of NLM incident, I=intensity on NLM firstly, then NLM

Again, from the familiar Snell's law of refraction, we have

$$n_L \sin\theta_1 = n_{NL} \sin\theta_2 \text{----------(2)}$$

Where, $n_L$is the RI of the concerned LM, θ_1 is called the Incident angle and θ_2 is the angle of Refraction.

By combing equation (1) and (2) an optical switch can be realized composed of LM &NLM (shown in fig.- 6.1).

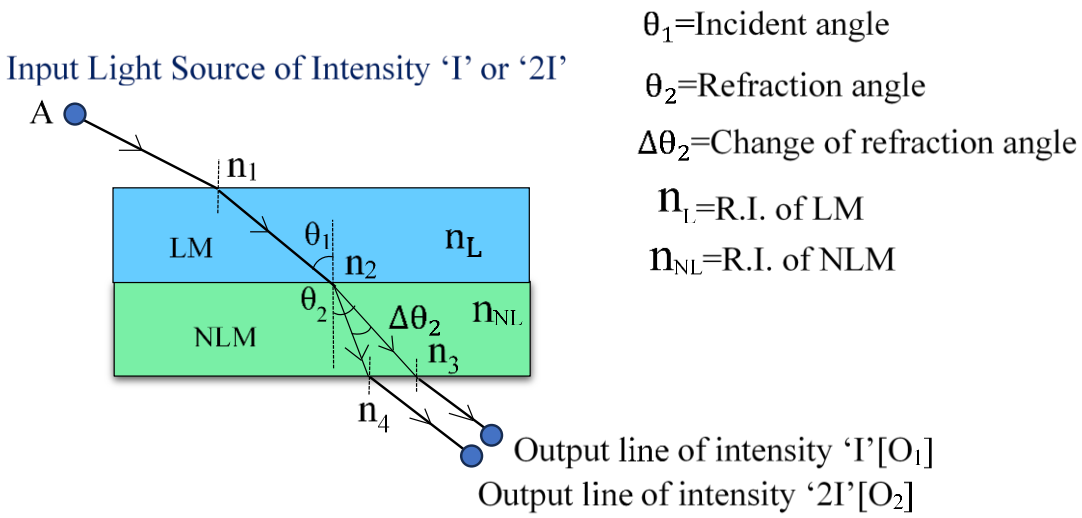

Fig. 6.1: Optical Kerr-type nonlinear materials as an optical switch

Now from equation (1), as the light intensity increases, the n_{NL} also increases. As a consequence (from equation (2))$\sin\theta_2$ as well as θ_2 is decreased.

So, when incident polarized light at the higher value of intensity first passes through the LM followed by NLM, the direction of O/P path from NLM is deflected shown in Fig.: -1, where θ_1 is fixed. Here in Fig.1, n_1 is the point of incidence of incident light beam An_1 of 'intensity I' on the interface between air medium and ordinary glass-made linear material of LM-NLM block; n_2 is the point of incidence of the refracted ray (through the linear material) of intensity 'I' on the boundary of LM & NLM; n_3 & n_4 are the points of incidence of the refracted rays (through the nonlinear material) of intensity 'I' & '2I' on the boundary of nonlinear material and air medium of LM-NLM block respectively. Here

it is also noted that in eqn. (1), n_2 is either positive or negative. But in this scheme, we select the material that has positive 2nd order correction term only. Here CS_2, SiO_2, GaAs are the example of positive NLM with self-focusing character. The focusing length (L) of NLM can be expressed as

$$P = \frac{\pi \epsilon_0 n_0 c a^4}{8 n_2 L^2} \quad \text{----------(3)}$$

Where 'P' is power of the laser beam, 'a' denotes the area of cross-section of the laser beam, 'C' is free space velocity of light.$\in_0$ is free space permittivity.

Consequently, for an integrated optical system [13-16], a high-power laser with limited diffraction is required. Here for I/P signal is a Q-switched pulse laser with 10^{-9}s pulse duration (on-time duration) can be utilized as coherent light source. It is also noted that the value of $n_0$and n_2 for SiO_2 is 1.46, and 3.2 × $10^{-2}m^2$/W respectively whereas, those value for CS_2 are 1.62 and 0.22 × $10^{-19}m^2$/W. For discussion the deviation of the light signal passing through CS_2 for different intensity level of the light beam can be calculated very easily. For an ordinary CW laser of 100m W power and 50μm^2 beam cross-section the intensity becomes 2×10^9 W/m^2. Now if the above continuous wave (CW) beam is changed to a pulsed beam of pulse duration 10^{-9}s the pulse power reaches a value of 2×10^{18} W/m^2. This pulsating beam can be obtained using a suitable Q-switching or mode locking mechanism. To excite the NLM, intense coherent laser beams may be treated as a polarized light source for desired optical operation. Nd:YAG (neodymium doped yttrium aluminum garnet) laser source is used as an ideal source to excite the NLM.

In the proposed design (shown in Fig.-13) when polarized light from the input section is incident on optical switch (N), the refracted light from it is forwarded in a different direction which follows different output path (named as O_1, O_2, O_3 ..., O_{10}) in accordance with the value of input intensity of the incident polarized light falling on it. Now it is discussed about the emergent polarized light from the optical switch in different output paths, followed by the equation (A). Thus, controlling the output path (entitled as O_1, O_2, O_3, ….., O_{10}) optical switch (N) interrelates the input section and output division through many definite optical devices, which is the key part of the OBED. Here it is noted that the intensity level of O_1, O_2, O_3, ..., and $O_{10}$are I, 2I, 3I, ……, and 10I, respectively.

3.2.3 Processing section

In the processing section of the proposed OBED, there are many optical devices named as P, Q, R, S, T, U, V, W & X which act as a processor. The O/P paths O_2, O_3, …..., and $O_{10}$from the control unit are connected with OD 'P', 'Q', 'R'…, and 'X', respectively. As a result, OD 'P', 'Q', 'R'… and 'X' are activated when I/P intensity on them are 2I, 3I, ……, and 10I respectively.

6.2.3.1. Construction of optical device (OD) -

Optical device (OD) is composed of following components

a) 50% Beam splitter (BS),

b) Beam combiner (BC),

c) Single constant polarized light source (SCL) and

d) Multiple constant polarized light sources (MCL).

Here it is noted that the additional constant light source (ACL) for specific OD is realized from a combination of a certain number of SCL and MCL i.e., here ACL consists of certain number of SCL and certain number of MCL (depending upon 'n'), i.e., SCL and MCL is termed as ACL. So, for specific OD, total intensity is offered by ACL as = intensity of certain no. of SCL (+) intensity of certain no. of MCL $=\{\frac{n(n+1)}{2}\}I$.

In the proposed scheme, the block diagram of OD in generalized form is designed as in **Fig. 6.2**.

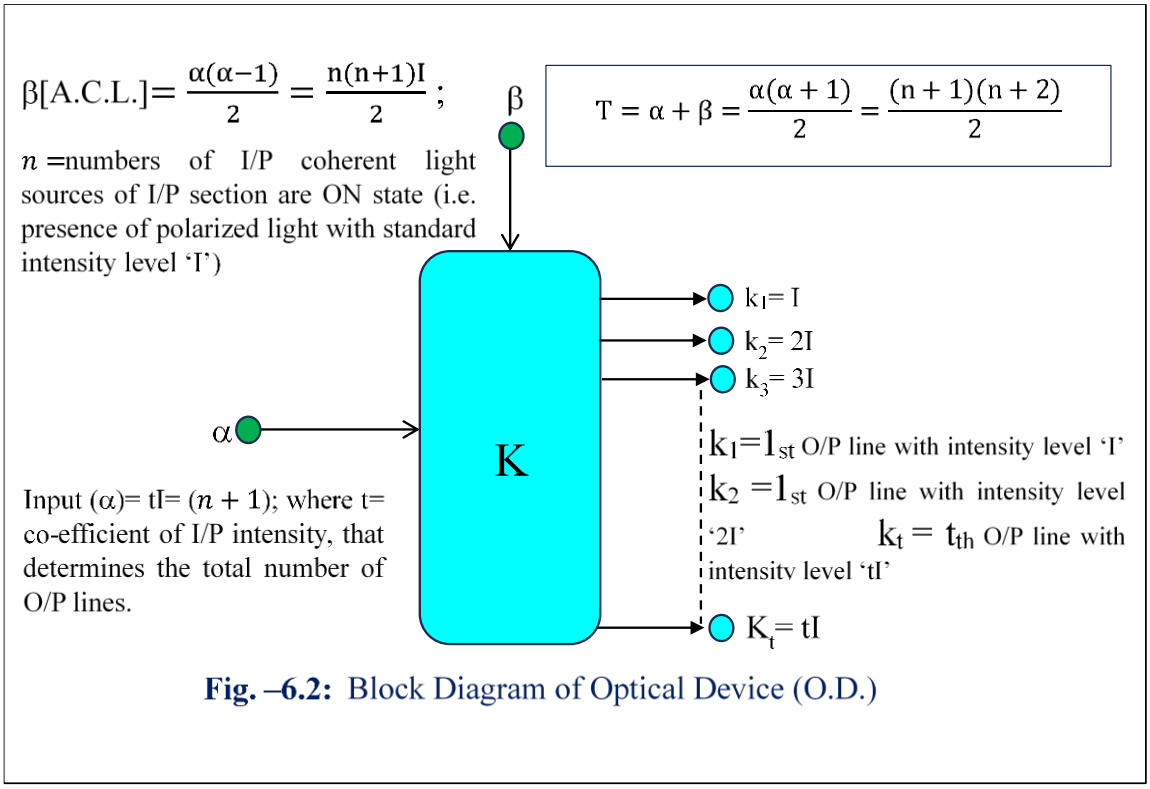

Fig. –6.2: Block Diagram of Optical Device (O.D.)

In the proposed OD, there are only one I/P line with several O/P lines emerging from it. The number of O/P lines from particular OD depends on the coefficient of I/P intensity of incident polarized light on that OD. Internal structure of 'K' in Fig.-2 is illustrated in Fig.-4(OD 'P') to Fig.-12(OD 'X') for n=1 to n=9. Moreover, for n=1 to n=9 i.e., t=2 to t=10, (here t=n+1) the block diagram is illustrated by 'P', 'Q', 'R, 'S', 'T', 'U', 'V', 'W' & 'X', which are shown in appendix-B, Fig.-S_1 to Fig.- S_9 respectively.

Here 50% BS is used to divide the intensity into two equal parts. The function of the BC is to add the intensity from different sources. Here it is also to be noted that there are two polarized light sources, such as SCL, which always provides the constant intensity level 'I' and MCL, which can provide multiple intensity levels such 2I, 3I,…….and so on as necessary. The MCL has alluded as L_m where 'm' stands for a natural number, but in our sketched OBED, the range of 'm' is 2 to 8. The significance of L_m is that the specific MCL consists of m number of coherent, constant light sources of single intensity 'I 'i.e., 'L_m' offers the specific intensity of value 'mI'. The block diagram of 'L_m'is shown in **Fig.-6.3**.

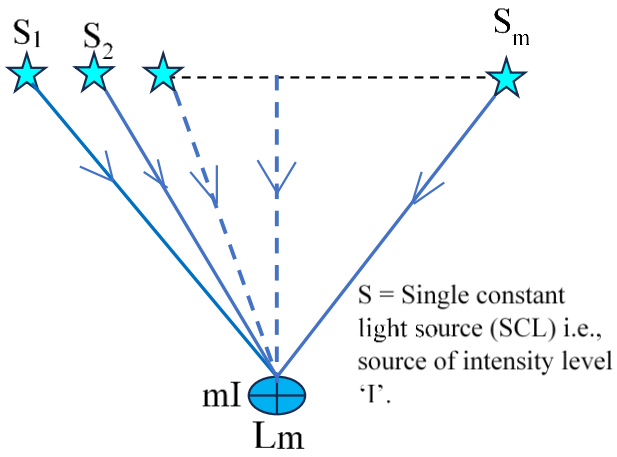

Fig. -6.3: Schematic diagram of MCL "Lm"; consists of 'm' number of SCL which acts as source of intensity level 'mI'.

6.2.3.2. Number of output paths from specific OD

To design OD such a way, so that the co-efficient of incident input intensity on a particular OD is equal to the number of output channels from that OD, i.e., when the input intensity is 'tI' on definite OD ('t' specifies the co-efficient of intensity I) then the number of output path from that OD is 't'. To compute the value of the intensity of each several output path out of 't' number of channels from the specific OD, total output intensity is TI (shown in **Table- 6.1**)

Table -6.1: Number of Input lighted sources (n) and concern net amount of gathered intensity level (TI) at specific optical devices.

Number of Input coherent sources (n)	Input intensity on Optical switch (N) = tI [t=co-efficient of input intensity] =(n+1) I	Output path from Optical switch (N)	Connecting Optical device	Value of Input intensity $=\alpha(=tI)$on definite Optical device	Value of additional constant light source (ACL) at concern Optical device $=\beta(=\frac{n(n+1)}{2})$	Total combined intensity into particular Optical device =TI $(=\alpha+\beta)$ [T=co-efficient of total combined intensity]
0	I	O_1	Direct	-	-	I
1	2I	O_2	P	2I	I	3I
2	3I	O_3	Q	3I	3I	6I
3	4I	O_4	R	4I	6I	10I
4	5I	O_5	S	5I	10I	15I
5	6I	O_6	T	6I	15I	21I
6	7I	O_7	U	7I	21I	28I
7	8I	O_8	V	8I	28I	36I
8	9I	O_9	W	9I	36I	45I
9	10I	O_{10}	X	10I	45I	55I

Where TI is the intensity of the incident polarized light on OD (tI) plus (+) excess intensity of the polarized light offered by ACL of the OD which is distributed in several output paths from it in the following manner

TI = (sum of first 't' natural numbers) × I

Or,$TI = k_1I + k_2I + k_3I + \ldots\ldots\ldots\ldots + k_tI$---------- (4)

where $T = (k_1 + k_2 + k_3 + \ldots\ldots\ldots + k_t)$denotes co-efficient of total output intensity (in Table- 1) of the definite OD; k_1, k_2, $k_{3,\ldots}$..., k_t express the natural number 1, 2, 3,……., t respectively. And 't' represents the co-efficient of input intensity on definite OD and determines the total number of O/P lines from OD.

Now from the equation – (4), the evolved situations as -

- When $t = 1$, then from the equation $TI = k_1I$or,$TI = I$. So, we get a single output path of intensity 'I'.

- When $t = 2$, then$TI = k_1I + k_2I$ or,$TI = I + 2I$ or, $TI = 3I$. So, in this case, number of output path from OD (named as P) are 2 (namely- P_1&P_2) and intensity in different output paths as –$P_1 = I$ &$P_2 = 2I$ (which is shown in Appendix-B, Fig. –S_1).
- In a similar way, when $t = 3$, then $TI = k_1I + k_2I + k_3I$or, $TI = I + 2I + 3I$ or,$TI = 6I$. Therefore, the number of output paths from the optical devices (named as Q) is three (such as Q_1, Q_2 and Q_3) and intensity distribution in different output paths of Q are as$Q_1 = I$; $Q_2 = 2I$ &$Q_3 = 3I$ (which is shown in Appendix-B, Fig. –S_2).
- When $t = 4$, then $TI = k_1I + k_2I + k_3I + k_4I$ or, $TI = I + 2I + 3I + 4I$ or, $TI = 10I$. In this case number of outlines from the optical device (mentioned as R) are four (namely,R_1, R_2, R_3& R_4), and intensity distribution in separate output paths from 'R' are as follows $R_1 = I$; $R_2 = 2I$; $R_3 = 3I$ &$R_4 = 4I$ (which is shown in Appendix-B, Fig. –S_3).
- Similarly, when $t = 5$, then $TI = k_1I + k_2I + k_3I + k_4I + k_5I$ or, TI = $\left\{\frac{5(5+1)}{2}\right\}$I = 15I. Hence output paths from OD (designated as 'S') are five (scilicet- S_1, S_2, S_3, S_4& S_5), and the value of intensity in different output lines of 'S' are like as $S_1 = I, S_2 = 2I, S_3 = 3I, S_4 = 4I$ &$S_5 = 5I$ (shown in Appendix-B, Fig. –S_4).
- In the same way $t = 6$, then TI = $\left\{\frac{6(6+1)}{2}\right\}$I = 21I. Consequently, number of output paths from OD (entitled as 'T') are six(namely- T_1, T_2, T_3, T_4, T_5& T_6) and intensity distribution at several output lines as $T_1 = I, T_2 = 2I, T_3 = 3I, T_4 = 4I, T_5 = 5I$ &$T_6 = 6I$ (shown in Appendix-B, Fig. – S_5).
- When $t = 7$, in similar way $TI = I + 2I + 3I + 4I + 5I + 6I + 7I$. After that intensity distribution in different output paths of denominated OD 'U' as $U_1 = I, U_2 = 2I, U_3 = 3I, U_4 = 4I, U_5 = 5I, U_6 = 6I$ &$U_7 = 7I$ (shown in Appendix-B, Fig. – S_6).
- For $t = 8$, then TI = $\left\{\frac{8(8+1)}{2}\right\}$I = 36I. So, output lines from OD (entitled as V) are eight(as- V_1, V_2, V_3, V_4, V_5, V_6, V_7& V_8) and intensity level in various output lines from this optical device (V) are as$V_1 = I, V_2 = 2I, V_3 = 3I, V_4 = 4I, V_5 = 5I, V_6 = 6I, V_7 = 7I$ &$V_8 = 8I$(shown in Appendix-B, Fig. –S_7).
- Similarly for $t = 9$, then TI = $\left\{\frac{t(t+1)}{2}\right\}$I = $\left\{\frac{9(9+1)}{2}\right\}$I = 45I. As consequences output lines from this optical device (mentioned as W) are nine(namely- W_1, W_2,

W_3, W_4, W_5, W_6, W_7, W_8& W_9) and intensity variation at separate output paths from it are as $W_1 = I, W_2 = 2I, W_3 = 3I, W_4 = 4I, W_5 = 5I, W_6 = 6I, W_7 = 7I, W_8 = 8I$ &$W_9 = 9I$ (shown in Appendix-B, Fig. –S_8).

- Now we discuss the equation – (4) for $t = 10$. Then$TI = k_1I + k_2I + k_3I + \dots\dots\dots + k_{10}I = \left\{\frac{10(10+1)}{2}\right\}$I = 55I. Here the number of output paths from the optical device (named as- 'X') are for t=10(denoted as- X_1, X_2, X_3, X_4, X_5, X_6, X_7, X_8, X_9 andX_{10}) and total intensity is distributed at several output paths from this optical device like as - $X_1 = I, X_2 = 2I, X_3 = 3I, X_4 = 4I, X_5 = 5I, X_6 = 6I, X_7 = 7I$ &$X_8 = 8I, X_9 = 9I$ &$X_{10} = 10I$(shown in Appendix-B, Fig. – S_9).

The output intensity level at separate O/P lines of each OD are shown in **Table-6.2**.

Table – 6.2: Intensity distribution at several Output channels of the activated optical devices

Number of input coherent light source (n)	Input (I/P) intensity on Optical Switch (OS) [N]	Output (O/P) path from OS	Name of the connecting optical device (OD) on O/P path from OS (N)	No. of O/P channel from OD	Name of the O/P channel from OD	Intensity level of each O/P channel from OD
0	I	O_1	Direct	-	-	I
1	2I	O_2	P	2	P_1	I
					P_2	2I
2	3I	O_3	Q	3	Q_1	I
					Q_2	2I
					Q_3	3I
3	4I	O_4	R	4	R_1	I
					R_2	2I
					R_3	3I
					R_4	4I
4	5I	O_5	S	5	S_1	I
					S_2	2I
					S_3	3I
					S_4	4I
					S_5	5I
5	6I	O_6	T	6	T_1	I
					T_2	2I
					T_3	3I
					T_4	4I
					T_5	5I
					T_6	6I
					U_1	I
					U_2	2I
					U_3	3I

6	7I	O_7	U	7	U_4	4I
					U_5	5I
					U_6	6I
					U_7	7I
7	8I	O_8	V	8	V_1	I
					V_2	2I
					V_3	3I
					V_4	4I
					V_5	5I
					V_6	6I
					V_7	7I
					V_8	8I
8	9I	O_9	W	9	W_1	I
					W_2	2I
					W_3	3I
					W_4	4I
					W_5	5I
					W_6	6I
					W_7	7I
					W_8	8I
					W_9	9I
9	10I	O_{10}	X	10	X_1	I
					X_2	2I
					X_3	3I
					X_4	4I
					X_5	5I
					X_6	6I
					X_7	7I
					X_8	8I
					X_9	9I
					X_{10}	10I

6.3.3 Mechanism of Optical Device (OD) [with python simulation result]

⇨ ***Optical Device 'P'***

To enliven the OD 'P', the input intensity of the incident polarized light on it is 2I which is due to O_2. This light beam of intensity '2I'splitted at the pt. p_1 by virtue of 50% Beam Splitter (BS). As a result, we get two paths of same intensity 'I'.

One of them acts as an output line 'P_1' of intensity I from the OD. Another path is faced with beam combiner (BC) at the pt. p_2. We get total intensity of the pt. p_2 is (I+I) =2I with the help of SCL, which acts as O/P path P_2 (of intensity 2I) from the OD. Now O/P lines P_1& P_2 are linked to Y_1& Y_2 (O/P division of OBED) respectively. Mechanism of OD 'P' is shown in **Fig. 6.4[a]** and it is also noted that O/P intensity level at separate O/P lines of

OD 'P' can be found in Appendix-B, Table no.-S_1. Python simulation result is shown in **Fig.- 6.4[b]**.

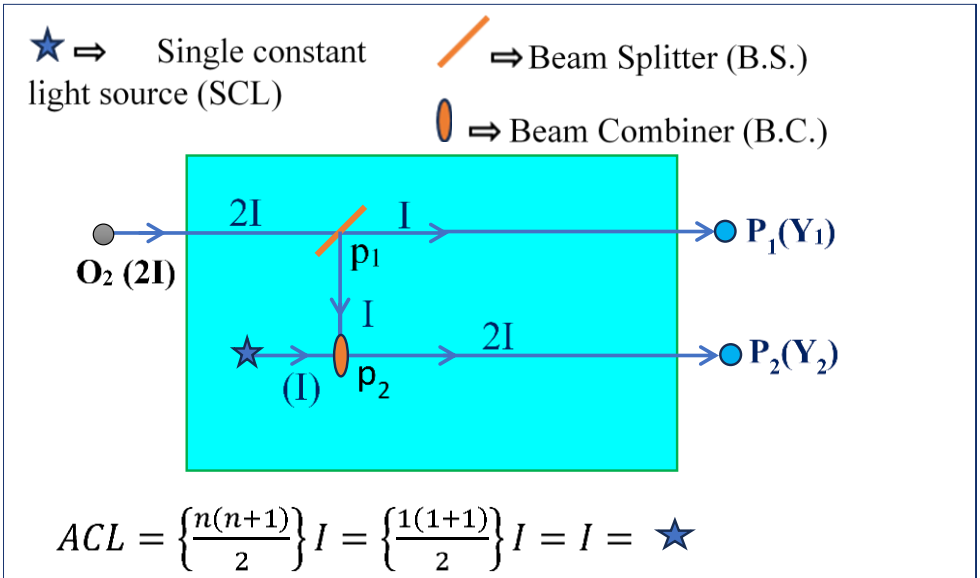

$$ACL = \left\{\frac{n(n+1)}{2}\right\} I = \left\{\frac{1(1+1)}{2}\right\} I = I = \bigstar$$

Fig. -6.4[a]: Intensity level at various pts. and final O/P intensity distribution of O.D. 'P'

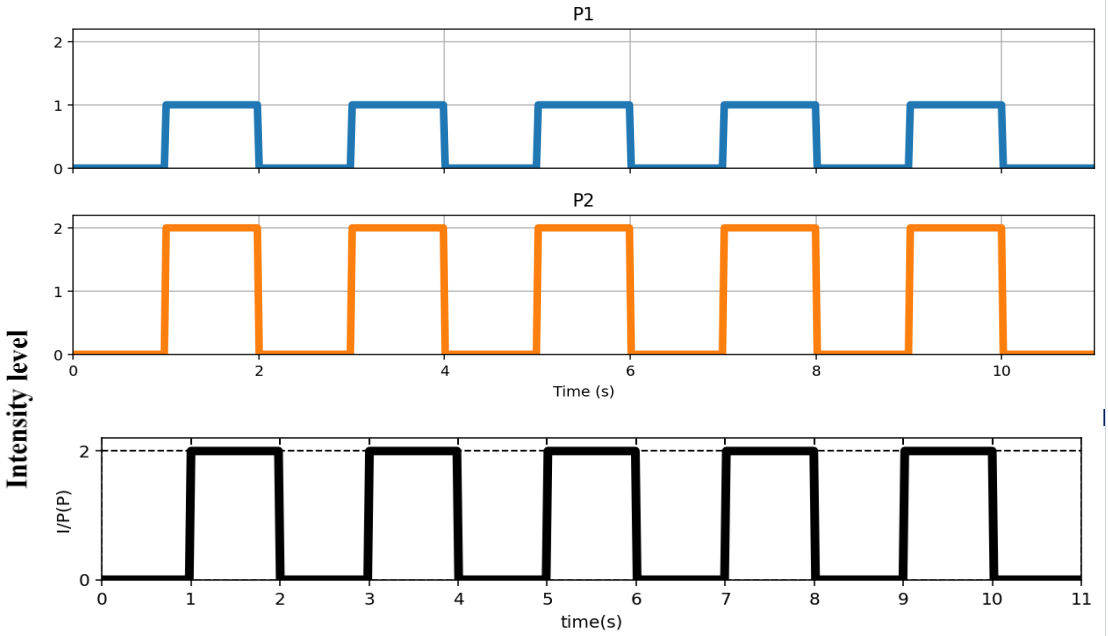

Fig. –6.4[b] Python simulation result for Optical Device [OD] **P,**

I/P Intensity[P]=2I; Output [P1] = I; [P2] = 2I.

⇨ *Optical Device 'Q'*

By dint of BC at the pt. q_1, the total intensity of light is (=3I+I) =4I. Here 3I & I am due to O_3 & SCL, respectively. Now, this amount of intensity of light is divided equally into two paths (where the intensity of each part is= 2I) at the pt. q_2. Now one part of them again is split by the BS into two parts (intensity I) at the pt. q_3. One of them acts as an O/P line Q_1 of intensity I from OD 'Q'. Another part of intensity I is joined to the pt. q_4. As a result, total intensity at the pt. q_4 with the help SCL is (I+I) =2I. Now in this path having intensity 2I from the pt. $q_4$behaves as O/P line Q_2 of the OD. Now at the pt. q_5, the total intensity of light is =2I (coming from the pt. q_2) + I (by virtue of SCL) = 3I, which is treated as O/P line Q_3 of the OD. After that, Q_1, Q_2& Q_3 are gradually adjoined with Y_1, Y_2& Y_3 (O/P division of OBED). Here accepted technique of OD 'Q' is shown in **Fig.-6.5[a]** & Appendix-B, Table – S_2. Python simulation result is shown in **Fig.- 6.5[b]**.

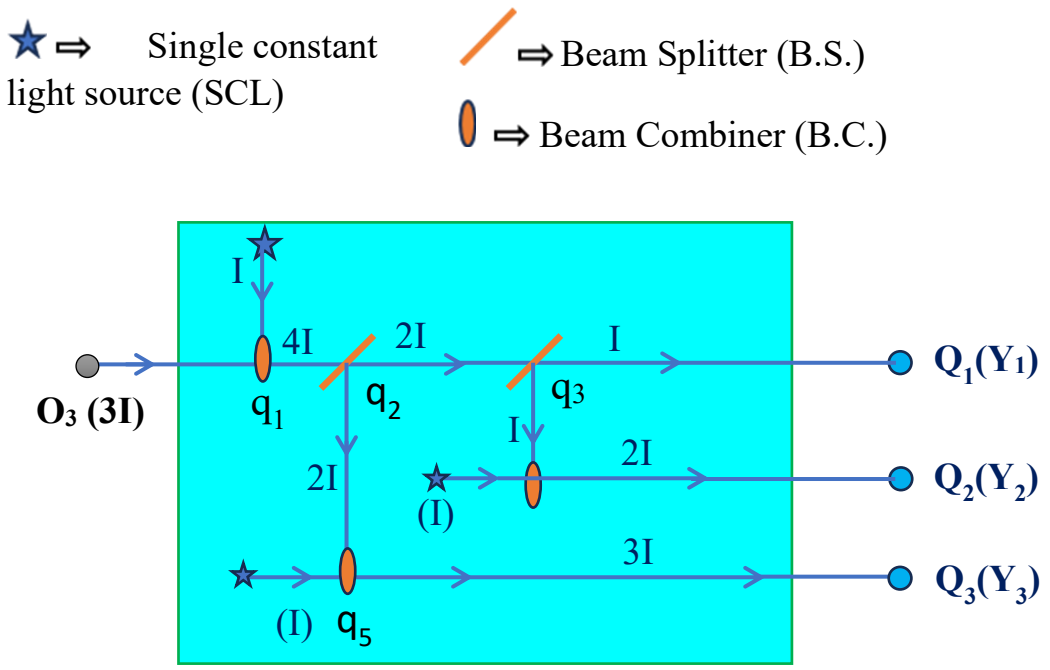

$$ACL = \left\{\frac{n(n+1)}{2}\right\} I = \left\{\frac{2(2+1)}{2}\right\} I = 3I = 3 \bigstar$$

Fig. -6.5[a]: Intensity level at various pts. and final O/P intensity distribution of O.D. 'Q'

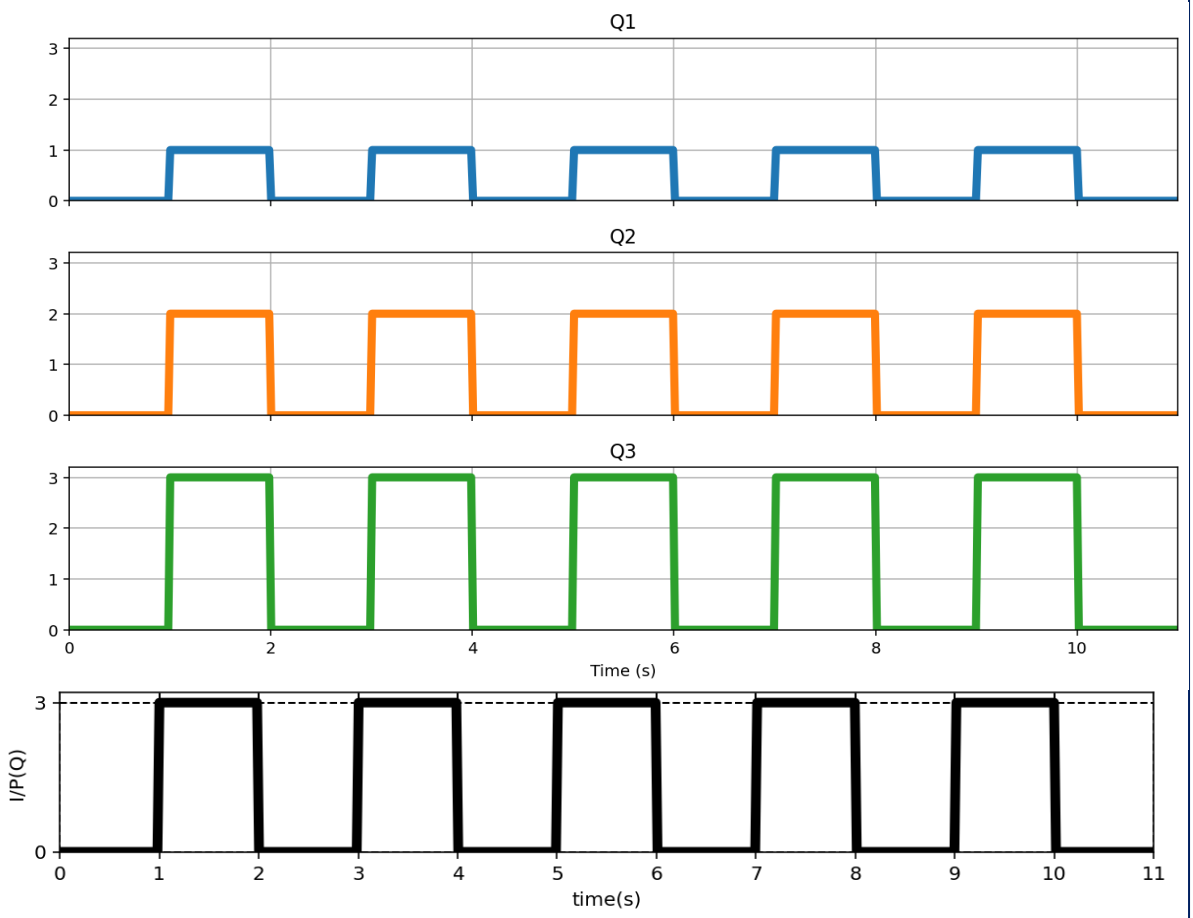

Input Intensity[Q]= 3I; Output [Q1] =I, [Q2] = 2I, [Q3] = 3I

Fig.– 6.5[b]: Python simulation result for Optical Device [OD] **Q**

⇨ *Optical Device 'R'*

Owing to O_4, the entrusted I/P light intensity into optical device 'R' is 4I. Now in the presence of 'L_2' (MCL) BS, BC, some number of SCL, there are four O/P lines as R_1, R_2, R_3& R_4 having intensity level I, 2I, 3I& 4I, respectively. Afterward, they are connected gradually with Y_1, Y_2, Y_3& Y_4, which are O/P channels of our proposed OBED. The mechanism of OD 'R' is shown in **Fig.-6.6[a]** & Appendix-B, Table-S_3. Python simulation result is shown in **Fig.- 6.6[b]**.

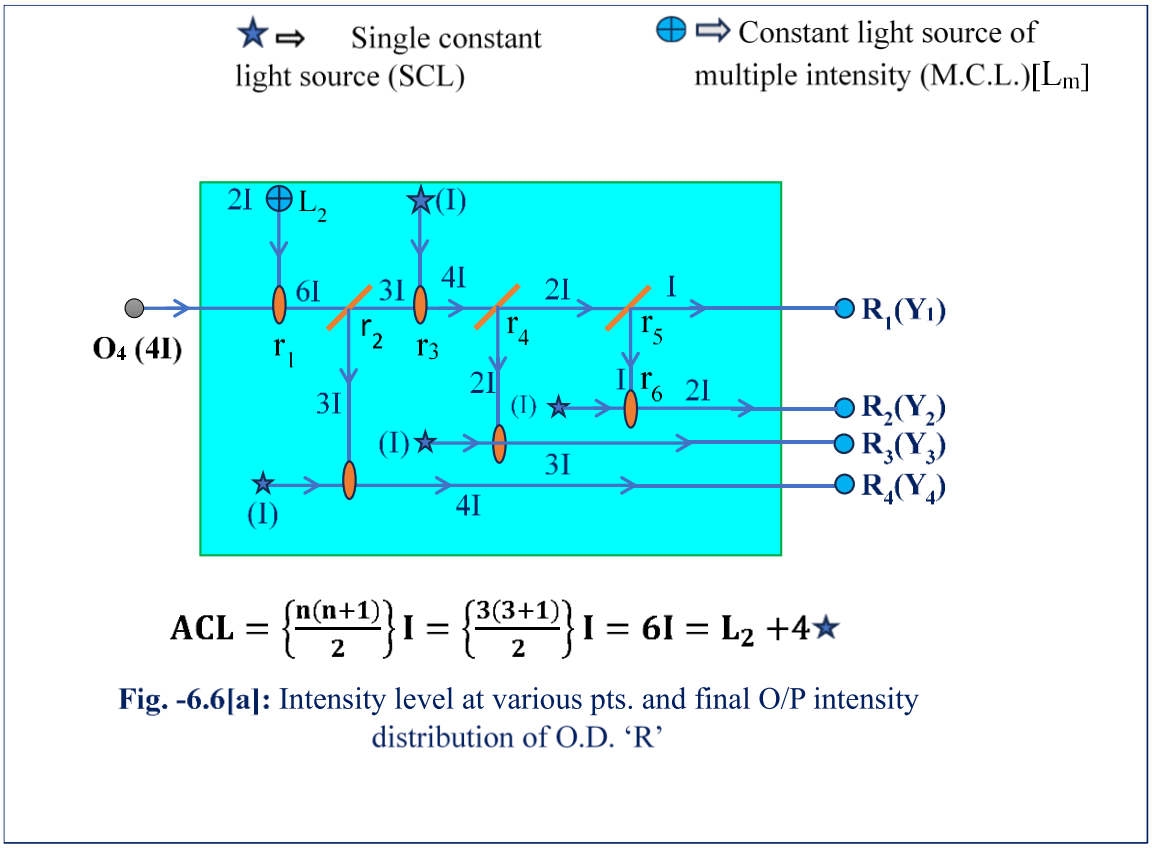

Fig. -6.6[a]: Intensity level at various pts. and final O/P intensity distribution of O.D. 'R'

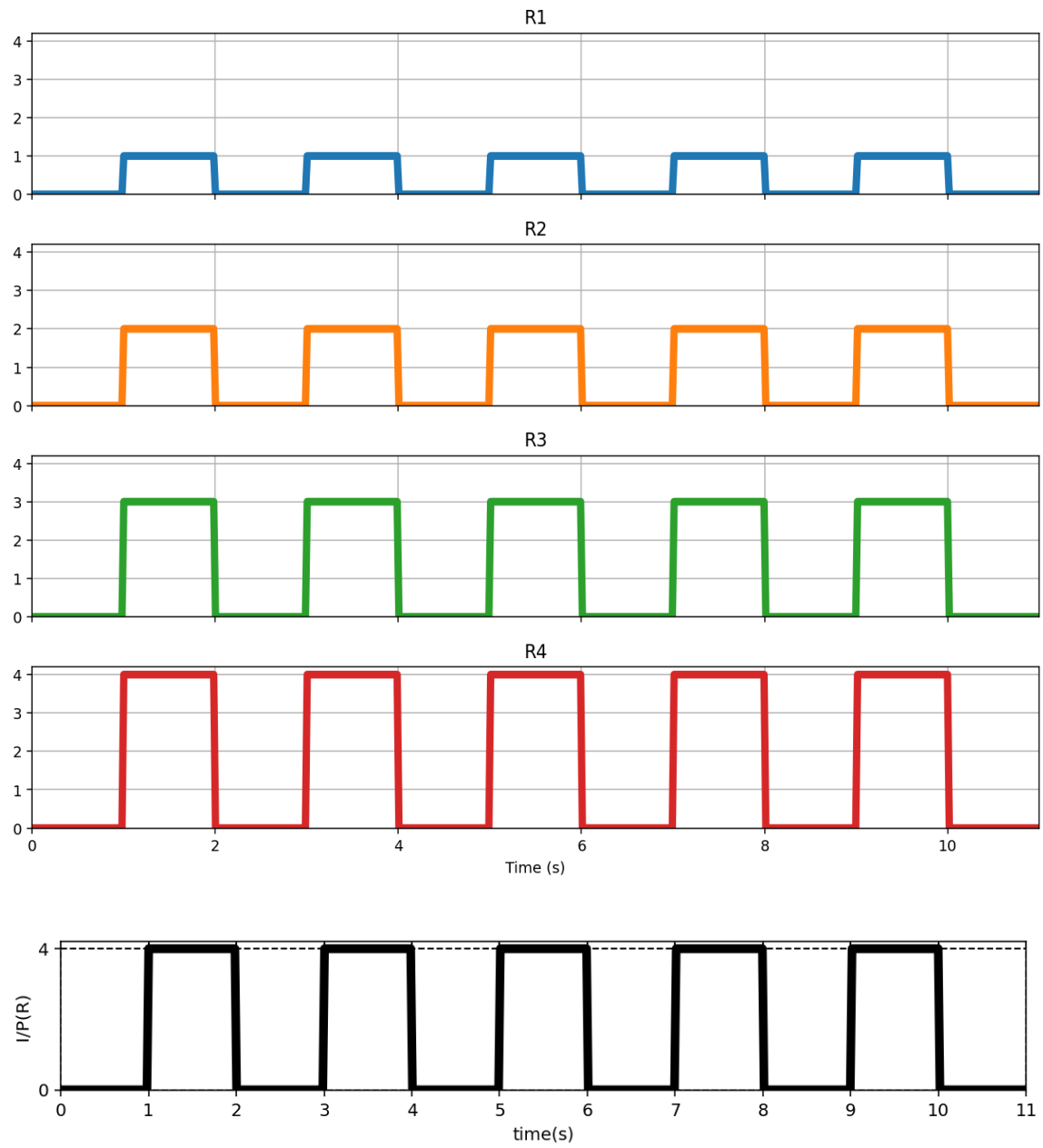

I/P Intensity [R] = 4I; O/P [R1] =1, [R2] =2I, [R3] =3I, [R4] =4I

Fig. 6.6[b]– Python simulation result for Optical Device [OD] **R**

⇨ *Optical Device 'S'*

Here the provided I/P intensity on OD 'S' is equal to 5I on account of O_5. By dint of two number of MCL (L_3& L_4), BS, & BC, O/P lines from OD 'S' are S_1(I), S_2(2I), S_3(3I), S_4(4I) & S_5 (5I) which are continued into Y_1, Y_2, Y_3, Y_4& Y_5. The function of OD 'S' is shown in **Fig.-6.7[a]** & Appendix-B, Table-S_4. Python simulation result is shown in **Fig.-6.7[b]**.

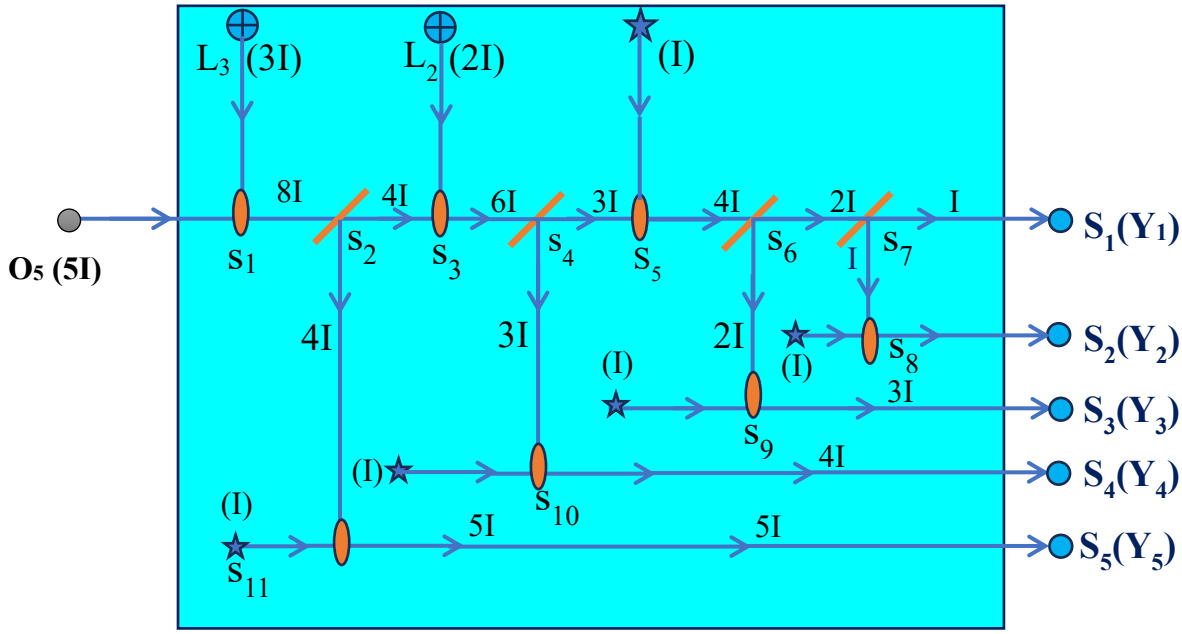

$$\mathbf{ACL} = \left\{\frac{\mathbf{n(n+1)}}{\mathbf{2}}\right\}\mathbf{I} = \left\{\frac{\mathbf{4(4+1)}}{\mathbf{2}}\right\}\mathbf{I} = \mathbf{10I} = \mathbf{L_3 + L_2 + 5\bigstar}$$

Fig. -6.7[a]: Intensity level at various pts. and final O/P intensity distribution of O.D. 'S'

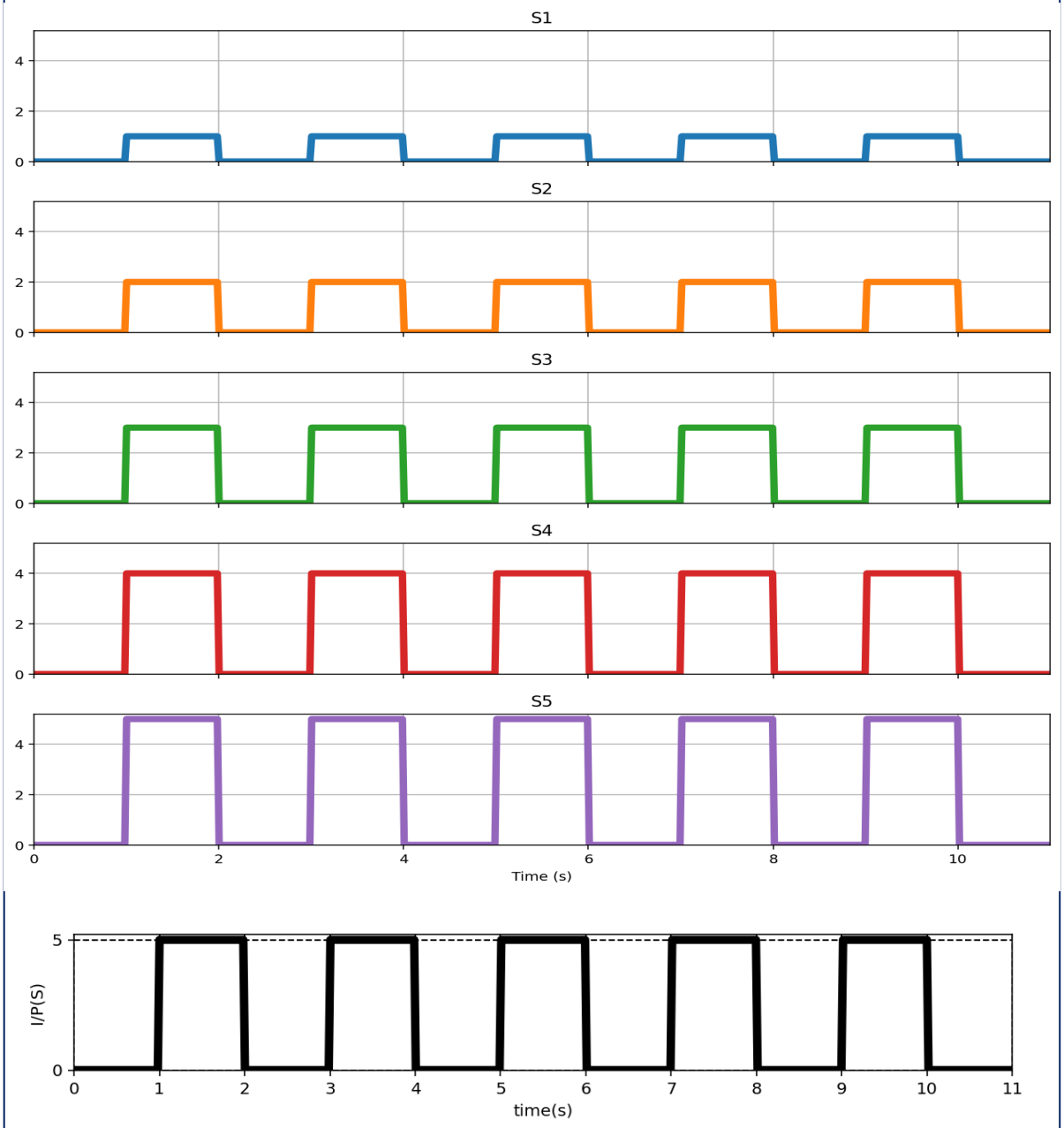

Input Intensity[S]= 5I; Output [S1] =I, [S2] = 2I, [S3] = 3I, [S4] = 4I, [S5] = 5I.

Fig.- 6.7[b]: PYTHON Simulation result for Optical Device [**S**].

» ***Optical Device 'T'***

With the collaboration of some number of MCL (L_4, L_3& L_2), BS, BC, and some number of SCL, when I/P intensity is 6I, then there exist six number of O/P lines from OD 'T' as T_1toT_6 with intensity level 'I' to '6I' respectively. The mechanism of OD 'T' is shown in **Fig.-6.8[a]** & Appendix-B, Table-S_5. At last, the O/P lines from OD 'T' such as T_1-T_6 are associated with Y_1-Y_6(O/P division of our proposed OBED), respectively. Python simulation result is shown in **Fig.- 6.8[b]**.

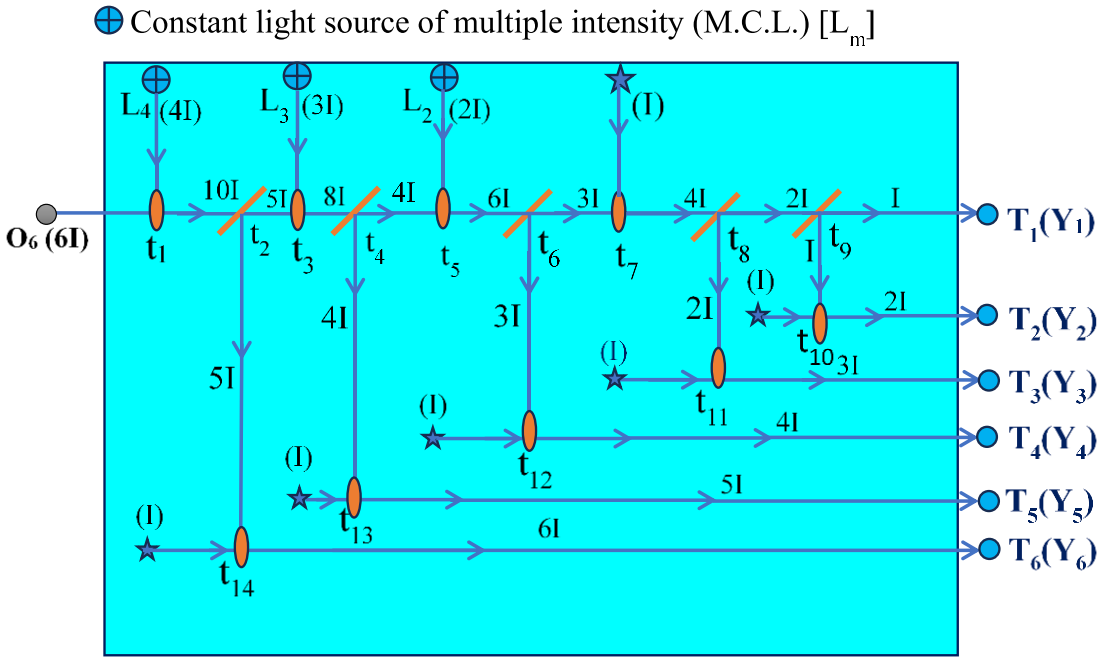

$$\mathbf{ACL} = \left\{\frac{n(n+1)}{2}\right\}\mathbf{I} = \left\{\frac{5(5+1)}{2}\right\}\mathbf{I} = 15\mathbf{I} = L_4 + L_3 + L_2 + 6\bigstar$$

Fig. -6.8[a]: Intensity level at various pts. and final O/P intensity distribution of O.D. 'T'

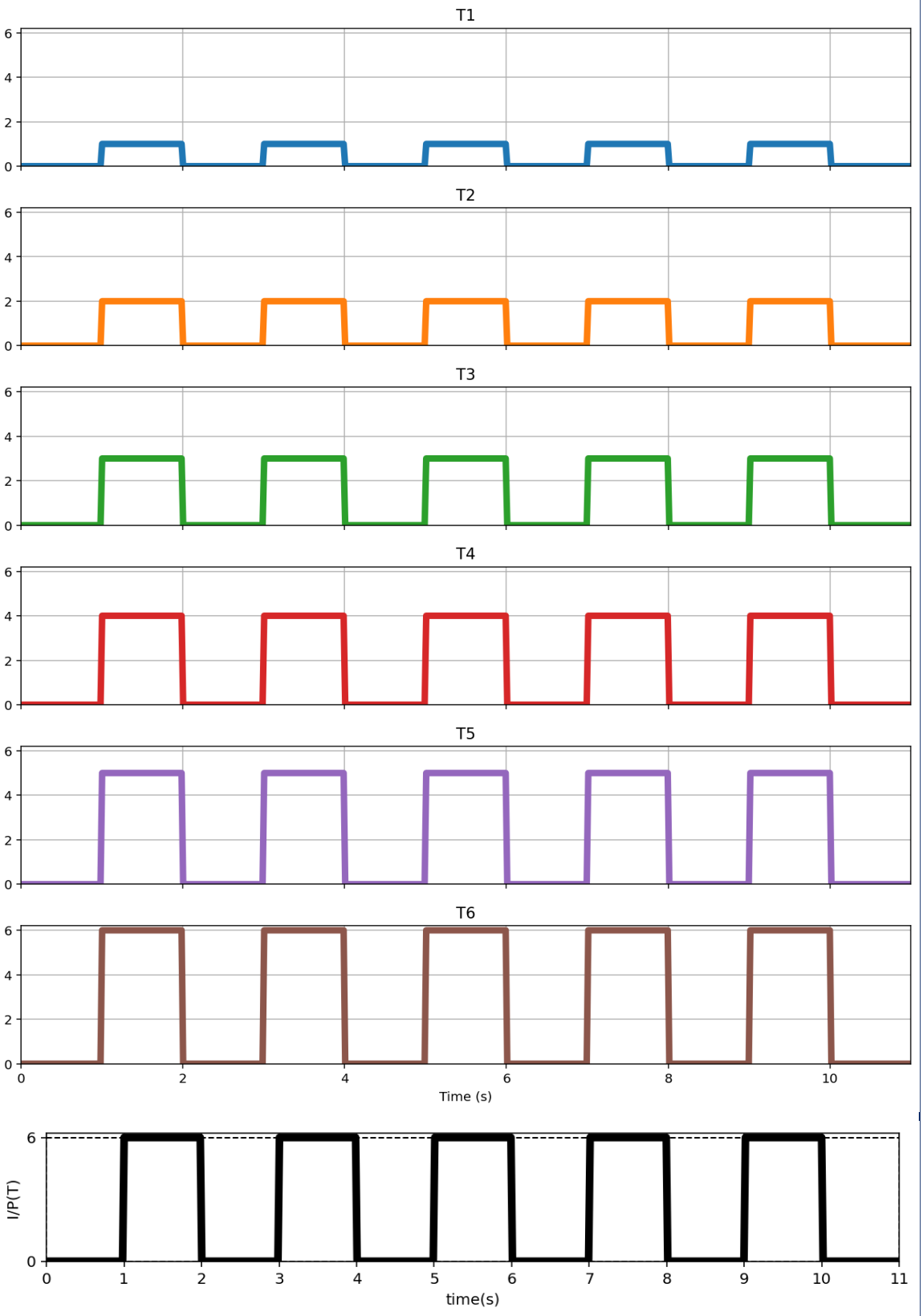

Fig. 6.8[b]: – SIMULATION result for OD [T]; I/P Intensity= 6I.

⇨ *Optical Device 'U'*

The optical device 'U' stimulates the ground of incident polarized light of intensity 7I on it. With the help of some number of MCL (L_5, L_4, L_3& L_2), BS, BC and some number of SCL, seven number of O/P lines U_1(I)-U_7 (7I) from OD 'U' are emitted with intensity level I to 7I respectively. The technique of OD 'U' is depicted in **Fig.-6.9[a]** & Appendix-B, Table – S_6. Finally, U_1, U_2, ….., U_7 from the OD 'U' is engaged with Y_1, Y_2, ….., Y_7 respectively (where they are the O/P channels of our proposed OBED.) Python simulation result is shown in **Fig.- 6.9[b]**.

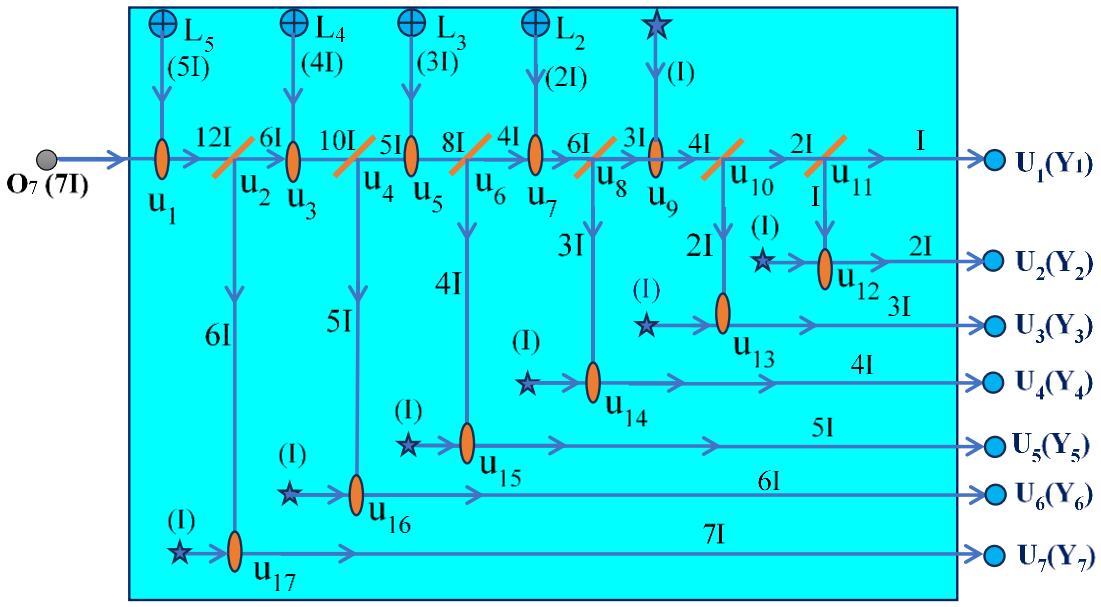

$$\mathbf{ACL} = \left\{\frac{n(n+1)}{2}\right\}\mathbf{I} = \left\{\frac{6(6+1)}{2}\right\}\mathbf{I} = \mathbf{21I} = \mathbf{L_5 + L_4 + L_3 + L_2 + 7\bigstar}$$

Fig. -6.9[a]: Intensity level at various pts. and final O/P intensity distribution of O.D. 'U'

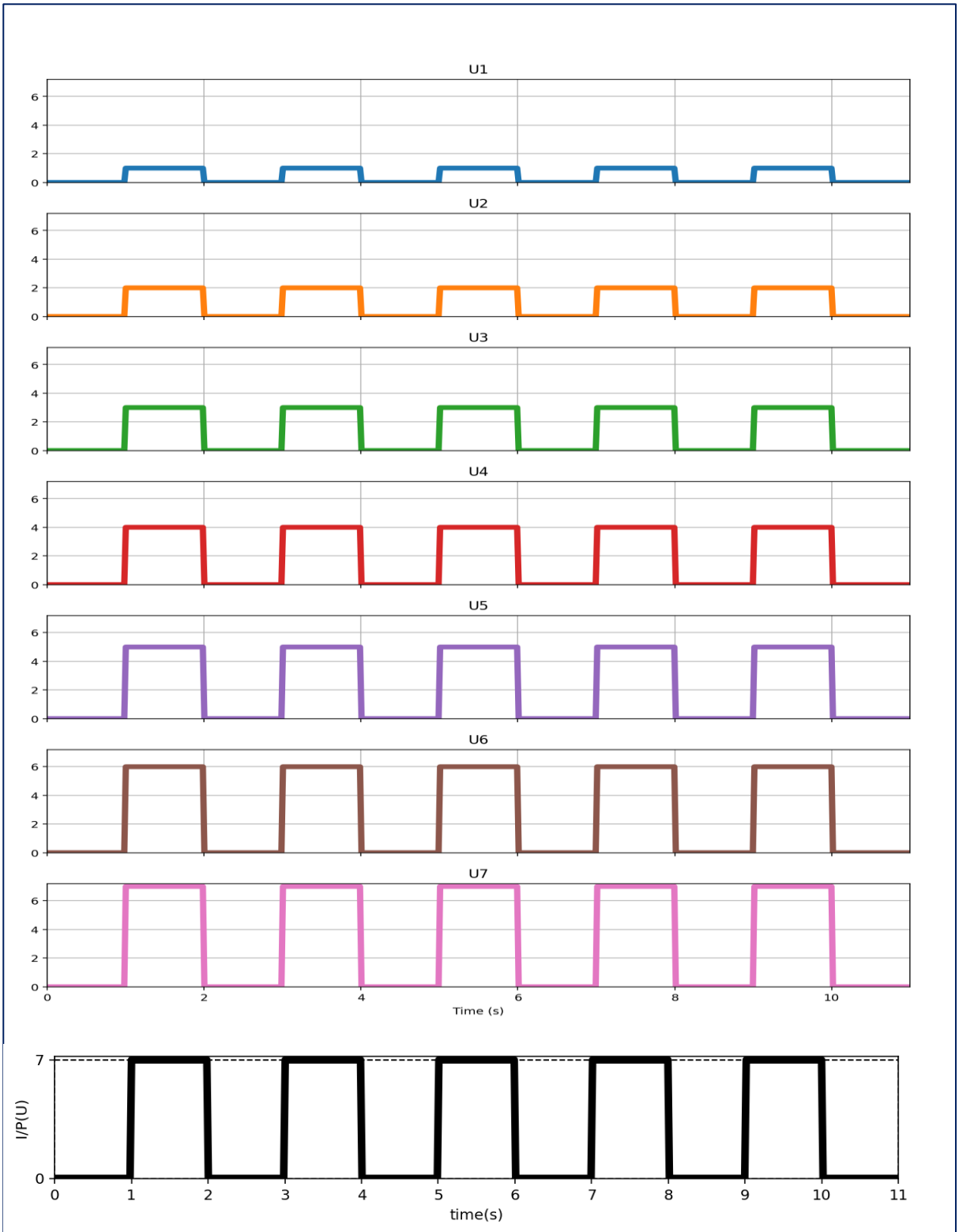

Fig.-6.9[b]: – SIMULATION result for OD [U]; I/P Intensity= 7I.

⇨ *Optical Device 'V'*

Conferred input intensity of incident polarized light on it is 8I owing to the presents of O_8. With the assistance of some number of MCL (L_6-L_2), BC, BS, and some number of SCL the O/P lines from OD 'V' are V_1-V_8 with intensity level I to 8I respectively. The operation of 'V' is shown in **Fig.-6.10[a]** and Appendix-B Table- S_7. At last, all O/P lines, i.e., V_1, V_2……., V_8 of the OD 'V' are leashed with Y_1, Y_2, ……., Y_8 (o/p channels of our submitted OBED) orderly. Python simulation result is shown in **Fig.- 6.10[b]**.

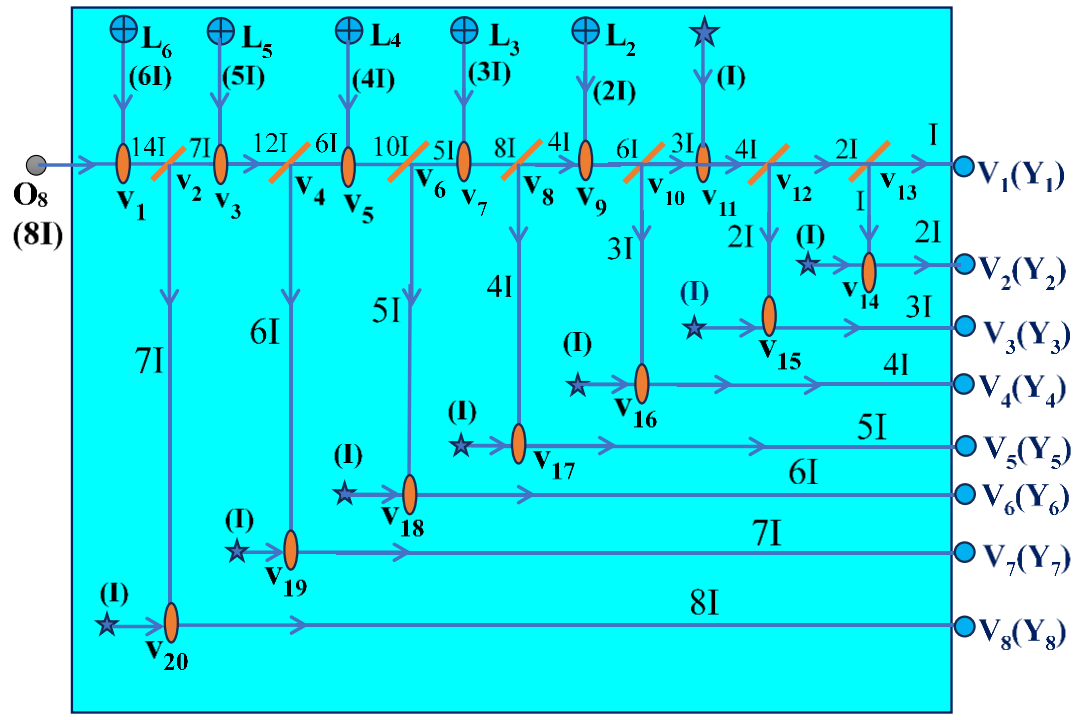

$$\mathbf{ACL} = \left\{\frac{n(n+1)}{2}\right\}\mathbf{I} = \left\{\frac{7(7+1)}{2}\right\}\mathbf{I} = \mathbf{28I} = \mathbf{L_6 + L_5 + L_4 + L_3 + L_2 + 8\bigstar}$$

Fig. -6.10[a]: Intensity level at various pts. and final O/P intensity distribution of O.D. 'V'

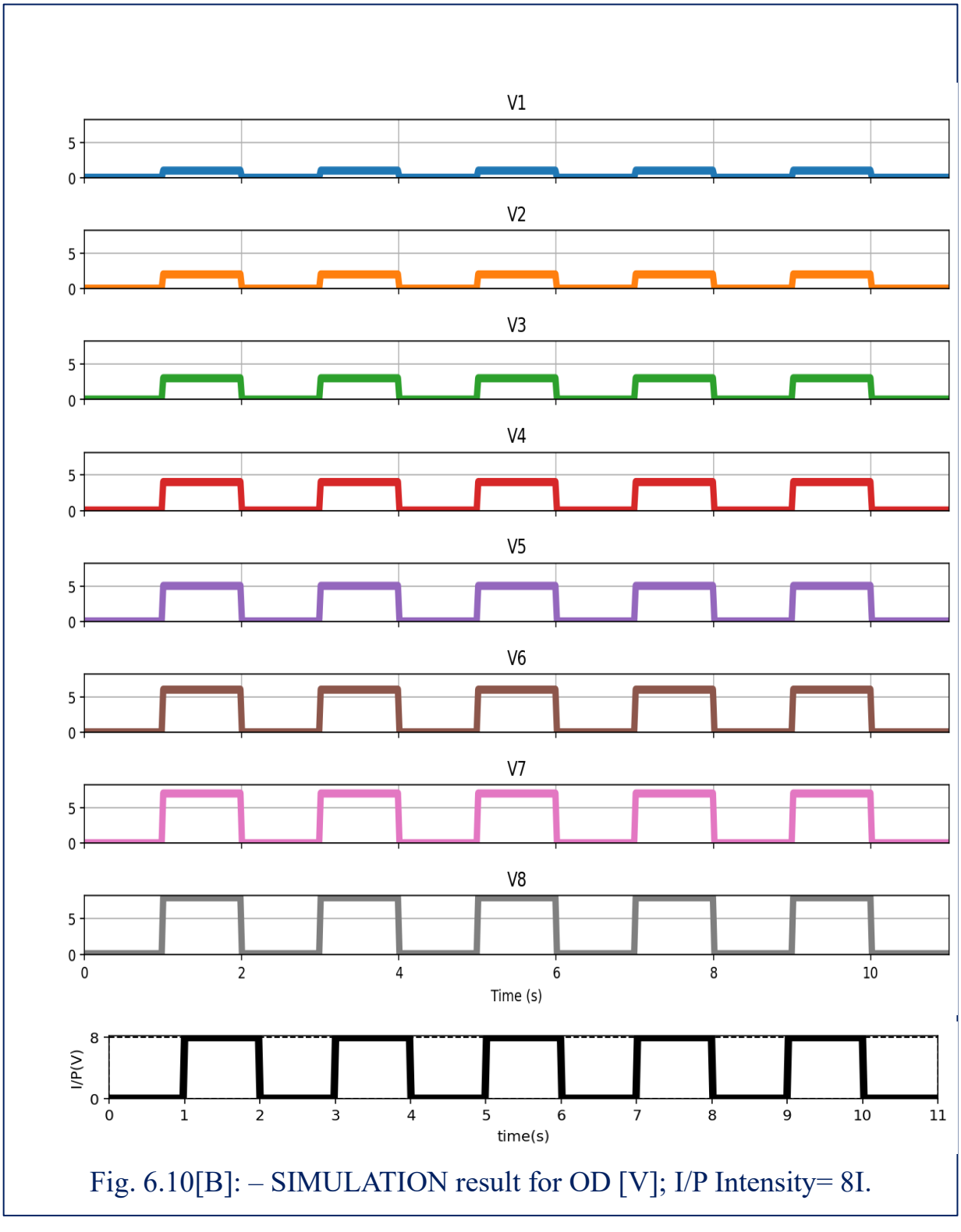

Fig. 6.10[B]: – SIMULATION result for OD [V]; I/P Intensity= 8I.

⇨ *Optical Device 'W'*

In order to activate the OD 'W', the supplied I/P intensity of incident polarized light on 'W' is set to be 9I obtained from 'O_9'. Here it is to be noticed that the nine number of O/P lines entitled as W_1 (I)-W_9(9I) are generated from OD 'W' by dint of some number of SCL, MCL (L_6-L_2), BC, BS; which is shown in **Fig.-6.11[a]** & Appendix-B, Table –S_8. Here all O/P lines i.e., W_1, W_2, ……., W_9 are attached with Y_1, Y_2, ……..., Y_9 (O/P channels of our introduced OBED) gradually. Python simulation result is shown in **Fig.-6.11[b]**.

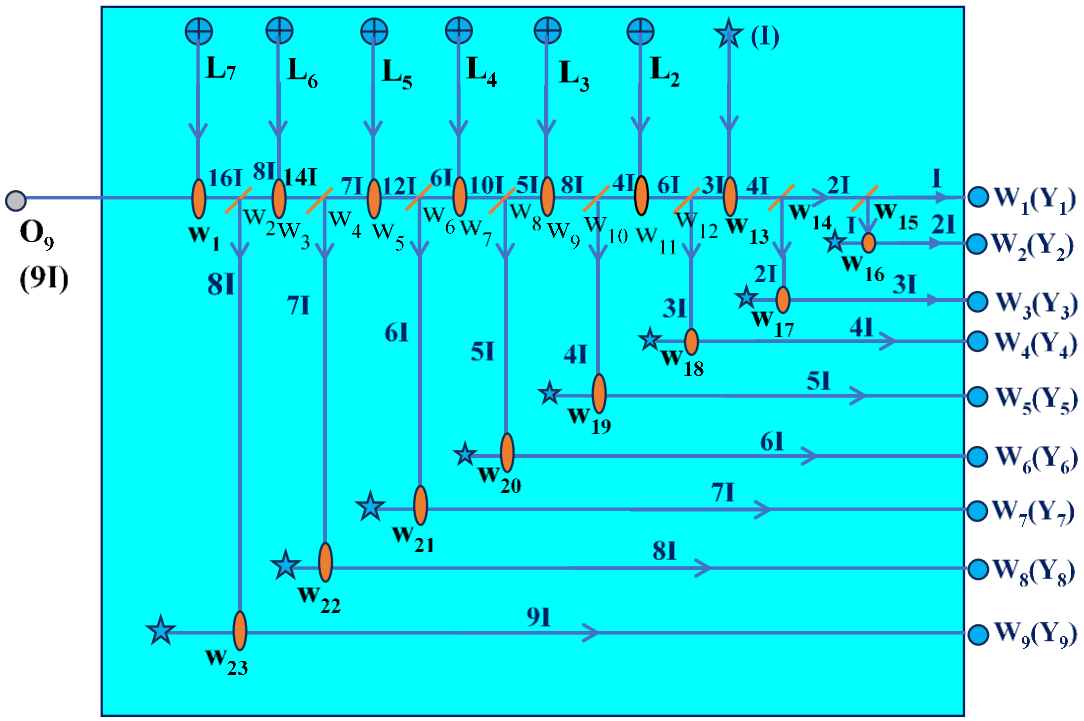

Fig. -6.11[a]: Intensity level at various pts. and final O/P intensity distribution of O.D. 'W'

$$\mathbf{ACL} = \left\{\frac{n(n+1)}{2}\right\}\mathbf{I} = \left\{\frac{8(8+1)}{2}\right\}\mathbf{I} = 36\mathbf{I} = L_7 + L_6 + L_5 + L_4 + L_3 + L_2 + 9\bigstar$$

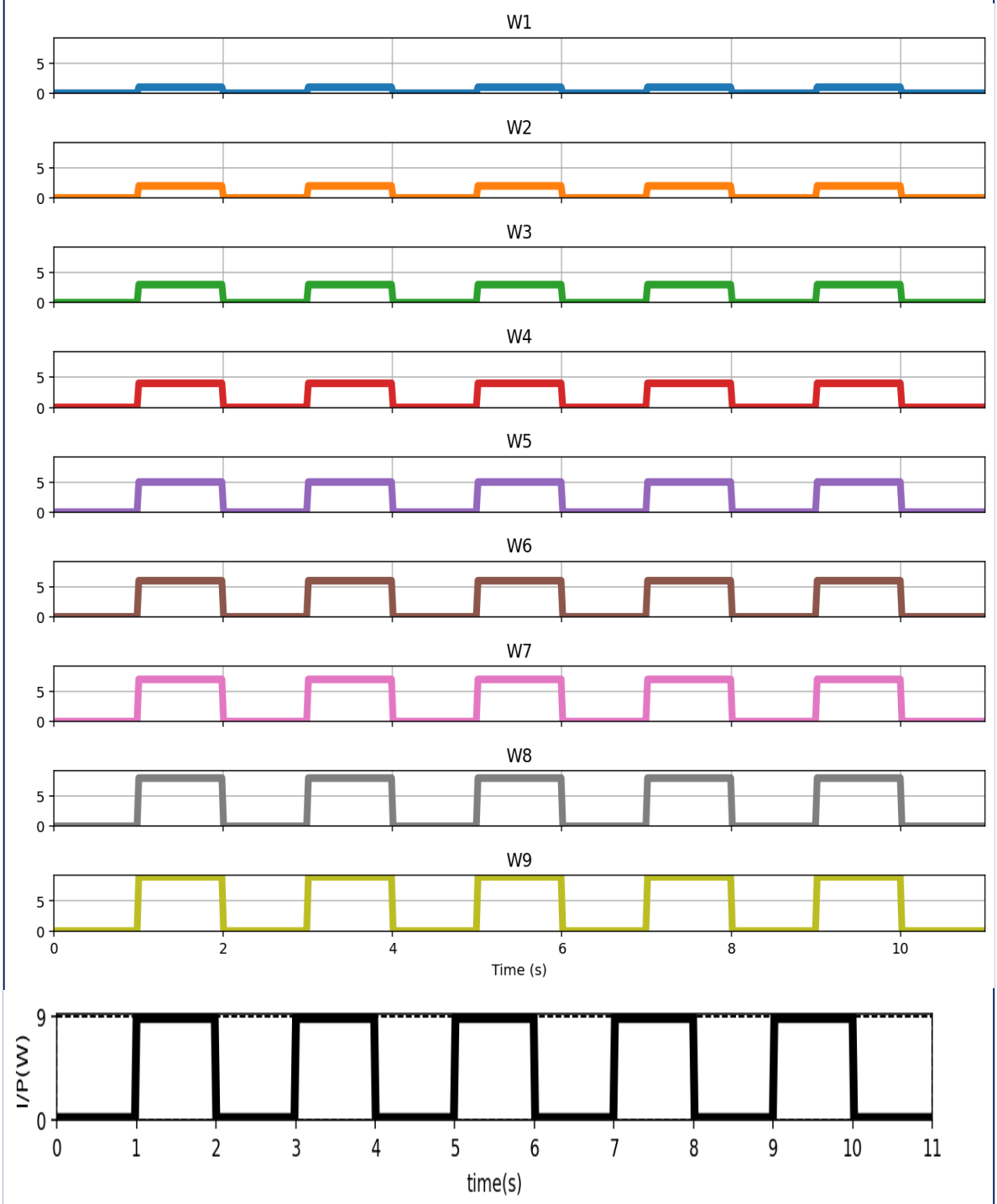

Fig.-6.11[b]: – SIMULATION result for OD [W]; I/P Intensity= 9I.

⇨ *Optical Device 'X'*

To incite the OD X, the I/P intensity must be consigned from the O/P path 'O_{10}' of the optical switch (N). As a consequence, the intensity of the incident as consequences the intensity of incident polarized light on OD 'X' from 'O_{10}' is =10I. Now by dint of some number of SCL, MCL (L_8-L_2) BC, BS, the total ten number of O/P lines such as X_1 (I) – X_{10} (10I) are transmitted to Y_1-Y_{10} (O/P channels of our mentioned OBED). The technique of OD 'S' is shown in **Fig.-6.12[a]** and Appendix-B, Table –S_9. Python simulation result is shown in **Fig.- 6.12[b]**.

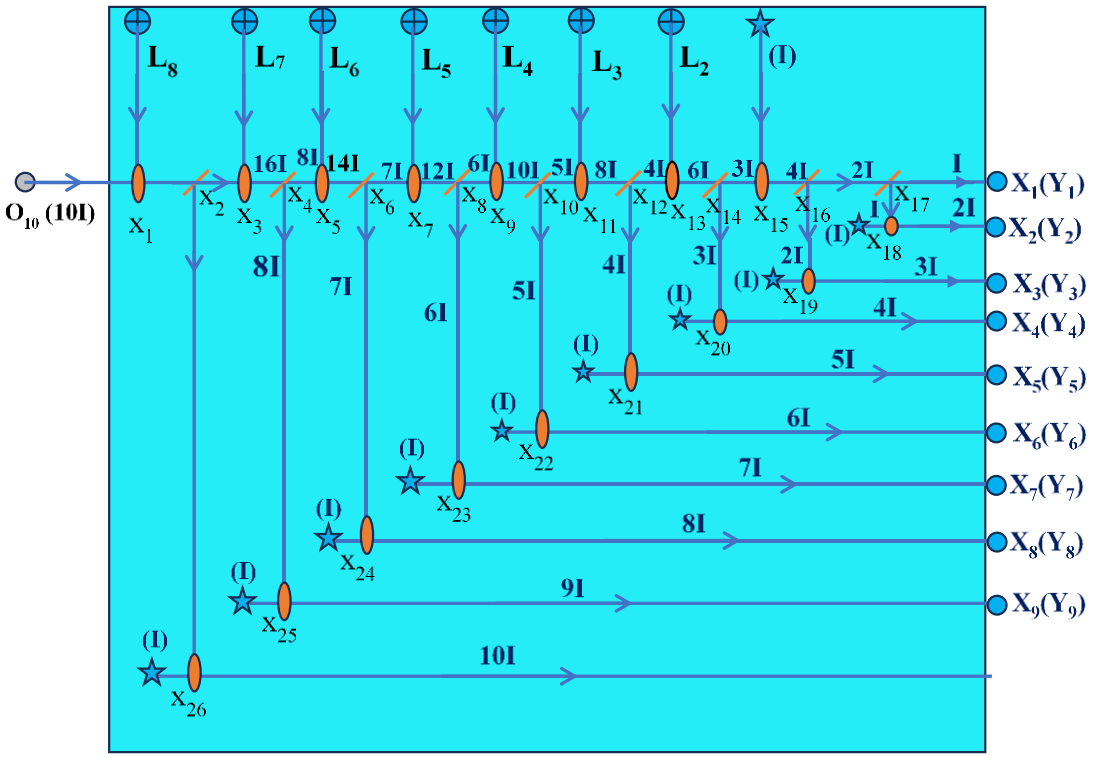

$$\text{ACL} = \left\{\frac{n(n+1)}{2}\right\} I = \left\{\frac{9(9+1)}{2}\right\} I = 45I = L_8 + L_7 + L_6 + L_5 + L_4 + L_3 + L_2 + 10\bigstar$$

Fig. -6.12[a]: Intensity level at various pts. and final O/P intensity distribution of O.D. 'X'

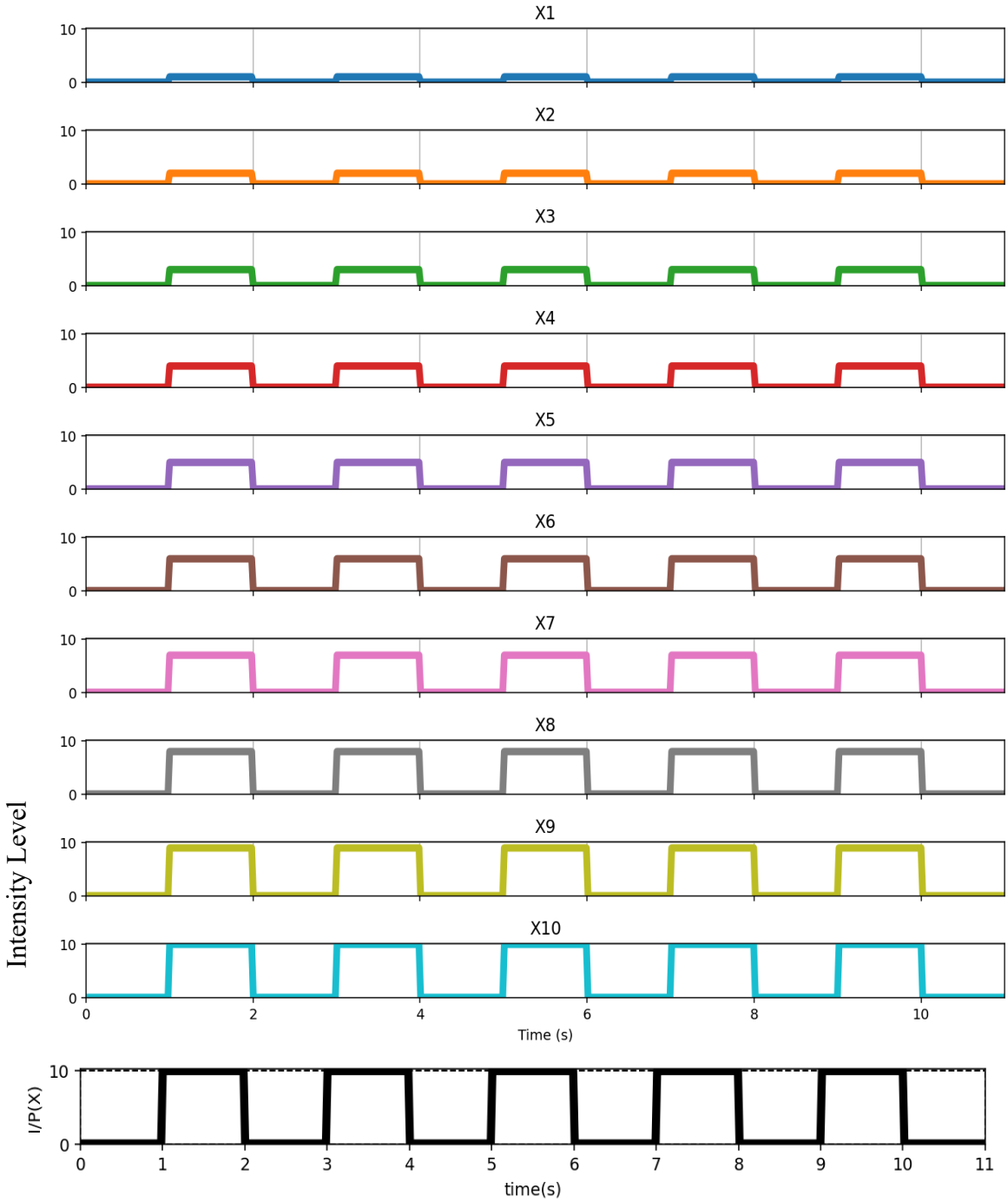

Fig. 6.12[b]– SIMULATION result for OD [X]; I/P Intensity= 10I.

6.2.4. Output division –

Depending upon the value of 't' from equation (A) of section 2.1, there are serially 't' number of output channels (in output division of OBED) i.e., Y_1, Y_2, Y_3, ……., Y_t are in ON state, i.e., polarized light is present with its specific intensity level like - intensity level of activated O/P channels Y_1, Y_2, Y_3, ……., Y_t are I, 2I, 3I,……., tI respectively. Such as in generalized form – intensity level of Y_t = tI where t= natural number (shown in **Table -6.3**).

Table – 6.3: [Number of lighted input sources and concern number of incited output channels with specific intensity level.]

Number of lighted sources (n)	Number of activated outputs channel of optical binomial expansion device (O.B.E.D)	Name of the output channels of OBED at specific intensity									
		I	2I	3I	4I	5I	6I	7I	8I	9I	10I
0	1	Y_1									
1	2	Y_1	Y_2								
2	3	Y_1	Y_2	Y_3							
3	4	Y_1	Y_2	Y_3	Y_4						
4	5	Y_1	Y_2	Y_3	Y_4	Y_5					
5	6	Y_1	Y_2	Y_3	Y_4	Y_5	Y_6				
6	7	Y_1	Y_2	Y_3	Y_4	Y_5	Y_6	Y_7			
7	8	Y_1	Y_2	Y_3	Y_4	Y_5	Y_6	Y_7	Y_8		
8	9	Y_1	Y_2	Y_3	Y_4	Y_5	Y_6	Y_7	Y_8	Y_9	
9	10	Y_1	Y_2	Y_3	Y_4	Y_5	Y_6	Y_7	Y_8	Y_9	Y_{10}

Here in our proposed scheme, it is considered that for particular number of I/P coherent lighted sources (n) the numerical values of O/P intensity levels I, 2I, 3I……., tI is in terms of combination as ${}^nC_0$, ${}^nC_1$, ${}^nC_2$, …., ${}^nC_{t-1}$ where $0 \leq t-1 \leq n$ (which is shown in **Table – 6.4**).

Table – 6.4: [For fixed number of lighted sources(n), the numerical value of incited output channels in terms of combination (by means of concern intensity level).]

Name of output channel of OBED.	Intensity Level of incited O/P channel of OBED (tI).	Value of (t-1) [t= =co-efficient of intensity level]	For particular number of lighted sources(n) the value of output of OBED in terms of combinations [C (n, t-1)] i.e., $\mathbf{Y_t={}^nC_{t-1}}$
Y_1	I	(1-1) =0	${}^nC_0$
Y_2	2I	(2-1) =1	${}^nC_1$
Y_3	3I	(3-1) =2	${}^nC_2$
Y_4	4I	(4-1) =3	${}^nC_3$
Y_5	5I	(5-1) =4	${}^nC_4$
Y_6	6I	(6-1) = 5	${}^nC_5$
Y_7	7I	(7-1) =6	${}^nC_6$
Y_8	8I	(8-1) =7	${}^nC_7$
Y_9	9I	(9-1) =8	${}^nC_8$
Y_{10}	10I	(10-1) =9	${}^nC_9$

In our designed scheme, there are in total of ten output channels entitled Y_1, Y_2, Y_3, ….., Y_{10}. The intensity level of activated output channels Y_1, Y_2, Y_3, ..., Y_{10} are of I, 2I, 3I, …,10I, respectively. It is now discussed how to calculate the numerical value of each output channel of our proposed OBED. This is as follows – $Y_t={}^nC_{t-1}$(see table – 15) where n⇒ total number of coherent input lighted sources as well as index of the binomial expansion. Here 't' is the coefficient of the intensity level of the definite O/P channel, for fixed 'n', t =(n+1) also indicates that the total no. of O/P channels of O/P division of our proposed architecture (OBED) which are in ON state. **Therefore, for the fixed value of 'n', activated O/P channels gradually are- Y_1, Y_2, Y_3, …. …..., Y_t, from which binomial coefficients can be calculated serially.** Moreover, the numerical value of serially output channels **Y_1, Y_2, Y_3, ……., Y_t** in terms of combination as **${}^nC_0$,${}^nC_1$, ${}^nC_2$, …., ${}^nC_{t-1}$** where $\mathbf{0 \leq t-1 \leq n}$ i.e., in numerical value at last term (Y_t) of the serially output channels (Y_1, Y_2, Y_3, ……., Y_t) of OBED, satisfying the relation **t−1=n, or t=n+1.**

6.3. Working Principle of Optical Binomial Expansion Device (OBED)

Now to design our proposed OBED (**Fig.-6.13**), we take the help of specific nine OD entitled as P, Q, R, S, T, U, V, W & X having no. of O/P lines from those are 2(P_1, P_2), 3(Q_1, Q_2, Q_3), 4(R_1 to R_4), 5(S_1 to S_5), 6(T_1 to T_6), 7(U_1 to U_7), 8(V_1 to V_8), 9(W_1 to W_9), & 10(X_1 to X_{10}) respectively, and there are 10 O/P channels as Y_1, Y_2, Y_3,……,Y_{10} where they are corresponding to intensity level I, 2I,…..10I respectively.

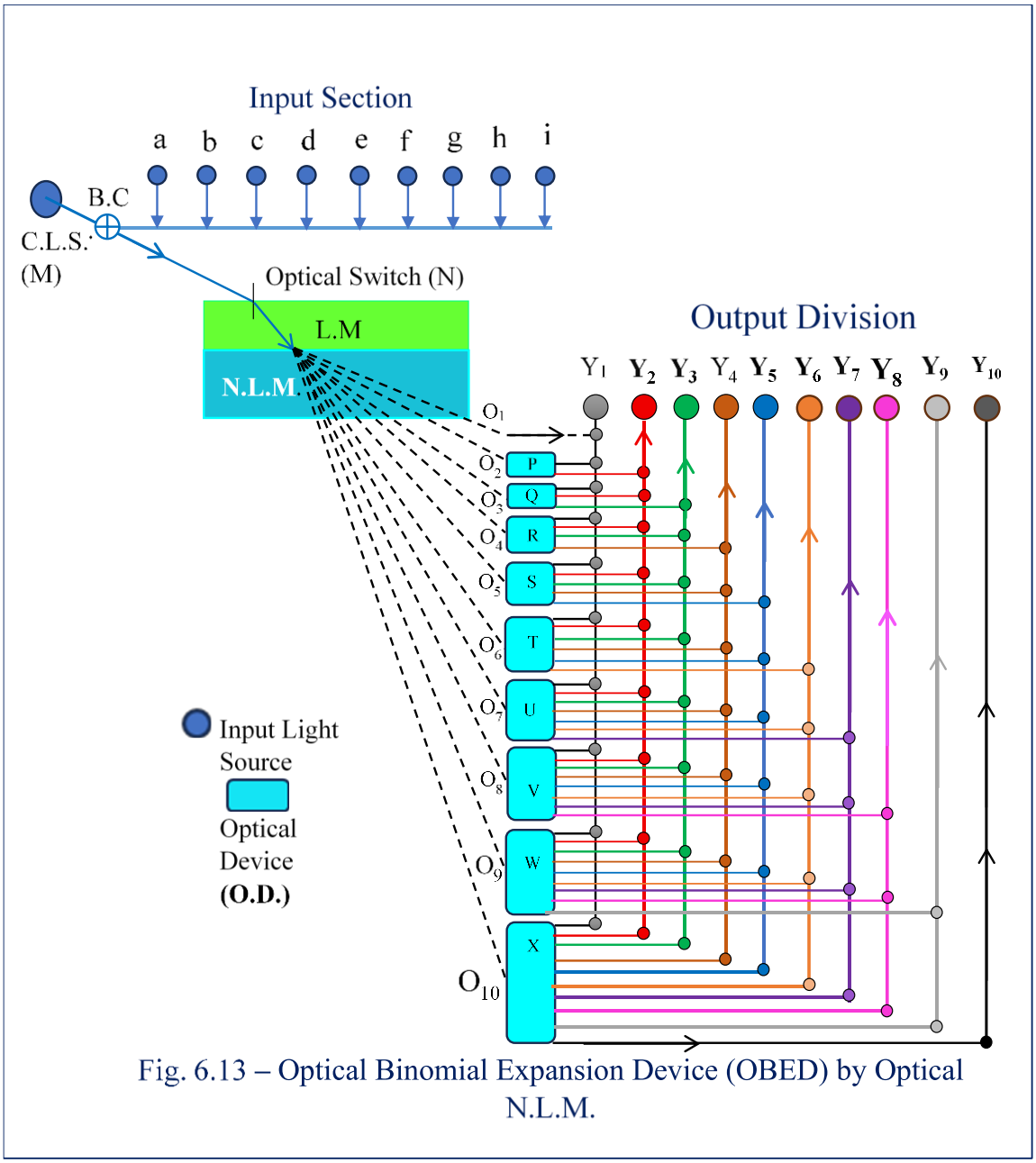

Fig. 6.13 – Optical Binomial Expansion Device (OBED) by Optical N.L.M.

It has to be noted that suffix of O/P lines from optical devices indicates the intensity level of themselves. All O/P channels of all-optical devices of which intensity level I, 2I, 3I,…..….,9I, 10I are to be connected to Y_1, Y_2, Y_3,……..,Y_9, $Y_{10,}$ respectively. So, O/P channels of each OD of which intensity level I, namely P_1, Q_1, R_1, S_1, T_1, U_1, V_1, W_1, X_1 are assembled to Y_1 and similarly O/P channels of each OD of which intensity level 2I namely P_2, Q_2, R_2, S_2, T_2, U_2, V_2, W_2, X_2 are joined to Y_2 and so on.

Now all o/p channels of each optical device (namely P, Q, R, S, T, U, V, W, X) and O/P channels of OBED (Y_1, Y_2, Y_3,…..,Y_{10}) are related as -

$$Y_1 = I_1 + P_1 + Q_1 + R_1 + S_1 + T_1 + U_1 + V_1 + W_1 + X_1 \quad \text{---------(5.1)}$$

$$Y_2 = P_2 + Q_2 + R_2 + S_2 + T_2 + U_2 + V_2 + W_2 + X_2 \quad \text{----------(5.2)}$$

$$Y_3 = Q_3 + R_3 + S_3 + T_3 + U_3 + V_3 + W_3 + X_3 \text{----------(5.3)}$$

$$Y_4 = R_4 + S_4 + P_4 + U_4 + V_4 + W_4 + X_4 \quad \text{---------(5.4)}$$

$$Y_5 = S_5 + T_5 + U_5 + V_5 + W_5 + X_5 \quad \text{----------(5.5)}$$

$$Y_6 = T_6 + U_6 + V_6 + W_6 + X_6 \text{----------(5.6)}$$

$$Y_7 = U_7 + V_7 + W_7 + X_7 \text{----------(5.7)}$$

$$Y_8 = V_8 + W_8 + X_8 \text{----------(5.8)}$$

$$Y_9 = W_9 + X_9 \text{----------(5.9)}$$

$$Y_{10} = X_{10} \text{----------(5.10)}$$

In our proposed OBED for particular no. of input lighted sources (n), the O/P intensity **I, 2I, 3I,……, tI** represents the binomial co-efficient with a numerical value in terms of combinations as $^nC_0$, $^nC_1$, $^nC_2$, ……$^nC_{t-1}$ respectively. Where **$0 \le t-1 \le n$**

Here it is also to be remarked that for coefficient of I/P intensity(t) on OS(N) which is designed in Fig.-13, there are 't' no of O/P channels like Y_1, Y_2, Y_3, ……Y_t are in the active state, i.e., light is present with their specific intensity level I, 2I, ……..., tI, respectively. When we want to know binomial co-efficient under definite positive index (n) of binomial expansion, it has to be incited 'n' no. of input light sources, where each input coherent light sources are in the same and standard intensity level I. This time input intensity of incident polarized light on OS (N) is (n+1) I with the help of additional CL(M).

Therefore, depending upon how many no. of coherent input sources is to be kept in ON state related with a definite index of the binomial expansion. Hence, as well as values of the intensity level of incident polarized light on OS (N) then by dint of specific optical devices we get definite no. of O/P channels like Y_1, Y_2, ……., Y_t according to co-efficient of I/P intensity 't' are in ON status. So, for fixed n, coefficient of I/P intensity of incident polarized on OS (N) is t=(n+1) then total no. of O/P channels as well as total no. of binomial co-efficient serially are as Y_1, Y_2, ……., Yt. Hence binomial co-efficient under index 'n', can be computed from the intensity level of **Y_1, Y_2, ……., Y_t** are $\boldsymbol{n_{c_0}}$, $\boldsymbol{n_{c_1}}$, $\boldsymbol{n_{c_2}}$, **……** $\boldsymbol{n_{c_{t-1}}}$ respectively wherein last term**, t-1=n.**

2. The calculation for Binomial Co-efficient from OBED -

- When none (n=0) of all I/P coherent light sources be lighted, then I/P intensity on optical switch (OS) 'N' is= [0+I (for the additional constant light source (CL) of single intensity I mentioned as 'M')] =I. So, it is noted that the O/P path from 'N' is of intensity I, which is named as 'O_1'. Moreover, this path 'O_1' is again directly linked with O/P channel 'Y_1' of OBED [from relation (5.1)]. So, for n=0, we get, binomial coefficient from the intensity level of 'Y_1' as-

  $Y_1 = n_{C_0} = 0_{C_0} = 1$.

- As for instance, when anyone I/P light source (i.e., here n=1) of I/P section (which are constructed by nine number of CL of same and standard intensity level I denominated as "a, b, c, d, e, f, g, h & i") be activated i.e., polarized light is present with intensity level I then intensity of incident light on optical switch (N) is =I+I (by additional CL source named as M) =2I. So here t=2 [t = co-efficient of I/P light on OS (N)]. Then from the property of OS (N) the O/P path from 'N' is denoted by 'O_2' with intensity level 2I. This path (O_2) is connected with OD 'P'. So, I/P intensity of OD 'P' is 2I then we get two O/P lines 'P_1' & 'P_2' with intensity level I & 2I respectively. Now from the relation (5.1) & (5.2), these are linked into the O/P channels Y_1& Y_2 gradually. So, for n=1, we get two number [for t=(n+1) =2] of binomial co-efficient, the numerical values of them as –

  $Y_1 = n_{C_0} = 1_{C_0} = 1$

  $Y_2 = n_{C_1} = 1_{C_1} = 1$.

- When 'a & b' are in ON state, then I/P intensity on O. S 'N' is = [2I+I (for 'M')] =3I.Then O/P path from 'N' is 'O_3', which is I/P line of O.D 'Q'. From the property

of 'Q', we have three O/P lines as Q_1, Q_2& Q_3 with intensity levels I,2I & 3I serially. Then they are newly conjoined into O/P channels Y_1, Y_2& Y_3 of OBED (relation 5.1-5.3). Therefore, for n (no. of lighted sources as well as the numerical value of the index of binomial expansion) =2, we have three no. of binomial coefficient with numerical values as follows-

$Y_1 = n_{C_0} = 2_{C_0}$=1

$Y_2 = n_{C_1} = 2_{C_1}$ =2

$Y_3 = n_{C_2} = 2_{C_2}$=1.

- When 'a, b & c' are in ON state, I/P intensity on OS 'N' is = [3I+I (for 'M')] =4I. So, O/P path 'O_4', from 'N' is of intensity level 4I. This is also I/P intensity of OD 'R'. We have four O/P lines from the OD 'R' feature, and we have four O/P lines as R_1, R_2, R_3& R_4 with intensity levels I, 2I, 3I & 4I, respectively. Again, those O/P lines are associated with O/P lines as Y_1, Y_2, Y_3& Y_4 orderly (relation 5.1 – 5.4). Hence for n=3, it will be taken noticed, four no. of binomial coefficient with numerical values such as-

  $Y_1 = n_{C_0} = 3_{C_0}$=1

  $Y_2 = n_{C_1} = 3_{C_1}$ =3

  $Y_3 = n_{C_2} = 3_{C_2}$=3

  $Y_4 = n_{C_3} = 3_{C_3}$=1.

- To calculate the binomial coefficient, when the index of binomial expansion is =4, there are four no. of I/P sources (such 'a, b, c & d') out of nine are actuated, i.e., polarized light is present with intensity level I separately. Then the intensity of incident polarized light on OS (N) is = [4I+I (for 'M')] =5I. Consequently, the emergent O/P path from OS (N) is 'O_5'. This is also joint with O.D 'S'. Due to 'O_5' the I/P intensity on 'N' is 5I, then characteristics of OS (S) we obtain five no. O/P lines as - S_1, S_2, S_3, S_4& S_5gradually increase intensity level I, 2I, 3I, 4I & 5I. Then they are also continued to Y_1, Y_2, Y_3, Y_4& Y_5 serially (relation 5.1-5.5). So, for n=4, it can be noticed that there are five no. of binomial coefficient with numerical values like as-

  $Y_1 = n_{C_0} = 4_{C_0}$ =1

  $Y_2 = n_{C_1} = 4_{C_1}$= 4

  $Y_3 = n_{C_2} = 4_{C_2}$=6

  $Y_4 = n_{C_3} = 4_{C_3}$=4

$Y_5 = n_{C_4} = 4_{C_4}$ =1

- To compute binomial coefficients for index 5, we have to actuate five no. of I/P sources (like – 'a, b, c, d & e') out of nine in the input section. Then the intensity of incident polarized light on OS 'N' is = [5I+I (for 'M')] =6I.Hence emanated polarized light from OS 'N' is of intensity 6I. So, O/P path of 'N' is O_6 which is also engaged with OD 'T'. As a result, after activation of 'T', there are six no. of O/P lines entitled as - T_1, T_2, T_3, T_4, T_5& T_6 from it where intensity level of them gradually are I, 2I, 3I, 4I,5I & 6I. From the relation (5.1) to (5.6), we have the activated O/P channels of OBED gradually - Y_1, Y_2, Y_3, Y_4, Y_5& Y_6. Finally, for n=5, the numerical values of binomial coefficients serially are-

  $Y_1 = n_{C_0} = 5_{C_0}$=1

  $Y_2 = n_{C_1} = 5_{C_1}$= =5

  $Y_3 = n_{C_2} = 5_{C_2}$ =10

  $Y_4 = n_{C_3} = 5_{C_3}$=10

  $Y_5 = n_{C_4} = 5_{C_4}$ =5

  $Y_6 = n_{C_5} = 5_{C_5}$ =1.

- When 'a, b, c, d, e & f' are in ON state, the intensity of incident polarized light on OS 'N' is = [6I+I (for 'M')] =7I. So, O/P path of 'N' is O_7, which is again I/P line of OD 'U'. So, due to O_7 inciting itself, it generates seven O/P lines named as- U_1, U_2, U_3, U_4, U_5, U_6& U_7 of intensity level I, 2I, 3I, 4I, 5I, 6I &7I serially. Now from the relation (5.1) to (5.7), when 'U' is enlivened, then O/P channels of OBED gradually are Y_1, Y_2, Y_3, Y_4, Y_5, Y_6 & Y_7. So, for n=6 the numerical values of binomial coefficients gradually are –

  $Y_1 = n_{C_0} = 6_{C_0}$ =1

  $Y_2 = n_{C_1} = 6_{C_1}$= 6

  $Y_3 = n_{C_2} = 6_{C_2}$ =15

  $Y_4 = n_{C_3} = 6_{C_3}$ =20

  $Y_5 = n_{C_4} = 6_{C_4}$ =15

  $Y_6 = n_{C_5} = 6_{C_5}$ =6

  $Y_7 = n_{C_6} = 6_{C_6}$ =1.

- To determine binomial coefficients for index seven, then the I/P sources such as 'a, b, c, d, e, f & g' are in ON state, i.e., polarized light is present with intensity

level I in each source. As a result, the intensity of the incident polarized on OS ('N') is = [7I+I (for 'M')] =8I. So, O/P polarized light of intensity 8I from OS 'N' goes forward along the path 'O_8'. This path is added to the OD 'V' as I/P line. Now owing to 'O_8', the OD 'V' is operated to transmit eight no. of O/P lines like as-V_1, V_2, V_3, V_4, V_5, V_6,V_7& V_8. From the relation (5.1) to (5.8), it can be cognized that there are eight no. O/P channels out of ten in the output division of OBED are in ON state (i.e., light is present with different specific intensity at several definite O/P channels), such as - Y_1, Y_2, Y_3, Y_4, Y_5, Y_6, Y_7& Y_8. Therefore, binomial coefficients for index 7(can be calculated from several O/P channels (where each different channel is in ON state with its different specific intensity) as well as different intensity levels like as-

$Y_1 = n_{C_0} = 7_{C_0} = 1$

$Y_2 = n_{C_1} = 7_{C_1} = 7$

$Y_3 = n_{C_2} = 7_{C_2} = 21$

$Y_4 = n_{C_3} = 7_{C_3} = 35$

$Y_5 = n_{C_4} = 7_{C_4} = 35$

$Y_6 = n_{C_5} = 7_{C_5} = 21$

$Y_7 = n_{C_6} = 7_{C_6} = 7$

$Y_8 = n_{C_7} = 7_{C_7} = 1$

- If eight input coherent sources are in ON state, then the intensity level of incident polarized light on optical switch 'N' is = [8I+I (owing to 'M')] =9I.Consequently O/P path from 'N' is of intensity level 9I, which O9 denotes. Again, this is directly entered into the optical device 'W'. Therefore, when eight input sources are being lighted, OD 'W' is stimulated with intensity level 9I. Now from the property of OD 'W', there are nine no. O/P lines (mentioned as 'W_1, W_2, W_3, --------, W_9') are ejected from it with intensity level gradually I to 9I. In this case, what no. of O/P channels of OBED are in ON state [from relation (5.1) to (5.9)] are -Y_1 to Y_9. So, binomial coefficients for n no. of lighted coherent sources from different O/P intensity levels as-

$Y_1 = n_{C_0} = 8_{C_0} = 1$

$Y_2 = n_{C_1} = 8_{C_1} = 8$

$Y_3 = n_{C_2} = 8_{C_2} = 28$

$Y_4 = n_{C_3} = 8_{C_3} = 56$

$Y_5 = n_{C_4} = 8_{C_4} = 70$

$Y_6 = n_{C_5} = 8_{C_5} = 56$

$Y_7 = n_{C_6} = 8_{C_6} = 28$

$Y_8 = n_{C_7} = 8_{C_7} = 8$

$Y_9 = n_{C_8} = 8_{C_8} = 1$

- Owing to the ON state of all I/P coherent sources, the intensity of incident polarized light on optical switch 'N' is [9I+I (on account of 'M')] =10I. So, the O/P path from OS 'N' is now the path of intensity 10I, which is adverted by 'O_{10}'. After entering its into OD 'X', there are ten no. O/P lines (X_1 to X_{10}) which are effused from OD 'X'. Therefore, when OD 'X' is enlivened, then from the relation (5.1) to (5.10), it can be observed that Y_1 to Y_{10} are in an activation state with their own specific intensity. So, binary coefficients for n = 9 can be calculated as –

$Y_1 = n_{C_0} = 9_{C_0} = 1$

$Y_2 = n_{C_1} = 9_{C_1} = 9$

$Y_3 = n_{C_2} = 9_{C_2} = 36$

$Y_4 = n_{C_3} = 9_{C_3} = 84$

$Y_5 = n_{C_4} = 9_{C_4} = 126$

$Y_6 = n_{C_5} = 9_{C_5} = 126$

$Y_7 = n_{C_6} = 9_{C_6} = 84$

$Y_8 = n_{C_7} = 9_{C_7} = 36$

$Y_9 = n_{C_8} = 9_{C_8} = 9$

$Y_{10} = n_{C_9} = 9_{C_9} = 1.$

After all, for particular no. of lighted sources and binomial index, we get binomial co-efficient from different O/P channel of proposed OBED (shown in **Table – 6.5**).

Table-6.5: [Index of binomial expansion Vs. numerical value from enlivened /ON stated output channels of OBED.]

Value of index	No. of light-ed sourc-es (n)	Value of (t-1) at particular Y_t where the maximum value of t at Y_t is =(n+1)										The numerical value of each output channel of OBED $Y_1 = n_{C_{t-1}}$									
		Y_1	Y_2	Y_3	Y_4	Y_5	Y_6	Y_7	Y_8	Y_9	Y_{10}	Y_1	Y_2	Y_3	Y_4	Y_5	Y_6	Y_7	Y_8	Y_9	Y_{10}
0	0	0																			
1	1	0	1									1_{C_0}	1_{C_1}								
2	2	0	1	2								2_{C_0}	2_{C_1}	2_{C_2}							
3	3	0	1	2	3							3_{C_0}	3_{C_1}	3_{C_2}	3_{C_3}						
4	4	0	1	2	3	4						4_{C_0}	4_{C_1}	4_{C_2}	4_{C_3}	4_{C_4}					
5	5	0	1	2	3	4	5					5_{C_0}	5_{C_1}	5_{C_2}	5_{C_3}	5_{C_4}	5_{C_5}				
6	6	0	1	2	3	4	5	6				6_{C_0}	6_{C_1}	6_{C_2}	6_{C_3}	6_{C_4}	6_{C_5}	6_{C_6}			
7	7	0	1	2	3	4	5	6	7			7_{C_0}	7_{C_1}	7_{C_2}	7_{C_3}	7_{C_4}	7_{C_5}	7_{C_6}	7_{C_7}		
8	8	0	1	2	3	4	5	6	7	8		8_{C_0}	8_{C_1}	8_{C_2}	8_{C_3}	8_{C_4}	8_{C_5}	8_{C_6}	8_{C_7}	8_{C_8}	
9	9	0	1	2	3	4	5	6	7	8	9	9_{C_0}	9_{C_1}	9_{C_2}	9_{C_3}	9_{C_4}	9_{C_5}	9_{C_6}	9_{C_7}	9_{C_8}	9_{C_9}

6.4 Conclusion:

The inherent parallelism of optic and intensity-based refractive index property of the nonlinear optical material has been successfully utilized in our proposed scheme (due to high relative RI of NLM with respect to air for making the optical switch LM & NLM are taken together). At the same time, 50% beam splitter and beam combiner are fully exploited in our architecture. Our proposed design (Fig.-13) can be envisaged for calculating binomial coefficient under maximum positive integral index nine. For activating our optical circuits, the I/P light beams should be polarized and coherent in nature. In the proposed OBED, the binomial coefficient can be accurately calculated from a different intensity level, where I, 2I, ……., tI represents the numerical value in terms of combination as – I= n_{c_0}; 2I=n_{c_1}; ……; tI= $n_{c_{t-1}}$ for 'n' number of lighted coherent I/P sources. The important condition for each specific OD (such 'P' to 'X') in our proposed architecture is such that the total provided intensity in it is TI=tI + $\frac{n(n+1)}{2}$I ; where t=(n+1); n is the number of lighted coherent I/P sources as well as the value of the positive integral index. t is co-efficient of I/P intensity of incident polarized light on that specific OD. It is also to be remarked that $\frac{n(n+1)}{2}$ amount of intensity is supplied by an additional constant light source which is briefed by ACL (in Table-1). Now total stored intensity for definite OD is = $TI = tI + \left\{\frac{n(n+1)}{2}\right\} I = \left\{\frac{t(t+1)}{2}\right\} I$. Now division of total stored intensity with in specific OD as $TI = k_1I + k_2I + ... + k_tI$. Where t is the total number of output channels for that OD as well as in our proposed architecture. Here k_1, k_2, ..., k_t denotes natural no. Moreover, k_1I is the amount of intensity at the 1st channel i.e., at Y_1; k_2I is the amount of intensity at the 2nd channel i.e., at Y_2. Similarly, k_tI is the amount of intensity at the 't' th channel i.e., at Y_t.

The system designed here is all optical in nature. To activate the NLM, coherent laser beams act as input. Also, we require a strong and purely polarized laser light for exploiting the non-linearity of the material. To produce the effect of 2nd order nonlinearity, the strong laser beam is significant.

However, there are some problems for implementing this scheme: At the time of refraction in optical switch a tiny reflection will also occur. Also, a small amount of absorption will take place at every step. This problem can be minimized by appropriate selection of the media and by use of some antireflection coating. Here another problem is diffraction due

to NLM cell sizes. To prevent this problem the size of the NLM and the laser wavelength should be selected gingerly. Taking these precautions properly, the whole system can be reduced to the sub-micron-level dimension. Now to activate the NLM, the laser source of high power is required. This can be done by application of a Q- switched pulsed laser. For example, Nd: YAG laser source with 532-nm light at 10W of O/P power is efficient of achieving an intensity of MW/sq.cm.

As the whole operation, ON state of Yt means that it always represents the const. intensity level 'tI' for any value of 'n' i.e., in different situations, ON state of definite O/P channel always represents the same intensity level. So, in our designed scheme (Fig.-13), Y_1, Y_2, Y_3, ……, Y_{10} in ON state always represents the intensity level I, 2I, 3I, …..., 10I. Here only depending upon 'n' as well as 't' (where t=n+1), we get there are serially 't' no. of O/P channels are in ON state.

So, the mentioned above problems will not create much trouble for receiving the desired result. As our proposed scheme is of fully optical in nature, we achieve high degree of processing speed. So, this scheme may be applied to the field of all optical computation.

6.5 References

1. S.D. Smith, "Optical bistability, photonic logic and optical computation," *Appl. Opt.* 25, 1550-1564 (1986).
2. G. Li, L. Lin, L. Shao, Y. Yin, J. Hua, "Parallel optical negabinary arithmetic based on logic operations," *Appl. Opt.* 36, 1011-1016 (1997).
3. H.J. Caulfield, "Perspectives in optical computing," *Computer* 31(2), 22-25 (1998).
4. S.P. Medhekar, P. Paltani, "Proposal for optical switch using non-linear refraction," *IEEE photonics Technol. Lett.* 18(15), 1579-1581 (2006).
5. N. Mitra, S. Mukhopadhyay, "Method of developing an all-optical synchronous counter by exploiting the kerr non-linearity of the medium," *Optics and photonics letters* Vol. 3, No.1 23-30 (2010).
6. Y. Fainman, C.C. Guest, S.H. Lee, "Optical digital logic operations by two beams coupling in photorefractive material," *Appl. Opt.* 25(10), 1598-1603 (1986).
7. N. Pahari, D.N. Das, S. Mukhopadhyay, "All-optical method for the addition of binary data by non-linear materials," *Appl. Opt.* 43(33), 6147-6150 (2004).
8. D. Psaltis, D. Brady, K. Wagner, "Adaptive optical networks using photorefractive crystals," *Appl. Opt.*27(9), 1752-1759 (1998).
9. N. Pahari, A. Guchhait, "All-optical serial data transfer between registers using optical mom-linear materials," *Optik* 123(5), 462-466 (2012).
10. N. Pahari, A. Guchhait, A.D. Jana, "Image edge detection scheme by the use of keer type non-linear material and the verification of the scheme by computer simulation," *Journal of optics (Optical Society of India)* 41,178-183 (2012).
11. A. Guchhait, N. Pahari, N.B. Manik, "All-optical decimal to ternary converter with the proper use of optical non-linear material," *Journal of optics (The Optical Society of India)* 49,59-68 (2019).
12. D. Samanta, S. Mukhopadhyay, "All-optical method for maintaining a fixed intensity level of a light signal in optical computation," *Optics communications* 281, 4851-4853 (2008).

13. M. A. Karim and A. A. S. Awwal, "Optical Computing: An Introduction," *(Wiley, New York, 2003)*, Chap. 3, pp. 35-56.

14. L. K. Cotter, T, J. Drabik, R. J. Dillon, and M. A. Handaschy, "Ferroelectric-liquid-crystal/silicon-integrated circuit spatial light modulator," *Opt. Lett.* 15(5), 291-293 (1990).

15. S. D. Smith, Tanossy, H. A. Mackenzie, J.G. H. Mathew, J.J.E. Reid, M.R. Taghizadeh, F.A.P. Tooley, A.C. Walker, "Nonlinear optical circuit elements, logic gates for optical computers: the first digital circuits," *Opt. Eng.* 24(4), 569-574 (1985).

16. N. Pahari, D. N. Das, S. Mukhopadhyay, "All-optical method for the addition of binary data nonlinear materials," *Appl. Opt.* 43(33), 6147-6150 (2004).

Chapter 7

Conclusions and future scope of works

7.2. Introduction

7.3. Summary of the thesis

7.4. Overall conclusions on the thesis

7.5. Future scope of works

Chapter

7

Conclusion and Future Scope of the Work

Optics has been an important contributor to logic operations and data processing in the last few decades. Although research in the field of optical computing is ongoing, it continues to be a highly researched field with tremendous untapped potential. In spite of all the numerous studies and models proposed thus far, there remains great potential for further research to be able to fully exploit the advantages that optics has to provide. This chapter gives a concluding overview of the thesis and sets out possible avenues for future research.

7.1. Introduction

Conventional electronic systems, while robust, face limitations in executing complex parallel operations at ultra-high speeds. As demand grows for faster computing reaching into terabit ranges optical and optoelectronic systems are being seen as the next frontier. Replacing electrons with photons as information carriers offers potential for significant performance gains, especially when paired with metamaterials and engineered crystal structures to precisely manage light signals. The last few decades have witnessed rapid advancements in this domain, with a focus on developing all-optical logic and arithmetic circuits. These circuits rely on the strategic use of non-linear optical materials for switching and computation. In such systems, binary '1' is typically represented by the presence of light, while binary '0' corresponds to its absence. As this field continues to evolve, the vision remains clear to design faster, energy-efficient, and more scalable computing systems where photons not electrons are at the heart of digital logic.

Optics is now a potential technology in optical computing and communication fields. Optical computing is an interdisciplinary field that encompasses science and engineering and interests' researchers and scientists from diverse backgrounds. Their persistent efforts have made tremendous progress and quick development in the application of optical systems, due to the increasing variety of real-life applications. This advancement has come

about through the establishment of new techniques, discovery and utilization of high optical materials, and development of special optical components. These are central to digital optical computers, where optical switches are particularly significant for facilitating parallel computation. Specifically, switches made from nonlinear optical materials have been extensively applied because of their speed and sensitivity.

Optical logic gates, being the building blocks of optical digital circuits, are at the center of this field. From the previous chapters, we have seen a number of optical logic, arithmetic, and data processing circuit designs. Due to their compact size and high speed, such systems promise to make ultra-fast data processing possible and play an enabling role in next-generation computing technologies.

7.2. Summary of the thesis

The final chapter consolidates the contributions made throughout the thesis. It emphasizes the advantages of using all-optical systems in digital logic, arithmetic, signal processing, and functional computation. Each proposed design demonstrates how nonlinear optical behavior, light routing, and intensity modulation can be combined to eliminate dependence on electronic components. Future work may involve experimental validation of the designs, integration with photonic integrated circuits, and the extension of current systems to handle more complex computations and logic operations. The research lays the groundwork for practical implementation of high-speed, scalable optical computing architectures

7.3. Overall conclusions on the thesis

This work presents an extensive set of all-optical design for executing a variety of data processing and computation tasks based on nonlinear optical materials (NLMs) and polarized coherent laser sources. Ranging from fast shift registers, encoders (binary, ternary, and quaternary), and decoders to image edge detection, binomial coefficient calculators, and trigonometric function generators, every scheme takes advantage of the ultrafast response times, parallelism, and gate-free logic realization inherent in optics.

Among the innovations in these designs is the elimination of conventional logic gates AND, OR, and NOT through the use of Kerr effect and intensity-based switching features of such NLMs as CS_2,, and silica glass. Both input sources are uniform in intensity and polarization to maintain consistency and coherence required for efficient nonlinear

activation. Reliability is also increased through the utilization of Nd: YAG lasers, which have appropriate wavelength and high coherence.

Compared to electronic counterparts, these optical schemes possess superior speed (in the terahertz range) and lower complexity, since the logic operations are intrinsically part of the material interactions. In multi-valued encoding/decoding applications, the ternary and quaternary systems provide representation of more states per bit, greatly increasing data handling capability with the same bit-width. The optical binomial coefficient calculator also demonstrates the capability of performing complex arithmetic operations without electronic computation in any form.

With meticulous architectural design-using beam splitters, optical combiners, and layered optical switching networks-these systems ensure accuracy while providing prospects for size reduction to the sub-micron scale, particularly when complemented with anti-reflection coatings and precision-controlled nonlinear media. Overall, the presented frameworks are a significant step towards the achievement of fully optical computing systems that are efficient, scalable, and possess outstanding speed.

7.4. Future scope of works

The schemes outlined here provide a number of promising avenues for future development:

1. Higher Radices Extension: The encoding principles can be generalized from quaternary to octal (radix-8), hexadecimal (radix-16), or higher, to offer greater data density and improve performance in photonic communication networks.
2. Gray and Colour Image Processing: Although present edge detection is tested and verified on binary images, the next-generation systems can be extended for processing Gray-level and colour images, making more powerful optical image processing possible.
3. Integration with Photonic Circuits: Such optical elements can be integrated into integrated photonic chips, enabling the realization of compact and scalable optical computers and AI accelerators.
4. Hybrid Optical-Electronic Systems: Hybridization of the speed of optics with the storage of electronics could yield hybrid architectures suited for high-performance computing and neuromorphic systems.

5. Smart Optics and Adaptive Materials: Tunable or smart nonlinear material research with improved Kerr effects can make logic systems more compact and reconfigurable.
6. Quantum-Enhanced Optical Computing: Certain of the switching and logic concepts described may be extended or adapted to be operational in quantum photonics for purposes of supporting quantum logic operations as well as secure optical communication.
7. Deep Learning Optical AI Blocks: These optical building blocks can form the basis for optical neural networks, facilitating ultra-fast inference in edge computing devices and data centers.
8. Energy Efficiency and Thermal Control: Next-generation designs could emphasize low power consumption and thermal impact management through novel material composites or passive heat removal methods.

With the development of these foundational ideas in this work, future progress may greatly expedite the shift from traditional electronic systems to **completely optical, ultrafast, and scalable computing platforms.**

APPENDICES

Appendix-A

Figure captions: -

1) Fig. S1.1: Block diagram of optical device ‘O’
2) Fig. S1.2: Block diagram of optical device ‘T’
3) Fig. S1.3: Block diagram of optical device ‘U’
4) Fig. S1.4: Block diagram of optical device ‘V’
5) Fig. S1.5: Block diagram of optical device ‘X’

Optical device 'O' [Fig: -S1.1]

It is one input but two outputs device. When the input intensity is 5I, then there are two output lines as 'O_1' & 'O_2' each of intensity level 'I' [which is revealed by Table: -s1.1].

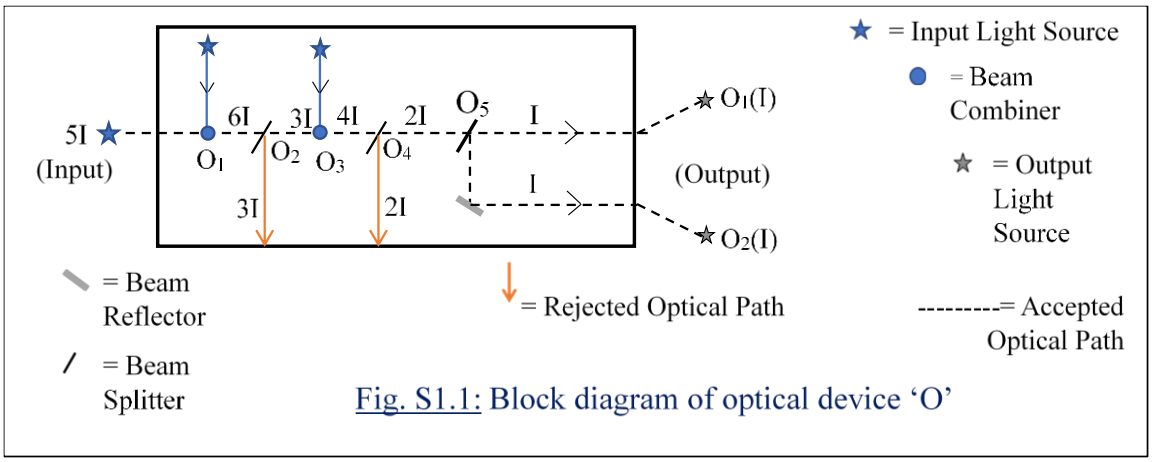

Fig. S1.1: Block diagram of optical device 'O'

Optical device 'T' [Fig: -S1.2]

This is also a single input and two outputs device. When it is actuated at input intensity 10I then there are two output lines 'T_1' and 'T_2' where each of them is of intensity level 2I [which is shown by Table: -s1.2].

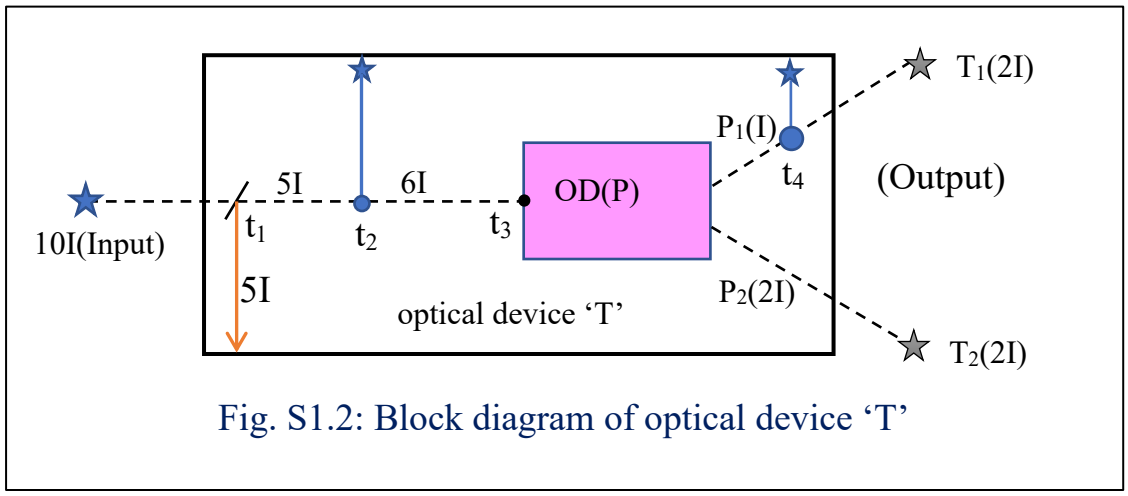

Fig. S1.2: Block diagram of optical device 'T'

Optical device 'U' [Fig: -S1.3].

This is a single input and two outputs device. It is incited for intensity level 11I. As an outcome, there are two outputs path 'U_1' and 'U_2' with intensity levels 2I and 3I respectively [which is revealed by Table: -s1.3].

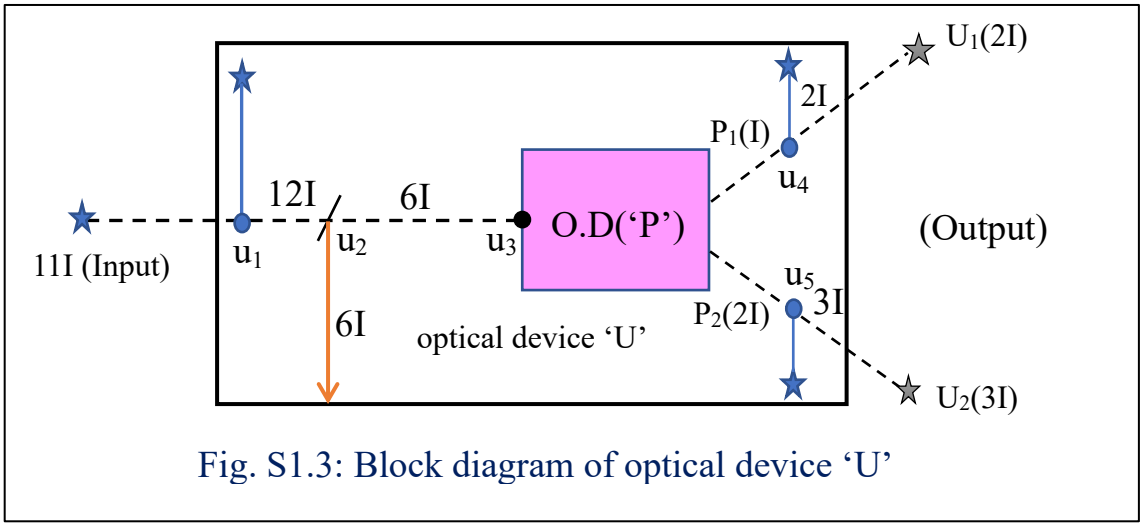

Fig. S1.3: Block diagram of optical device 'U'

Optical device 'V' [Fig: -S1.4].

It is a single input (12I) and single output (3I) device [which is displayed in Table: -s1.4].

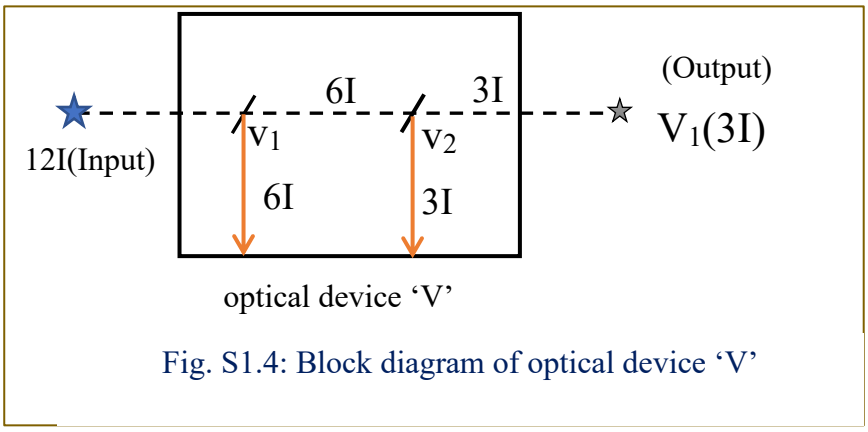

Fig. S1.4: Block diagram of optical device 'V'

Optical device 'X' [Fig: -S1.5]

It is operated at input intensity level 14I. For activated 'X' there are two output lines 'X_1' and 'X_2' of intensity level 2I and 3I respectively [which is revealed by Table: -s1.5].

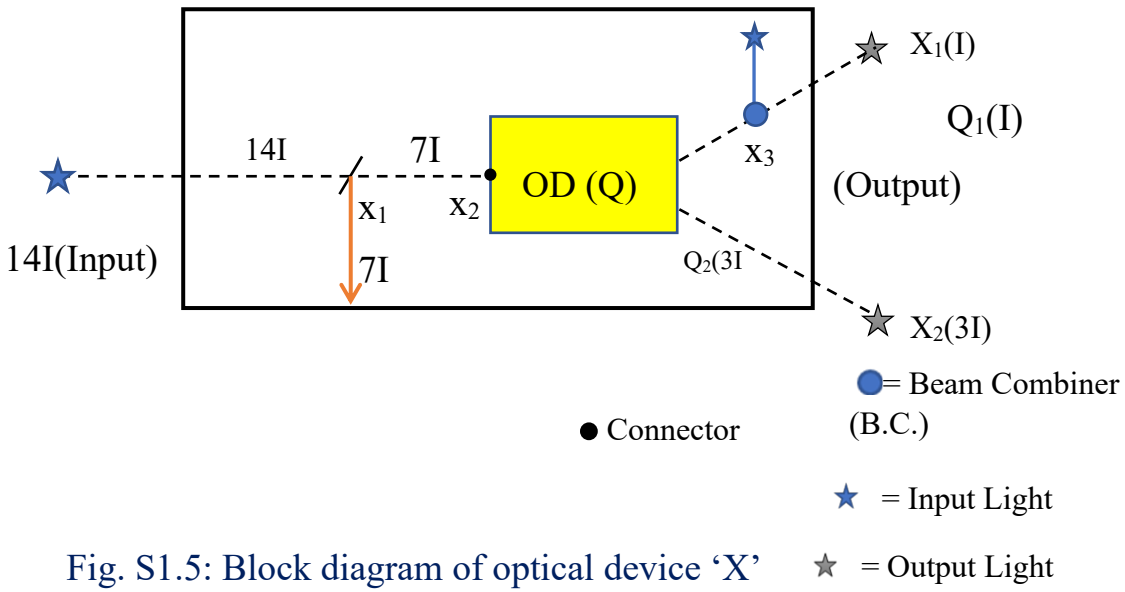

Fig. S1.5: Block diagram of optical device 'X'

Table captions: -

1. Table – s1.1: Input intensity versus Output intensity of the optical device ‘O’
2. Table – s1.2: Input intensity versus Output intensity of the optical device ‘T’
3. Table – s1.3: Input intensity versus Output intensity of the optical device ‘U’
4. Table – s1.4: Input intensity versus Output intensity of the optical device ‘V’
5. Table – s1.5: Input intensity versus Output intensity of the optical device ‘X’
6. Table – s2: Decimal number versus connected optical device
7. Table – s3: Comparison among Binary, Ternary, and Quaternary encoders of 3-bit

Table – s1.1: Input intensity versus Output intensity of the optical device 'O'

Name of the specific point of O.D. 'O'	Input intensity into the specific point	Helping element [Beam splitter (B.S.)/ Beam combiner (B.C.) /another O.D.]	Output intensity of progressive light beam from the specific point by the helping element	Name of the output line from the O.D. 'O' (with the intensity level)
o_1	5I	B.C.	6I	
o_2	6I	B.S.	3I	
			3I	
o_3	3I	B.C.	4I	
o_4	4I	B.S.	2I	
			2I	
o_5	2I	B.S.	I	O_1(I)
			I	O_1(I)

Table – s1.2: Input intensity versus Output intensity of the optical device 'T'

Input intensity [into the specific point]	Helping element [Beam splitter (B.S.)/ Beam combiner (B.C.) /another O.D.]	Output intensity of progressive light beam from the specific point by the helping element	Name of the output line from the O.D. 'T' (with the intensity level)
10I [t_1]	B.S.	5I	
		5I	
5I [t_2]	B.C.	6I	
6I [t_3]	O.D.(P)	I(P_1)	
		2I(P_2)	T_2(2I)
I(P_1) [t_4]	B.C.	2I	T_1(2I)

Table – s1.3: Input intensity versus Output intensity of the optical device 'U'

Input intensity [into the specific point]	Helping element [Beam splitter (B.S.)/ Beam combiner (B.C.) /another O.D.]	Output intensity of progressive light beam from the specific point by the helping element	Name of the output line from the O.D. 'U' (with the intensity level)
11I [u_1]	B.C.	12I	
12I [u_2]	B.S.	6I	
		6I	
6I [u_3]	O.D.(P)	I(P_1)	
		2I(P_2)	
I(P_1) [u_4]	B.C.	2I	U_1(2I)
2I(P_1) [u_5]	B.C.	3I	U_2(3I)

Table – s1.4: Input intensity versus Output intensity of the optical device 'V'

Input intensity [into the specific point]	Helping element [Beam splitter (B.S.)/ Beam combiner (B.C.) /another O.D.]	Output intensity of progressive light beam from the specific point by the helping element	Name of the output line from the O.D. 'V' (with the intensity level)
12I [v_1]	B.S.	6I	
		6I	
6I [v_2]	B.S.	3I	V_1(3I)
		3I	

Table s1.5: Input intensity versus Output intensity of the optical device 'X'

Input intensity [into the specific point]	Helping element [Beam splitter (B.S.)/ Beam combiner (B.C.) /another O.D.]	Output intensity of progressive light beam from the specific point by the helping element	Name of the output line from the O.D. 'W' (with the intensity level)
14I [x_1]	B.S.	7I	
		7I	
7I [x_2]	O.D.(Q)	I(Q_1)	
		3I(Q_2)	X_2(3I)
I [x_3]	B.C.	2I	X_1(2I)

Table. – s2: Decimal number versus connected optical device

Decimal number	Number of active input sources	Output intensity from optical regulator (O.R.)	Name of the connected optical device
1	1	I	None
2	2	2I	None
3	3	3I	None
4	4	4I	'N'
5	5	5I	'O'
6	6	6I	'P'
7	7	7I	'Q'
8	8	8I	'R'
9	9	9I	'S'
10	10	10I	'T'
11	11	11I	'U'
12	12	12I	'V'
13	13	13I	'W'
14	14	14I	'X'
15	15	15I	'Y'
16	16	16I	'Z'

Table: - s3: Comparison among Binary, Ternary and Quaternary encoder of 3 bit

Encoder	Bit(n)	Maximum number of coding data(decimal)
Binary	3	$[2^n - 1]$ =07
Ternary	3	$[3^n - 1]$ =26
Quaternary	3	$[4^n - 1]$ =63

Conversion (decimal to quaternary) process: -

For coding a particular decimal number then it has to be activated that particular number of input sources as-

1. To code the decimal number 1 to its quaternary form, any one input optical source out of 16 sources is to be lighted. Then there is the output line of intensity 'I' from O.R. This light beam of intensity 'I' is directly joined into the port 'F_1'. As an outcome, quaternary form of decimal number 1 is as - $F_3 = 0$; $F_2 = 0$; $F_1 = \bar{0}$
2. To code the decimal number 2 into its quaternary form, any two input optical sources out of 16 sources are to be kept in a high state (i.e. light is present). Then there is an output line of intensity level 2I from the optical regulator (O.R). This polarized light of intensity 2I is directly linked with port F_1. As a result, the output optical state will be - $F_3 = 0$; $F_2 = 0$; $F_1 = 1$
3. For the conversion of decimal number 3, any three input optical sources are in a high state. Then O.R. emerges the output line of intensity 3I which is directly connected with port F_1. For this case situation will be- $F_3\, F_2\, F_1 = 0\ 0\ \bar{1}$
4. To express the decimal number 4, any four input sources are in High state. As a result, a polarized light beam of intensity 4I from O.R is followed to the O.D(N). Then a polarized light beam of intensity 'I' as an output beam from O.D 'N' is connected to the port 'F_2'. Again, F_2 is also attached to an optical switch $(O.S)_2$. As a consequence, the output of 'F_2' is $\bar{0}$. Finally, the quaternary form of decimal number 4 is as- $F_3\, F_2\, F_1 = 0\ \bar{0}\ 0$
5. To convert the decimal number 5, any 5 out of 16 input sources have to be incited. Thereafter refracted ray from O.R. follows the path of intensity 5I. This light beam of intensity 5I enters into the optical device 'O'. Now from the feature of 'O' for input intensity 5I, there are two output lines 'O_1' & 'O_2' from optical device 'O' with the same intensity level 'I', where 'O_1' & 'O_2' are again joined to the port 'F_1' & 'F_2' respectively. After that the output quaternary form of the decimal number 5 is as $F_3 = 0$; $F_2 = \bar{0}$; $F_1 = \bar{0}$
6. When 6 input sources are in active state, then output lines from O.R. are of intensity level 6I. This polarized light beam is joined to the O.D 'P'. Then O.D 'P' transmits two output lines 'P_1' & 'P_2' with the intensity I and 2I respectively. These are added

to the port 'F_2' & 'F_1' respectively. Finally, the output quaternary form of the decimal number '6' is as -$F_3 = 0$; $F_2 = \bar{0}$; $F_1 = 1$

7. To change the decimal number 7 to its quaternary form, the input intensity level of O.R. has to be 7I. Then the output path of intensity 7I is put in O.D 'Q'. After processing by O.D. two emanated output lines Q_1(I) & Q_2(3I) further connected to the port F_2 & F_1 respectively. As a consequence, the output quaternary form of decimal number 7 is as $F_3 = 0$; $F_2 = \bar{0}$; $F_1 = \bar{1}$
8. The decimal number 8 can be converted by any 8 number of input sources out of 16 are in High state. Then a refracted ray of intensity 8I from O.R. is concerned to the O.D 'R'. From the feature of 'R', we get output line R_1 of intensity 2I. This output line R_1(2I) is associated with optical port F_2. Now quaternary form of decimal number 8 is as- $F_3 = 0$; $F_2 = 1$; $F_1 = 0$
9. For coding the decimal number 9, the input intensity level of O.R. is to be 9I. Then refracted ray from O.R. is directed along the O.D 'S'. Then two output lines S_1(I) & S_2(2I) from 'S' are entered into the port F_1 & F_2 respectively. So, output quaternary form of decimal number 9 is as- $F_3 = 0$; $F_2 = 1$; $F_1 = \bar{0}$
10. To convert the decimal number 10 to its quaternary form, any 10 input light sources are in a high state, in this case, the optical device 'T' is activated. As a result, two output lines T_1 & T_2 of the same intensity level 2I conjoined to ports F_1 & F_2 respectively. Now output quaternary form of 10 is –$F_3 = 0$; $F_2 = 1$; $F_1 = 1$
11. When the input intensity on O.R is 11I, the refracted ray enters in O.D. 'U'. Now two output lines U_1 and U_2 of intensity 2I & 3I from O.D 'U' are linked with optical ports F_2 & F_1 respectively. Therefore, the quaternary form of the decimal number 11 is as -$F_3 = 0$; $F_2 = 1$; $F_1 = \bar{1}$
12. To turn the decimal number 12 to its quaternary form, the input intensity on O.R. is to be 12I. Thereafter light beam of intensity 12I from O.R. is accumulated into optical device 'V'. After processing 'V' grants output line V_1 of intensity level 3I. Then this output line is directly connected to the port 'F_2'. So, the quaternary form of the decimal number 12 is as - $F_3 = 0$; $F_2 = \bar{1}$; $F_1 = 0$
13. For converting, the decimal number 13 to its quaternary form, any 13 input sources are to be kept in a high state. Hence the output line from O.R propagates along the path of intensity 13I and enters into the optical device 'W'. After the process 'W' yields two output lines 'W_1' & 'W_2' with intensity levels 'I' & '3I' respectively.

Afterwards $W_1(I)$ & $W_2(3I)$ are engaged with optical port 'F_1' & 'F_2' orderly. Finally, the output quaternary form of decimal number 13 is as – $F_3 = 0$; $F_2 =$; $F_1 = \bar{0}$

14. The transformation of decimal number 14 to its quaternary form, is already discussed in the main manuscript. The output quaternary form of decimal number 14 is as – $F_3F_2F_1 = 0\ \bar{1}\ 1$
15. For expressing decimal number 15 to its quaternary form, it is to be stimulated any 15 numbers of input sources out of 16 light sources. Then the refracted light beam from O.R. is along the path of intensity 15I. This polarized light beam is now connected to the optical device as an input source. From the characteristics of 'Y', there are two output lines 'Y_1' & 'Y_2' of the same intensity level 3I where they are again joined to the optical port F_1 & F_2 respectively. As an outcome, the quaternary form of decimal number 15 is as – $F_3 = 0$; $F_2 = \bar{1}$; $F_1 = \bar{1}$
16. To code decimal number 16, all of the input sources are to remain in a high state (i.e. light is present). Then O.R emanates an output line of intensity 16I, which is linked with O.D 'Z'. Receiving input intensity 16I, O.D 'Z' provides a single output line of intensity 'I', which is further connected with optical port 'F_3'. As ending quaternary form of the decimal number 16 is as follows- $F_3 = \bar{0}$; $F_2 = 0$; $F_1 = 0$.

Appendix-B

List of Figures: -

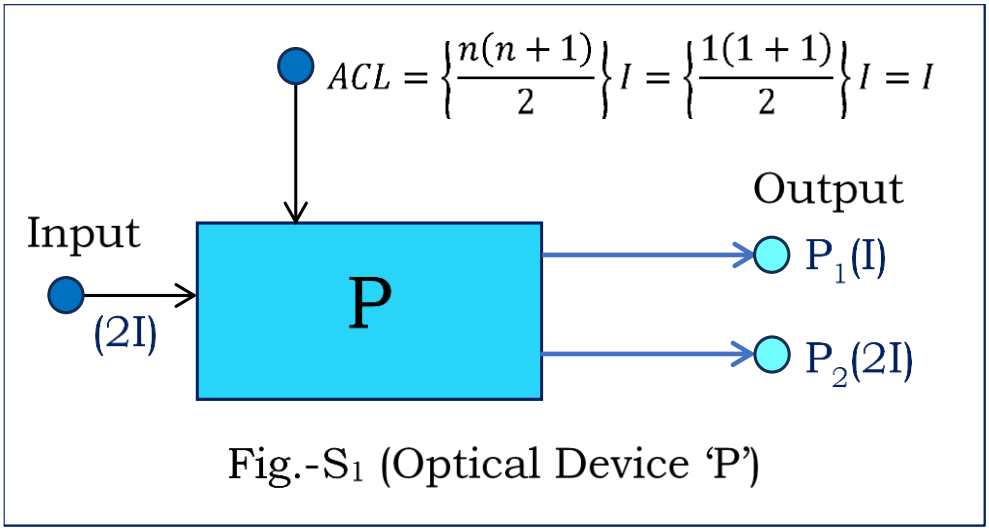

Fig.-S_1 (Optical Device 'P')

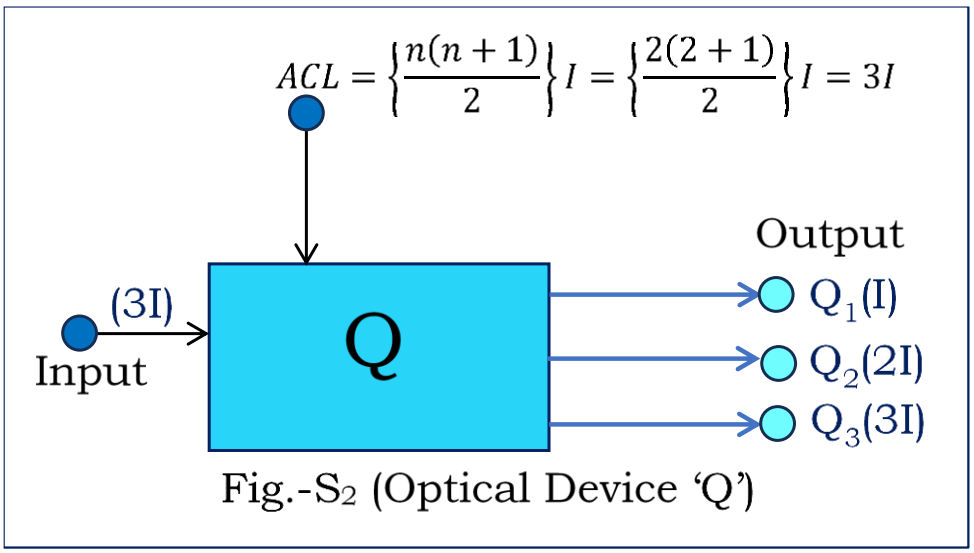

Fig.-S_2 (Optical Device 'Q')

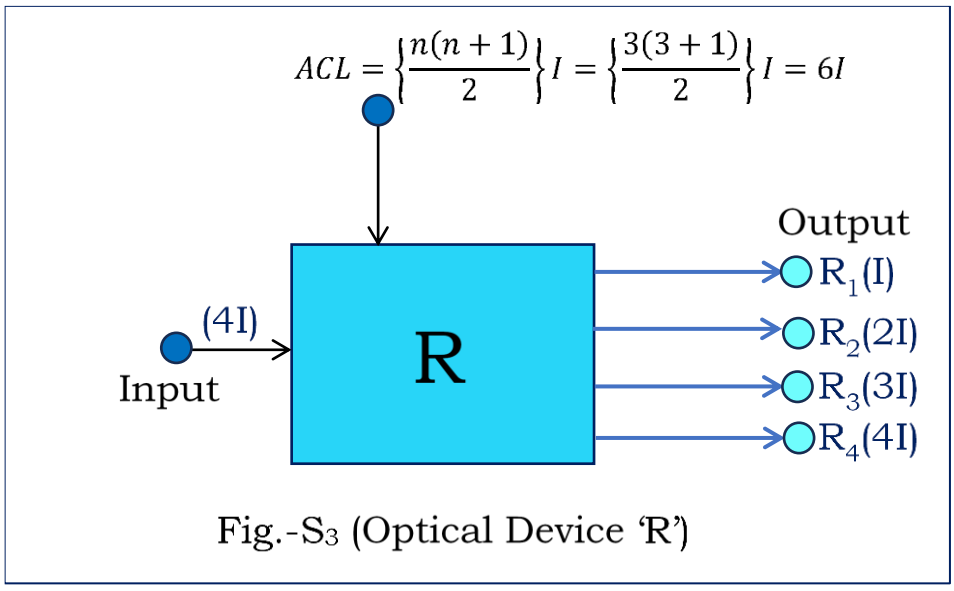

Fig.-S_3 (Optical Device 'R')

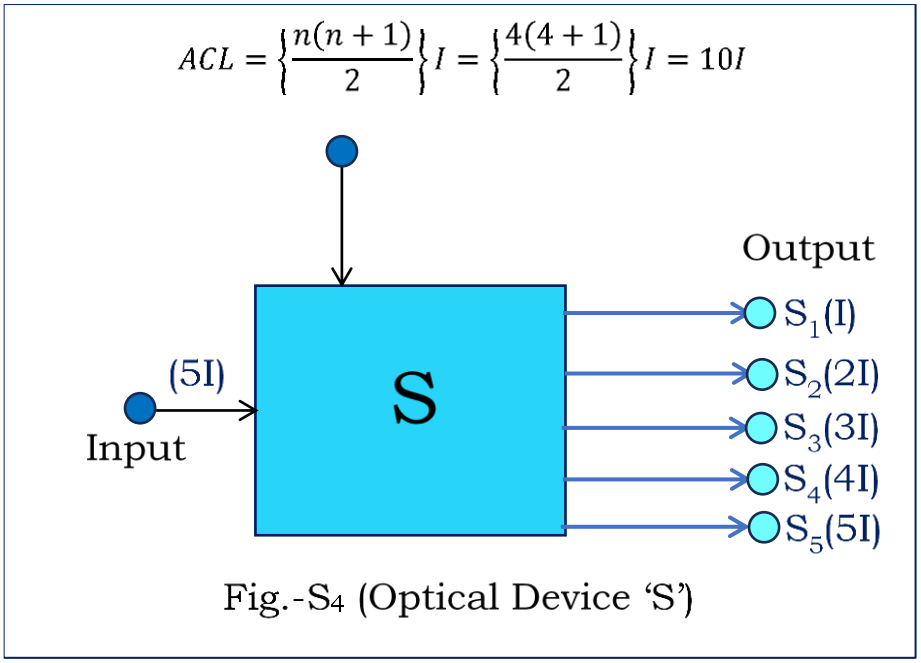

Fig.-S4 (Optical Device 'S')

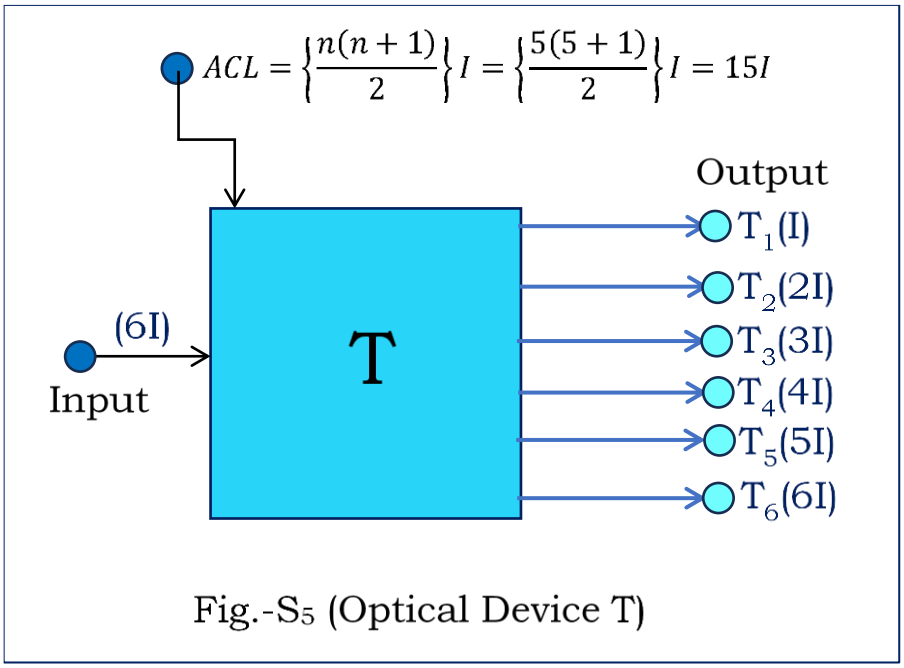

Fig.-S5 (Optical Device T)

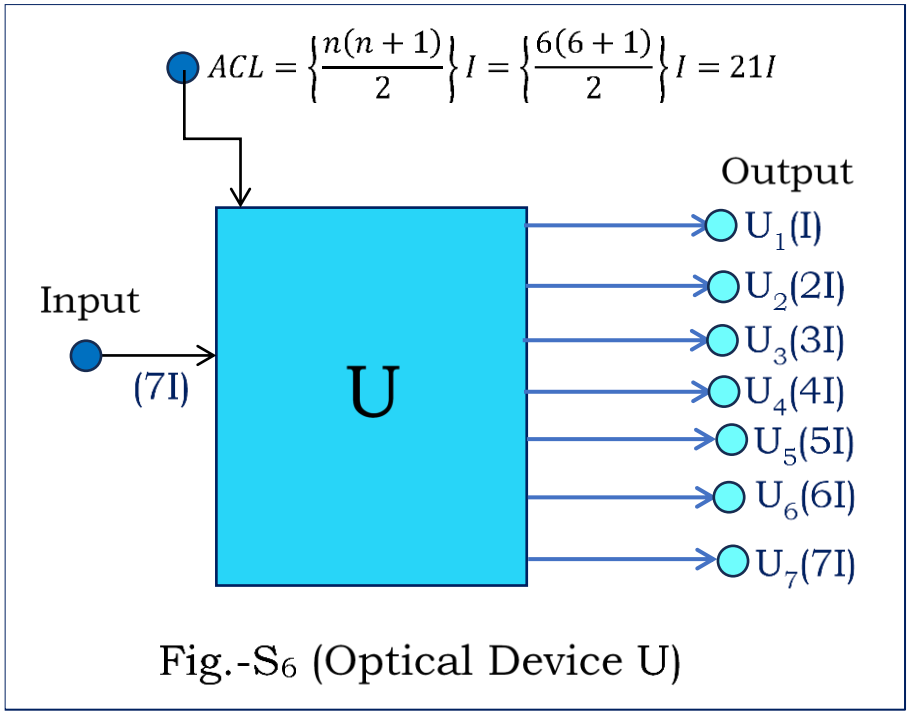

Fig.-S6 (Optical Device U)

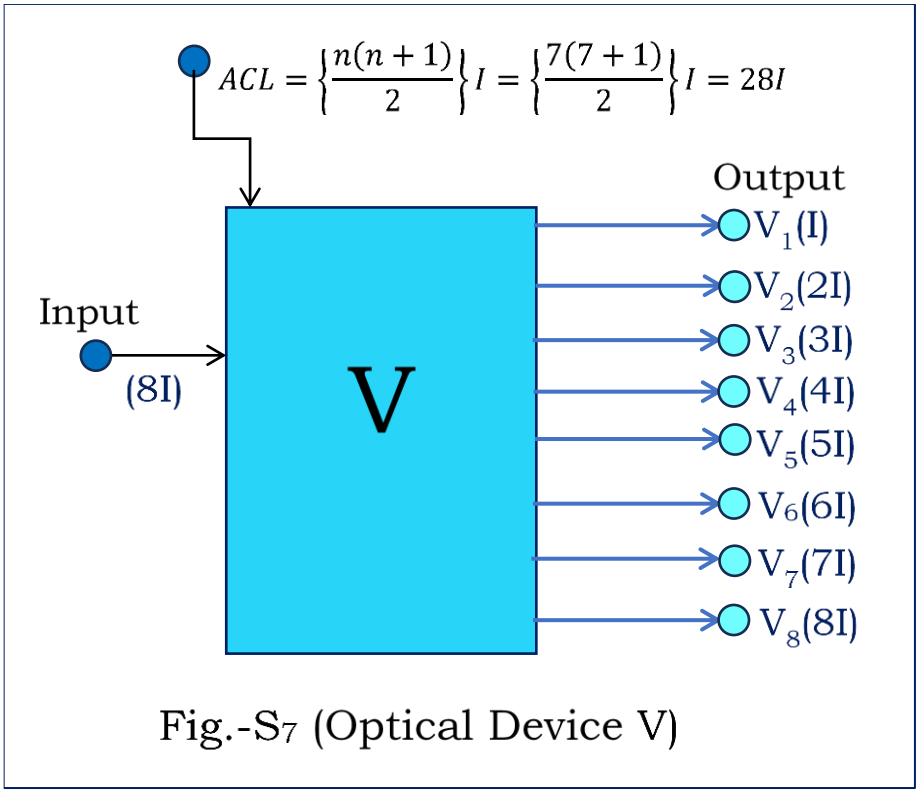

Fig.-S7 (Optical Device V)

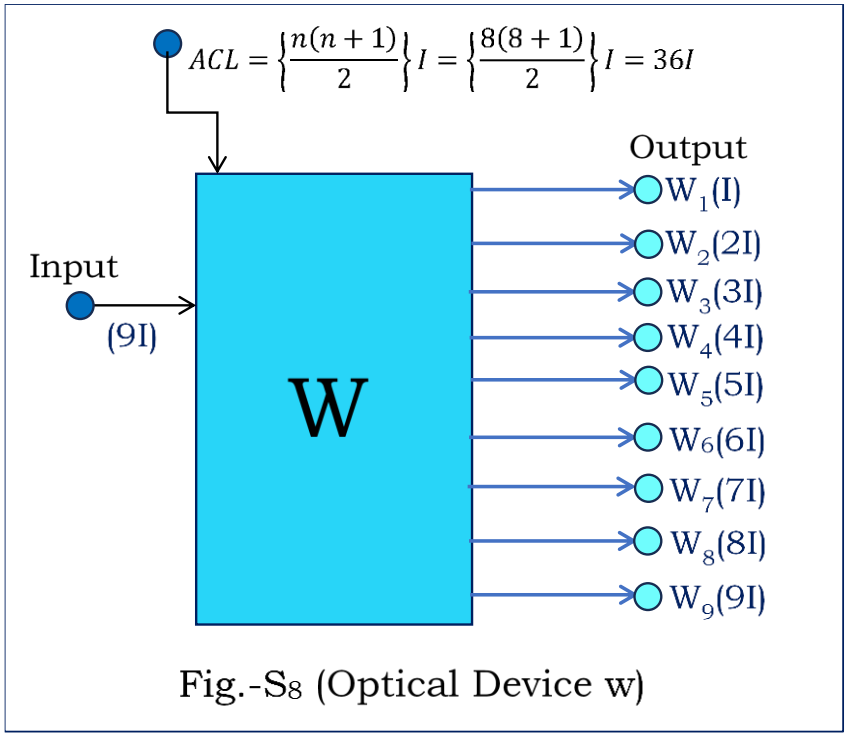

Fig.-S8 (Optical Device w)

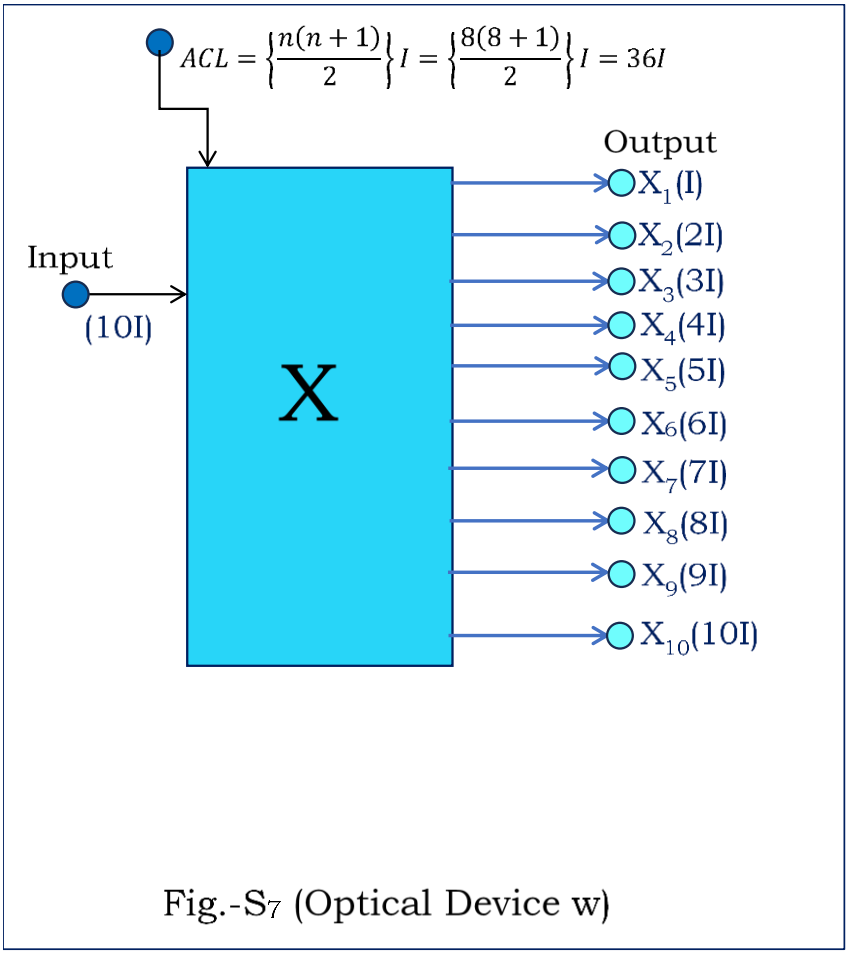

Fig.-S7 (Optical Device w)

List of Tables: -

Table – S_1 (Optical Device – P)

Name of the output lines with the intensity level of optical device 'P'

Input Intensity of light	At the definite point	By dint of BC (Beam Combiner) or BS (Beam Splitter)	Output Intensity of light at the definite point	Name of the output lines & [connected to output channel of OBED (Optical Binomial Expansion Device)]
2I	P_1	BS	I	P_1 [Y_1]
			I	
I	P_2	BC	2I	P_2 [Y_2]

Table – S_2 (Optical Device – Q)

[Name of the output lines with the intensity level of optical device 'Q'.]

Input Intensity of light	At the definite point	By dint of BC (Beam Combiner) or BS (Beam Splitter)	Output Intensity of light at the definite point	Name of the output lines & [connected to output channel of OBED (Optical Binomial Expansion Device)]
3I	q_1	BC	4I	
4I	q_2	BS	2I	
			2I	
2I	q_3	BS	I	Q_1 [Y_1]
			I	
I	q_4	BC	2I	Q_2 [Y_2]
2I	q_5	BC	3I	Q_3 [Y_3]

Table –S_3 (Optical Device – R)

[Name of the output lines with the intensity level of optical device 'R'.]

Input Intensity of light	At the definite point	By dint of BC (Beam Combiner) or BS (Beam Splitter)	Output Intensity of light at the definite point	Name of the output lines & [connected to output channel of OBED (Optical Binomial Expansion Device)]
4I	r_1	BC	6I	
6I	r_2	BS	3I	
			3I	
3I	r_3	BC	4I	
4I	r_4	BS	2I	
			2I	
2I	r_5	BS	I	R_1 [Y_1]
			I	
I	r_6	BC	2I	R_2 [Y_2]
2I	r_7	BC	3I	R_3 [Y_3]
3I	r_8	BC	4I	R_4 [Y_4]

Table – S_4 (Optical Device – S)

[Name of the output lines with the intensity level of optical device 'S'.]

Input Intensity of light	At the definite point	By dint of BC (Beam Combiner) or BS (Beam Splitter)	Output Intensity of light at the definite point	Name of the output line & [connected output channel of OBED (Optical Binomial Expansion Device)]
5I	s_1	BC	8I	
8I	s_2	BS	4I	
			4I	
4I	s_3	BC	6I	
6I	s_4	BS	3I	
			3I	
3I	s_5	BC	4I	
4I	s_6	BS	2I	
			2I	
2I	s_7	BS	I	S_1 [Y_1]
			I	
I	s_8	BC	2I	S_2 [Y_2]
2I	s_9	BC	3I	S_3 [Y_3]
3I	s_{10}	BC	4I	S_4 [Y_4]
4I	s_{11}	BC	5I	S_5 [Y_5]

Table – S_5 (Optical Device – T)

[Name of the output lines with the intensity level of optical device 'T'.]

Input Intensity of light	At the definite point	By dint of BC (Beam Combiner) or BS (Beam Splitter)	Output Intensity of light at the definite point	Name of the output line & [connected to output channel of OBED (Optical Binomial Expansion Device)]
6I	t_1	BC	10I	
10I	t_2	BS	5I	
			5I	
5I	t_3	BC	8I	
8I	t_4	BS	4I	
			4I	
4I	t_5	BC	6I	
6I	t_6	BS	3I	
			3I	
3I	t_7	BC	4I	
4I	t_8	BS	2I	
			2I	
2I	t_9	BS	I	T_1 [Y_1]
			I	
I	t_{10}	BC	2I	T_2 [Y_2]
2I	t_{11}	BC	3I	T_3 [Y_3]
3I	t_{12}	BC	4I	T_4 [Y_4]
4I	t_{13}	BC	5I	T_5 [Y_5]
5I	t_{14}	BC	6I	T_6 [Y_6]

Table – S_6 (Optical Device – U)

[Name of the output lines with the intensity level of optical device 'U'.]

Input Intensity of light	At the definite point	By dint of BC (Beam Combiner) or BS (Beam Splitter)	Output Intensity of light at the definite point	Name of the output line & [connected to output channel of OBED (Optical Binomial Expansion Device)
7I	u_1	BC	12I	
12I	u_2	BS	6I	
			6I	
6I	u_3	BC	10I	
10I	u_4	BS	5I	
			5I	
5I	u_5	BC	8I	
8I	u_6	BS	4I	
			4I	
4I	u_7	BC	6I	
6I	u_8	BS	3I	
			3I	
3I	u_9	BC	4I	
4I	u_{10}	BS	2I	
			2I	
2I	u_{11}	BS	I	U_1 [Y_1]
			I	
I	u_{12}	BC	2I	U_2 [Y_2]
2I	u_{13}	BC	3I	U_3 [Y_3]
3I	u_{14}	BC	4I	U_4 [Y_4]
4I	u_{15}	BC	5I	U_5 [Y_5]
5I	u_{16}	BC	6I	U_6 [Y_6]
6I	u_{17}	BC	7I	U_7 [Y_7]

Table – S_7(Optical Device – V)

[Name of the output lines with the intensity level of optical device 'V'.]

Input Intensity of light	At the definite point	By dint of BC (Beam Combiner) or BS (Beam Splitter)	Output Intensity of light at the definite point	Name of the output line & [connected to output channel of OBED (Optical Binomial Expansion Device)]
8I	v_1	BC	14I	
14I	v_2	BS	7I	
			7I	
7I	v_3	BC	12I	
12I	v_4	BS	6I	
			6I	
6I	v_5	BC	10I	
10I	v_6	BS	5I	
			5I	
5I	v_7	BC	8I	
8I	v_8	BS	4I	
			4I	
4I	v_9	BC	6I	
6I	v_{10}	BS	3I	
			3I	
3I	v_{11}	BC	4I	
4I	v_{12}	BS	2I	
			2I	
2I	v_{13}	BS	I	V_1 [Y_1]
			I	
I	v_{14}	BC	2I	V_2 [Y_2]
2I	v_{15}	BC	3I	V_3 [Y_3]
3I	v_{16}	BC	4I	V_4 [Y_4]
4I	v_{17}	BC	5I	V_5 [Y_5]
5I	v_{18}	BC	6I	V_6 [Y_6]
6I	v_{19}	BC	7I	V_7 [Y_7]
7I	v_{20}	BC	8I	V_8 [Y_8]

Table – S_8 (Optical Device – W)

[Name of the output lines with intensity level of optical device 'W'.]

Input Intensity of light	At the definite point	By dint of BC (Beam Combiner) or BS (Beam Splitter)	Output Intensity of light at the definite point	Name of the output line & [connected to output channel of OBED (Optical Binomial Expansion Device)]
9I	w_1	BC	16I	
16I	w_2	BS	8I	
			8I	
8I	w_3	BC	14I	
14I	w_4	BS	7I	
			7I	
7I	w_5	BC	12I	
12I	w_6	BS	6I	
			6I	
6I	w_7	BC	10I	
10I	w_8	BS	5I	
			5I	
5I	w_9	BC	8I	
8I	w_{10}	BS	4I	
			4I	
4I	w_{11}	BC	6I	
6I	w_{12}	BS	3I	
			3I	
3I	w_{13}	BC	4I	
4I	w_{14}	BS	2I	
			2I	
2I	w_{15}	BS	I	W_1 [Y_1]
			I	
I	w_{16}	BC	2I	W_2 [Y_2]
2I	w_{17}	BC	3I	W_3 [Y_3]
3I	w_{18}	BC	4I	W_4 [Y_4]
4I	w_{19}	BC	5I	W_5 [Y_5]
5I	w_{20}	BC	6I	W_6 [Y_6]
6I	w_{21}	BC	7I	W_7 [Y_7]
7I	w_{22}	BC	8I	W_8 [Y_8]
8I	w_{23}	BC	9I	W_9 [Y_9]

Table – S_9 (Optical Device – X)

[Name of the output lines with intensity level of optical device 'X'.]

Input Intensity of light	At the definite point	By dint of BC (Beam Combiner) or BS (Beam Splitter)	Output Intensity of light at the definite point	Name of the output line & [connected to output channel of OBED (Optical Binomial Expansion Device)]
10I	x_1	BC	18I	
18I	x_2	BS	9I	
			9I	
9I	x_3	BC	16I	
16I	x_4	BS	8I	
			8I	
8I	x_5	BC	14I	
14I	x_6	BS	7I	
			7I	
7I	x_7	BC	12I	
12I	x_8	BS	6I	
			6I	
6I	x_9	BC	10I	
10I	x_{10}	BS	5I	
			5I	
5I	x_{11}	BC	8I	
8I	x_{12}	BS	4I	
			4I	
4I	x_{13}	BC	6I	
6I	x_{14}	BS	3I	
			3I	
3I	x_{15}	BC	4I	
4I	x_{16}	BS	2I	
			2I	
2I	x_{17}	BS	I	X_1 [Y_1]
			I	
I	x_{18}	BC	2I	X_2 [Y_2]
2I	x_{19}	BC	3I	X_3 [Y_3]
3I	x_{20}	BC	4I	X_4 [Y_4]
4I	x_{21}	BC	5I	X_5 [Y_5]
5I	x_{22}	BC	6I	X_6 [Y_6]
6I	x_{23}	BC	7I	X_7 [Y_7]
7I	x_{24}	BC	8I	X_8 [Y_8]
8I	x_{25}	BC	9I	X_9 [Y_9]
9I	x_{26}	BC	10I	X_{10} [Y_{10}]

List of my publications and presentations

Journal Publications

1. Nirmalya Pahari, **Apurba Guchhait**, "All-optical Serial Data Transfer between Registers using optical non-linear materials, *Optik 123 (2012) 462–466*, Doi: 10.1016/j.ijleo.2011.05.006

2. Nirmalya Pahari, **Apurba Guchhait**, Atish Dipankar Jana, "Image edge detection scheme by the use of Kerr type nonlinear material and the verification of the scheme by computer simulation", *Journal of Optics 41 (2012) 178-183*, Doi: 10.1007/s12596-012-0082-0.

3. **Apurba Guchhait**, Nirmalya Pahari, Nabin Baran Manik, "All-optical decimal to ternary converter with the proper use of optical non-linear material, *Journal of Optics 49 (2019) 59-68,* https://doi.org/10.1007/s12596-019-00579-1.

4. **Apurba Guchhait**, Nirmalya Pahari, Nabin Baran Manik, Optical Kerr nonlinear material for calculating the coefficient of binomial expansion under any positive integral index, *Journal of Optics 51 (2022) 851-865,* https://doi.org/10.1007/s12596-021-00823-7.

5. **Apurba Guchhait**, Nirmalya Pahari, Nabin Baran Manik, Optical Kerr nonlinear material for expressing the trigonometric ratios of compound angles, *Journal of Optics 53 (2023) 892-905*, https://doi.org/10.1007/s12596-023-01245-3.

6. **Apurba Guchhait**, Nirmalya Pahari, Nabin Baran Manik, Design of an all-optical quaternary encoder to code decimal numbers by utilizing optical Kerr nonlinear material, *Discover Electronics 02 (2025) article 43*, https://doi.org/10.1007/s44291-025- 00064-z.

Book Chapters-

1. **Apurba Guchhait**, Nirmalya Pahari, Nabin Baran Manik,"Optical Non-Linear Material for Designing All-Optical Binary Encoder to Code Decimal Number",*Materials Science and Engineering*, accepted on June 2025**,** **ISBN:978-93-49897-15-1,** NEW DELHI PUBLISHERS

2. **Apurba Guchhait**, Nirmalya Pahari, Nabin Baran Manik**,**"Optical Circuit for Decoding Ternary Code to Decimal Number by Exploiting Kerr Optical Non-Linear Material",*Materials Science and Engineering***,** accepted on June 2025, **ISBN:978-93-49897-15-1,** NEW DELHI PUBLISHERS

Seminar papers –

1. **Apurba Guchhait,** Dr. Nirmalya Pahari, ''A new scheme for coding decimal numbers to binary numbers by optical Encoder with the help of optical non-linear material'',*(UGC sponsored) National seminar on Photonics and nano sciences*, Department of Physics; Garhbeta College; Paschim Medinipur; 721127 in collaboration with Indian Association of Physics Teachers, 20-21 December 2011.

2. **Apurba Guchhait,** Dr. Nirmalya Pahari, ''A new scheme for decoding binary numbers to decimal numbers by optical Decoder'',*Recent Trends in Optoelectronics [Sponsored by University Grants Commission (New Delhi)],* Department of Physics; Sripat Singh College; Jiaganj, Murshidabad in collaboration with Dumkal College, 3rd February, 2012.

3. **Apurba Guchhait,** Dr. Nirmalya Pahari, ''An all-optical decoder by optical non-linear material'', *Second national seminar on recent trends in condensed matter Physics including Laser application (Sponsored by UGC),* Department of Physics Centre of Advanced Study, The University of Burdwan Golap bag Burdwan, 22nd -23rd March, 2012.

4. **Apurba Guchhait,** Dr. Nirmalya Pahari, Prof. Nabin Baran Manik, ‘‘Optical non-linear material for designing all-optical quaternary encoder to code decimal number’’ *One Day International Seminar on Recent Advancement in materials Science and Engineering,* Department of Physics in collaboration With IQAC of Vivekananda Mahavidyalaya, Burdwan, 30th January, 2025.

5. **Apurba Guchhait,** Dr. Nirmalya Pahari, Prof. Nabin Baran Manik, ‘‘Optical Non-linear Material for Designing All-Optical Ternary to Binary Converter’’*, Scientific Innovation and Skill Development for Societal Advancement*, Department of Physics, Jadavpur University, 7th March, 2025.